



**UNIVERSITÀ DEGLI STUDI DI TRIESTE**

**e**

**UNIVERSITÀ CA' FOSCARI DI VENEZIA**

**XXXIII CICLO DEL DOTTORATO DI RICERCA IN  
CHIMICA**

**SYNTHESIS AND USE OF TRIAZINYL QACs AS  
ANTIMICROBIAL AGENTS**

Settore scientifico-disciplinare: **CHIM/04**

DOTTORANDO / A

**ANDREA MORANDINI**

COORDINATORE

**PROF. ENZO ALESSIO**

SUPERVISORE DI TESI

**PROF. VALENTINA BEGHETTO**

**ANNO ACCADEMICO 2019/2020**



*Se la conoscenza può creare dei problemi, non è con l'ignoranza che possiamo risolverli.*

*If knowledge can create trouble, it is not with ignorance that we can solve it.*

*-Isaac Asimov-*

## Abstract

The development of resistance to adverse substances by microorganisms is a natural mechanism that they have exploited since ancient times to be able to preserve the species. The unusual acceleration in the development of microorganisms capable of resisting the most common antimicrobial substances in recent years is a phenomenon of recent concern to various global health organizations.

With the onset of industrialization in the early 20th century and the discovery of powerful antibiotic drugs, mankind has been able to significantly improve its lifestyle. But, after decades of irresponsible use and squandering of these antimicrobial substances in the environment, the inexorable generation of new antibiotic-resistant species has arrived.

Humanity, if it wants to better contain this phenomenon, in the future will have to act with more conscience, limiting waste, using products that better preserve the environment and developing new effective antimicrobial substances.

In this PhD work we describe the synthesis of novel antimicrobial compounds based on quaternary ammonium salts (QACs). QACs are widespread hygienizers commonly used in detergent products. Normally they are prepared from reactions exploiting high-temperature alkyl-halides. Taking advantage of the high reactivity of chlorotriazines, it has been possible to obtain new libraries of triazine QACs using more sustainable processes with less impact on the environment.

In the first instance, we focused on the synthesis of a library of morpholino-triazine QACs directly inspired by the structure of 4-(4,6-dimethoxy-1,3,5-triazin-2-yl)-4-methylmorpholinium chloride or DMTMM. Then evaluating its efficacy against Gram-positive and Gram-negative bacterial strains such as *Staphylococcus aureus* and *Escherichia coli*. Next, we moved on to the synthesis of a library of imidazole-triazine QACs that showed superior performance compared to the first morpholino-triazine QACs, both in terms of yield and antimicrobial activity. Finally, the synthesis of various blockcopolymers based on 2-*N*-morpholinoethyl methacrylate (MEMA) and their use in the preparation of polymeric QACs and antimicrobial surfaces was described.

## Sommario

Lo sviluppo della resistenza alle sostanze avverse nei microorganismi è un meccanismo naturale che essi hanno sfruttato fin dall'antichità per poter preservare la specie. L'inusuale accelerazione nello sviluppo di microorganismi in grado di resistere alle più comuni sostanze antimicrobiche negli ultimi anni è un fenomeno che recentemente preoccupa le varie organizzazioni della salute mondiale.

Con l'avvio verso l'industrializzazione ai primi del XX secolo e la scoperta di potenti farmaci antibiotici, l'umanità ha potuto notevolmente migliorare il suo stile di vita. Ma, dopo decenni di utilizzo irresponsabile e sperpero nell'ambiente di queste sostanze antimicrobiche, si è giunti all'inesorabile generazione di nuove specie antibiotico resistenti.

L'umanità, se meglio vuole arginare questo fenomeno, in futuro dovrà agire con più coscienza, limitando gli sprechi, utilizzando prodotti che meglio preservino l'ambiente e sviluppando nuove sostanze antimicrobiche efficaci.

In questo lavoro di dottorato si descrive la sintesi di nuovi composti antimicrobici basati sui sali d'ammonio quaternario (QACs). I QACs sono degli igienizzanti molto diffusi nei prodotti detergenti di uso comune e normalmente vengono preparati a partire da reazioni che sfruttano alchil-alogenuri ad alta temperatura. Sfruttando la grande reattività delle clorotriazine è stato possibile ottenere nuove librerie di QACs triazinici utilizzando processi più sostenibili e di minor impatto sull'ambiente.

In prima istanza ci si è concentrati sulla sintesi di una libreria di QACs morfolino-triazinici di diretta ispirazione alla struttura della 4-(4,6-dimetossi-1,3,5-triazin-2-il)-4-metil-morfolinio cloruro o DMTMM. Valutandone poi l'efficacia contro ceppi batterici Gram-positivi e Gram-negativi come *Staphylococcus aureus* ed *Escherichia coli*. Successivamente si è passati alla sintesi di una libreria di QACs imidazolo-triazinici che hanno mostrato prestazioni superiori rispetto ai primi QACs morfolino-triazinici, sia in termini di resa delle reazioni che in termini di attività antimicrobica. Infine, è stata descritta la sintesi di vari polimeri a blocchi basati sulla 2-*N*-morfolinoetil metilmetacrilato (MEMA) e il loro utilizzo nella preparazione di QACs polimerici e superfici antimicrobiche.

## List of abbreviation

|                  |  |
|------------------|--|
| AA-MoPA          | Morpholinopropyl-alkylamide  |
| AMR              | Antimicrobial Resistance   |
| ATRP             | Atom transfer radical polymerization   |
| BAC              | Benzalkonium chloride  |
| BuMO-CC          | 4,4'-(6-chloro-1,3,5-triazine-2,4-diyl)bis(4-(3-alkylamidopropyl)morpholin-4-ium) chloride     |
| BuMO-MMT         | 4,6-bis(4-(3-alkylamidopropyl)morpholino-4-ium)-2-oxo-2 <i>H</i> -1,3,5-triazin-1-ide chloride |
| C.a.             | <i>Candida albicans</i>  |
| CC               | Cyanuric chloride  |
| CDMT             | 2-chloro-4,6-dimethoxy-1,3,5-triazine  |
| CFU              | Colony Forming Units   |
| CMC              | Critical Micelle Concentration   |
| COSY             | 2D NMR Correlation Spectroscopy  |
| CPC              | Cetylpyridinium chloride   |
| DDAC             | Didecyl-methyl-ammonium chloride   |
| DFT              | Density Functional Theory  |
| DMTM             | 4-(4,6-dimethoxy-1,3,5-triazin-2-yl)-morpholine  |
| DMTMM            | 4-(4,6-dimethoxy-1,3,5-triazin-2-yl)-4-methyl-morpholinium chloride                            |
| DMTOH            | 2-hydroxy-4,6-dimethoxy-1,3,5-triazine   |
| dNbpy            | 4,4'-dinonyl-2,2'-bipyridyl  |
| EBiB             | Ethyl 2-bromoisobutyrate   |
| E.c.             | <i>Escherichia coli</i>  |
| E.f.             | <i>Enterococcus faecalis</i>   |
| FT-IR            | Fourier-transform infrared spectroscopy  |
| GC               | Gas Chromatography   |
| HMBC             | 2D NMR Heteronuclear Multiple Bond Correlation   |
| HMQC             | 2D NMR Heteronuclear Multiple Quantum Coherence  |
| IC <sub>50</sub> | Half maximal inhibitory concentration  |
| MAT              | 4,6-dichloro-N-alkyl-1,3,5-triazin-2-amine   |
| MATdMIMI         | 3,3'-(6-(alkylamino)-1,3,5-triazine-2,4-diyl)bis(1-methyl-1 <i>H</i> -imidazol-3-ium) chloride |

|                         |  |
|-------------------------|--|
| MAT <sub>12</sub> mMIMI | 3-(4-chloro-6-(dodecylamino)-1,3,5-triazin-2-yl)-1-methyl-1 <i>H</i> -imidazol-3-ium chloride                  |
| MAT <sub>12</sub> MBP   | 1',1''-(6-(dodecylamino)-1,3,5-triazine-2,4-diyl)bis(1-methyl-[4,4'-bipyridine]-1,1'-dium) dichloride diiodide |
| MBP                     | 1-methyl-[4,4'-bipyridin]-1-ium iodide   |
| MEMA                    | 2- <i>N</i> -morpholinoethyl methacrylate  |
| MIC                     | Minimal Inhibitory Concentration   |
| MMA                     | Methyl methacrylate  |
| MMT                     | 2,4-dichloro-6-methoxy-1,3,5-triazine  |
| MoPALA-CC               | 4,4'-(6-chloro-1,3,5-triazine-2,4-diyl)bis(4-(3-alkylamidopropyl)morpholin-4-ium) chloride                     |
| MoPALA-MMT              | 4,6-bis(4-(3-alkylamidopropyl)morpholino-4-ium)-2-oxo-2 <i>H</i> -1,3,5-triazin-1-ide chloride                 |
| MRSA                    | Methicillin-Resistant <i>Staphylococcus aureus</i>   |
| NMM                     | <i>N</i> -methylmorpholine   |
| NMR                     | Nuclear Magnetic Resonance   |
| P.a.                    | <i>Pseudomonas aeruginosa</i>  |
| PFU                     | Plague Forming Units   |
| PMDETA                  | <i>N,N',N'',N'''</i> -pentamethyldiethylenetriamine  |
| PMEMA                   | Poly-2- <i>N</i> -morpholinoethyl methacrylate   |
| PMMA                    | Polymethylmetacrylate  |
| PS                      | Polystyrene  |
| QACs                    | Quaternary ammonium salts  |
| ROS                     | Reactive Oxygen Species  |
| S.a.                    | <i>Staphylococcus aureus</i>   |
| TQACs                   | Triazine Quaternary ammonium salts   |
| WHO                     | World Health Organization  |

# Index

| Chapters  | Pages     |
|---|-----------|
| <b>SYNTHESIS OF NEW ANTIMICROBIAL TRIAZINE-BASED QUATERNARY AMMONIUM SALTS</b>  |           |
| <b>1 INTRODUCTION</b>   | <b>1</b>  |
| 1.1 Global health: Current scenario   | 2         |
| 1.2 Increment of antimicrobial resistance   | 3         |
| 1.3 Antibiotics, antiseptics and disinfectant   | 5         |
| 1.4 Quaternary Ammonium Salts (QACs)  | 7         |
| 1.4.1 Quaternary ammonium salts as antimicrobial agents   | 9         |
| 1.4.2 Bacteriolytic effect of QACs  | 12        |
| 1.4.3 Relation between QACs and Antimicrobial Resistance  | 13        |
| 1.5 Triazine: Structure, Reactivity and Uses  | 15        |
| <b>2 SCOPE OF THE WORK</b>  | <b>22</b> |
| <b>3 RESULT AND DISCUSSION</b>  | <b>25</b> |
| 3.1 Introduction  | 26        |
| 3.2 Morpholine-based antimicrobial triazine quaternary ammonium salts (TQACs)   | 29        |
| 3.2.1 Development of new sustainable protocol in use of Triazine-Based Dehydro-Condensation Agents for Amide Synthesis                                    | 30        |
| 3.2.2 Preparation of <i>N</i> -(3-morpholinopropyl)alkylamide (MoPALA)  | 32        |
| 3.2.3 Synthesis of 4-butylmorpholine  | 37        |
| 3.2.4 Synthesis of 2,4-dichloro-6-methyl-1,3,5-triazine (MMT)   | 40        |
| 3.2.5 Preparation of 4,4'-(6-chloro-1,3,5-triazine-2,4-diyl)bis(4-(3-alkylamidopropyl)morpholin-4-ium) chloride (MoPALA-CC)                               | 42        |
| 3.2.6 Synthesis of 4,6-bis(4-(3-alkylamidopropyl)morpholino-4-ium)-2-oxo-2 <i>H</i> -1,3,5-triazin-1-ide chloride (MoPALA-MMT)                            | 50        |
| 3.2.7 Synthesis of 4,4'-(6-chloro-1,3,5-triazine-2,4-diyl)bis(4-butylmorpholin-4-ium) chloride (BuMO-CC)  | 56        |
| 3.2.8 Synthesis of 4,6-bis(4-butylmorpholino-4-ium)-2-oxo-2 <i>H</i> -1,3,5-triazin-1-ide chloride (BuMO-MMT)   | 59        |
| 3.3 Imidazole-based antimicrobial triazine quaternary ammonium salts (TQACs)  | 63        |
| 3.3.1 Synthesis of 4,6-dichloro- <i>N</i> -alkyl-1,3,5-triazin-2-amine (MAT)  | 64        |
| 3.3.2 Synthesis of 1-methyl-[4,4'-bipyridin]-1-ium iodide (MBP)   | 69        |
| 3.3.3 Synthesis of 3,3'-(6-(alkylamino)-1,3,5-triazine-2,4-diyl)bis(1-methyl-1 <i>H</i> -imidazol-3-ium) chloride (MATdMIMI)                              | 71        |
| 3.3.4 Synthesis of 3-(4-chloro-6-(dodecylamino)-1,3,5-triazin-2-yl)-1-methyl-1 <i>H</i> -imidazol-3-ium chloride (MAT <sub>12</sub> mMIMI)                | 79        |
| 3.3.5 Synthesis of 1',1''-(6-(dodecylamino)-1,3,5-triazine-2,4-diyl)bis(1-methyl-[4,4'-bipyridine]-1,1'-dium) dichloride diiodide (MAT <sub>12</sub> MBP) | 83        |
| 3.4 TQACs biological test and antimicrobial evaluation  | 86        |
| 3.4.1 Evaluation of MoPALA-CC, MoPALA-MMT, BuMO-CC and BuMO-MMT TQACs   | 87        |
| 3.4.2 Evaluation of MATdMIMI TQACs  | 89        |
| 3.4.3 Evaluation of MAT <sub>12</sub> mMIMI and MAT <sub>12</sub> MBP   | 93        |
| <b>4 CONCLUSIONS</b>  | <b>95</b> |
| <b>5 EXPERIMENTAL SECTION</b>   | <b>97</b> |
| 5.1 Methods and instrumentation   | 98        |
| 5.2 Reagents and solvents   | 99        |



|  |  |     |
|--|--|-----|
| 5.3  | Synthesis of precursors and substituted chloro triazine  | 100 |
| 5.3.1  | Synthesis of 2,4-dichloro-6-methoxy-1,3,5-triazine (MMT)   | 100 |
| 5.3.2  | Synthesis of <i>N</i> -(3-morpholinopropyl) dodecanamide (via Dean-Stark)  | 101 |
| 5.3.3  | Synthesis of <i>N</i> -(3-morpholinopropyl) dodecylamide via CDMT/NMM system   | 102 |
| 5.3.4  | Synthesis of <i>N</i> -(3-morpholinopropyl) alkylamide via DMTMM (MoPALA)  | 103 |
| 5.3.5  | Synthesis of 4-butylmorpholine   | 107 |
| 5.3.6  | Synthesis of 1,3,5-triazin-2-alkylamine  | 108 |
| 5.3.7  | Synthesis of 1-methyl-[4,4'bipyridin] iodide (MBP)   | 113 |
| 5.4  | Synthesis of triazinyl quaternary ammonium salts   | 114 |
| 5.4.1  | Synthesis of 4,4'-(6-chloro-1,3,5-triazine-2,4-diyl)bis(4-(3-alkylamidopropyl) morpholin-4-ium) chloride MoPALA-CC   | 114 |
| 5.4.2  | Synthesis of 4,4'-(6-chloro-1,3,5-triazine-2,4-diyl)bis(4-(3-alkylamidopropyl) morpholin-4-ium) chloride (MoPALA-MMT)  | 118 |
| 5.4.3  | Synthesis of 4-butyl-4-(4,6-dichloro-1,3,5-triazin-2-yl)morpholin-4-ium chloride   | 122 |
| 5.4.4  | Synthesis of 4,6-bis(4-butylmorpholino-4-ium)-2-oxo-2 <i>H</i> -1,3,5-triazin-1-ide chloride   | 123 |
| 5.4.5  | Synthesis of 3,3'-(6-(alkylamino)-1,3,5-triazin)bis(1-methyl-1 <i>H</i> -imidazol-3-ium) chloride (MATdMIMI)   | 124 |
| 5.4.6  | Synthesis of 3-(4-chloro-6-(dodecylamino)-1,3,5-triazin-2-yl)-1-methyl-1 <i>H</i> -imidazol-3-ium chloride (MAT <sub>12</sub> mMIMI)   | 129 |
| 5.4.7  | Synthesis of 1'.1''-(6-(dodecylamino-1,3,5-triazin-2,4,-diyl)bis(1-methyl-[4,4'-bipyridin]-1,1'-io) salt (MAT <sub>12</sub> dMBP)  | 130 |
| 5.5  | Biological assays  | 131 |
| 5.6  | Determination of critical micelle concentration  | 132 |
| 5.7  | LogP calculation method  | 133 |
| <b>6 REFERENCES</b>  |  | 134 |
| <b>POLYMERIC QACS SYNTHESIS AND THEIR SURFACE ADHESION TREATMENT</b> |  | 148 |
| <b>7 INTRODUCTION</b>  |  | 149 |
| 7.1  | Biofilm  | 150 |
| 7.2  | New Challenge in infectious diseases   | 152 |
| 7.3  | Active surfaces for biofilm formation prevention   | 153 |
| 7.4  | Contact-killing surfaces containing quaternary ammonium salts  | 155 |
| 7.4.1  | Surface containing quaternary ammonium polymers  | 155 |
| 7.5  | Surface grafting techniques  | 157 |
| 7.6  | Reversible-deactivation radical polymerization   | 159 |
| 7.6.1  | Atom transfer radical polymerization (ATRP)  | 160 |
| <b>8 SCOPE OF THE WORK</b>   |  | 162 |
| <b>9 RESULT AND DISCUSSION</b>                                       |  | 164 |
| 9.1  | Introduction   | 165 |
| 9.2  | Atom transfer radical polymerization (ATRP) polymers synthesis and characterization  | 166 |
| 9.2.1  | Synthesis of poly-2- <i>N</i> -morpholinoethyl methacrylate (PMEMA)  | 168 |
| 9.2.2  | Synthesis of polystyrene- <i>b</i> -poly-2- <i>N</i> -morpholinoethyl methacrylate diblock copolymers (PS- <i>b</i> -PMEMA)  | 169 |
| 9.2.3  | Synthesis of polystyrene- <i>b</i> -[poly-2- <i>N</i> -morpholinoethyl methacrylate-co-polymethyl methacrylate] diblock copolymer (PS- <i>b</i> -(PMEMA-co-PMMA))  | 173 |
| 9.2.4  | Synthesis of polystyrene- <i>b</i> -poly-2- <i>N</i> -morpholinoethyl methacrylate- <i>b</i> -polystyrene triblock copolymers (PS- <i>b</i> -PMEMA- <i>b</i> -PS) and polystyrene- <i>b</i> -[poly-2- <i>N</i> -morpholinoethyl methacrylate-co-polymethyl methacrylate]- <i>b</i> -polystyrene triblock copolymer (PS- <i>b</i> -(PMEMA-co-PMMA)- <i>b</i> -PS) | 175 |

|                                |   |     |
|--------------------------------|---|-----|
| 9.3                            | Synthesis of polymeric TQACs  | 177 |
| 9.4                            | Polypropylene film surface modification with (PS- <i>b</i> -(PMAT <sub>12</sub> MEMA- <i>co</i> -PMMA)- <i>b</i> -PS) triblock copolymer  | 181 |
| 9.5                            | Polypropylene modified surface antibiofilm evaluation   | 183 |
| <b>10 CONCLUSIONS</b>          |   | 185 |
| <b>11 EXPERIMENTAL SECTION</b> |   | 187 |
| 11.1                           | Methods and instrumentation   | 188 |
| 11.2                           | Reagents and solvents used  | 188 |
| 11.3                           | Atom transfer radical polymerization (ATRP) polymers synthesis and characterization   | 189 |
| 11.3.1                         | Synthesis of poly-2- <i>N</i> -morpholinoethyl methacrylate (PMEMA)   | 191 |
| 11.3.2                         | Synthesis of polystyrene (PS)   | 193 |
| 11.3.3                         | Synthesis of polystyrene- <i>b</i> -[poly-2- <i>N</i> -morpholinoethyl methacrylate] diblockcopolymer (PS- <i>b</i> -(PMEMA))   | 194 |
| 11.3.4                         | Synthesis of polystyrene- <i>b</i> -[poly-2- <i>N</i> -morpholinoethyl methacrylate- <i>co</i> -polymethylmetacrilate] diblockcopolymer (PS- <i>b</i> -(PMEMA- <i>co</i> -PMMA))  | 196 |
| 11.3.5                         | Synthesis of polystyrene- <i>b</i> -[poly-2- <i>N</i> -morpholinoethyl methacrylate]- <i>b</i> -polystyrene triblockcopolymer (PS- <i>b</i> -PMEMA- <i>b</i> -PS)   | 197 |
| 11.3.6                         | Synthesis of polystyrene- <i>b</i> -[poly-2- <i>N</i> -morpholinoethyl methacrylate- <i>co</i> -polymethylmetacrilate]- <i>b</i> -polystyrene triblockcopolymer (PS- <i>b</i> -(PMEMA- <i>co</i> -PMMA)- <i>b</i> -PS)  | 198 |
| 11.4                           | Synthesis of polystyrene- <i>b</i> -[4-(4-chloro-6-(dodecylamino)-1,3,5-triazin-2-yl)-4-(2-methacrylamidoethyl) morpholin-4-ium chloride- <i>co</i> -polymethyl metacrilate]- <i>b</i> -polystyrene triblock copolymer (PS- <i>b</i> -(PMAT <sub>12</sub> MEMA- <i>co</i> -PMMA)- <i>b</i> -PS) | 199 |
| 11.5                           | Polypropylene film surface modification with (PS- <i>b</i> -(PMAT <sub>12</sub> MEMA- <i>co</i> -PMMA)- <i>b</i> -PS) triblockcopolymer   | 200 |
| 11.6                           | Biofilm formation inhibition assay on surfaces  | 201 |
| <b>12 REFERENCES</b>           |   | 202 |
| <b>ACKNOWLEDGEMENTS</b>        |   | 213 |

# **SYNTHESIS OF NEW ANTIMICROBIAL TRIAZINE- BASED QUATERNARY AMMONIUM SALTS**

# **CHAPTER 1**

## **INTRODUCTION**

**Synthesis of new antimicrobial triazine-based quaternary ammonium salts**

## 1.1 Global health: Current scenario

High life expectancy in our modern society is in part correlated to our capacity to prevent pathogens spread. The last 200 years of our history have been the cradle of great innovations generating better control of infectious diseases, improvement of food preservation and safety, drastic advancement of sanitary conditions and multiple social improvements.<sup>[1]</sup>

In fact, we must not forget how the world was before the invention of penicillin discovered thanks to the observations of Alexander Fleming.<sup>[2]</sup> Before that, diseases such as pneumonia or small infections due to harmless scratches could lead to death for septicemia. After the discovery of antibiotics or more generally of antimicrobials, there has been a drastic increase in the control of infectious diseases, managing to reduce the mortality rate both in humans and animals, contributing to the progress of public health and improving life expectancy (Figure 1.1).

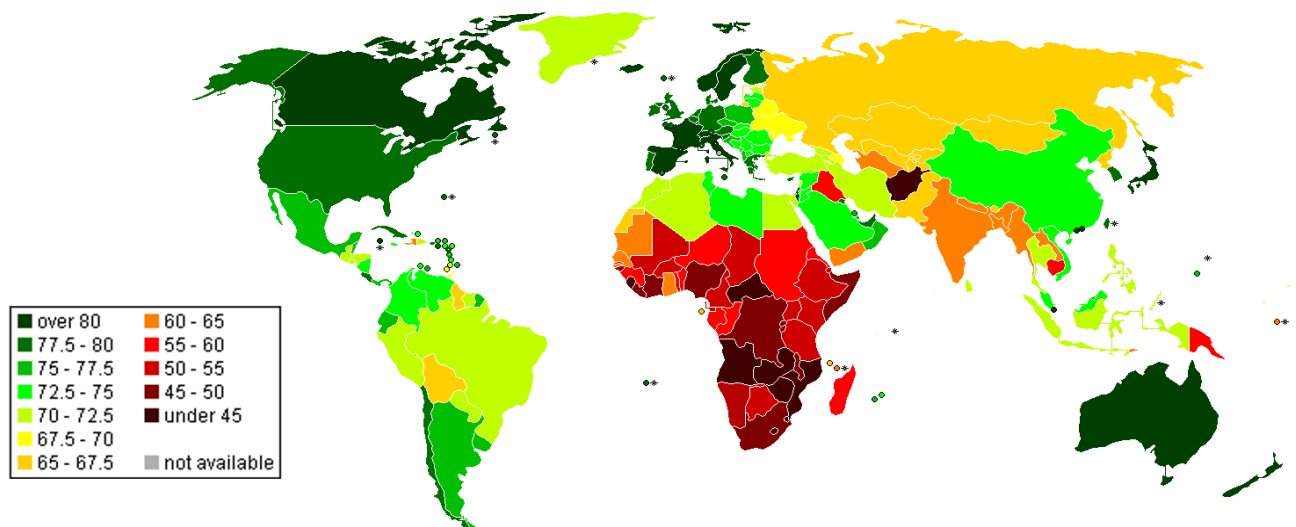


**Figure 1.1** - World map of Life expectancy at birth (years) 2005-2010<sup>[3]</sup>

In particular, a modern society is marked by a massive use of disinfection techniques, with a special attention in disinfection of sensible material like medical devices, drugs, surgical equipment, dental restorations and bone cements.<sup>[4]</sup> From physical sterilization technique that use heat, light or mechanical stress like cavitation to kill or inhibit microorganisms<sup>[5]</sup>, to chemical substances like disinfecting detergents, oxidation agents and antimicrobial drugs.<sup>[6]</sup>

This class of compounds, in particular, has gained increasing attention in the last decades, because they are broad spectrum molecules, acting against infections caused by bacteria, viruses, fungi and parasites.

## 1.2 Increment of antimicrobial resistance

Antimicrobial resistance (AMR) is a phenomenon that occurs when microorganisms (for example a bacterium) survive after the exposure to an agent, which would usually cause their death or inhibit reproduction and growth. This natural process of evolution and consequent resistance of microorganisms was discovered after the diffusion of the first antibiotics.<sup>[7]</sup> Historically bacteria have become increasingly resistant to adverse conditions of nature carrying in their genes the information of survive to substances capable of causing damage. This defense mechanism is obviously a resilient behavior that microorganisms implement in order to preserve the species, and in some cases allowing them to survive even when exposed to a particular drug.<sup>[8-10]</sup>

This inevitably leads to the emergence of new super-resistant species such as, for example, the well-known methicillin-resistant *Staphylococcus aureus* (MRSA) or drug-resistant Tuberculosis that are difficult or impossible to treat with existing drugs. The indiscriminate and excessive use of antimicrobials has increased the rate of development of bacterial resistant species increasing the need for new drugs and their responsible use.<sup>[11,12]</sup>

Disease is the antithesis of health and antimicrobial resistance is increasingly becoming a problem, so that humanity is facing a growing enemy with a largely ineffective strategy. Previously, these resistant microorganisms developed primarily in hospital settings, but with the widespread dissemination of drugs and other antimicrobial substances, resistant infections have also been found outside of hospital settings.<sup>[13-16]</sup> With the rise of resistance, our advantage of treatment and prevention against infections that had accumulated over the past 100 years is decreasing, according to some estimates it is expected that by 2050 the number of deaths caused but resistant bacterial strains will rise over 10 million (figure 1.2). In 2014, the

World Health Organization (WHO) drafted a report on the global surveillance of antimicrobial resistance speculating that the world is heading into an era where diseases that would not constitute a health hazard today may become difficult to treat with modern medical treatment. WHO then issued a warning to the scientific communities to make a concerted effort to stop the diffusion of antibiotic-resistant microorganisms.<sup>[17]</sup> In addition, during 2016 Jim O’Neill has drawn a report<sup>[18]</sup> on drug-resistance pathogens in which he summarized a ten-points action program to fight AMR and prevent their onset. These points include: improvement of sanitation, reduction of unnecessary use of antimicrobials, promotion of new and rapid diagnostics, promotion of development and use of vaccines, promotion of investment for new drugs and improving existing ones. This attention to the phenomenon is a clear indication of how serious the issue is.

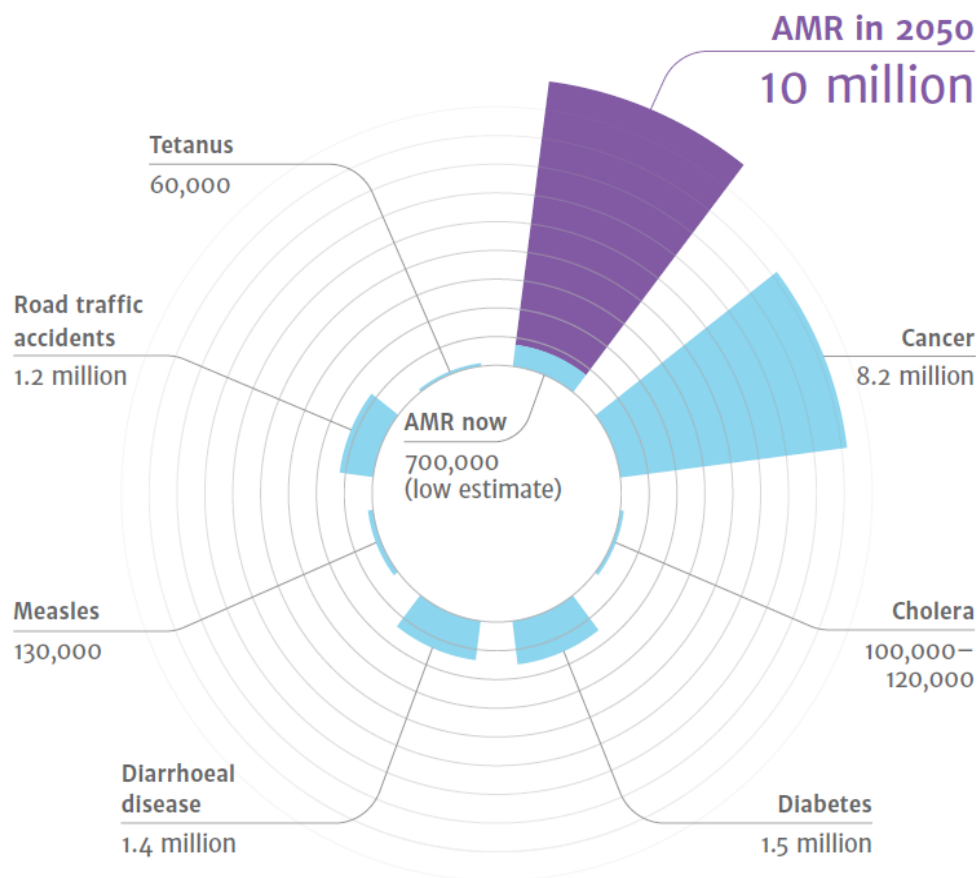


**Figure 1.2** – Numbers of death attributable to various disease in comparison to AMR nowadays and a prediction for 2050.<sup>[18]</sup>

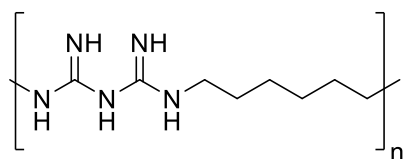
### 1.3 Antibiotics, antiseptics and disinfectant

As mentioned above, prevention is essential nowadays, and it is done through immunization and diagnosis as well as hygiene and disinfection practices. There are several techniques of disinfection and eradication of infections; they can be divided into those that use physical methods such as sterilization in autoclave or ionizing radiation<sup>[19,20]</sup> and those more widespread using chemical substances.<sup>[19,21]</sup>

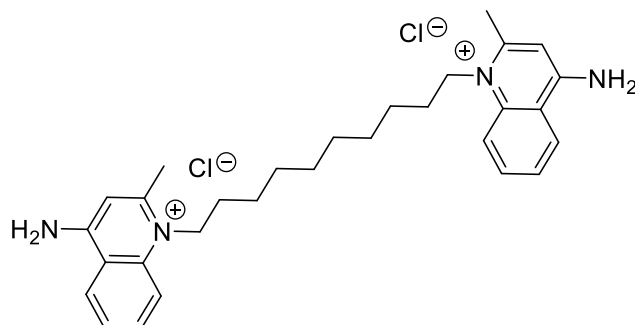
The latter may be divided into three categories according the field of application:

- Disinfectants: they are a type of chemical agents that act on inert surfaces by destroying or inactivating microorganisms or viruses. Not always these substances are able to kill all microorganisms, some of the most resistant ones such as spores are able to resist. Although this makes them less effective in treatment than physical methods, chemical methods however are extremely easier to apply and above all can be used in extremely different contexts. This class includes, for example, alcohols,<sup>[22]</sup> aldehydes,<sup>[23]</sup> oxidizing substances such as ozone,<sup>[24]</sup> sodium hypochlorite,<sup>[25]</sup> hydrogen peroxide,<sup>[26]</sup> and quaternary ammonium salts.<sup>[27]</sup>
- Antiseptics: these are antimicrobial substances used to reduce infection and sepsis on tissue and skin, some of which may be normal disinfectants (alcohol, quaternary ammonium salts), while others act as true germicides such as bis-guanidine compounds such as chlorhexidine<sup>[28]</sup> and polyhexanide<sup>[29]</sup> or quinolines such as hydroxyquinoline,<sup>[30]</sup> dequalinium chloride,<sup>[31]</sup> or chlorquinaldol<sup>[32]</sup> (Figure 1.3).
- Antibiotics: probably the most important type of antimicrobial substance available, which act within the body to eradicate bacterial infections that cause illness or disease. Antibiotics can kill or inhibit bacterial growth even in extremely low doses and are used exclusively for medical purposes. Initially discovered as natural substances like penicillin<sup>[2]</sup> secreted by molds or other microorganisms, they have evolved into synthetic surrogates such as sulfonamides<sup>[33]</sup> like Sulfamethoxazol and Sulfanilamide (figure 1.3).<sup>[34]</sup>

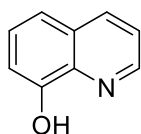




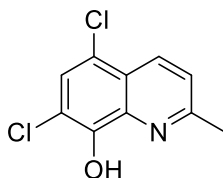
Polyhexanide



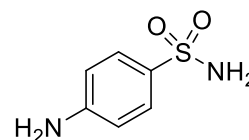
Dequalinium chloride



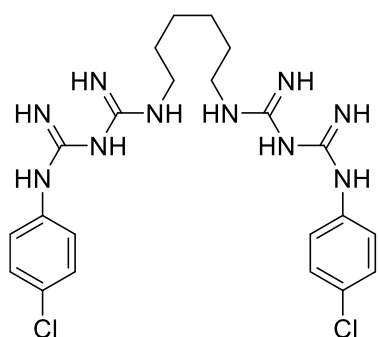
Hydroxyquinoline



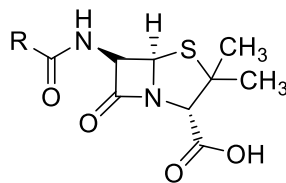
Chlorquinaldol



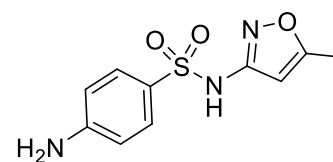
Sulfanilamide



Chlorhexidine



Penicillin



Sulfamethoxazole

**Figure 1.3** – Structure of Polyhexanide, Dequalinium chloride, Hydroxyquinoline, Chlorquinaldol, Chlorhexidine (antiseptic), Penicillin Sulfanilamide and Sulfamethoxazole (antibiotics)

## 1.4 Quaternary Ammonium Salts (QACs)

Chemically speaking, quaternary ammonium salts (QACs) (Figure 1.4) are molecules having the brute formula  $R_4N^+$ , in which a nitrogen atom is covalently bonded to four alkyl/aryl groups or three alkyl/aryl group in which one is double-bonded to nitrogen. The positive charge on

nitrogen is balanced by a counter ion, typically  $\text{Cl}^-$  or  $\text{Br}^-$ , alternatively  $\text{BF}_4^-$  or  $\text{ClO}_4^-$ <sup>[35,36]</sup> or others. They possess good stability and, contrary to amines (primary, secondary, tertiary), QACs have a lower basicity and therefore cannot be protonated.<sup>[37]</sup>

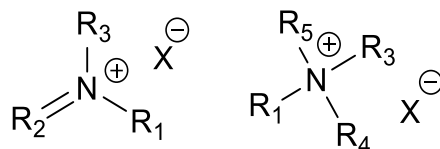
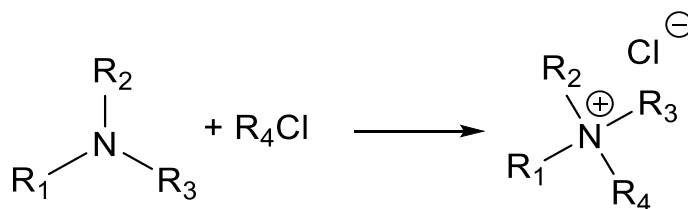


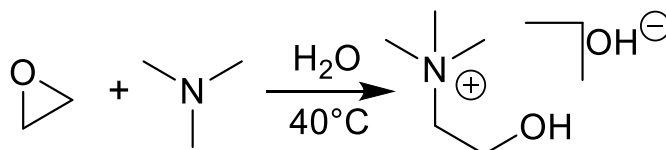
**Figure 1.4** - General structure of quaternary amines

Historically, quaternary ammonium salts have been prepared by reacting a tertiary amine with an alkyl halide, commonly alkyl bromide or chloride. This reaction, called the Menshutkin reaction, dating back to 1890<sup>[38]</sup> and is generally referred to as quaternarization reaction (Scheme 1.1).



**Scheme 1.1** – Quaternarization reaction

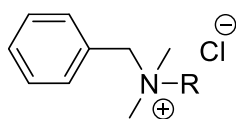
Alternatively, these salts can be synthesized via epoxide. For example, trimethylcholine may be synthesized by reaction of a tertiary amine (trimethylamine) in the presence of ethylene oxide (Scheme 1.2).<sup>[39]</sup>



**Scheme 1.2** – Synthesis of trimethylcholine

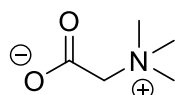
In the literature, QACs with amphiphilic characteristics are also referred to as ammonium surfactants or QAS. Generally, QACs possess a hydrophilic group (head) due to the positive charge of the quaternary nitrogen and a hydrophobic group (tail) formed by a long alkyl chain or an aromatic group. This type of structure provides these compounds with a number of useful properties for a variety of different applications, such as for example (Figure 1.8):

- Disinfectants (Benzalkonium chloride)<sup>[40]</sup>
- Cationic<sup>[41]</sup> or amphoteric<sup>[42]</sup> (betaines such as N,N,N-trimethylglycine) surfactants
- Softeners (Quaternium-52)<sup>[43]</sup>
- Alkylating agents (Chlorocholine chloride)<sup>[44]</sup>
- Dyes (Malachite green, Crystal violet)<sup>[45]</sup>

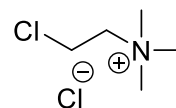


R = C<sub>8</sub>H<sub>17</sub>...C<sub>18</sub>H<sub>37</sub>

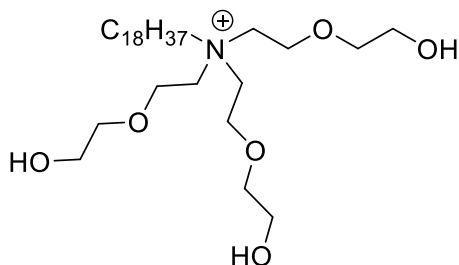
Benzalkonium chloride



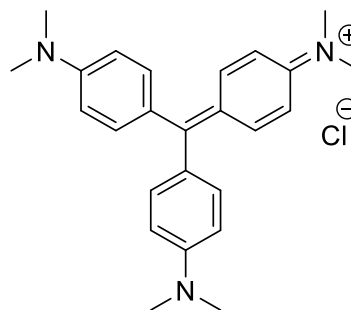
Trimethylglycine



Chlorocholine chloride



Quaternium-52



Christal Violet

**Figure 1.8** – Some examples of commercially available QACs

### 1.4.1 Quaternary ammonium salts as antimicrobial agents

The first uses of QACs as antiseptics or disinfectants were carried out by Dogmak<sup>[46]</sup> who had already discovered sulphonamides a few years earlier.<sup>[47]</sup> At that time, QACs were a real revolution especially for tissue disinfection. Today it is estimated that the use of QACs is around 500.000 tons per year.<sup>[48]</sup> Their biocidal action is due to their ability to destroy the cell membrane, for this reason their action is similar to antimicrobial peptides exploited by animals in animal kingdom.<sup>[49-51]</sup> QACs are potential candidates to combat antibiotic resistance, with a broad spectrum of activity.<sup>[52]</sup> They result lethal to a wide variety of microorganisms, including Gram-positive and Gram-negative bacteria (figure 1.9), fungi, yeast, and some viruses.<sup>[53-56]</sup>

The factors which regulate the antimicrobial effect are multiple.<sup>[57]</sup> It has been demonstrated that in many occasions the length of the alkyl side chain is relevant in determining the activity of QACs,<sup>[58-61]</sup> additionally, also molecular weight in the case of polymeric QACs has great influence on its efficacy.<sup>[57]</sup> For many bacterial species, the optimal length of the alkyl chain present on QACs varies from 14 carbon units for Gram-positive bacteria to 16 units for Gram-negative bacteria, a 12-unit chain is often more effective for fungi and yeast.<sup>[62,63]</sup>

A correlation between antimicrobial activity and the rigidity of the QACs structure was also investigated, revealing that, although with slight difference, less rigid structures are more effective.<sup>[64,65]</sup> Regarding the effect of the counter anion there seems to be conflicting opinions among researchers. Some state that the counter anion has a marked effect on the efficacy and selectivity;<sup>[66-69]</sup> for examples according to the work by Panarin and Mizerska, the efficacy of some dendrimeric QACs depends significantly on the counterion. In particular it seems that the compound with bromide anions is more effective than the compound with chloride anions.<sup>[70,71]</sup> However, other studies state that counterions do not affect antimicrobial activity at all.<sup>[72,73]</sup> It is therefore clear that trying to predict the correlation between the structure of a QACs and its antimicrobial action is quite difficult. Although there are some generic rules such as chain length that govern their antimicrobial character others such as counter ion seem to influence in specific cases and not in others.

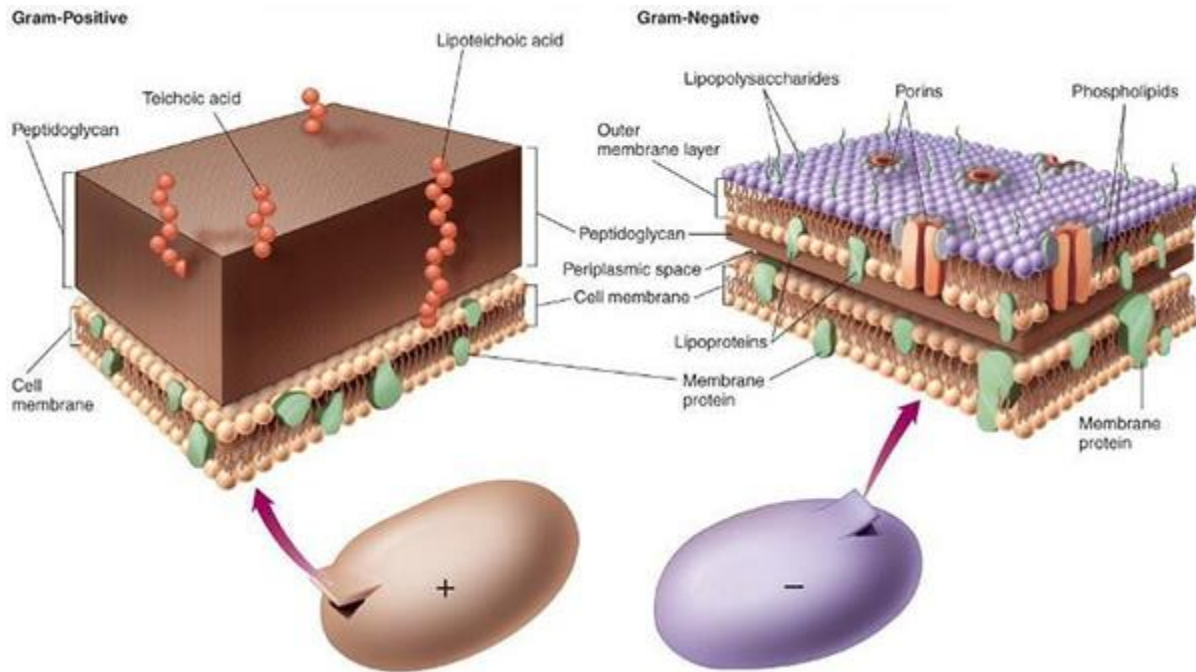


**Figure 1.9** - Different membrane structure of Gram-Negative and Gram-Positive strains

Another characteristic that can vary the antimicrobial activity of QACs is the number of positively charged nitrogen in the molecule. We can differentiate the types of QACs based on the number of permanent positive charges into Mono-QACs, Bis-QACs or Multi-QACs:

- **Mono-QACs:** are ammonium salts containing a single charge; these include Benzalkonium chloride (BAC, Figure 1.10) the most commercially available and most widely used ammonium salt in the world.<sup>[74]</sup> First synthesized in the 30s, it was one of the first QACs to be used as a disinfectant. In 2006, C.J. Ioannou and his research group<sup>[75]</sup> performed studies on the disinfectant action of BAC and DDAC (Didecyl-methyl-ammonium chloride, Figure 1.10) against a bacterial strain of *Staphylococcus aureus*. The authors report that QACs with an alkyl chain containing 12 to 18 carbons can penetrate more easily through the bacterial outer membrane than homologs with a shorter chain, thus being more effective.

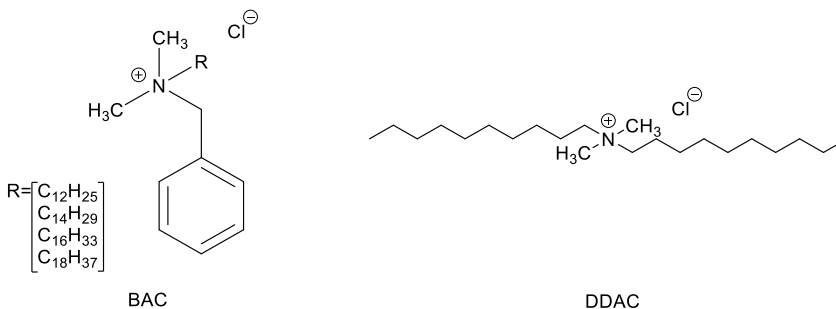


**Figure 1.10** - Benzalkonium Chloride (BAC) and Didecyl-methyl-ammonium chloride (DDAC)

- **Bis-QACs:** based on what has been reported in the literature, these compounds have two permanent positive charges that increase their bactericidal power.<sup>[76]</sup> Furthermore, as reported in experiments by Jennings and colleagues<sup>[77]</sup> bis-QACs show reduced susceptibility to antimicrobial resistance cases. Some examples are reported in Figure 1.11.

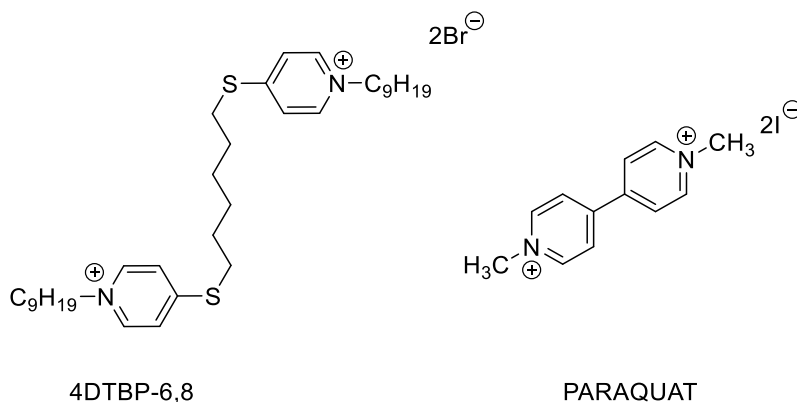


**Figure 1.11** - Exemple of Bis-QAC; 4,4'-(1,6-hexamethylenedithio)bis(1-octylpyridinium bromide) (4DTBP-6,8), 1,1'-Dimethyl-4,4'-bipyridinium diiodide (PARAQUAT)

- **Multi-QACs:** these compounds are characterized by the presence of more than two permanent positive charges. Recently some studies have been performed on this type of compounds demonstrating, however, their lower efficacy as antimicrobials compared to Mono- and Bis-QACs. An example of Multi-QACs is shown in Figure 1.12.<sup>[78]</sup>

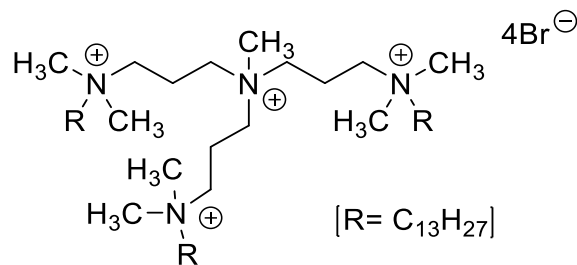


**Figure 1.12** - Example of Tetra-QACs (sT-12,12,12-1)

## 1.4.2 Bacteriolytic effect of QACs

QACs are essentially lytic bioactive agents. In fact, their mode of action involves the disruption of the cytoplasmic membrane composed of a phospholipid bilayer in both Gram-positive and Gram-negative bacteria. This perturbation causes a real lysis in the phospholipid tissue favoring the escape of cytoplasmic material leading to cell death. The interaction between QACs and cell membrane follows 3 steps: (Figure 1.13)<sup>[76]</sup>:

1. Initially, QACs migrate from the bulk solution, by electrostatic interaction, to the surface of the negatively charged cell membrane. In doing so, they carry out a substitution reaction with Mg<sup>2+</sup> ions present on the surface causing them to be released.
2. The hydrophobic tail (alkyl groups) then penetrates in the inner part of the phospholipid bilayer. These interactions increase the surface pressure in the outer layer of the membrane causing it to stiffen and decrease its fluidity. This stiffening promotes a transition of the membrane state from crystalline fluid to liquid losing its osmotic regulatory functions.<sup>[79,80]</sup>
3. In a short time, vesicle-like swellings are formed on the membrane surface. The vesicles gradually swell to the point of rupture, initiating membrane lysis, and eventually, external diffusion of all intracellular material is observed, leading to the death of the bacterium.<sup>[81]</sup>

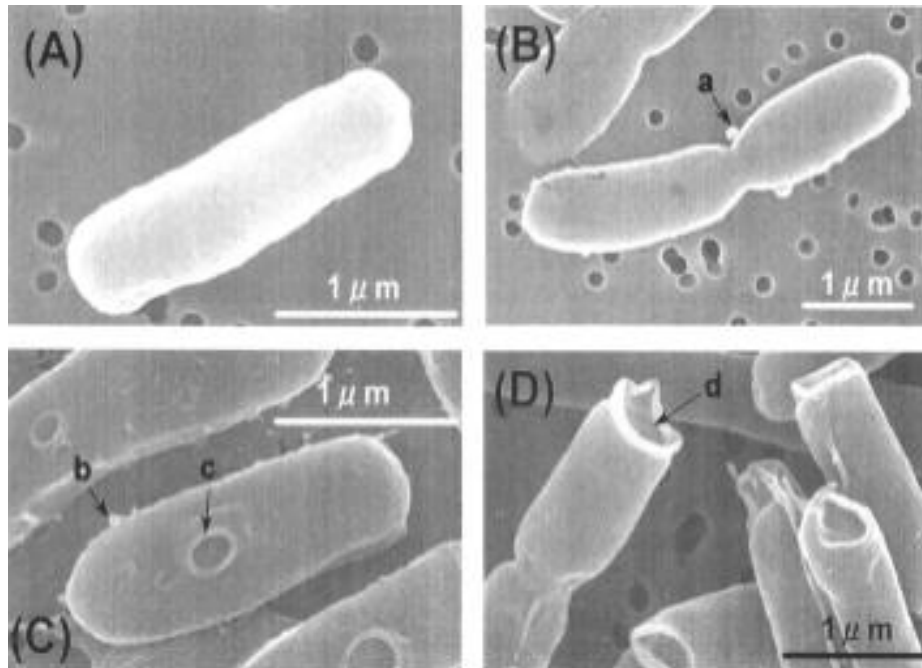


**Figure 1.13** - Box (A): *E. coli* bacteria. Box (B): arrow "a" shows bubble formation. Box (C): arrow "b" shows a vesicle while arrow "c" shows a hole in the cell wall. Box (D): destruction of the surface of the bacterium. <sup>[81]</sup>

### 1.4.3. Relation between QACs and Antimicrobial Resistance

QACs in the present day are ubiquitous, being used in a wide variety of disinfectant formulations for domestic uses, agriculture, cosmetics, and industry.<sup>[82]</sup> Approximately 75% of the QACs used each year are released into wastewater treatment plant, while the rest are discharged directly into the environment.<sup>[83-86]</sup>

This massive use can lead to the selection in the environment of microorganisms that are multi-resistant to many pharmaceuticals through co-resistance mechanisms (Figure 1.14). Compared to antibiotics, QACs possess a profoundly different mechanism of action; antibiotics interact with very specific target sites in the cell, whereas QACs act indiscriminately across the membrane.<sup>[87]</sup> However, both can stimulate the production of reactive oxygen species (ROS) by the cell, which can induce genetic mutations. This can lead to the development of QAC and antibiotic resistance by the cell through mutation of the gene expressing a multidrug efflux pump



by increasing its efficiency<sup>[88]</sup> or through mutation of the target site of the specific antibiotic.<sup>[89,90]</sup> These mutations due to oxidative stress have been shown to generate cross-resistance to many clinically important antibiotics by mutant species resistant to QACs.<sup>[91]</sup>

Another physiological mechanism that microorganisms put in place when they are in an environment having a subinhibitory concentration of QACs is the reduction of the number of porin proteins present on the surface: these proteins are responsible for the intermembrane exchange of substances of various natures. This results in a less permeable membrane, which consequently limits the interaction not only with QACs but also with other antimicrobial substances. As a consequence, the antibiotics themselves become ineffective as they are unable to reach their target sites.<sup>[91,92]</sup>

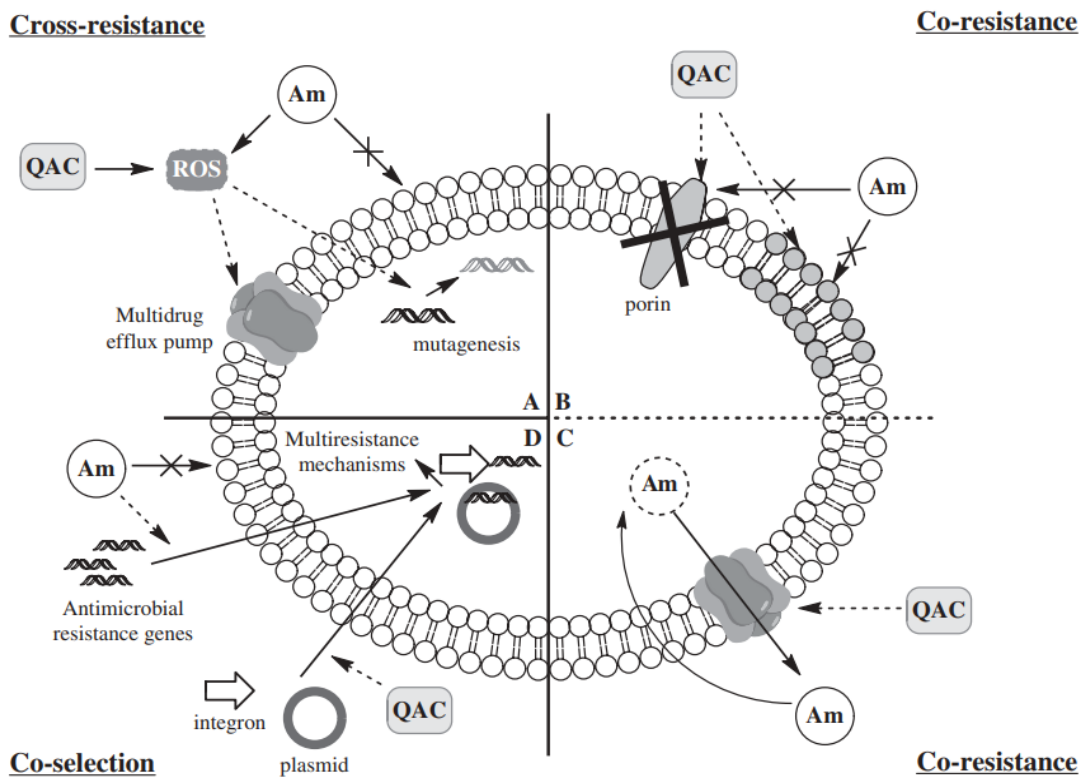


**Figure 1.14** - QAC-induced or selected antibiotic/antimicrobial resistance mechanisms **A)** Cross-resistance: Tolerance by the cell of an antimicrobial agent acquired by a mechanism developed against a different antimicrobial agent having the same mode of action. **B-C)** Co-resistance: Tolerance by the cell of an antimicrobial agent acquired by a mechanism developed against a different antimicrobial agent having a distinct mode of action. **D)** Co-selection: Tolerance by the cell of multiple antimicrobial agents having different modes of action by acquisition of new mobile genetic material (e.g.: plasmids, integrons) during exposure to one of the agents.<sup>[48]</sup>

Finally, QACs can lead to an increase in resistant species by a mechanism called co-selection (figure 1.14). This type of resistance is associated with the acquisition by the cell of plasmids and integrons, which are nothing more than sections of genetic material containing elements that express several characteristics, including that of antibiotic resistance. These genes in particular have been found in high concentrations in water treatment plants, an environment in which the concentrations of QACs are relatively high. This facilitates the acquisition by bacteria of integrons<sup>[93,94]</sup> and allows them to develop resistance to other antimicrobials.<sup>[95]</sup>

## 1.5 Triazine: Structure, Reactivity and Uses

Triazines, or s-triazines, are aromatic heterocyclic compounds, formed by a six-atom ring with alternating carbon and nitrogen. There are three types of ring isomers such as 1,3,5-, 1,2,4-, and 1,2,3-triazines, distinguished by the different position of the carbon atoms, as shown in Figure 1.15.

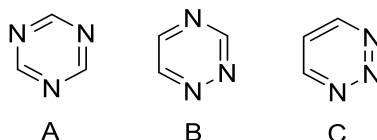
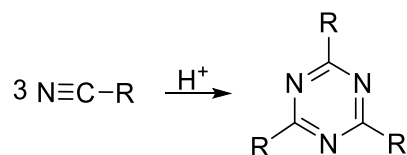


**Figure 1.15** - A. 1,3,5-triazine; B. 1,2,4-triazine; C. 1,2,3-triazine

Specifically, 1,3,5-triazines are prepared by trimerization of various nitriles in the presence of an acid catalyst (Scheme 1.3).<sup>[96]</sup>



**Scheme 1.3** – General synthesis of 1,3,5-triazines.

In fact, they are often used in organic syntheses to replace hydrogen cyanide as a reagent,<sup>[97]</sup>



analytical form by the Hammett equation (Equation 1.1)<sup>[100]</sup> which can be used to calculate the "Hammett sigma", a parameter that quantifies the influence that the presence of a particular substituent has on the reactivity of the molecule.

$$\log \frac{K}{K^{\circ}} = \sigma \rho$$

**Equation 1.1** – Hammett equation that describes a linear free-energy relationship relating reaction rates and equilibrium constants

The reaction mechanism follows a two-stage  $S_N2Ar$  pathway called addition-elimination with second-order kinetics.<sup>[101]</sup> In the first stage of the reaction which is the rate determining step, the nucleophile reacts with the triazine leading to the formation of a resonance-stabilized carbanion (Meisenheimer intermediate), followed by fast elimination of the leaving group (second step) (Figure 1.17).

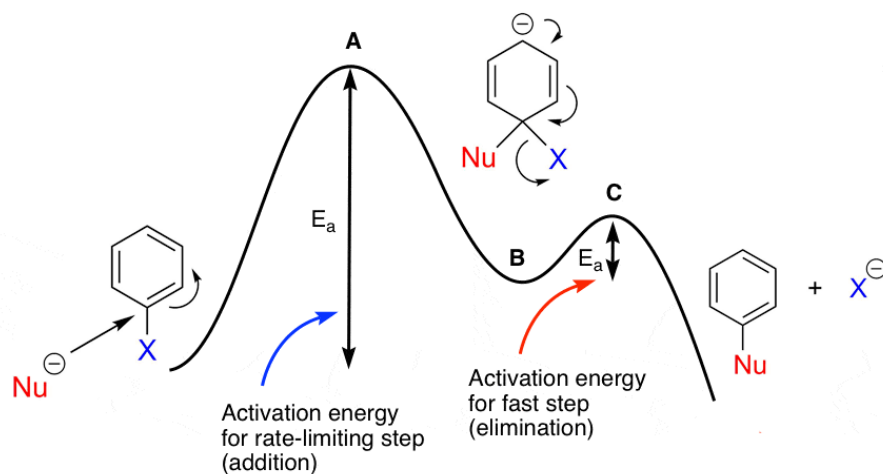


**Figure 1.17** – Kinetic of  $S_N2Ar$  reaction A) transition state for addition, B) intermediate, C) transition state for elimination

Triazines have been conquering several commodity and fine chemical market sectors for several decades now. Some of the most common use of thiazines are:

- Herbizides: perhaps the sector that has been the most successful, the best known of these are compounds such as Atrazine, Simazine and Cyanazine.<sup>[102]</sup> Synthesized for the first time in the 50's with the purpose of eliminating weeds from the train tracks, they found a wide use for water control in marine farms or in agriculture helping considerably the production of maize, sorghum, grapes, asparagus, so that, many companies around the world developed and patented different triazine derivatives for this purpose.<sup>[103-106]</sup>

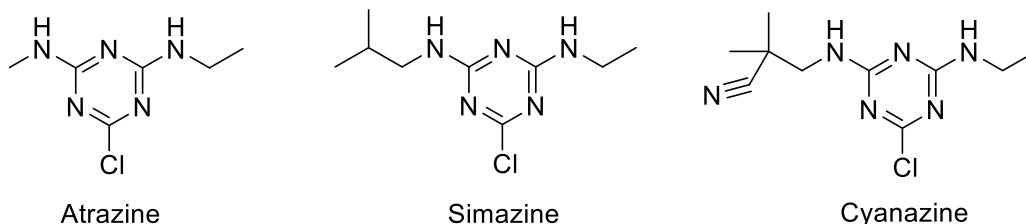


**Figure 1.18** - Herbicides derived from triazine

- Dyes: widely used in textile dyeing as reactive dyes able to covalently attach to fibers such as wool and cotton, the most famous of which is certainly Procion® developed by Imperial Chemical Industries (Figure 1.19). But they are also used in chromatography for the separation of some biological molecules such as proteins and enzymes, famous is the case of Cibacron blue 3GA (Figure 1.19).<sup>[107]</sup>

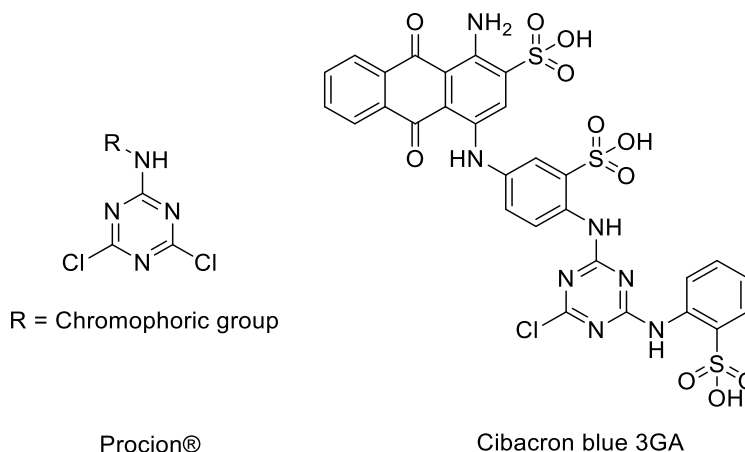
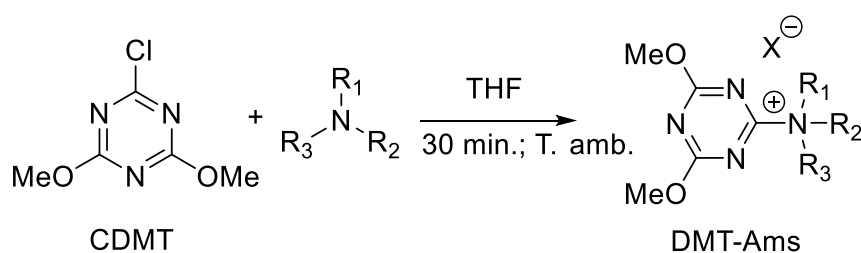


**Figure 1.19** - Structure of Procion® and Cibacron blue 3GA

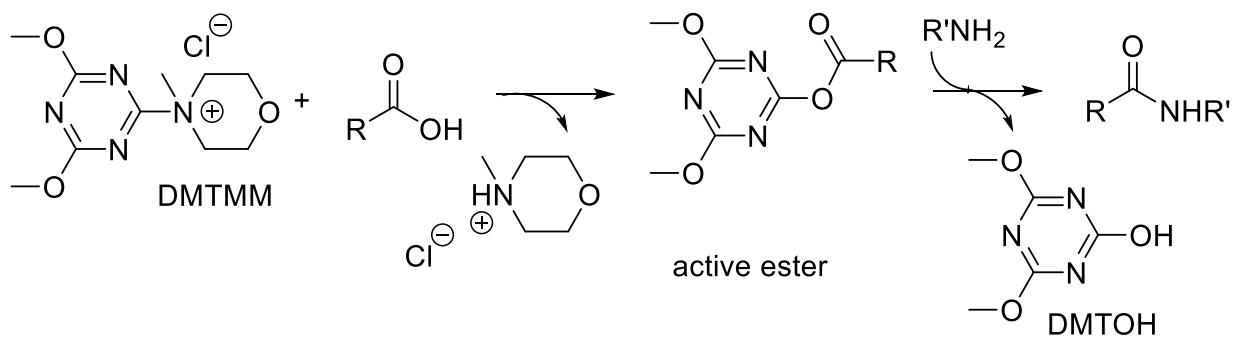
- Condensation agents: Definitely of more recent development than the others,<sup>[108]</sup> this class of triazine compounds in the form of ammonium salts<sup>[36]</sup> (scheme 1.5) are

activators for condensation reactions, used for the synthesis of amides and esters, whose most famous is 4-(4,6-dimethoxy-1,3,5-triazin-2-yl)-4-methyl-morpholinium chloride or DMTMM [109,110]. The advantage of these compounds is in allowing to obtain very good yields in condensation reactions in a short time and at room temperature, this opens the way for many synthesis routes for thermolabile substances that could not be obtained in a classical thermal condensation.<sup>[111]</sup> Remarkable are the applications in the biomedical field for the synthesis of peptides,<sup>[112-114]</sup> synthesis of pharmaceutical substances<sup>[115]</sup> and in leather tanning<sup>[116,117]</sup>.



**Scheme 1.5** - Synthesis of DMT-Ams condensation agents

The reaction mechanism for condensation reactions with DMTMM has been proposed by Kunishima<sup>[118]</sup> (scheme 1.6). In the first step, the nucleophilic substitution reaction of the carboxylic acid on the triazine carbon bounded to the *N*-methylmorpholinium group takes place, resulting in the formation of an active ester and as a co-product leaving group *N*-methylmorpholinium chloride.<sup>[111]</sup> In the second step, the triazine-activated ester species reacts with a nucleophilic group such as an amine or alcohol completing the condensation reaction. Removal of the condensation product from the triazine ring leads to the formation of 2-hydroxy-4,6-dimethoxy-1,3,5-triazine (DMTOH) and *N*-methylmorpholinium chloride as reaction byproducts.



**Scheme 1.6** - Mechanism of activation of carboxylic acids in amidation reaction with DMTMM

## **CHAPTER 2**

### **SCOPE OF THE WORK**

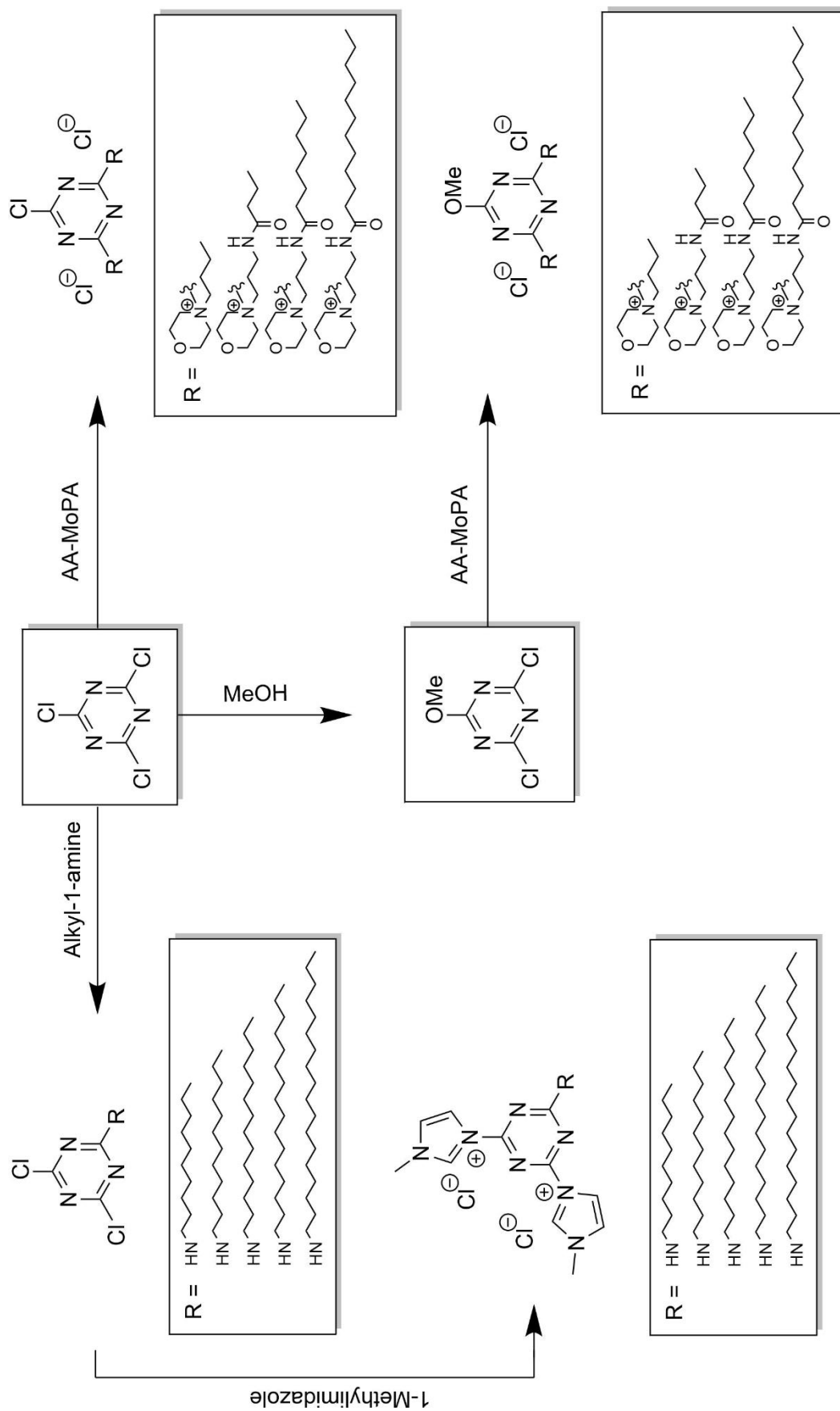
**Synthesis of new antimicrobial-triazine based quaternary ammonium salts**



The PhD project, of which this thesis is the final result, was carried out with the objective of producing a new class of triazine-based quaternary ammonium salts (QACs) that would show antimicrobial characteristics comparable to common disinfectant agents of the same category such as benzalkonium chloride and cetylpyridinium chloride. The advantage of this new class of compounds lies in exploiting the ability of chlorotriazines to form ammonium compounds in a short time and at room temperature adversely to what would be done by a classical quaternization reaction using alkyl halides at high temperature and with more toxic reagents.

The first part of this thesis is dedicated to the synthesis and study of new triazine QACs that have 2,4,6-trichloro-1,3,5-triazine as a common precursor (Figure 2.1). The research group that hosted me in order to perform my PhD has long been interested in the development of sustainable processes and triazine based chemical compounds. In addition, Ca' Foscari University itself has always distinguished for its commitment to technological development that is at the same time environmentally friendly. Therefore, efforts have been made to use mild reaction conditions, such as ambient temperatures/pressures and short reaction times, so that they can be easily applied in the industrial field. The development of more environmentally friendly QAC substitutes, as well as the proper management and healthier handling of QAC-containing waste streams, along with new biotechnologies based on recent discoveries regarding QAC biodegradation, are all promising methods to reduce the release of QACs into an increasingly stressed natural environment.

All the compounds obtained were then tested on different bacterial strains in order to evaluate their antimicrobial power and those with the most promising results in terms of efficacy will be used in the second part of this work to create antimicrobial active surfaces.



**Scheme 2.1** - Synthesis of new antimicrobial-triazine based quaternary ammonium salts

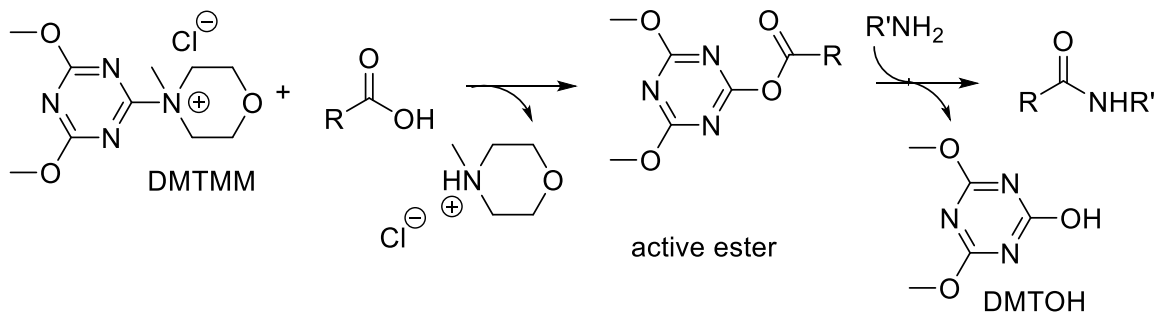
## **CHAPTER 3**

### **RESULT AND DISCUSSION**

**Synthesis of new antimicrobial triazine-based quaternary ammonium salts**

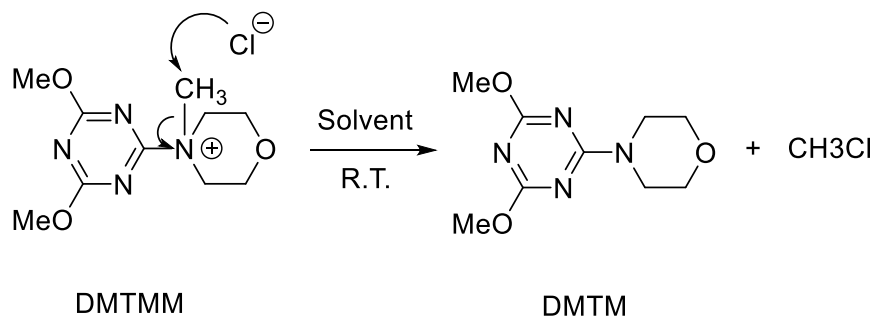
### 3.1 Introduction

To date the only triazines known in literature in the form of quaternary ammonium salts, are those based on 4-(4,6-dimethoxy-1,3,5-triazin-2-yl)-4-methylmorpholinium chloride (DMTMM) and their derivatives as condensation agents<sup>[109,119-121]</sup>. Many works regarding the use of these quaternary ammonium salts as condensation agents have been reported by Kaminsky<sup>[108,112,122,123]</sup> and Kunishima<sup>[36,111,118]</sup>. Main characteristic of these condensation agent is their reactivity, promoting the formation of an active ester species and formation of the amide with consequent decomposition of the condensation agent (scheme 3.1).



**Scheme 3.1** - Mechanism of activation of carboxylic acids in amidation reaction with DMTMM

Additionally, as reported by Kunishima<sup>[111]</sup>, triazine based quaternary ammonium salts are unstable in solution and can dealkylate as reported in scheme 3.2 in a process analogous to the Von Braun reaction<sup>[124]</sup>. Dealkylated product are stable organic compounds totally inactive as condensation agents.



**Scheme 3.2** – Demethylation reaction of DMTMM<sup>[111]</sup>

In fact, in organic solvents the nucleophilic attack by the chloride anion of DMTMM, on the *N*-CH<sub>3</sub> group of the morpholino cation is particularly favored, bringing the formation of chloromethane and 4-(4,6-dimethoxy-1,3,5-triazin-2-yl)-morpholine (DMTM) (scheme 3.2). Specifically, as shown in table 3.1, the decomposition of DMTMM is almost complete after just 3 hours in dichloromethane and chloroform, and decomposition in acetonitrile and dimethyl sulfoxide is also significant in the same period of time. Decomposition is slower in polar protic solvents such as water and alcohols where the chloride ion is better stabilized by the solvent itself.

**Table 3.1** – Stability of DMTMM in several solvent<sup>[111]</sup> [a] Isolate yields. [b] Determined by NMR

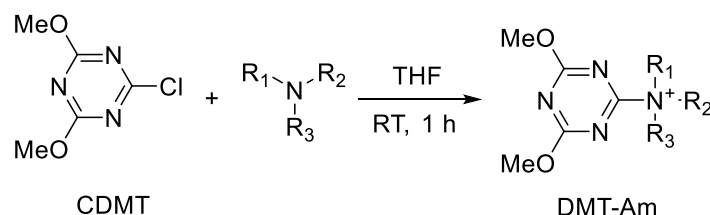
| Solvent                         | Stirring time | DMTMM (recovery) <sup>[a]</sup> | DMTM <sup>[a]</sup> |
|---------------------------------|---------------|---------------------------------|---------------------|
| CH <sub>2</sub> Cl <sub>2</sub> | 3h            | 0%                              | 96%                 |
| CHCl <sub>3</sub>               | 3h            | 11%                             | 83%                 |
| THF                             | 3h            | 95%                             | 2%                  |
| THF                             | 18h           | 85%                             | 13%                 |
| Hexane                          | 3h            | 85%                             | 1%                  |
| Et <sub>2</sub> O               | 3h            | 96%                             | 1%                  |
| AcOEt                           | 3h            | 95%                             | 2%                  |
| DMSO-d <sub>6</sub>             | 3h            | 57% <sup>b</sup>                | 43% <sup>b</sup>    |
| Acetonitrile-d <sub>6</sub>     | 3h            | 38% <sup>b</sup>                | 62% <sup>b</sup>    |
| Methanol-d <sub>6</sub>         | 3h            | 100% <sup>b</sup>               | 0% <sup>b</sup>     |
| D <sub>2</sub> O                | 3h            | 100% <sup>b</sup>               | 0% <sup>b</sup>     |

Reaction Conditions. Substrate: DMTMM, Temperature: 25°C

To achieve the primary goal of the thesis and obtain antimicrobial quaternary ammonium salts derived from triazine ammonium salts it is therefore necessary to stabilize them, and generate stable antimicrobial quaternary ammonium salts.

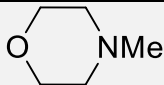
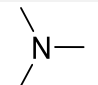
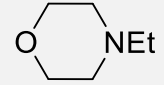
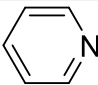
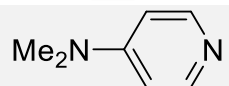
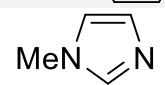
Kunishima further described the synthesis of some quaternary triazine ammonium salts (DMT-Ams) obtained by reaction of 2-chloro-4,6-dimethoxy-1,3,5-triazine (CDMT) with other tertiary amines than *N*-methylmorpholine (scheme 3.3)<sup>[36]</sup>. In his work he reports some examples of condensation reactions of benzoic acid and phenylethylamine, in the presence of different

quaternary ammonium salts obtained by reaction between CDMT and a tertiary amine other than NMM, demonstrating that different reactivity may be achieved changing the *tert*-amine used. Generally, condensation reagents which are highly reactive have low stability in solution (table 3.3).



**Scheme 3.3** – Preparation of DMT-Ams

**Table 3.2** – Preparation, stability, and condensation activity of DMT-Ams<sup>[36]</sup>.

| Tertiary amine  | Yield <sup>[a]</sup> | Stability in CH <sub>2</sub> Cl <sub>2</sub> | Yield in condensation reaction <sup>[b]</sup> |
|---|----------------------|--|---|
|  | 96%                  | Demethylation 100%                           | 77%   |
|  | 85%                  | Demethylation 100%                           | 98%   |
|  | 30%                  | Deethylation 62%                             | 58%   |
|  | 32%                  | Recovery 100%                                | 0%  |
|  | 87%                  | Recovery 91%                                 | 0%  |
|  | 69%                  | Recovery 97%                                 | 0%  |

Reaction conditions: [a] in THF at 25 °C, [b] Dehydrocondensation between 3-phenylpropionic acid and phenethylamine with DMT-Am, in THF at 25 °C

As can be seen from data reported in Table 3.2, DMT-Ams that have no decomposition are the more stable and consequently are the least active as condensation agents. The most stable DMT-Ams appear to be those obtained through the reaction of CDMT with aromatic amines. In addition, if we compare the degree of demethylation of DMTMM with the degree of deethylation

of DMTEM, the latter is less susceptible to dealkylation. This fact suggests that a longer alkyl chain group on the quaternary ammonium on a cyclic amine disfavors the decomposition reaction.

### **3.2 Morpholine-based antimicrobial triazine quaternary ammonium salts (TQACs)**

In this section will be discussed the synthesis of long alkyl chain morpholines with variable chain length and then its triazine ammonium salts.

The first class of compounds synthesized in this work for which antimicrobial activity has been evaluated, is represented by morpholine-based TQACs, inspired by DMTMM. Based on the previous paragraph, since the DMT-Ams reported by Kunishima<sup>[36]</sup> with ethyl substituent on morpholine seem to have a lower tendency to dealkylation we tried to synthesize TQACs based on morpholine having long side chains. Several TQACs were prepared using chlorotriazines such as cyanuric chloride (CC) and 2,4-dichloro-6-methoxy-1,3,5-triazine (MMT) in combination with different morpholines with variable chain lengths. These morpholines precursor were obtained via amidation reactions between 3-morpholinopropylamine and variable-length fatty acids. The choice to use fatty acids amidation reaction instead of, for example, using long chain alkyl halides, stems in the extensive experience of our group to carry out condensation reaction at room temperature using DMTMM, in addition we want to pursuit of the goal of the thesis of seeking reaction conditions more sustainable as possible, avoiding use of toxic compound like alkyl halides.

The long alkyl chains present in QACs can modulate the antimicrobial properties, as explained in section 1.4. The choice of using long chains was therefore necessary to give to our TQACs an antimicrobial behaviour.

### 3.2.1 Development of new sustainable protocol in use of Triazine-Based Dehydro-Condensation Agents for Amide Synthesis

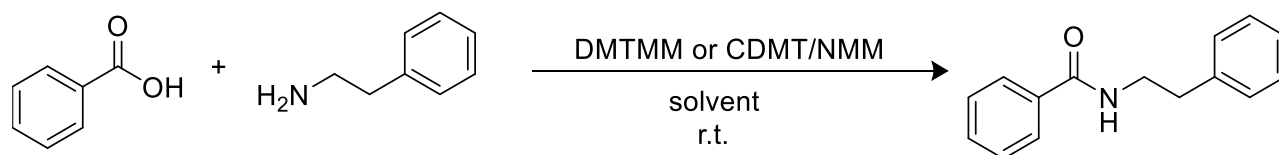
The study of innovative and sustainable processes for the production of fine chemicals has long characterized our research group<sup>[125-128]</sup>. Recently, our efforts have focused on the development of new condensation agents<sup>[120]</sup>. Among the goals of this thesis work there is sustainability, seeking processes that use non-toxic reagents and operating conditions that involve less energy waste and fewer steps between synthesis and work up.

In anticipation of the synthesis of a large library of morpholino-amides in which DMTMM will be used as a dehydro-condensation agent, we investigated the use of an alternative protocol that does not involve the use of DMTMM as preformed compound. In fact, according to the procedure reported in the literature the preparation of DMTMM is carried out by reaction with an equivalent of 2-chloro-4,6-dimethoxy-1,3,5-triazine (CDMT) and 1.2 equivalents of *N*-methyl morpholine (NMM) in THF at room temperature for 1 hr.

The goal is to avoid the DMTMM synthesis step, reducing the complexity of the production and less use of solvents and work up processes, exploiting a CDMT/NMM system. To the best of our knowledge, no in-depth study has been reported on the advantages derived from the use of different CDMT/NMM systems compared to isolated DMTMM.

The activity of CDMT/NMM systems for dehydro-condensation reactions has been compared with the activity of the corresponding isolated DMTMM.

In this paragraph, the CDMT/NMM protocol was investigated by studying the amidation reaction between benzoic acid and phenylethylamine. The procedure involves the dissolution of 1.3 mmoles of benzoic acid in the reaction solvent, followed by the addition (within seconds) of 1.3 mmoles of CDMT, 1.3 mmoles of NMM, and 1.2 mmoles of phenylethylamine (Scheme 3.4).



**Scheme 3.4** - Dehydro-condensation reaction for the synthesis of amide *N*-phenethylbenzamide.



The data obtained from the various tests are shown in Table 3.3. Data from reactions performed in the presence of DMTMM and the CDMT/NMM system were compared. All data shown in Table 3.3 are the average values obtained in triplicate monitored after 15 min and 1 h.

**Table 3.3** Dehydro-condensation reaction between benzoic acid and phenylethylamine by 2-chloro-4,6-dimethoxy-1,3,5-triazine (CDMT)/*N*-methyl morpholine (NMM) system or isolated 4-(4,6-dimethoxy-1,3,5-triazin-2-yl)-4-methylmorpholinium (DMTMM) in different solvents.

| Run | Solvent                         | Coupling Agent | Yield (%) (15/60) min |
|-----|---------------------------------|----------------|-----------------------|
| 1   | THF                             | CDMT/NMM       | 74/78                 |
| 2   | THF                             | DMTMM          | 80/89                 |
| 3   | CH <sub>3</sub> OH              | CDMT/NMM       | 93/95                 |
| 4   | CH <sub>3</sub> OH              | DMTMM          | 98/99                 |
| 5   | EtOH                            | CDMT/NMM       | 92/95                 |
| 6   | EtOH                            | DMTMM          | 98/99                 |
| 7   | CH <sub>3</sub> CN              | CDMT/NMM       | 78/82                 |
| 8   | CH <sub>3</sub> CN              | DMTMM          | 58/66                 |
| 9   | Acetone                         | CDMT/NMM       | 82/83                 |
| 10  | Acetone                         | DMTMM          | 73/97                 |
| 11  | CH <sub>2</sub> Cl <sub>2</sub> | CDMT/NMM       | 86/93                 |
| 12  | CH <sub>2</sub> Cl <sub>2</sub> | DMTMM          | 85/92                 |
| 13  | Toluene                         | CDMT/NMM       | 69/90                 |
| 14  | Toluene                         | DMTMM          | 65/72                 |
| 15  | H <sub>2</sub> O                | CDMT/NMM       | 45/52 <sup>(c)</sup>  |
| 16  | H <sub>2</sub> O                | DMTMM          | 49/53 <sup>(c)</sup>  |

Reaction conditions: benzoic acid: 1.3 mmol, phenylethylamine: 1.2 mmol, Solvent: 6 mL, T: 25 °C. [a] Coupling agent: 1.3 mmol of CDMT and 1.3 mmol of NMM were added; for isolated DMTMM, 1.3 mmol were used. [b] Yield of *N*-phenethylbenzamide was measured by GLC using mesitylene as internal standard. [c] Yields were measured on weight of *N*-phenethylbenzamide recovered after workup.

Interestingly, after 15 min, the CDMT/NMM system, in most of the organic solvents used, has equivalent or even better yields than DMTMM. In CH<sub>3</sub>OH and EtOH, near quantitative yields of

*N*-phenethylbenzamide were measured with both DMTMM (98%) and CDMT/NMM (93%) within 15 min (run 3-6, Table 3.3).

The CDMT/NMM protocol also showed excellent performance in relatively nonpolar solvents. In fact, in toluene as a solvent, CDMT/NMM resulted in a very good yield of *N*-phenethylbenzamide (90%) after 1 h, which was higher than that in the presence of DMTMM (entries 13 and 14, Table 3.3). We also highlight the significantly low yield of *N*-phenethylbenzamide obtained in water as a solvent (run 15 and 16 of Table 3.3), probably due to low water solubility of the starting substrates.

Thus, according to the data shown in Table 3.3, the activity and selectivity of the CDMT/NMM system and the isolated DMTMM were shown to be very similar. The use of alcohols promoted better performance for both dehydro-condensation systems tested.

### 3.2.2 Preparation of *N*-(3-morpholinopropyl)alkylamide (MoPALA)

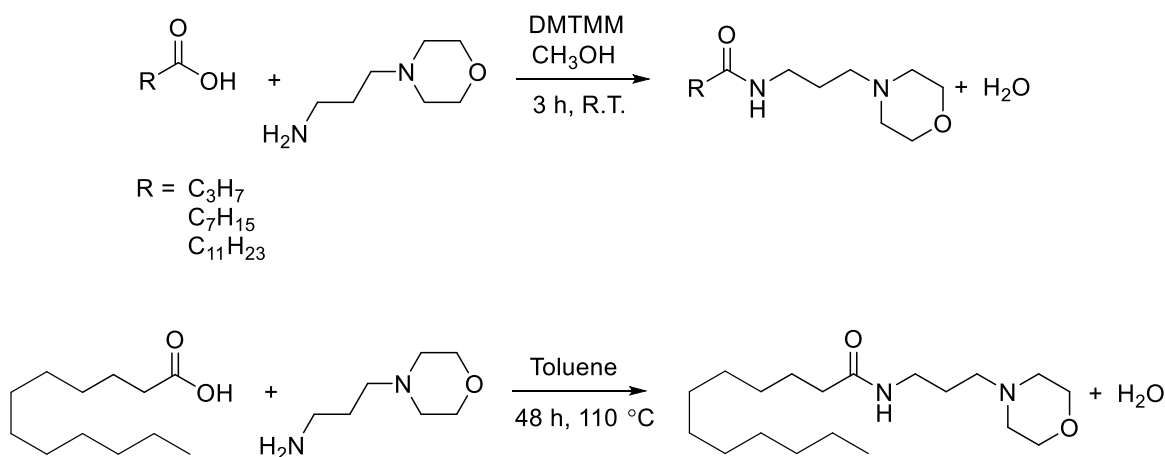
To achieve this, two synthesis approach were compared. A classical dehydro condensation route that exploits heat and water removal with a Dean-Stark trap, and one that exploits DMTMM and CDMT/NMM system as a condensation agent were tested. Several *N*-substituted morpholines were readily prepared by amidation between 3-morpholinopropylamine and several fatty acids of 4, 8 and 12 carbon units respectively (scheme 3.5).

Initially, the synthesis of *N*-(3-morpholinopropyl)dodecylamide (MoPALA<sub>12</sub>) was investigated as standard reaction to verify which of the two methodologies above reported was more efficient.

The classical amidation reaction with Dean-Stark trap was carried out in toluene at reflux. Toluene was chosen as a solvent since it has a higher boiling temperature and a lower density than water. This makes it easy to remove water from the reaction environment and accumulate it in the Dean-Stark trap. The reaction was followed by gas chromatography, and 66% conversion in *N*-(3-morpholinopropyl)dodecylamide was achieved in 48 hours.

The reaction with DMTMM was carried out in methanol at room temperature. This choice has been based on the results obtained through the amidation tests reported in table 3.3 where the reactions conducted in methanol reported the highest performance both in terms of selectivity and in terms of yield of the final product. Moreover, Kunishima reports that demethylation of DMTMM occurs less in polar solvents such as alcohols<sup>[36]</sup>. The reaction was followed by gas chromatography and 70% conversion in *N*-(3-morpholinopropyl)dodecylamide was achieved in 3 hours using isolate DMTMM, and 55% conversion in CDMT/NMM system.

Thus isolate DMTMM protocol was chosen for the synthesis of *N*-(3-morpholinopropyl)octylamide (MoPALA<sub>8</sub>) and *N*-(3-morpholinopropyl)butylamide (MoPALA<sub>4</sub>).



**Scheme 3.5** – Synthesis of different *N*-(3-morpholinopropyl)alkylamide

Isolation of end products was achieved by removal of DMTMM reaction residues by basic washing (see experimental part). The final yields obtained were 60% MoPALA<sub>4</sub>, 62% for MoPALA<sub>8</sub>, and 52% for MoPALA<sub>12</sub> (table 3.4). The amides obtained result in yellow oily products in the case of MoPALA<sub>4</sub> and MoPALA<sub>8</sub> and a white waxy product in the case of MoPALA<sub>12</sub>.

**Table 3.4** – Yield percentile in isolated product of MoPALA<sub>4</sub>, MoPALA<sub>8</sub> and MoPALA<sub>12</sub>

| Compound            | Yield | Purity |
|---------------------|-------|--------|
| MoPALA <sub>4</sub> | 60%   | 85%    |
| MoPALA <sub>8</sub> | 62%   | 87%    |

|                            |     |     |
|----------------------------|-----|-----|
| <b>MoPALA<sub>12</sub></b> | 52% | 98% |
|----------------------------|-----|-----|

The <sup>1</sup>H NMR and <sup>13</sup>C NMR spectra MoPALA<sub>4</sub>, MoPALA<sub>8</sub> and MoPALA<sub>12</sub> obtained (figure 3.1 and figure 3.3) show that the ppm value are almost identical among the three compounds, varying only the integration of the pick referred to the alkyl chain. As a reference, therefore, we comment only on the <sup>1</sup>H NMR and <sup>13</sup>C NMR spectrum of MoPALA<sub>12</sub> (figure 3.2 and figure 3.4). Signal assignment was done using both single-dimensional and two-dimensional techniques such as COSY, HMQC, and HMBC.

From the <sup>1</sup>H NMR spectrum shown in figure 3.2, it can be seen that the synthesis results in an extremely clean product without using of chromatographic techniques or recrystallization. At 6.78 ppm we can recognize the NH amide signal that is broad by quadrupolar relaxation due to nitrogen atom (**NH**). The alkyl side chain is characterized by four signals: at 0.89 ppm fall the terminal methyl (CH<sub>2</sub>**CH<sub>3</sub>**), at 1.21 ppm falls the eight CH<sub>2</sub> within the chain (CH<sub>2</sub>(**CH<sub>2</sub>**)<sub>8</sub>CH<sub>2</sub>), at 1.63 ppm fall the CH<sub>2</sub> in β to the carbonyl (COCH<sub>2</sub>**CH<sub>2</sub>**), and at 2.16 ppm fall the CH<sub>2</sub> signal in α to the carbonyl (**CH<sub>2</sub>**CO). The signals from the propyl linker between the morpholine and the amide are characterized by three signals: at 1.70 ppm fall the central CH<sub>2</sub> (**CH<sub>2</sub>**CH<sub>2</sub>NH), at 2.46 ppm fall the CH<sub>2</sub> in α to the morpholino nitrogen (CH<sub>2</sub>**CH<sub>2</sub>**N(CH<sub>2</sub>)<sub>2</sub>), which is superimposed on the signals of the morpholino CH<sub>2</sub> in α to the nitrogen ((**CH<sub>2</sub>**)<sub>2</sub>NCH<sub>2</sub>), at 3.36 ppm fall the protons in α to the amide (NH**CH<sub>2</sub>**CH<sub>2</sub>). To conclude at 3.73 ppm there is the signal represented by the four protons of the two CH<sub>2</sub> of the morpholino ring proximal to the oxygen atom (**CH<sub>2</sub>**O**CH<sub>2</sub>**).

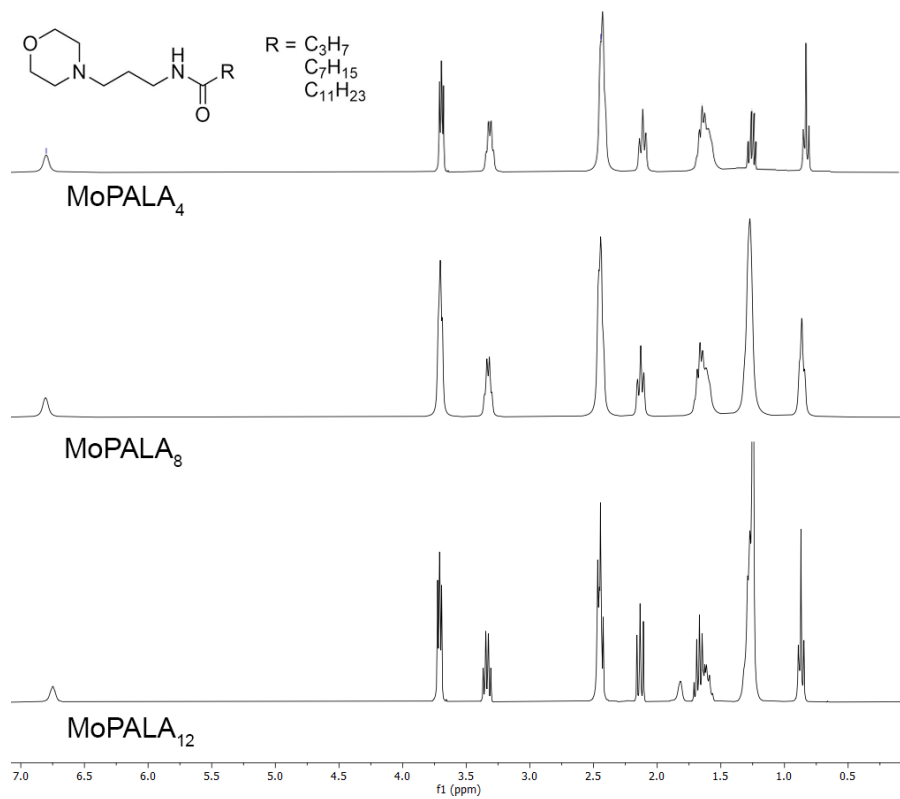
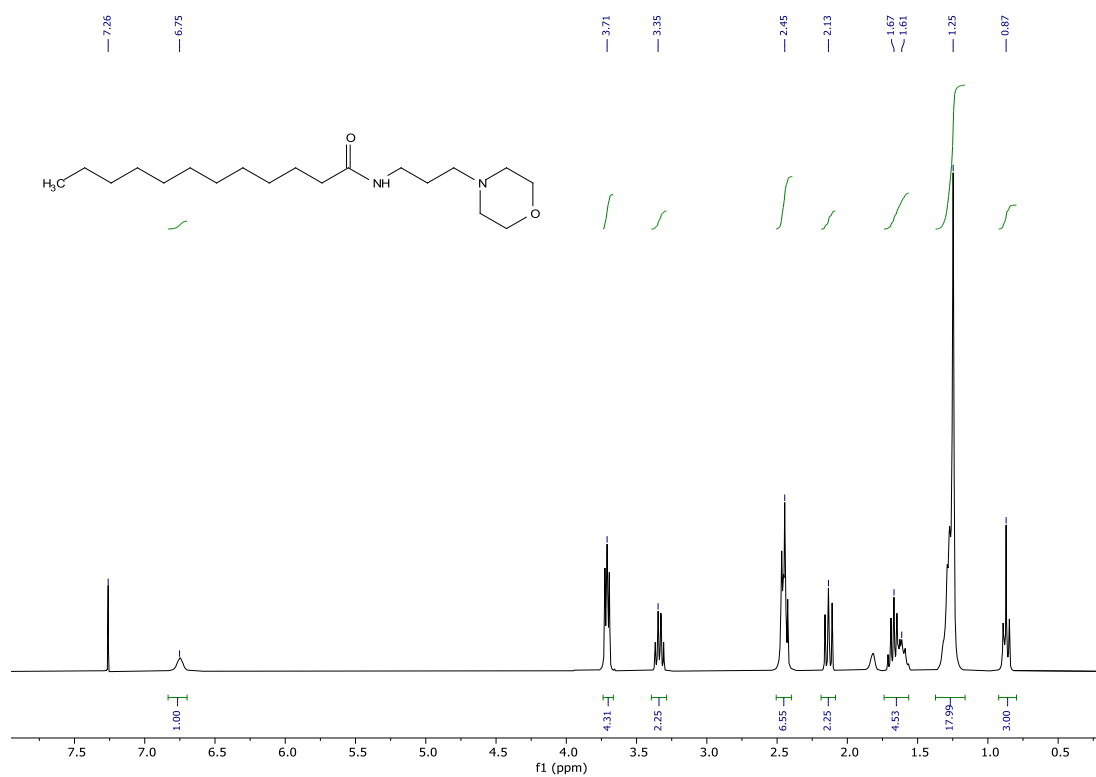
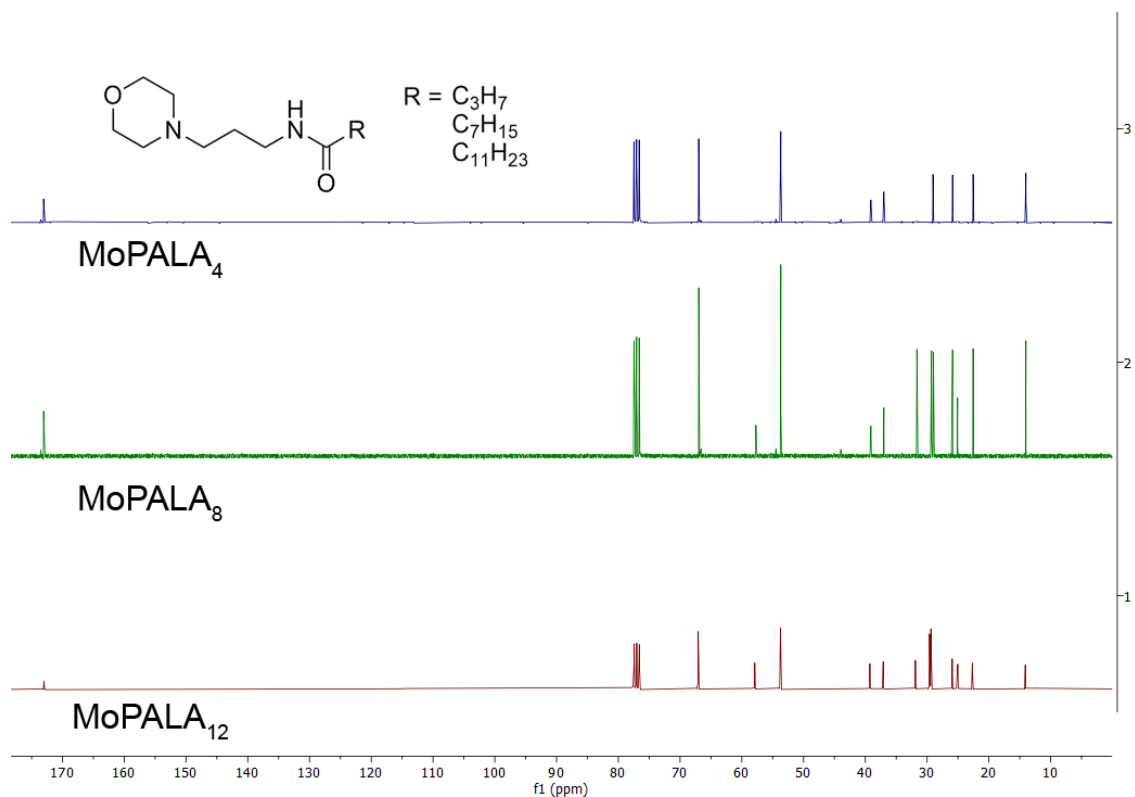


Figure 3.1 - <sup>1</sup>H NMR (CDCl<sub>3</sub>) spectrum of MoPALAs



**Figure 3.2** -  $^1\text{H}$  NMR ( $\text{CDCl}_3$ ) spectrum of MoPALA<sub>12</sub>



**Figure 3.3** –  $^{13}\text{C}$  NMR ( $\text{CDCl}_3$ ) spectrum of MoPALA<sub>s</sub>

The  $^{13}\text{C}$  NMR spectrum of MoPALA<sub>12</sub> in figure 3.4, the long alkyl chain is characterized by the signal at; 14.10 ppm for terminal CH<sub>3</sub> signal, 22.67, 25.93, 29.32, 29.60 for the internal CH<sub>2</sub> and 172.99 ppm for carbonyl carbon. Propyl linker chain signals fall at 67.06, 37.10 and 31.89 ppm. Morpholine carbons fall at 57.90 ppm those are in  $\alpha$  to the oxygen and 53.74 ppm those are in  $\alpha$  to the amine nitrogen.

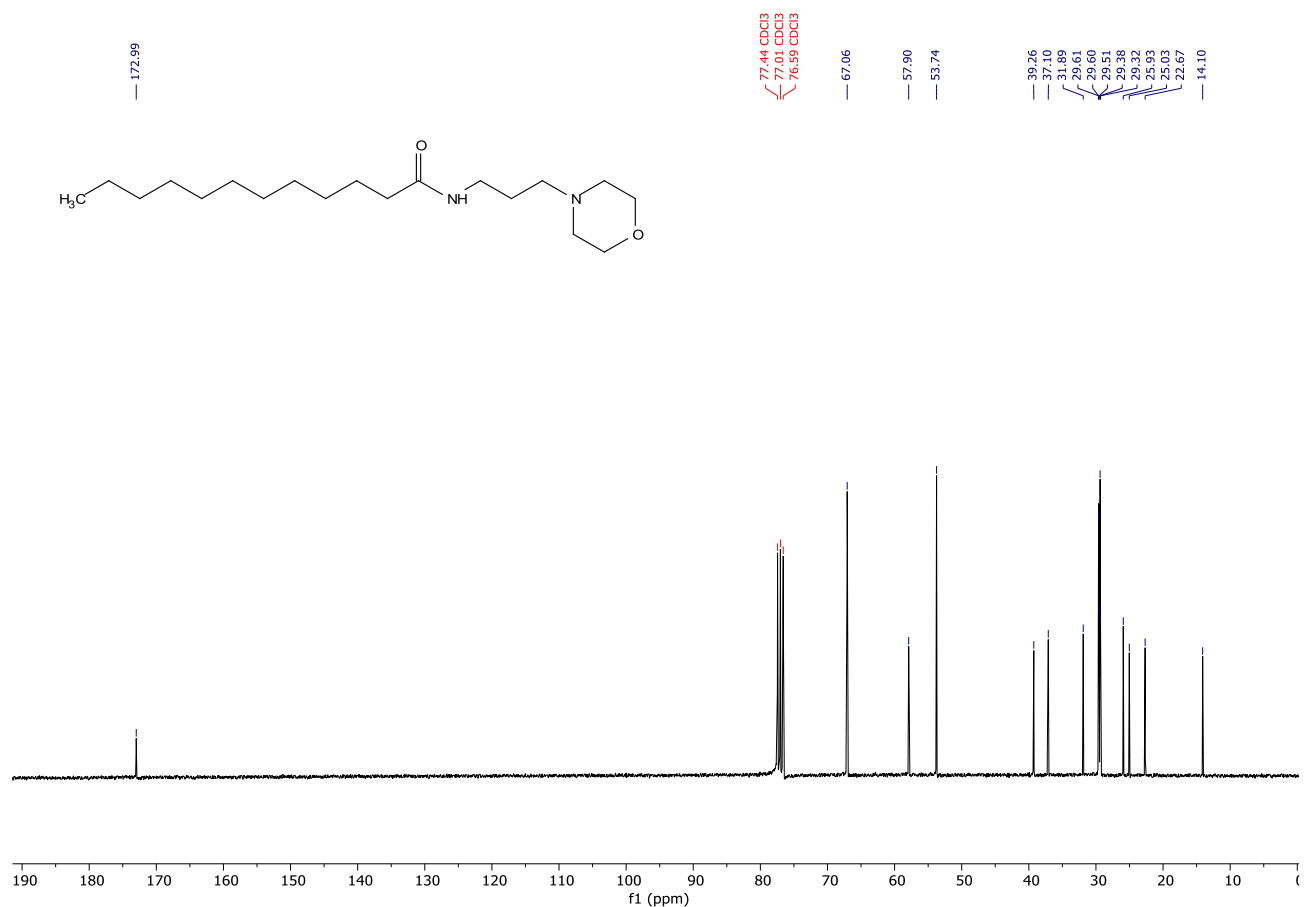
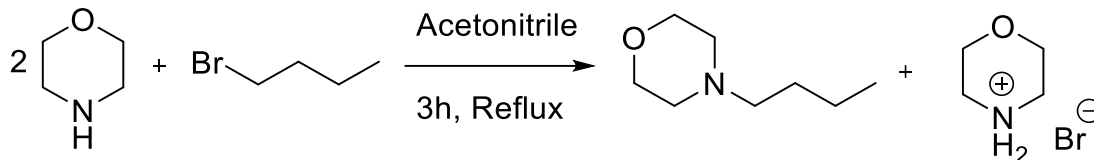


**Figure 3.4** – <sup>13</sup>C NMR (CDCl<sub>3</sub>) spectrum of MoPALA<sub>12</sub>

### 3.2.2 Synthesis of 4-butylmorpholine

As often reported in the literature, QACs with carbon side chains ranging from 8 to 16 are the most active as antimicrobial agents<sup>[58-61]</sup>. In this work for a better investigation, we wanted to evaluate the antimicrobial activity of a short chain morpholine TQACs.

The synthesis of 4-butylmorpholine by reaction with bromobutane is reported here (scheme 3.6). The reaction was conducted in refluxed acetonitrile using an excess of morpholine as a scavenger for the hydrobromic acid that forms during the reaction.



**Scheme 3.6** – Synthesis of 4-butylmorpholine by reaction between morpholine and bromobutane

The reaction was monitored by gas chromatograph and after 3h hours it is achieved the full conversion in 4-butylmorpholine. In order to remove the morpholine residue that could then cause problems in subsequent quaternization reactions, the reaction crude was distilled under vacuum. The clear liquid product obtained from the distillation was then characterized by  $^1\text{H}$  NMR and  $^{13}\text{C}$  NMR which revealed it to be 4-butylmorpholine with a yield of 86% for 98% purity. Signal assignment was done using both single-dimensional and two-dimensional techniques such as COSY, HMQC, and HMBC.

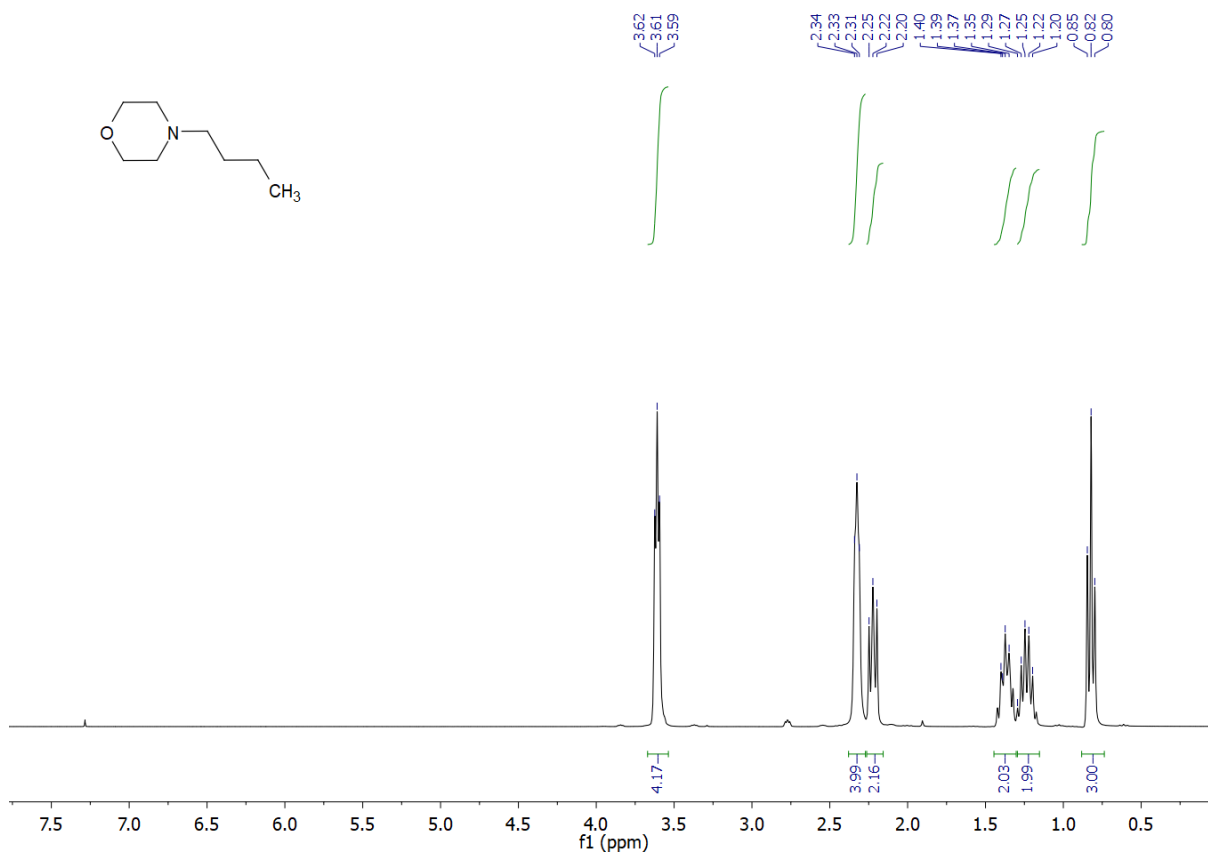


**Figure 3.5** -  $^1\text{H}$  NMR ( $\text{CDCl}_3$ ) spectrum of 4-butylmorpholine



The  $^1\text{H}$  NMR spectrum (figures 3.5) shows 6 different signals. The first four, at lower fields, belong to the butyl chain. A triplet at 0.82 ppm may be attributed to the  $\text{CH}_3$  terminal of the alkyl chain ( $\text{CH}_2\text{CH}_3$ ), while the triplet at 1.25 belongs to the vicinal  $\text{CH}_2$  ( $\text{CH}_2\text{CH}_2\text{CH}_3$ ), the inner  $\text{CH}_2$  is located at 1.38 ppm showing a triplet signal ( $\text{CH}_2\text{CH}_2\text{CH}_2\text{N}$ ) and finally the  $\text{CH}_2$  in  $\alpha$  to the nitrogen atom is described by the triplet at 2.25 ppm ( $\text{CH}_2\text{CH}_2\text{CH}_2\text{N}$ ). The other two signals belong to the morpholino residue signals, which are described by the triplet integrating for 4H at 2.33 which represents the  $\text{CH}_2$ s in  $\alpha$  to the nitrogen ( $(\text{CH}_2)_2\text{NCH}_2$ ) and the triplet at 3.61 which describes the  $\text{CH}_2$  pair directly bound to the oxygen atom ( $\text{CH}_2\text{OCH}_2$ ).

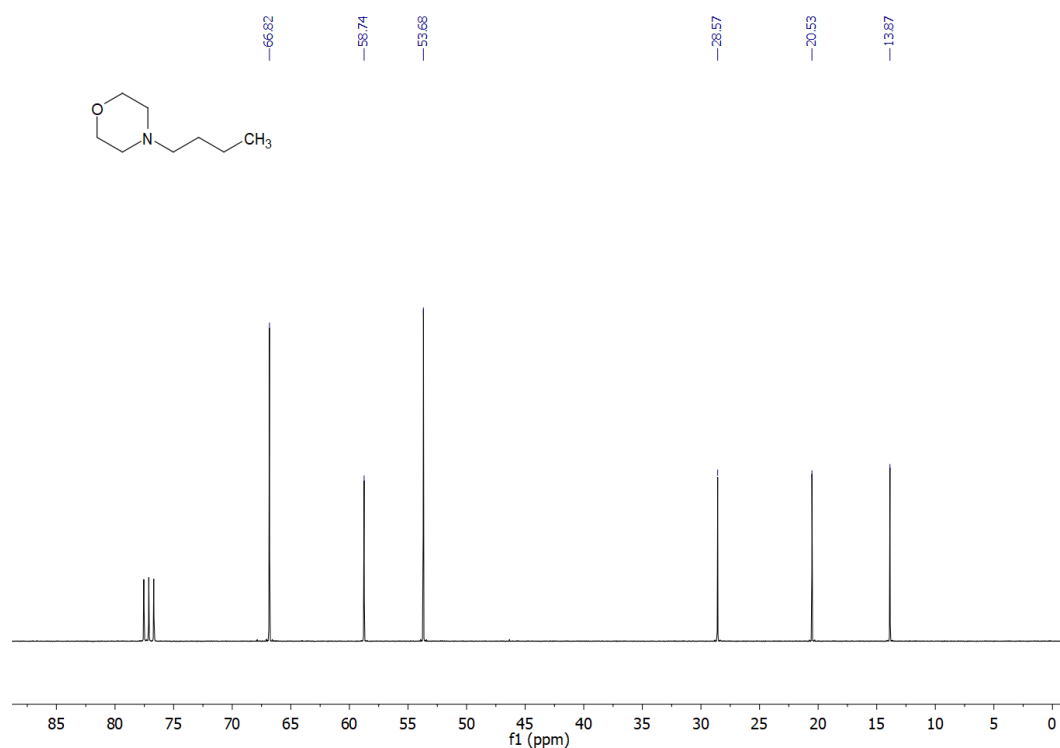


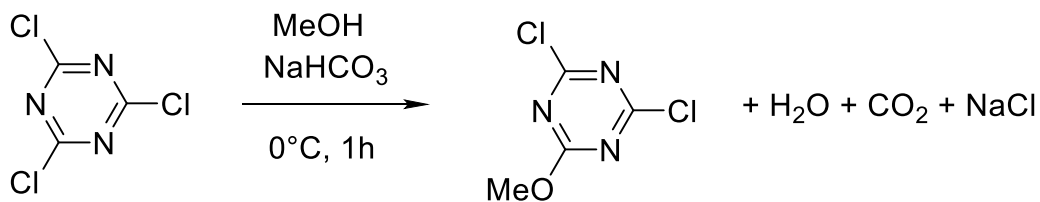
**Figure 3.6** –  $^{13}\text{C}$  NMR ( $\text{CDCl}_3$ ) spectrum of 4-butylmorpholine

In the  $^{13}\text{C}$  NMR spectrum of 4-butylmorpholine (figure 3.6), the butyl side chain signals can be distinguished at 13.87, 20.53, 28.57, and 58.74 ppm, respectively. The signals belong to the morpholino carbons falls at 53.68 ppm for the carbons in  $\alpha$  to the amine nitrogen and at 66.82 ppm for the carbons in  $\alpha$  to the oxygen.

### 3.2.3 Synthesis of 2,4-dichloro-6-methyl-1,3,5-triazine (MMT)

MMT is well known in the literature as a building block for various technological applications. For example, it is used for development of OLED technologies<sup>[129]</sup>, synthesis of antimicrobials and peptides<sup>[130,131]</sup>, or in patents for anticancer drugs<sup>[132,133]</sup>. It was also investigated in our recent article as a basis for the synthesis of novel condensation agents<sup>[120]</sup>.

MMT was obtained using the method reported by Kaminsky<sup>[123]</sup>, by vigorously stirring a solution of cyanuric chloride in methanol in the presence of NaHCO<sub>3</sub>. To avoid double substitution on the triazine ring by methoxy groups and thus formation of CDMT, the reaction was carried out at low temperature (0 °C) (scheme 3.7).



**Scheme 3.7** - Synthesis of MMT

Using gas chromatographic analysis, it was possible to monitor the progress of the reaction which results in complete conversion into the monosubstituted product in 1h. The <sup>1</sup>H NMR, <sup>13</sup>C NMR and FT-IR spectra confirmed the isolation of MMT as a white solid with yields of 97% and 98% purity.

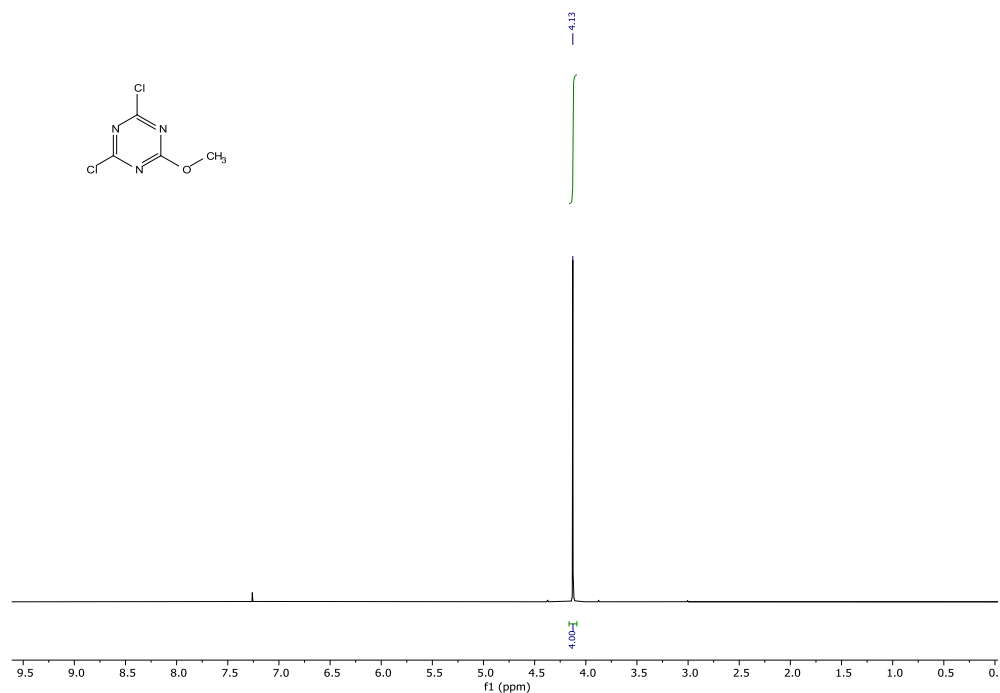


**Figure 3.7** - <sup>1</sup>H NMR (CDCl<sub>3</sub>) spectrum of MMT

In the <sup>1</sup>H NMR spectrum (figure 3.7) there is a singlet at 4.17 ppm corresponding to the protons of the methoxyl group present in the molecule.

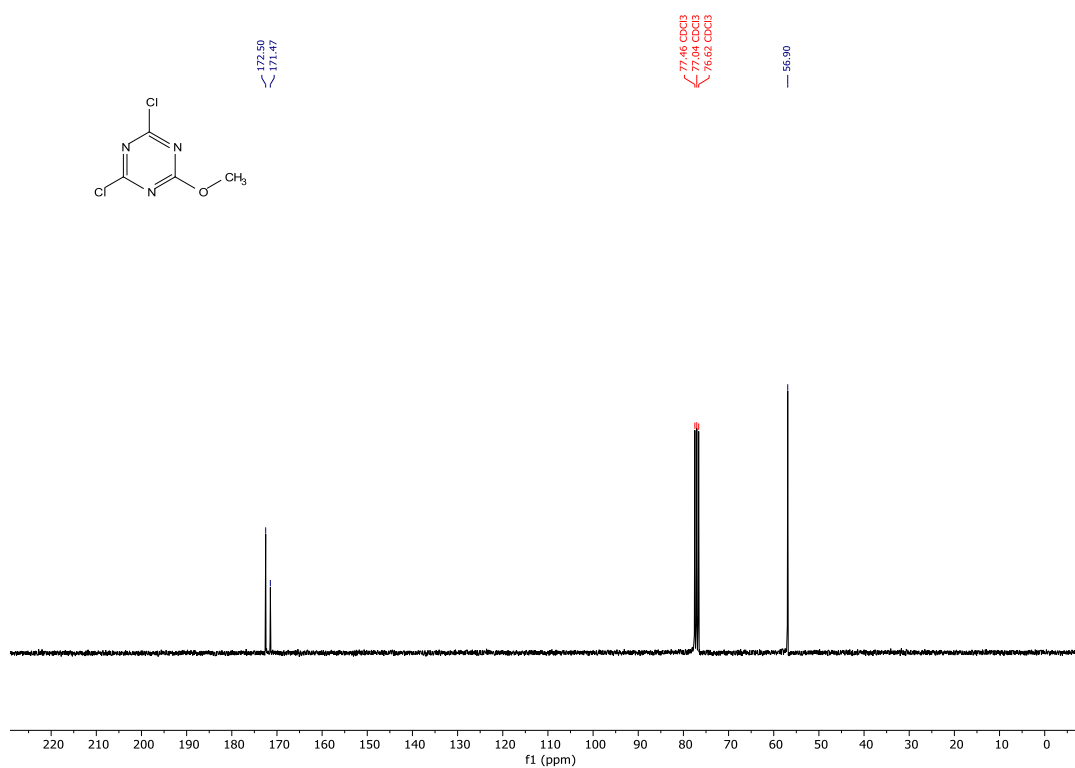
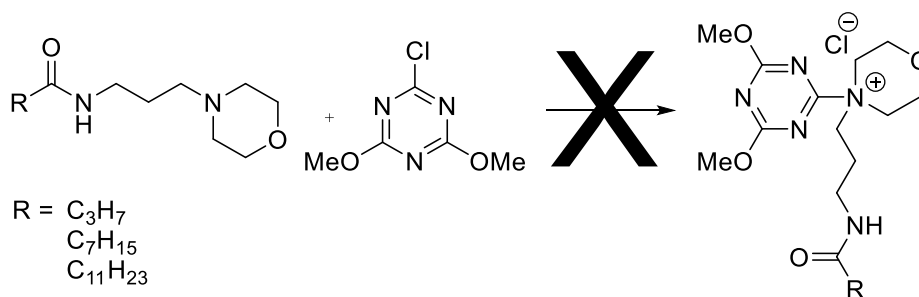


**Figure 3.8**- <sup>13</sup>C NMR (CDCl<sub>3</sub>) spectrum of MMT

In the  $^{13}\text{C}$  NMR spectrum (figure 3.8), the signals at 172.50 ppm and 172.47 ppm correspond to the quaternary triazine carbons, the chlorine-substituted carbon atoms and the carbon bound to the methoxy group, respectively. Finally, the signal at 56.90 ppm is assignable to the carbon of the methoxy substituent.

### 3.2.4 Preparation of 4,4'-(6-chloro-1,3,5-triazine-2,4-diyl)bis(4-(3-alkylamidopropyl) morpholin-4-ium) chloride (MoPALA-CC)

As mentioned in the introduction, in devising the design of these morpholino TQACs we were inspired by the work of Kunishima<sup>[36]</sup> and his studies on ammonium salts obtained by reaction with CDMT and tertiary amines of various nature. Initially our idea was to exploit the long chain morpholino-amides previously obtained and form its quaternary ammonium derivatives with CDMT. But despite several attempts even using reflux reaction mixtures, CDMT did not give the desired results. In fact, in all the tests carried out it was never possible to obtain the desired 4-(4,6-dimethoxy-1,3,5-triazin-2-yl)-4-(3-alkylamidopropyl)morpholin-4-ium (scheme 3.8).

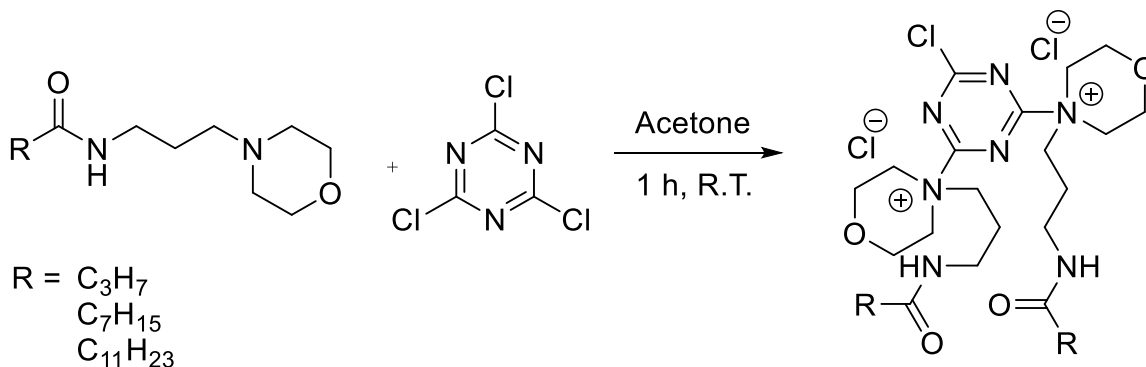


**Scheme 3.8** – Synthesis of 4-(4,6-dimethoxy-1,3,5-triazin-2-yl)-4-(3-alkylamidopropyl)morpholin-4-ium by reaction of CDMT with *N*-(3-morpholinopropyl)alkylamide

We suppose that the low reactivity of CDMT towards long chain morpholino-amides might reside in its poor tendency to react with morpholines that have hindered substituents. As reported in the work of Kunishima and colleagues<sup>[36]</sup>, reactions between CDMT and ethyl morpholine give low yields compared to those with methyl morpholine, in another work Kunishima<sup>[134]</sup> reports the synthesis of an DMT-Ams using benzyl morpholine. For make this he

replaced the chlorine of CDMT with a triflate group in order to increase its reactivity. In fact, as also described by Hammett's<sup>[100]</sup>, substituents of different nature can change the reactivity of a molecule. In particular this mechanism is regulated by a parameter  $\sigma$  that changes according to the nature of the substituent, higher value of  $\sigma$  tend to make the molecule less reactive. Methoxy substituents, in our case, according to Hammett's  $\sigma$ , lower the reactivity of the triazine respect the chloro substituents. The use of a less methoxy-substituted chlorotriazine was therefore tested. So, as a first approach, we moved from using CDMT to using cyanuric chloride (CC) that is the most chloro-carrier triazine species available.

Here after are reported the synthesis of different 4,4'-(6-chloro-1,3,5-triazine-2,4-diyl)bis(4-(3-alkylamidopropyl) morpholin-4-ium) chloride by reaction of various *N*-(3-morpholinopropyl)alkylamide with cyanuric chloride (CC) in acetone (scheme 3.9). The product was recovered by simple filtration as they precipitate from the reaction solvent.



**Scheme 3.9** – Synthesis of 4,4'-(6-chloro-1,3,5-triazine-2,4-diyl)bis(4-(3-alkylamidopropyl) morpholin-4-ium) chloride by reaction of cyanuric chloride with *N*-(3-morpholinopropyl)alkylamide

The final yields obtained were 19% for 4'-(6-chloro-1,3,5-triazine-2,4-diyl)bis(4-(3-butylamidopropyl)morpholin-4-ium) chloride (MoPALA<sub>4</sub>CC), 18% for 4,4'-(6-chloro-1,3,5-triazine-2,4-diyl)bis(4-(3-octanamidopropyl)morpholin-4-ium) chloride (MoPALA<sub>8</sub>CC), and 15% for 4,4'-(6-chloro-1,3,5-triazine-2,4-diyl)bis(4-(3-dodecanamidopropyl)morpholin-4-ium) chloride (MoPALA<sub>12</sub>CC) (table 3.5). The product are all fine white powders.

**Table 3.5** - Yield percentile in isolated product of MoPALA<sub>4</sub>CC, MoPALA<sub>8</sub>CC and MoPALA<sub>12</sub>CC

| Compounds                    | Yield | Purity |
|------------------------------|-------|--------|
| <b>MoPALA<sub>4</sub>CC</b>  | 19%   | 89%    |
| <b>MoPALA<sub>8</sub>CC</b>  | 18%   | 91%    |
| <b>MoPALA<sub>12</sub>CC</b> | 15%   | 96%    |

The NMR spectrum of MoPALA<sub>4</sub>CC, MoPALA<sub>8</sub>CC, MoPALA<sub>12</sub>CC (figure 3.9 and figure 3.10) shows that the signal's shift is almost identical among the three compounds, varying only the integrations of the peaks related to the alkyl chain. As an example, therefore, we comment only the <sup>1</sup>H NMR and <sup>13</sup>C NMR spectrum of MoPALA<sub>12</sub>CC (figure 3.11 and figure 3.12). Signal assignment was done using both single-dimensional and two-dimensional techniques such as COSY, HMQC, and HMBC.

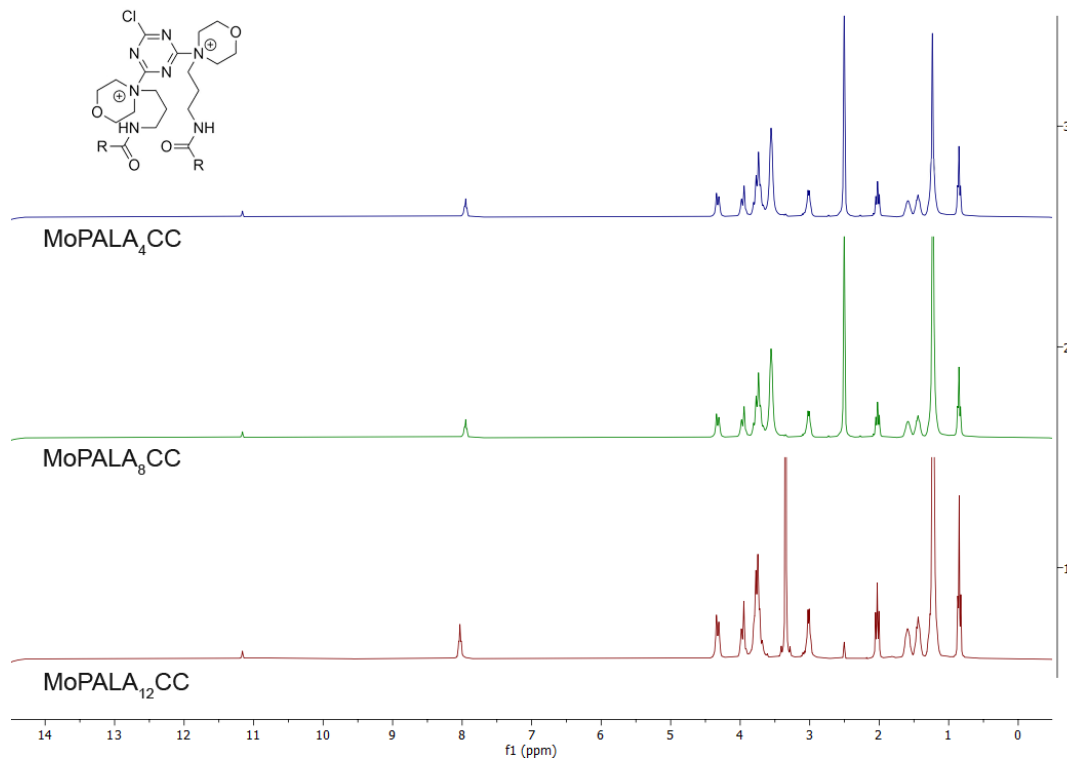


**Figure 3.9** <sup>1</sup>H NMR (DMSO-d<sub>6</sub>) spectrums of MoPALACC

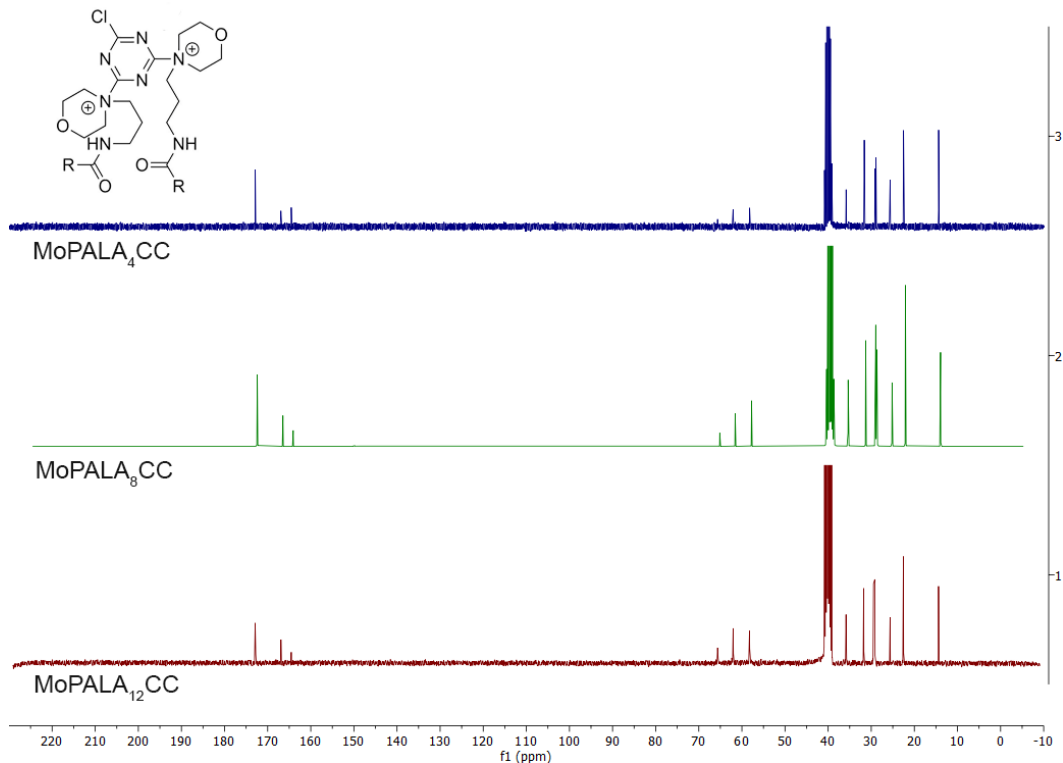


**Figure 3.10**  $^{13}\text{C}$  NMR (DMSO- $d_6$ ) spectra of MoPALACC

From the comparison of the  $^1\text{H}$  NMR spectrum reported in figure 3.11 with the  $^1\text{H}$  NMR spectrum of MoPALA<sub>12</sub> reported in figure 3.2 many signals appear similar making assignment easier. At 7.95 ppm we can recognize the NH amide signal that is broad by quadrupolar relaxation due to nitrogen atom (NH). The alkyl side chain is characterized by four signals: at 0.85 ppm fall the terminal methyl ( $\text{CH}_2\text{CH}_3$ ), at 1.23 ppm falls the eight  $\text{CH}_2$  within the chain ( $\text{CH}_2(\text{CH}_2)_8\text{CH}_2$ ), at 1.44 ppm fall the  $\text{CH}_2$  in  $\beta$  to the carbonyl ( $\text{COCH}_2\text{CH}_2$ ), and at 2.02 ppm fall the  $\text{CH}_2$  signal in  $\alpha$  to the carbonyl ( $\text{CH}_2\text{CO}$ ). The signals from the propyl linker between the morpholine and the amide are characterized by three signals: at 1.59 ppm fall the central  $\text{CH}_2$  ( $\text{CH}_2\text{CH}_2\text{NH}$ ), at 3.01 ppm fall the protons in  $\alpha$  to the amide ( $\text{NHCH}_2\text{CH}_2$ ), at 3.74 ppm fall the  $\text{CH}_2$  in  $\alpha$  to the morpholino nitrogen ( $\text{CH}_2\text{CH}_2\text{N}^+(\text{CH}_2)_2$ ), which is superimposed on the signals of the morpholino  $\text{CH}_2$  in  $\alpha$  to oxygen atom ( $\text{CH}_2\text{OCH}_2$ ). The signal of the morpholine  $\text{CH}_2$  in  $\alpha$  to the nitrogen atom result split into 2 different signals. According to Kunishima and Kaminsky<sup>[36,122]</sup>, a morpholino triazinyl ammonium salt structure, like DMTMM, exists in 2 different conformers (figure 3.12), for this reason the signals of axial and equatorial hydrogens are discriminated in

NMR analysis. In the case of MoPALA<sub>12</sub>CC the signals fall at 3.96 ppm and 4.32 ppm (CH<sub>2</sub>CN<sup>+</sup>(CH<sub>2</sub>)<sub>2</sub>)

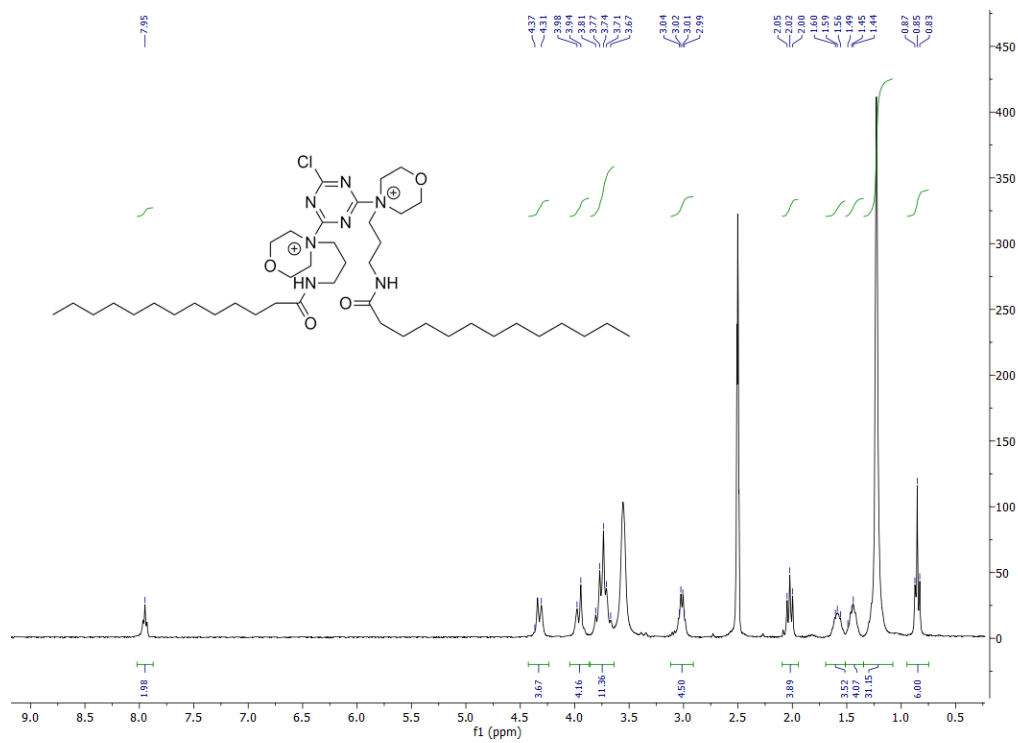
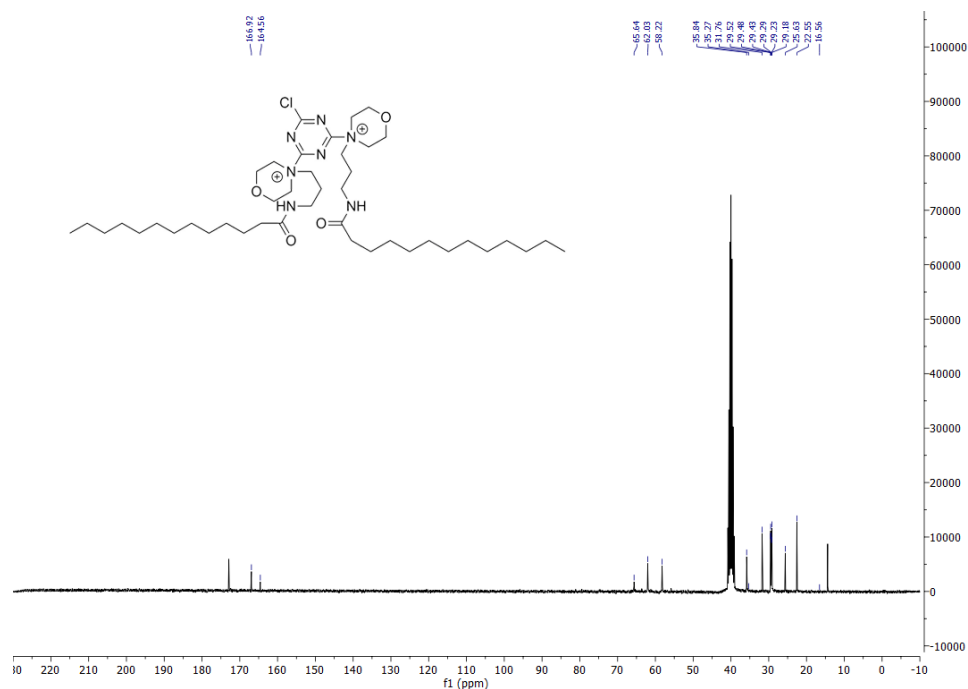


Figure 3.11 <sup>1</sup>H NMR (DMSO-d<sub>6</sub>) spectrum of MoPALA<sub>12</sub>CC





**Figure 3.12**  $^{13}\text{C}$  NMR (DMSO- $d_6$ ) spectrum of MoPALA $_{12}$ CC

The  $^{13}\text{C}$  NMR spectrum in figure 3.11 also bears many similarities to MoPALA $_{12}$ . The signal at 13.92 ppm corresponds to the terminal  $\text{CH}_3$  of the alkyl chain, the rest of the chain is then characterized by signals at 22.07, 25.16, 28.68, 28.76, 28.95, 29.00, 29.05, 35.33 and 172.41 ppm with the latter representing carbonyl carbon. Propyl chain signals fall at 65.13, 35.36 and 31.28 ppm. Morpholine carbons fall at 57.76 ppm those proximal to the oxygen atom and 61.56 ppm those proximal to the nitrogen atom. At 164.08 ppm and 166.46 ppm fall the triazine carbon atoms.

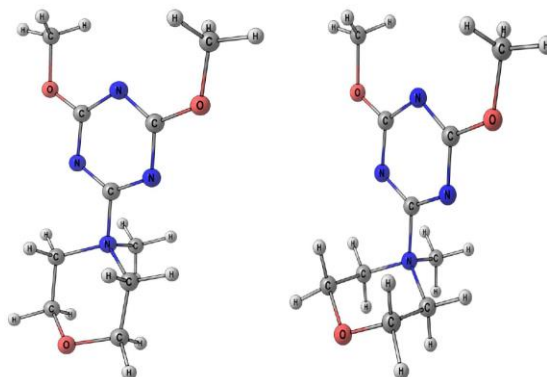


**Figure 3.13** – DMTMM possible conformers with the triazine in equatorial position (left) an axial position (right) to morpholine ring

The substitution on the triazine ring was confirmed by ESI-MS analysis (Figure 3.14). The compounds MoPALA<sub>4</sub>CC and MoPALA<sub>12</sub>CC under the analytical conditions used (30% H<sub>2</sub>O, 70% ACN) their chlorine moieties are hydrolyzed.

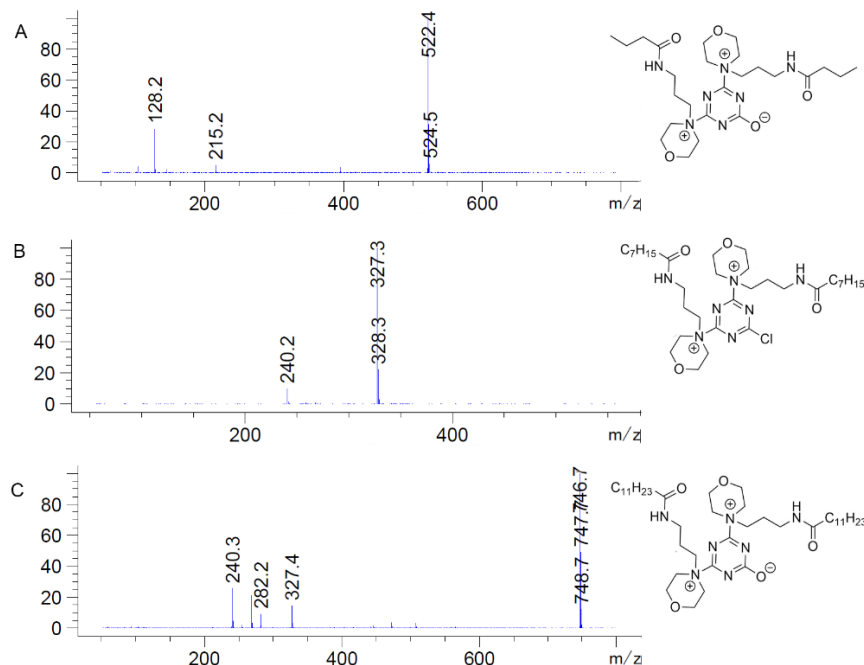
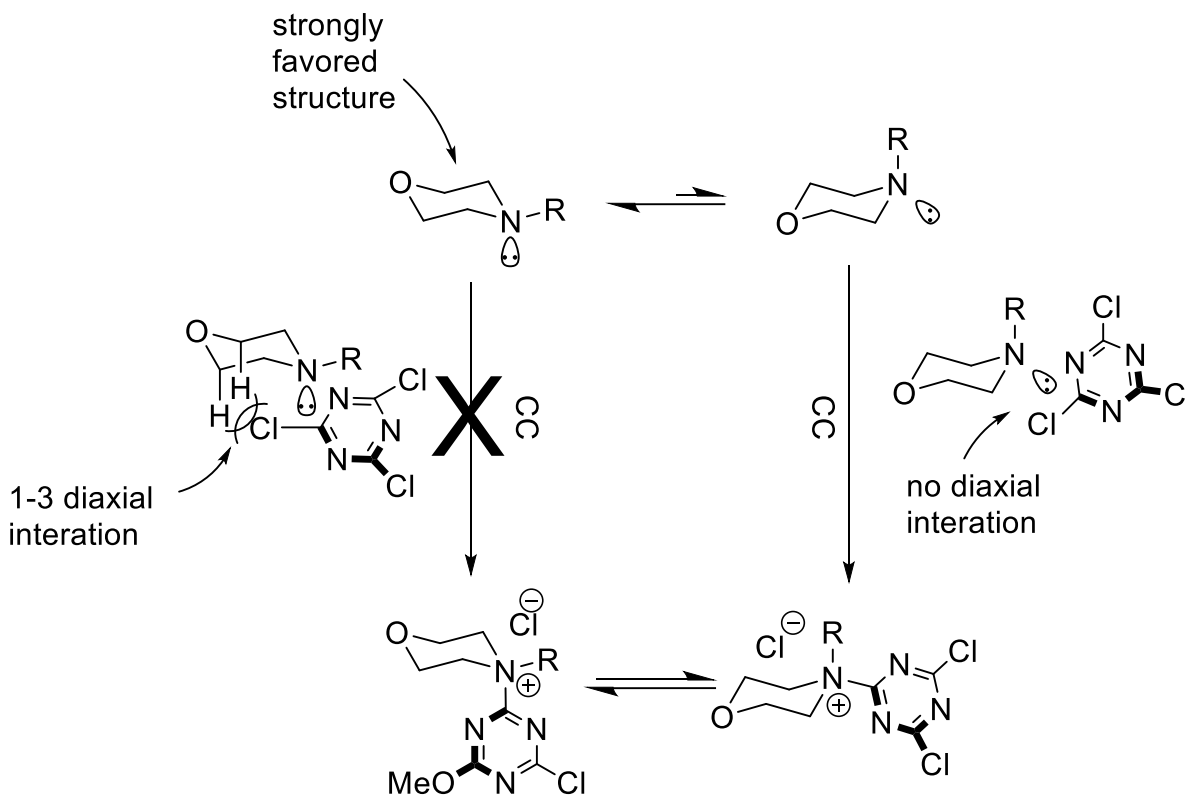


**Figure 3.14** – Mass spectrum of MoPALACCs. A) MoPALA<sub>4</sub>CC, the chlorine moiety was hydrolyzed in HPLC-ESI condition,  $[M]^+ = 522.4$   $m/z$ . B) MoPALA<sub>8</sub>CC,  $[M]^{2+} = 327.3$   $m/z$ . C) MoPALA<sub>12</sub>CC, the chlorine moiety was hydrolyzed in HPLC-ESI condition,  $[M]^+ = 746.7$ .

Although initially the intention was to obtain a monosubstituted TQACs, with the precaution of using CC in excess respect to the morpholine, the reaction inevitably leads to the formation of a disubstituted product. This behavior could be a consequence of the disactivating character of the  $NR_3^+$  substituent. This substituent in fact, is a strong electron-withdrawing, which are generally meta directors. The result of these electronic are promoting nucleophilic substitution in the meta position. For this reason, further substitution reactions could be thermodynamically favored. The reason why a trisubstituted product is not formed is not well understood, it could be due to the high steric hindrance of the two substituents or to the fact that the increase of positive charges on the product drastically decrease its solubility in the reaction solvent, and preventing further substitution.

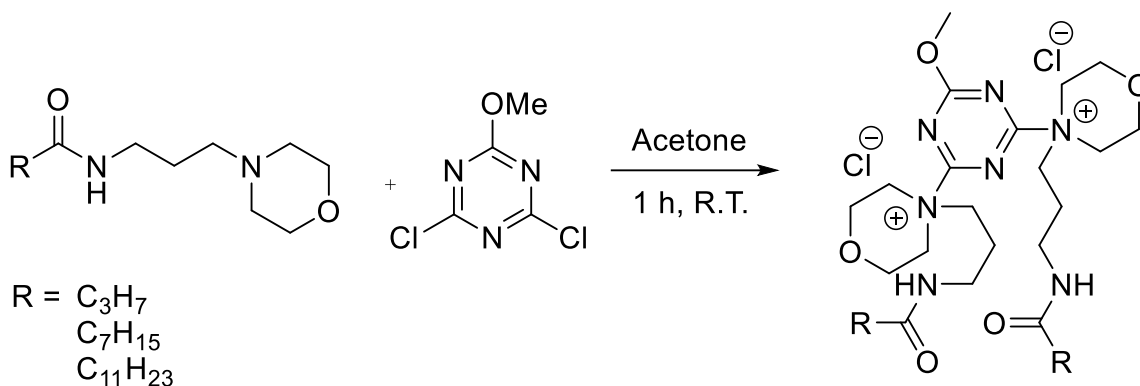


**Scheme 3.10** - Reaction path of chlorotriazine with cyclic amines. Scheme adapted from work of Kunishima et al.<sup>[36]</sup>

Despite the great reactivity of CC, the final yields were unexpectedly low. The reason for this behavior could be attributable to a kinetic effect. According to Kunishima<sup>[36]</sup>, the attack of a triazine ring on the nitrogen atom of a cyclic aliphatic amine can occur only when the nitrogen lone pair is in equatorial position, while the attack in the axial position is prevented by 1,3-diaxial interaction of the morpholine hydrogens with the chlorine atom (scheme 3.10). In our case, the cyclic amine has a very bulky long-chain group and it may be supposed that the equilibrium between the conformers is shifted towards the form in which the long alkyl chain is in equatorial position and the lone pair in axial position. Since the latter is the less reactive of the two forms, it consequently disfavors the attack of triazine on the nitrogen of the tertiary amine.

#### 5.4.2 Synthesis of 4,4'-(6-methoxy-1,3,5-triazine-2,4-diyl)bis(4-(3-alkylamidopropyl)morpholin-4-ium) chloride (MoPALA-MMT)

The following is the synthesis of 4,4'-(6-methoxy-1,3,5-triazine-2,4-diyl)bis(4-(3-alkylamidopropyl)morpholin-4-ium) chloride (scheme 3.11) by reaction between *N*-(3-morpholinopropyl)alkylamide and an MMT in acetone. The products were recovered by simple filtration because they precipitate in the reaction environment.



**Scheme 3.11** – Synthesis of 4,4'-(6-chloro-1,3,5-triazine-2,4-diyl)bis(4-(3-alkylamidopropyl) morpholin-4-ium) chloride by reaction of MMT with *N*-(3-morpholinopropyl)alkylamide

Similar to the MoPALA-CCs, the final performance of the reaction is very poor in terms of yield. The final yields obtained were 15% for 4,4'-(6-methoxy-1,3,5-triazine-2,4-diyl)bis(4-(3-butylamidopropyl)morpholin-4-ium) chloride (MoPALA<sub>4</sub>MMT), 12% for 4,4'-(6-methoxy-1,3,5-triazine-2,4-diyl)bis(4-(3-octylamidopropyl)morpholin-4-ium) chloride (MoPALA<sub>8</sub>MMT), and 8% for 4,4'-(6-methoxy-1,3,5-triazine-2,4-diyl)bis(4-(3-dodecylamidopropyl)morpholin-4-ium) chloride (MoPALA<sub>12</sub>MMT) (table 3.6). The product results in fine white powder.

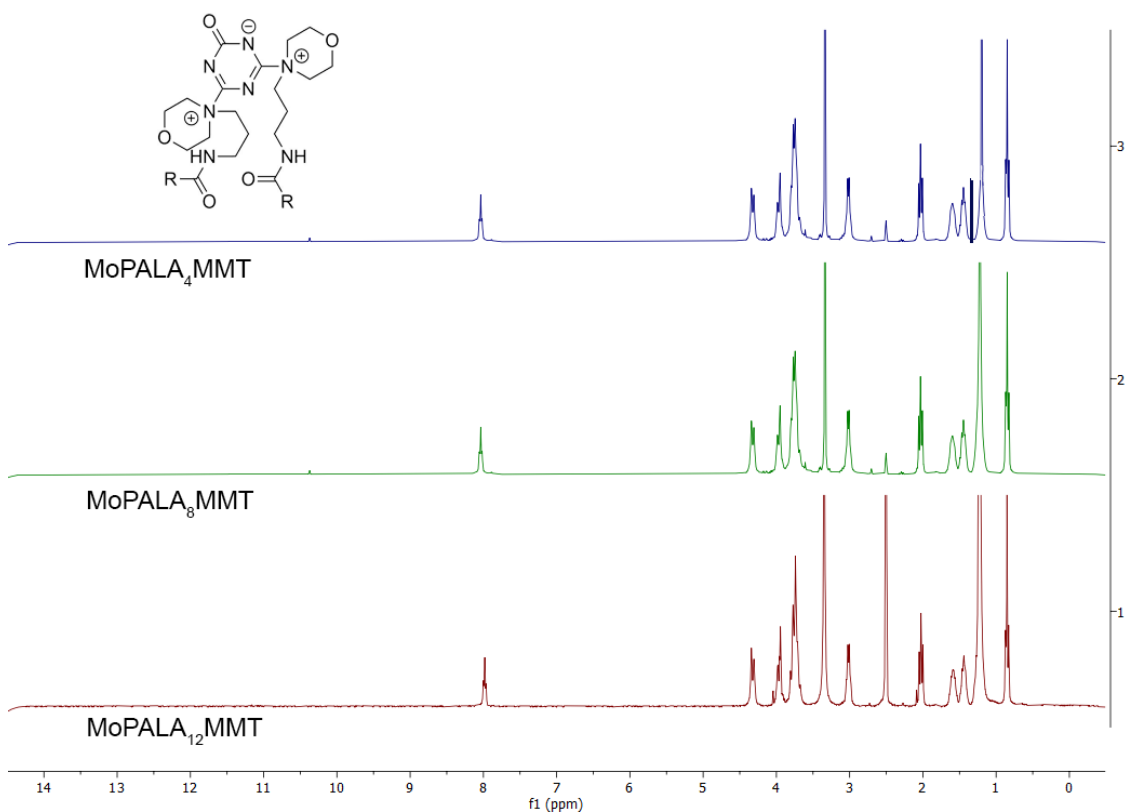
**Table 3.6** - Yield percentile in isolated product of MoPALA<sub>4</sub>CC, MoPALA<sub>8</sub>CC and MoPALA<sub>12</sub>CC

| Compounds                | Yield | Purity |
|--------------------------|-------|--------|
| MoPALA <sub>4</sub> MMT  | 15%   | 89%    |
| MoPALA <sub>8</sub> MMT  | 12%   | 85%    |
| MoPALA <sub>12</sub> MMT | 8%    | 87%    |

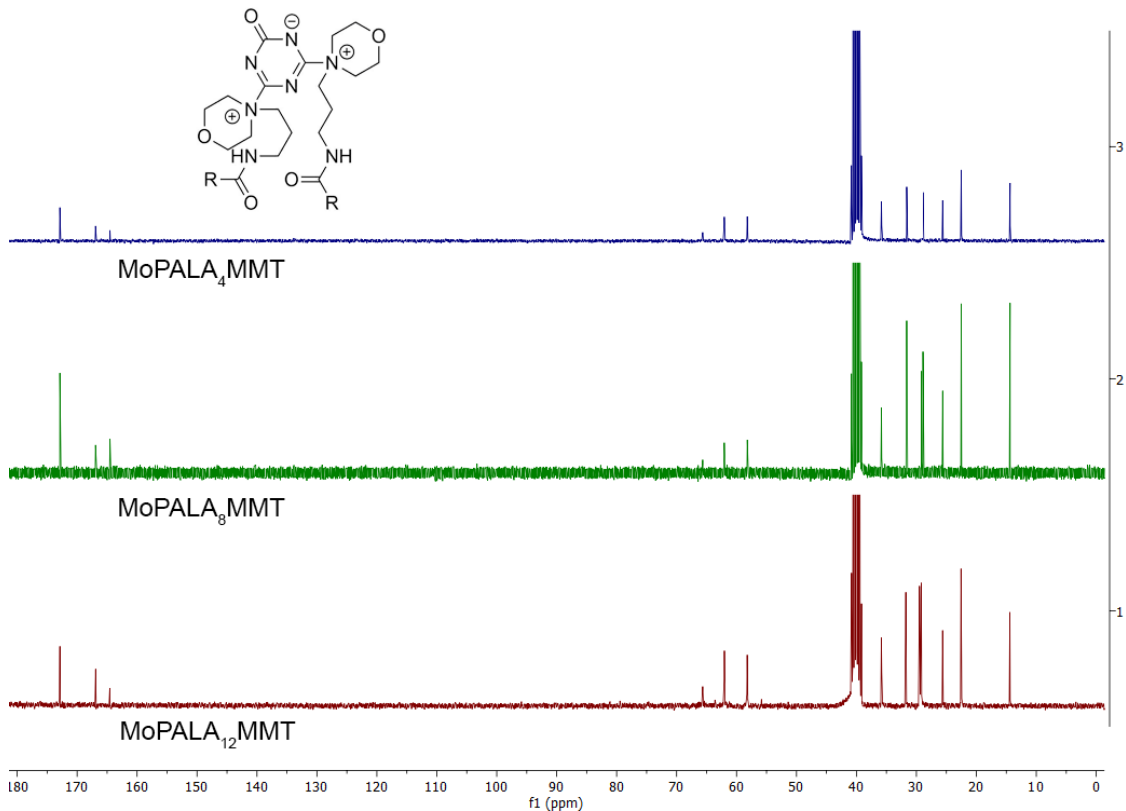
The <sup>1</sup>H NMR and <sup>13</sup>C NMR spectra (figure 3.15 and figure 3.16) of MoPALA-MMTs are almost identical to the MoPALA-CCs compounds. One of the first things we notice is the lack of the

characteristic CH<sub>3</sub> signal of the methoxy group, it does not appear in the spectrum. Typically, this signal falls at 4.13 ppm for the proton and 56.90 ppm for the carbon.

As an example, therefore, we comment only the <sup>1</sup>H NMR and <sup>13</sup>C NMR spectrum of MoPALA<sub>12</sub>MMT (figure 3.17 and figure 3.18). Signal assignment was done using both single-dimensional and two-dimensional techniques such as COSY, HMQC, and HMBC.

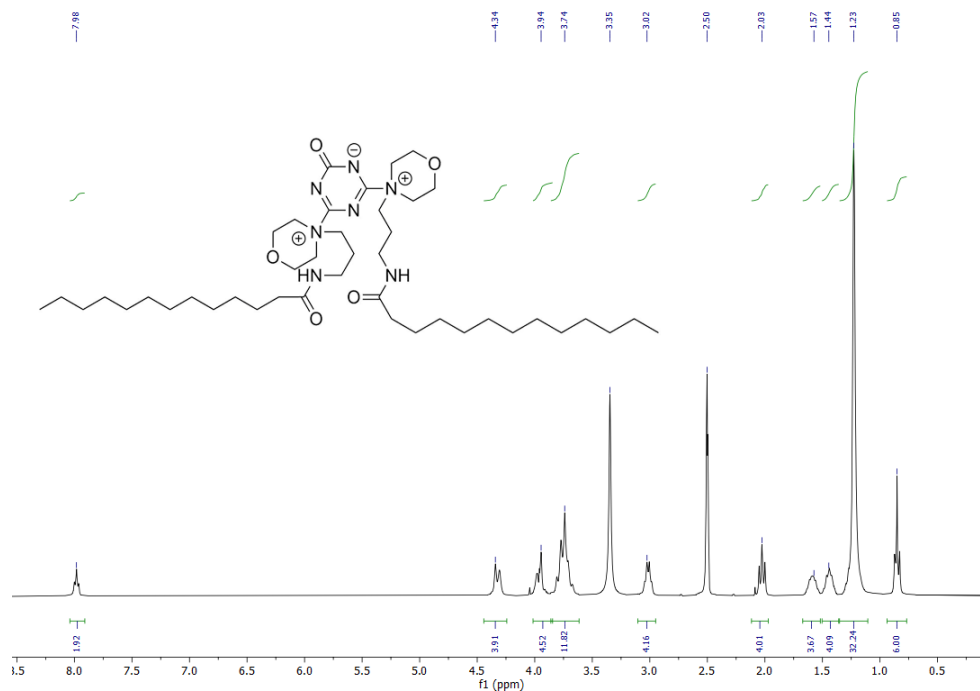


**Figure 3.15** – <sup>1</sup>H NMR (DMSO-d<sub>6</sub>) spectra of MoPALA-MMTs



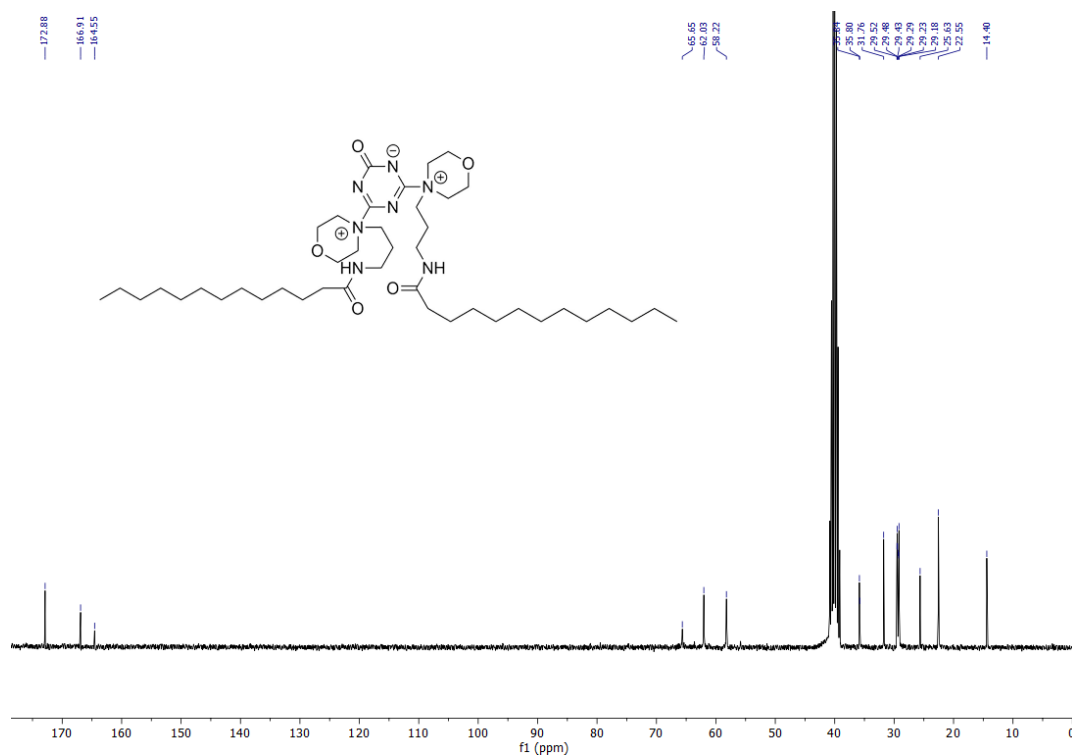
**Figure 3.16** –  $^{13}\text{C}$  NMR (DMSO- $d_6$ ) spectrums of MoPALA-MMTs

Figure 3.17 shows the  $^1\text{H}$  NMR spectrum of the compound MoPALA<sub>12</sub>MMT. At 7.99 ppm we can recognize the NH amide signal that is broad by quadrupolar relaxation due to nitrogen atom (**NH**). The alkyl side chain is characterized by four signals: at 0.85 ppm fall the terminal methyl ( $\text{CH}_2\text{CH}_3$ ), at 1.22 ppm falls the eight  $\text{CH}_2$  within the chain ( $\text{CH}_2(\text{CH}_2)_8\text{CH}_2$ ), at 1.44 ppm fall the  $\text{CH}_2$  in  $\beta$  to the carbonyl ( $\text{COCH}_2\text{CH}_2$ ), and at 2.02 ppm fall the  $\text{CH}_2$  signal in  $\alpha$  to the carbonyl ( $\text{CH}_2\text{CO}$ ). The signals from the propyl linker between the morpholine and the amide are characterized by three signals: at 1.58 ppm fall the central  $\text{CH}_2$  ( $\text{CH}_2\text{CH}_2\text{NH}$ ), at 3.01 ppm fall the protons in  $\alpha$  to the amide ( $\text{NHCH}_2\text{CH}_2$ ), at 3.74 ppm fall the  $\text{CH}_2$  in  $\alpha$  to the morpholino nitrogen ( $\text{CH}_2\text{CH}_2\text{N}^+(\text{CH}_2)_2$ ), which is superimposed on the signals of the morpholino  $\text{CH}_2$  in  $\alpha$  to oxygen atom ( $\text{CH}_2\text{OCH}_2$ ). Again, the morpholino proton signals in  $\alpha$  to the nitrogen are split due to the two structural conformers at 3.94 ppm and 4.32 ppm ( $(\text{CH}_2)_2\text{N}^+\text{CH}_2$ )



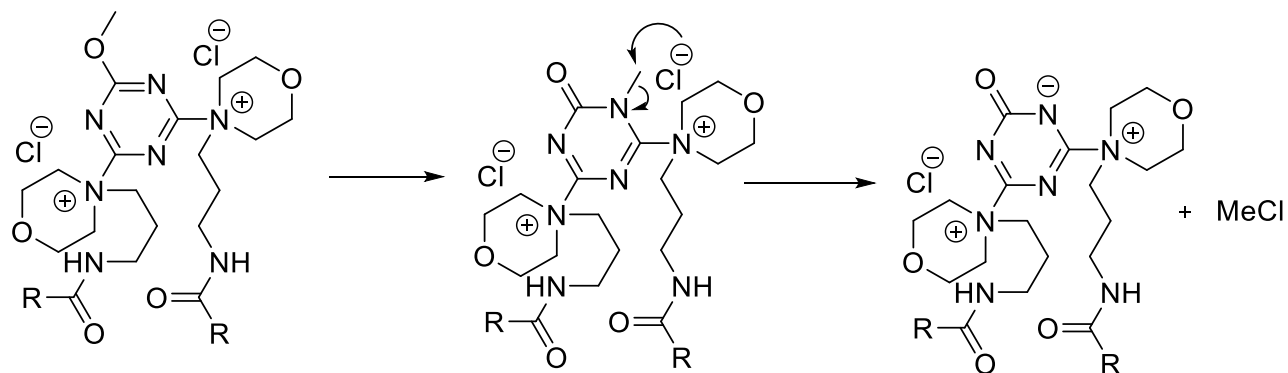
**Figure 3.17** -  $^1\text{H}$  NMR (DMSO- $d_6$ ) spectrum of MoPALA $_{12}$ MMT

The  $^{13}\text{C}$  NMR in figure 3.18 shows the spectrum of the MoPALA $_{12}$ MMT. 14.40 ppm signal corresponds to the terminal  $\text{CH}_3$  of the alkyl chain, the rest of the chain is then characterized by signals at 22.55, 25.63, 29.18, 29.23, 29.29, 29.43, 29.48, 29.52, 35.80, and 172.88 ppm with the latter representing carbonyl carbon. Propyl chain signals fall at 65.65, 35.84 and 31.76 ppm. Morpholine carbons fall at 58.22 ppm those proximal to oxygen and 61.56 ppm those proximal to nitrogen. At 164.55 ppm and 166.91 ppm fall the triazine carbon which have bounded chlorine and the triazine carbons which have bounded the morpholino residues, respectively.



**Figure 3.18** –  $^{13}\text{C}$  NMR (DMSO- $d_6$ ) spectrum of MoPALA $_{12}$ MMT

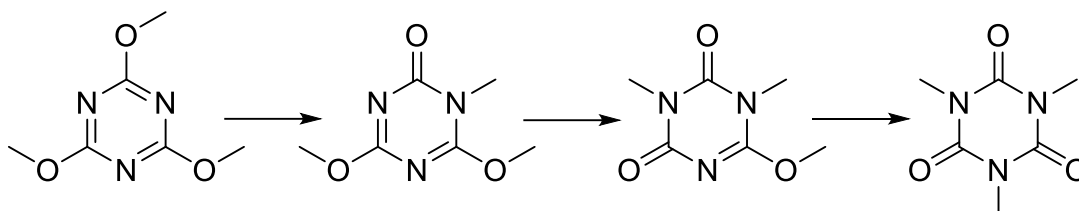
The lack of signal met by the spectrum can be attributed to demethylation by a nucleophilic attack of the chloride ion as a result of ring rearrangement, bringing the formation of 4,6-bis(4-(3-alkylamidopropyl)morpholino-4-ium)-2-oxo-2H-1,3,5-triazin-1-ide chloride (scheme 3.12).



**Scheme 3.12** – Formation of ,6-bis(4-(3-alkylamidopropyl)morpholino-4-ium)-2-oxo-2H-1,3,5-triazin-1-ide chloride from 4'-(6-methoxy-1,3,5-triazine-2,4-diyl)bis(4-(3-alkylamidopropyl)morpholin-4-ium) chloride by chlorine ion's nucleophilic attack on methyl after triazine rearrangement.



In fact, it is reported in the literature that methoxy-triazines undergo a rearrangement phenomenon that leads to the formation of the respective 1,3,5-triazinone<sup>[135-137]</sup>. This phenomenon, according to the work made by Handelsman-Benory et al.<sup>[138]</sup>, occurs through an intramolecular mechanism that leads to the formation of the final triazinone in various steps (scheme 3.13).

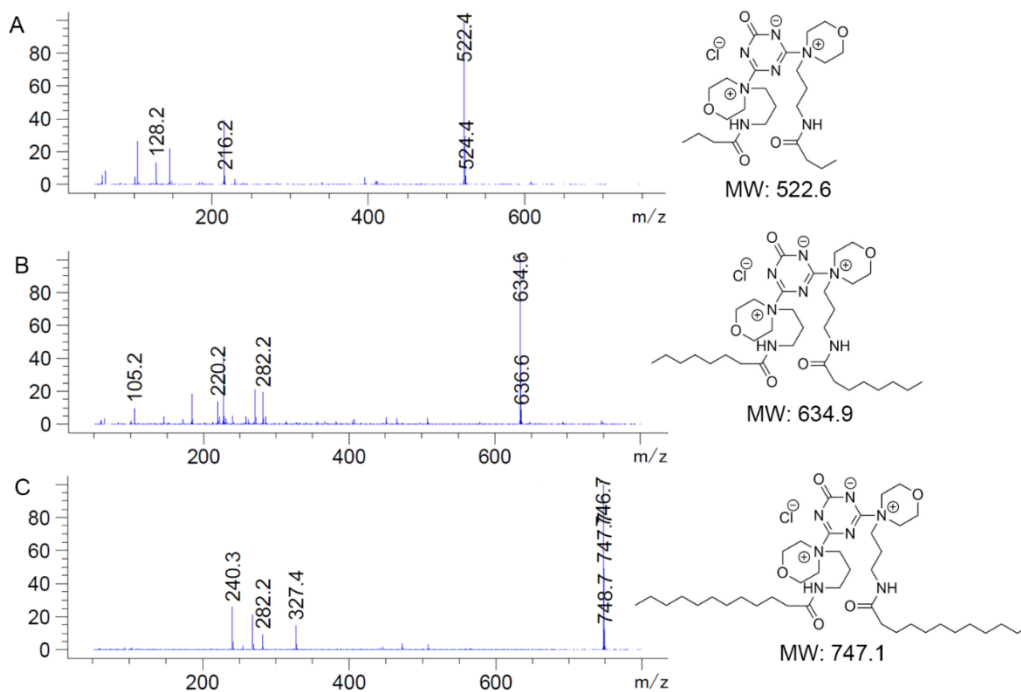


**Scheme 3.13** - Rearrangement accompanying methoxy substituents on triazine rings.

It is still not well understood why this phenomenon did not occur with bis-morpholino triazine ammonium salts that we have reported as condensation agents in our paper<sup>[120]</sup>. Seems there is a direct correlation between the steric hinderance of the morpholino substituent and the endocyclic bonding angles N-C-N bond angle of the triazine ring. This phenomenon is in fact described by Fridman et al<sup>[136]</sup> and an increase in the N-C-N triazine angle could favor the rearrangement phenomenon. However, further investigations are needed to better understand the course of the rearrangement.

As a result of the rearrangement, the nucleophilic attack of the chloride ion on methyl occurs as described in scheme 3.12, leading to the formation of methyl chloride and the 1,3,5-triazinone anion. This behavior of the chloride ion to react towards amine methyl has already been seen in the decomposition of DMTMM reported previously.<sup>[36]</sup>

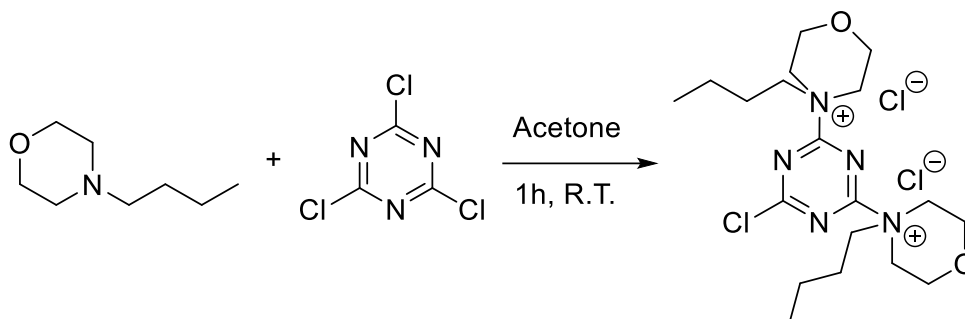
ESI-MS analyses also seem to support this thesis. From the mass spectra (figure 3.19) it is denoted that the molecular ion of the compound indicates a monocationic specie. We can also see that the final mass coincides with the hypothesized demethylated compound.



**Figure 3.19** –ESI-MS spectrum of MoPALA-MMT, A) MoPALA<sub>4</sub>MMT, [M]<sup>+</sup> = 522.4 m/z. B) MoPALA<sub>8</sub>CC, [M]<sup>+</sup> = 634.6 m/z. C) MoPALA<sub>12</sub>CC [M]<sup>+</sup> = 746.7.

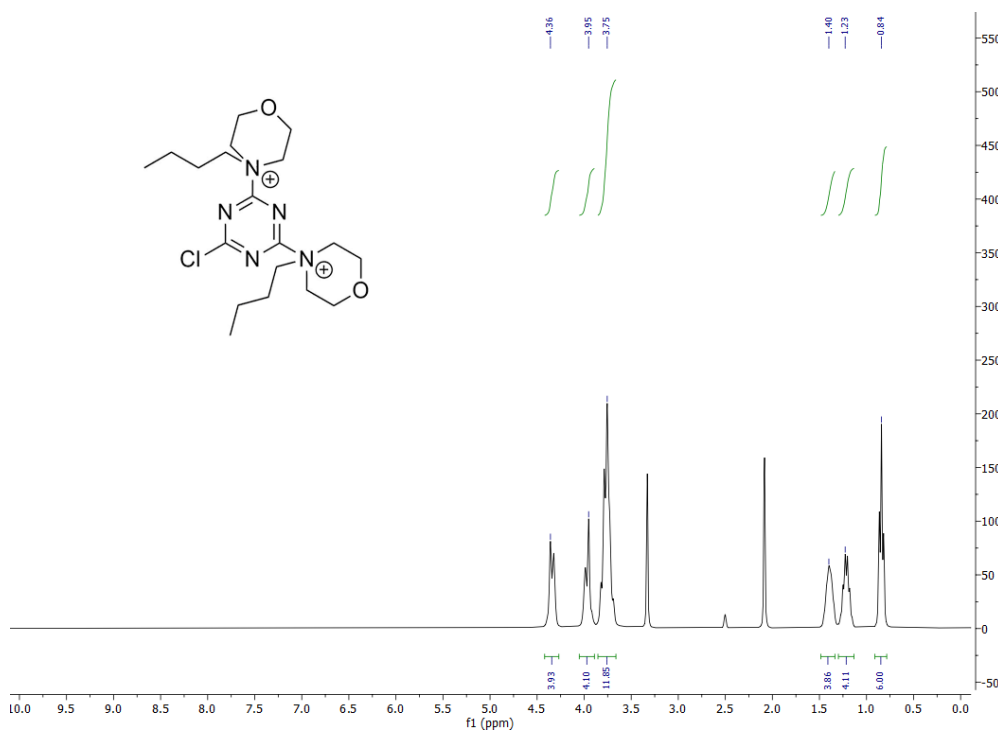
### 5.4.3 Synthesis of 4,4'-(6-chloro-1,3,5-triazine-2,4-diyl)bis(4-butylmorpholin-4-ium) chloride (BuMO-CC).

The synthesis of 4,4'-(6-chloro-1,3,5-triazine-2,4-diyl)bis(4-butylmorpholin-4-ium) chloride (BuMO-CC) (scheme 3.14) by reaction between butylmorpholine and cyanuric chloride is reported below. The reaction conditions are similar for those described in the synthesis of MoPALA-CC. The product is recovered by filtration for a yield of 26% resulting in 92% purity BuMO-CC.



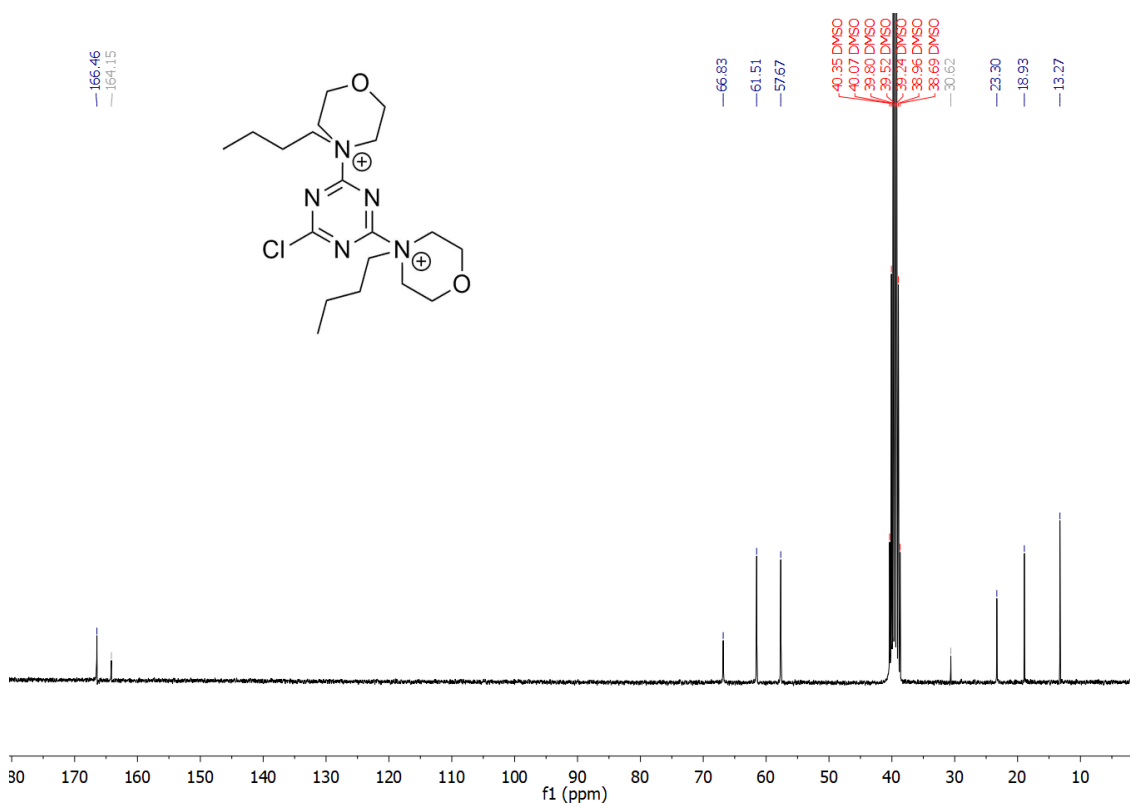
**Scheme 3.14** - Synthesis of 4,4'-(6-chloro-1,3,5-triazine-2,4-diyl)bis(4-butylmorpholin-4-ium) chloride

Figure 3.20 shows the  $^1\text{H}$  NMR spectrum of BuMO-CC. Signal assignment was done using both single-dimensional and two-dimensional techniques such as COSY, HMQC, and HMBC. The butyl side chain is characterized by four signals: at 0.84 ppm fall the terminal methyl ( $\text{CH}_2\text{CH}_3$ ), at 1.23 ppm falls the signal of the  $\text{CH}_2$  in  $\alpha$  to  $\text{CH}_3$  ( $\text{CH}_2\text{CH}_2\text{CH}_3$ ), at 1.40 ppm fall the signal of the  $\text{CH}_2$  in  $\beta$  to the ammonium ion ( $\text{CH}_2\text{CH}_2\text{N}^+$ ), and at 2.02 ppm fall the  $\text{CH}_2$  signal in  $\alpha$  to the carbonyl ( $\text{CH}_2\text{CO}$ ). At 3.74 ppm there is the peak which is the result of the superimposition of the signal of the  $\text{CH}_2$  in  $\alpha$  to the ammonium ( $\text{N}^+\text{CH}_2\text{CH}_2$ ) and the morpholine  $\text{CH}_2$  proximal to the oxygen ( $\text{CH}_2\text{OCH}_2$ ). Finally, the signals of morpholino  $\text{CH}_2$  in  $\alpha$  to the ammonium ion discriminated in axial and equatorial protons at 3.95 ppm and 4.36 ppm ( $\text{CH}_2\text{CN}^+(\text{CH}_2)_2$ ).



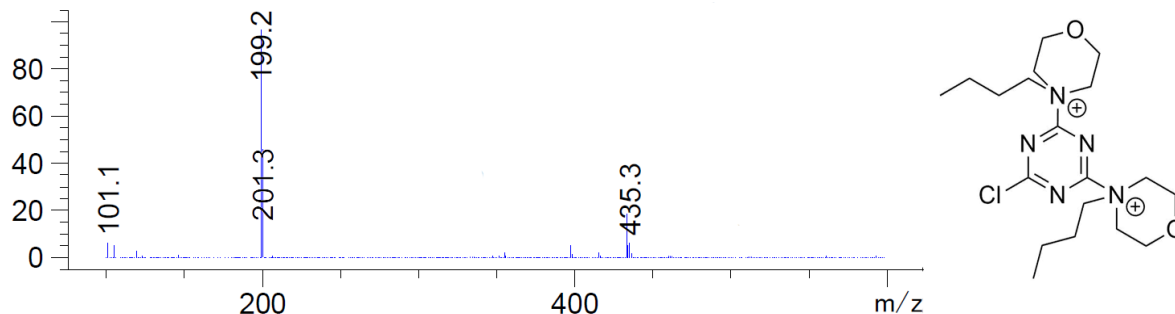
**Figure 3.20** –  $^1\text{H}$  NMR ( $\text{DMSO-d}_6$ ) spectrum of 4,4'-(6-chloro-1,3,5-triazine-2,4-diyl)bis(4-butylmorpholin-4-ium) chloride

Figure 3.21 shows the  $^{13}\text{C}$  NMR spectrum of 4,4'-(6-chloro-1,3,5-triazine-2,4-diyl)bis(4-butylmorpholin-4-ium) chloride. Butyl chain signals are clearly distinguishable at 13.27, 18.93, 23.30, and 66.83 ppm, with the first signal representing terminal  $\text{CH}_3$  and the last representing  $\text{CH}_2$  in  $\alpha$  to ammonium ion. At 57.67 the signals of the morpholino carbons adjacent to the oxygen atom fall, and at 61.51 fall the signals of the morpholino carbons in  $\alpha$  to the ammonium ion. The signals of the triazine carbons fall at 164.15 and 166.46, respectively, the carbon bound to the chlorine atom and those bound to the ammonium ion. It is also visible the signal of some residual acetone at 30.62.



**Figure 3.21** –  $^{13}\text{C}$  NMR ( $\text{DMSO-d}_6$ ) spectrum of 4,4'-(6-chloro-1,3,5-triazine-2,4-diyl)bis(4-butylmorpholin-4-ium) chloride

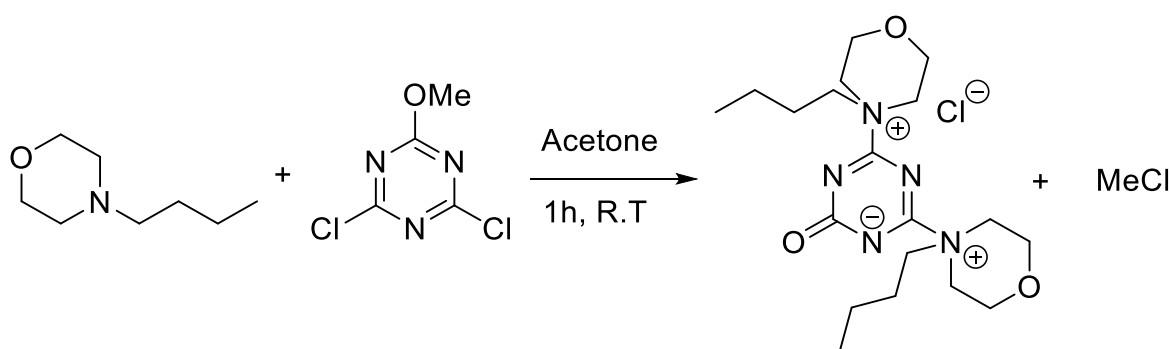
Finally, the ESI-MS analysis shown in the mass spectrum in figure 3.22 reports the molecular ion peak of the product at 199.2 m/z.



**Figure 3.22** – ESI-MS spectrum of 4,4'-(6-chloro-1,3,5-triazine-2,4-diyl)bis(4-butylmorpholin-4-ium) chloride  $[M]^{2+} = 199.2$

#### 5.4.4 Synthesis of 4,6-bis(4-butylmorpholino-4-ium)-2-oxo-2H-1,3,5-triazin-1-ide chloride (BuMO-MMT)

A test with MMT was also attempted with butylmorpholine. The same demethylation effect was found to occur as in the case of MoPALA-MMT. In the following, the synthesis of 4,6-bis(4-butylmorpholin-4-ium)-2-oxo-2H-1,3,5-triazin-1-ide chloride (BuMO-MMT) is described (scheme 3.15), using the same procedure as for the synthesis of BuMO-CC.



**Scheme 3.15** - Synthesis of 4,6-bis(4-butylmorpholino-4-ium)-2-oxo-2H-1,3,5-triazin-1-ide chloride

The final precipitates in the reaction environment and it is recovered by filtration. The final product result in a fine white powder for a yield of 20% consistent in 4,6-bis(4-butylmorpholino-4-ium)-2-oxo-2H-1,3,5-triazin-1-ide chloride.

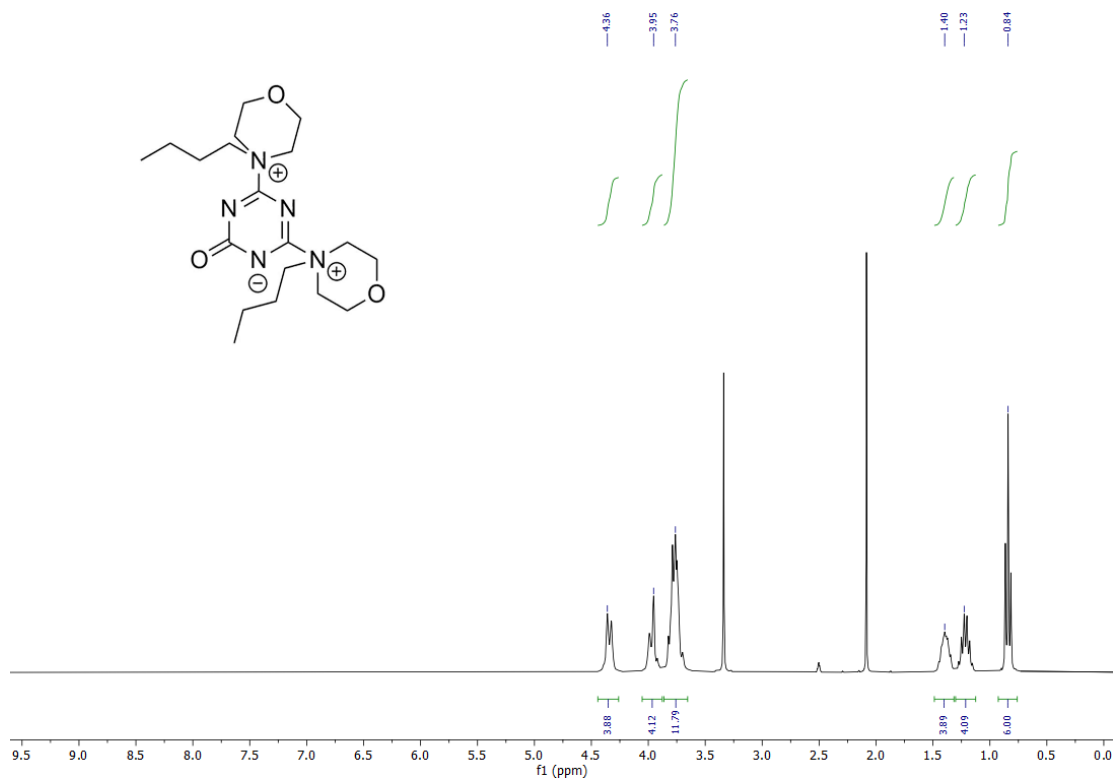


**Figure 3.23** –  $^1\text{H}$  NMR ( $\text{DMSO-d}_6$ ) spectrum of 4,6-bis(4-butylmorpholino-4-ium)-2-oxo-2H-1,3,5-triazin-1-ide chloride

Figure 3.23 shows the  $^1\text{H}$  NMR spectrum of BuMO-MMT. Signal assignment was done using both single-dimensional and two-dimensional techniques such as COSY, HMQC, and HMBC. The butyl side chain is characterized by four signals: at 0.84 ppm fall the terminal methyl ( $\text{CH}_2\text{CH}_3$ ), at 1.23 ppm falls the signal of the  $\text{CH}_2$  in  $\alpha$  to  $\text{CH}_3$  ( $\text{CH}_2\text{CH}_2\text{CH}_3$ ), at 1.40 ppm fall the signal of the  $\text{CH}_2$  in  $\beta$  to the ammonium ion ( $\text{CH}_2\text{CH}_2\text{N}^+$ ), and at 2.02 ppm fall the  $\text{CH}_2$  signal in  $\alpha$  to the carbonyl ( $\text{CH}_2\text{CO}$ ). At 3.76 ppm there is the peak which is the result of the superimposition of the signal of the  $\text{CH}_2$  in  $\alpha$  to the ammonium ( $\text{N}^+\text{CH}_2\text{CH}_2$ ) and the morpholinic  $\text{CH}_2$  proximal to the oxygen ( $\text{CH}_2\text{OCH}_2$ ). Finally, the signals of morpholine  $\text{CH}_2$  in  $\alpha$  to the ammonium ion discriminated in axial and equatorial protons at 3.95 ppm and 4.36 ppm ( $\text{CH}_2\text{CN}^+(\text{CH}_2)_2$ ).

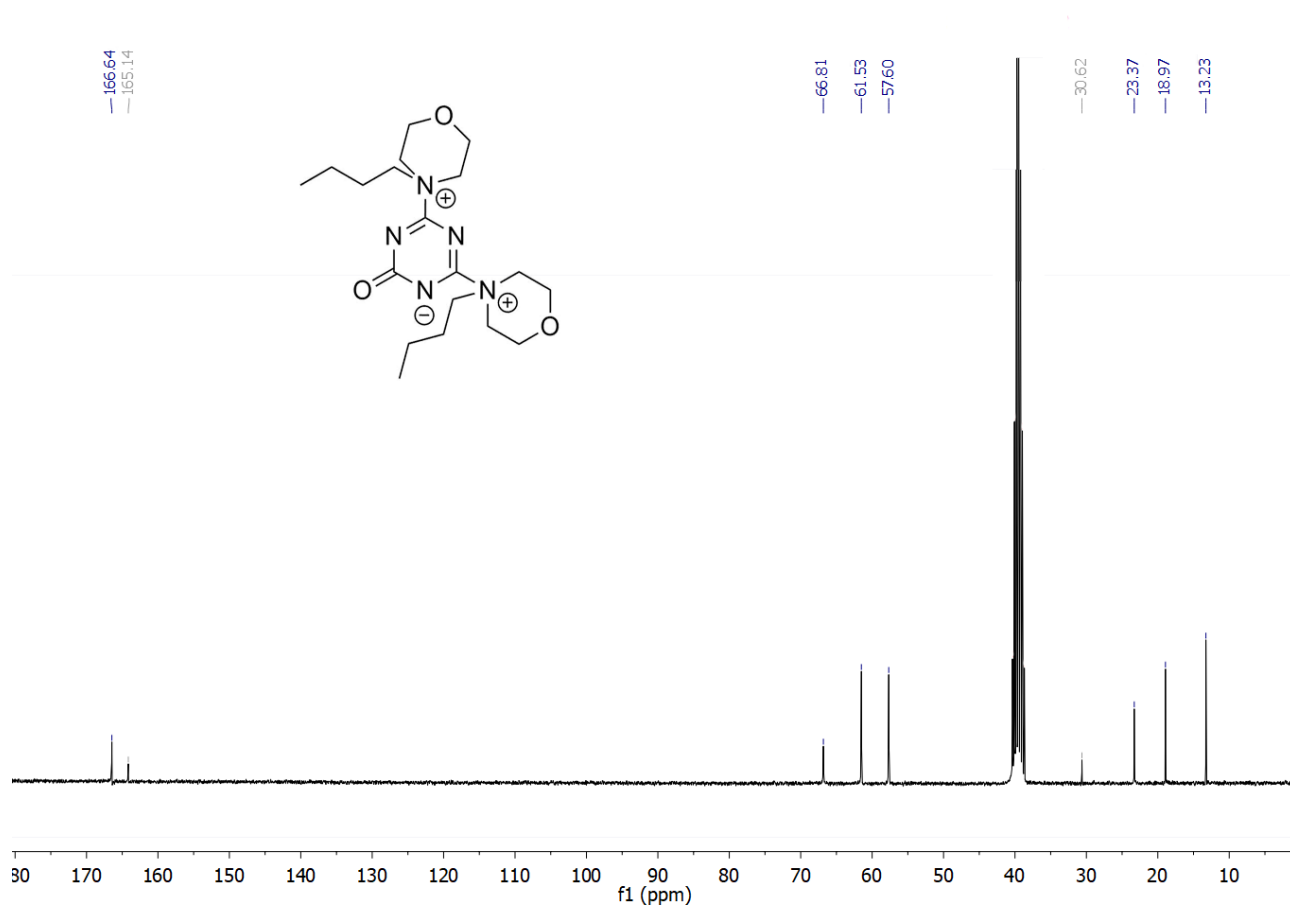


**Figure 3.24**  $^{13}\text{C}$  NMR (DMSO- $d_6$ ) spectrum of 4,6-bis(4-butylmorpholino-4-ium)-2-oxo-2H-1,3,5-triazin-1-ide chloride

Figure 3.24 shows the  $^{13}\text{C}$  NMR spectrum of 4,6-bis(4-butylmorpholino-4-ium)-2-oxo-2H-1,3,5-triazin-1-ide chloride. Butyl chain signals are clearly distinguishable at 13.23, 18.97, 23.37, and 66.81 ppm, with the first signal representing terminal  $\text{CH}_3$  and the last representing  $\text{CH}_2$  in  $\alpha$  to ammonium ion. At 57.60 fall the signals of the morpholino carbons adjacent to the oxygen atom, and at 61.53 the signals of the morpholino carbons in  $\alpha$  to the ammonium ion fall. The signals of the triazine carbons fall at 165.14 and 166.64, respectively, the carbon bound to the chlorine atom and those bound to the ammonium ion. It is also visible the signal of some residual acetone at 30.62.

The mass spectrum in figure 3.25 shows a molecular ion peak of 380.3 m/z which is attributable to 4,6-bis(4-butylmorpholino-4-ium)-2-oxo-2H-1,3,5-triazin-1-ide that have a molar mass of 380.51.

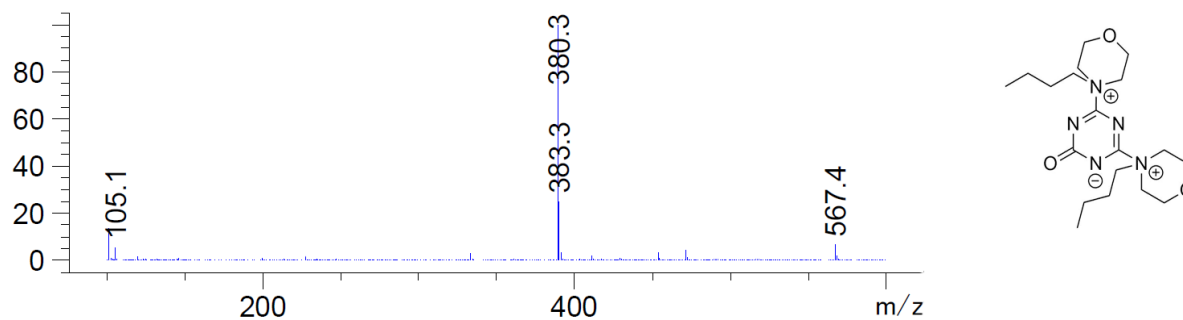


**Figure 3.25** ESI-MS spectrum of 4,4'-(6-chloro-1,3,5-triazine-2,4-diyl)bis(4-butylmorpholin-4-ium) chloride  $[M]^+ = 380.3$ .



### 3.3 Imidazole-based antimicrobial triazine quaternary ammonium salts

The second class of triazine compounds reported in this work are imidazole-based TQACs. As mentioned above (chapter 3.1), imidazole-CDMT ammonium salts, and more generally CDMT-Ams derived from aromatic amines, are extremely stable in various solvents. In fact, these structure reported in figure 3.26 not show reactivity towards condensation reactions and can be recovered entirely from solution<sup>[36]</sup>. Similarly to the case of morpholino-triazine compounds also imidazole-triazine compounds can be exploited for the synthesis of TQACs. In addition, imidazole is well known in the scientific community in the medical and veterinary fields as an antifungal<sup>[139-141]</sup> and antiviral<sup>[142,143]</sup>.

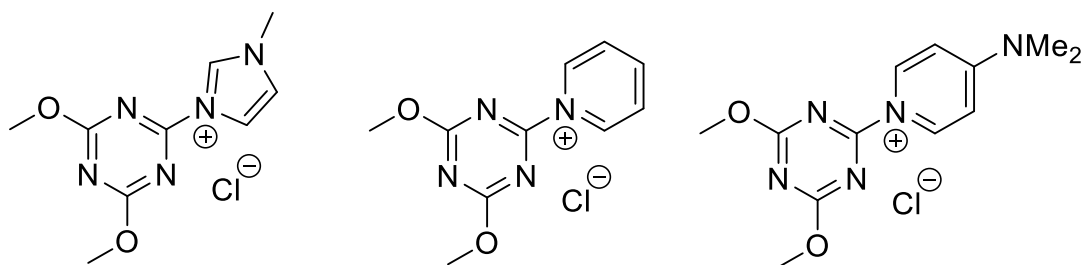


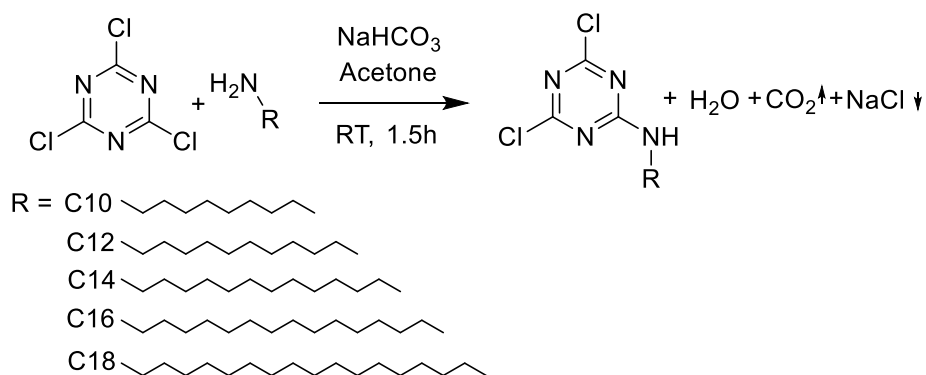
**Figure 3.26** – Stable CDMT-Ams salts that are unable to perform dehydrocondensation reactions

In this section are reported the data achieved by exploiting cyanuric chloride for the design of TQACs by use of long alkyl chains directly bonded to the triazine ring. In Fact, the difficulties we encountered in the synthesis of morpholino triazine TQACs, such as poor yield in terms of isolated product, seems lie in the inability of the chlorotriazines to react with hindered tertiary amines. Therefore, we changed our approach going to insert the long side chain directly on the chloro triazine precursor. We then synthesize dichloro mono alkyl triazines (MAT) with alkyl chains of variable length. We will then discuss their use for the synthesis of imidazole bis-TQACs, imidazole mono-TQACs and bipyridyl multi-TQACs.

### 3.3.1 Synthesis of 4,6-dichloro-*N*-alkyl-1,3,5-triazin-2-amine (MAT)

At first, we proceeded to synthesize precursors exhibiting a hydrophobic alkyl residue by directly binding long-chain alkyl amine to cyanuric chloride taking advantage of its high reactivity towards amine compounds.

Scheme 3.16 describe the synthesis of different 4,6-dichloro-*N*-alkyl-1,3,5-triazin-2-amine (MAT) having alkyl chains of variable length by reacting cyanuric chloride with *N*-alkylamine using NaHCO<sub>3</sub> as a scavenger of the HCl formed during the reaction.



**Scheme 3.16** – General synthesis of MATs

The reaction was monitored by GC and after 1.5h total conversion in the corresponding 4,6-dichloro-*N*-alkyl-1,3,5-triazin-2-amine achieved in all cases. The final products were obtained after a reprecipitation in hexane and final yields obtained were 51% for 4,6-dichloro-*N*-decyl-1,3,5-triazin-2-amine (MAT<sub>10</sub>), 96% for 4,6-dichloro-*N*-dodecyl-1,3,5-triazin-2-amine (MAT<sub>12</sub>), 52% for 4,6-dichloro-*N*-tetradecyl-1,3,5-triazin-2-amine (MAT<sub>14</sub>), 71% for 4,6-dichloro-*N*-hexadecyl-1,3,5-triazin-2-amine, 50% for 4,6-dichloro-*N*-octadecyl-1,3,5-triazin-2-amine (table 3.7).

**Table 3.7** - Yield in isolated product of MAT<sub>10</sub>, MAT<sub>12</sub>, MAT<sub>14</sub>, MAT<sub>16</sub> and MAT<sub>18</sub>

| Compounds         | Yield | Purity |
|-------------------|-------|--------|
| MAT <sub>10</sub> | 51%   | 87%    |

|                         |     |     |
|-------------------------|-----|-----|
| <b>MAT<sub>12</sub></b> | 96% | 93% |
| <b>MAT<sub>14</sub></b> | 52% | 91% |
| <b>MAT<sub>16</sub></b> | 71% | 94% |
| <b>MAT<sub>18</sub></b> | 50% | 86% |

The <sup>1</sup>H NMR and <sup>13</sup>C NMR spectrum of MAT<sub>10</sub>, MAT<sub>12</sub>, MAT<sub>14</sub>, MAT<sub>16</sub> and MAT<sub>18</sub> (figure 3.27 and figure 3.28) are very similar, varying for the integrations of the peaks related to the alkyl chain and the chemical shift of the amine hydrogen. As reference, therefore, we comment only the <sup>1</sup>H NMR and <sup>13</sup>C NMR spectrum of MAT<sub>12</sub> (figure 3.29 and figure 3.30). Signal assignment was done using both single-dimensional and two-dimensional techniques such as COSY, HMQC, and HMBC.

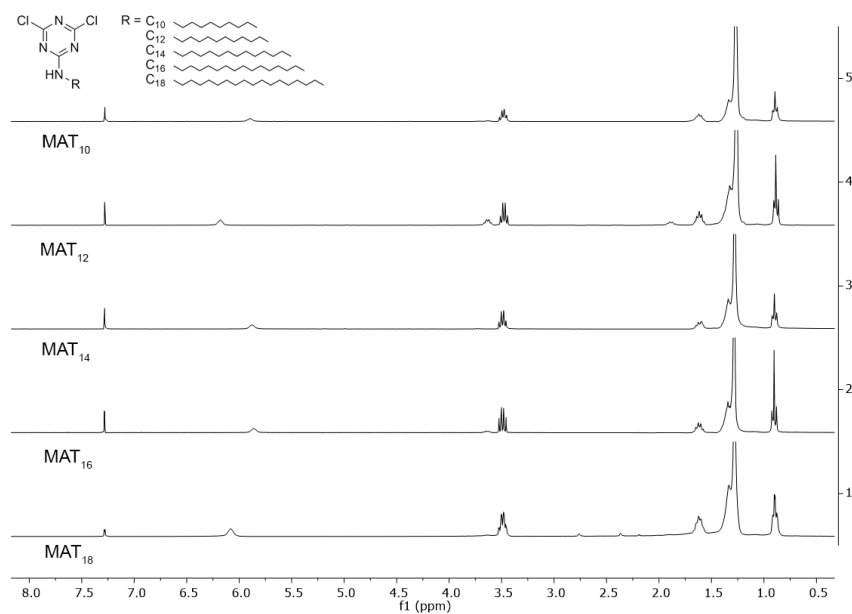


**Figure 3.27** - <sup>1</sup>H NMR (CDCl<sub>3</sub>) spectrum of MATs

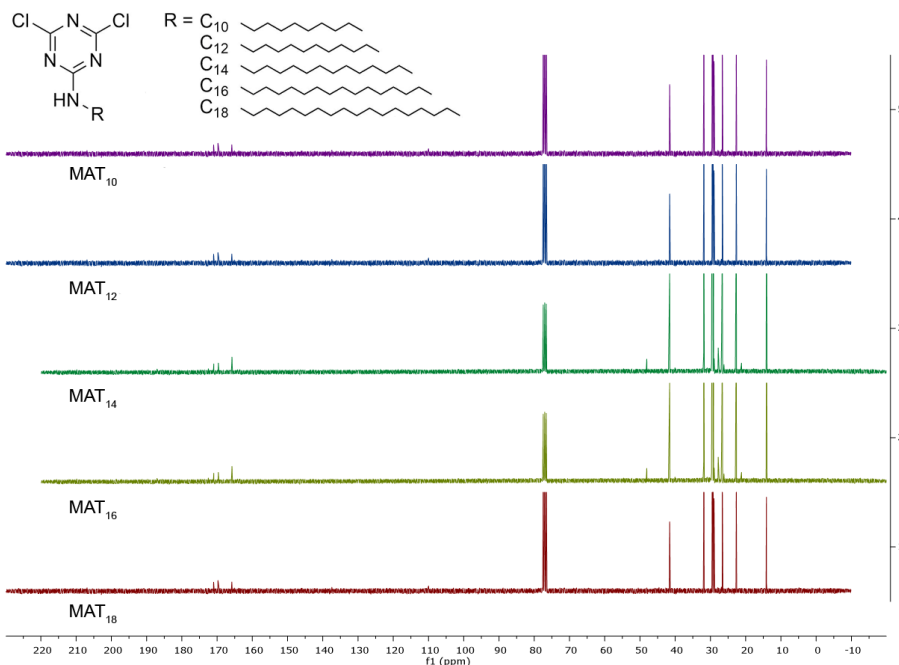


**Figure 3.28** -  $^{13}\text{C}$  NMR ( $\text{CDCl}_3$ ) spectrum of MATs

In figure 3.29 is reported the  $^1\text{H}$  NMR spectrum of  $\text{MAT}_{12}$ . We can recognize the signal at 6.42 ppm corresponds to hydrogen bonded to nitrogen ( $\text{NH}$ ), that is broad due to the effect of quadrupolar relaxation of the nitrogen atom. The signal at 3.47 ppm corresponds to the  $\text{CH}_2$  of the alkyl chain in  $\alpha$  to the amine group ( $\text{HNCH}_2\text{CH}_2$ ), at 1.62 ppm there is a signal that corresponds to the  $\text{CH}_2$  of the alkyl chain in  $\beta$  to the amine group ( $\text{CH}_2\text{CH}_2\text{CH}_2\text{NH}$ ), signal at 1.25 ppm corresponds to the  $\text{CH}_2$  in the middle of the alkyl chain ( $\text{CH}_2(\text{CH}_2)_9\text{CH}_2$ ), finally the signal at 0.85 ppm corresponds to the signal of terminal methyl ( $\text{CH}_3\text{CH}_2$ ).

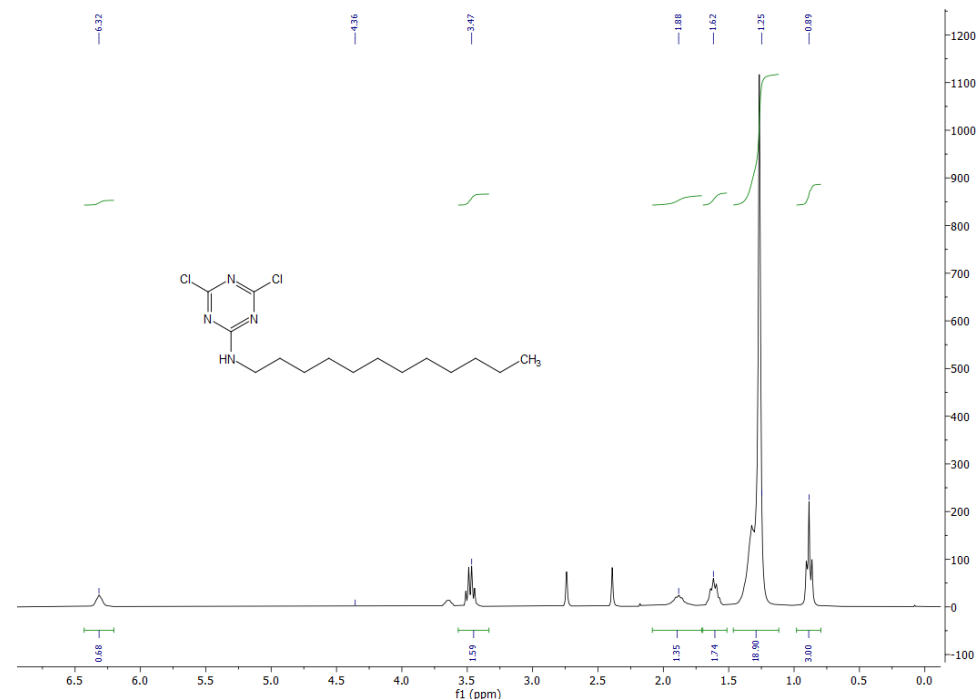
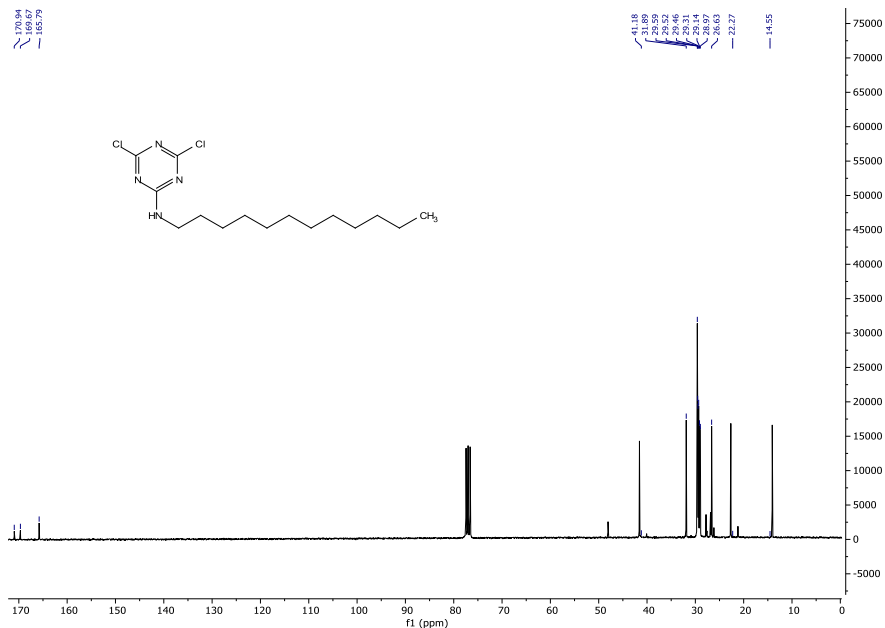


**Figure 3.29** -  $^1\text{H}$  NMR spectrum (DMSO- $d_6$ ) of MAT<sub>12</sub>

In figure 3.30 is reported the  $^{13}\text{C}$  NMR spectrum of MAT<sub>12</sub>, the signals at 171.07 and 169.80 ppm correspond to the carbon atoms of triazine ring bounded to chlorine atoms ( $\text{N}_2\text{C}\text{Cl}$ ), these signals are split due to the formation of two atropoisomers in solution as a result of the impediment of free rotation of the alkyl chain on the  $\text{C}(\text{Ar})\text{-N}$  axis. The signal at 165.92 ppm corresponds to the carbon of the triazine ring bounded to the amine nitrogen of the alkyl amine ( $\text{N}_2\text{C}\text{NH}$ ). The signal at 41.70 ppm corresponds to the carbon atom bounded to the amine nitrogen of the alkyl chain ( $\text{HN}\text{CH}_2\text{CH}_2$ ), the signals at 32.02, 29.73, 26.77 and 22.80 ppm correspond to the carbons ( $\text{CH}_2(\text{CH}_2)_9\text{CH}_2$ ) of the long alkyl chain and finally the signal at 14.22 ppm corresponds to the primary terminal carbon of the alkyl chain ( $\text{CH}_2\text{CH}_3$ ).



**Spettro 3.30** -  $^{13}\text{C}$  NMR ( $\text{CDCl}_3$ ) spectrum of  $\text{MAT}_{12}$

The storage of MATs should be carried out in a cool, dry environment since, as shown in figure 3.31, with advancing time the two residual chlorine atoms tend to react with the moisture giving as by-products 4-chloro-6-(alkylamino)-1,3,5-triazin-2-ol  $\text{MAT}(\text{OH})$  or 6-(alkylamino)-1,3,5-triazine-2,4-diol  $\text{MAT}(\text{OH})_2$ . The products were then stored in a dryer equipped with drying agents. The presence of OH is easily detected by the signal at 11.16 ppm corresponds to hydroxyl protons (**COH**), integrations confirm the presence of the disubstituted product.

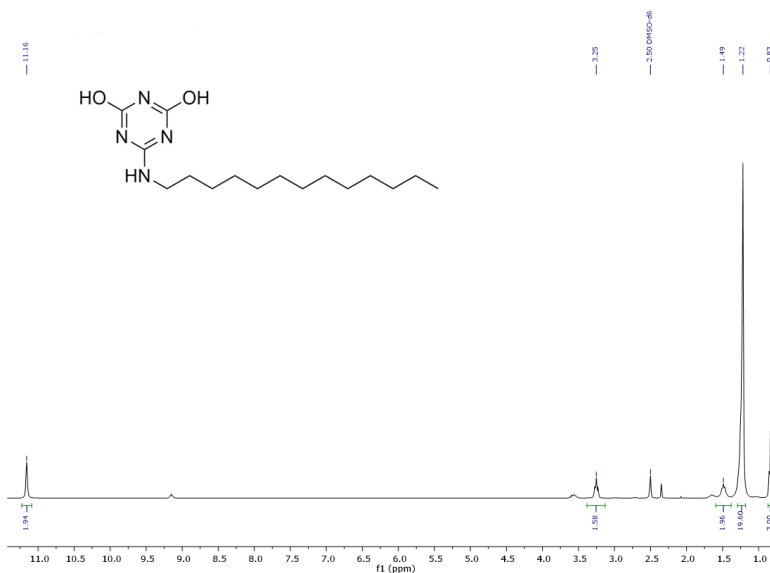


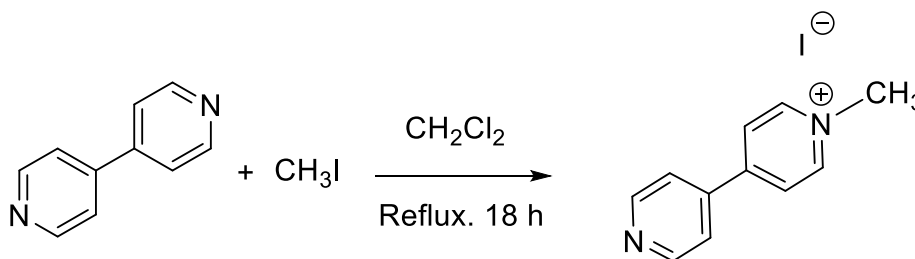
**Figure 3.31** -  $^1\text{H}$  NMR ( $\text{DMSO-d}_6$ ) spectrum of  $\text{MAT}_{12}(\text{OH})_2$

### 3.2 Synthesis of 1-methyl-[4,4'-bipyridin]-1-ium iodide (MBP)

Several examples for the synthesis of antimicrobial multi-QACs exist in the literature<sup>[144,145]</sup>, showing an activity more or less comparable with bis-QACs.

For further investigation, we tried to devise multi-TQACs to compare their antimicrobial activity with bis-TQACs. Exploiting the potential of an aromatic compound such as bipyridyl to form two ammonium groups, we used it in combination with MATs to obtain a compound with four ammonium groups.

Therefore, we proceeded with the synthesis of 1-methyl-[4,4'-bipyridin]-1-ium iodide as shown in scheme 3.17. This compound was already used by Minbiole's group<sup>[146]</sup> for the synthesis of several multi-QACs.



**Scheme 3.17** – Synthesis of 1-methyl-[4,4'-bipyridin]-1-ium iodide (MBP)

The synthesis was carried out as reported by Minbiole et al.<sup>[146]</sup>. 4,4'-bipyridine was mixed with methyl iodide in refluxed dichloromethane and reacted for at least one night. According to Minbiole<sup>[146]</sup> the final product was a mixture of mono substituted bipyridine and a bis substituted bipyridine. The monosubstituted product was separated from the bis substituted product by fractional solubilization in methanol. After filtration, the organic solvent was evaporated obtaining a brown solid powder which was characterized by <sup>1</sup>H NMR and <sup>13</sup>C NMR corresponding to 1-methyl-[4,4'-bipyridin]-1-ium iodide (96% yield).

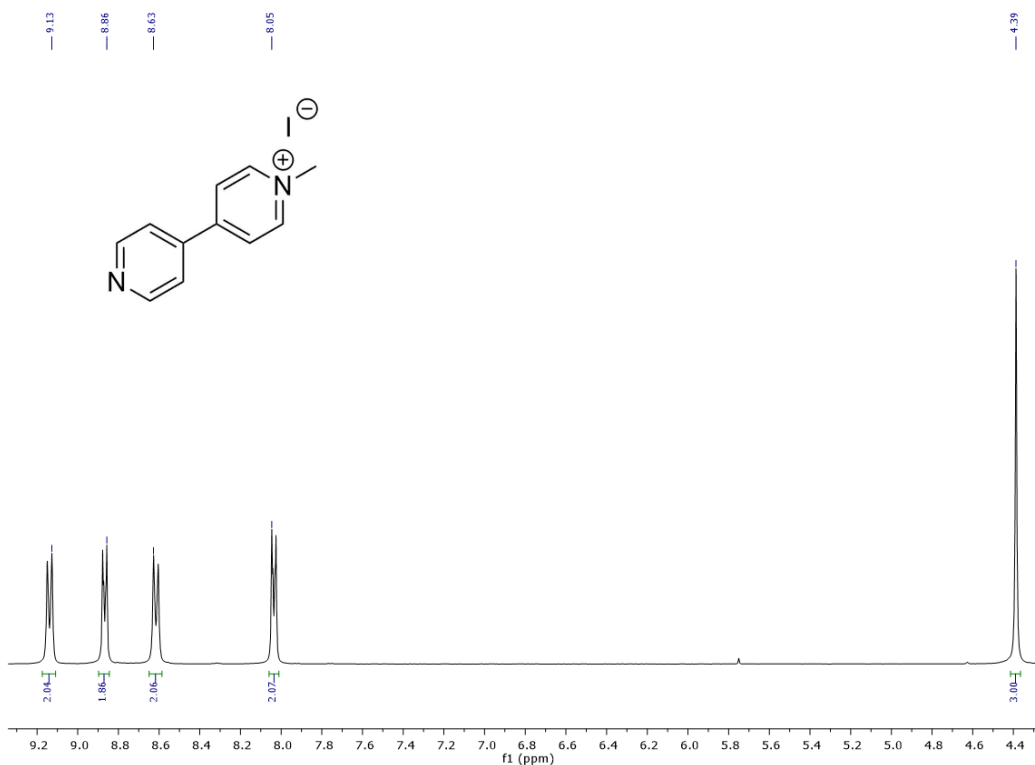


**Figure 3.32** -  $^1\text{H}$  NMR (DMSO- $d_6$ ) of MBP

The  $^1\text{H}$  NMR and  $^{13}\text{C}$  NMR are reported in figure 3.32 and figure 3.33. Signal assignment was done using both single-dimensional and two-dimensional techniques such as COSY, HMQC, and HMBC.

Figure 3.32 represent the  $^1\text{H}$  NMR spectrum; it is possible to recognize the signal at 9.13 ppm corresponds to CH of the pyridine ring in ortho to quaternary nitrogen ( $\text{CHCHN}^+$ ), the signal at 8.86 ppm corresponds to CH of the pyridine ring in ortho to tertiary nitrogen ( $\text{CHCHN}$ ), the signal at 8.63 ppm corresponds to the CH of the pyridine ring in meta to quaternary nitrogen ( $^+\text{NCHCHC}$ ), the signal at 8.05 ppm corresponds to the CH of the pyridine ring in meta to tertiary nitrogen ( $\text{NCHCHC}$ ), and finally, the signal at 4.39 ppm corresponds to the protons of the methyl group ( $\text{CH}_3\text{N}^+$ ).



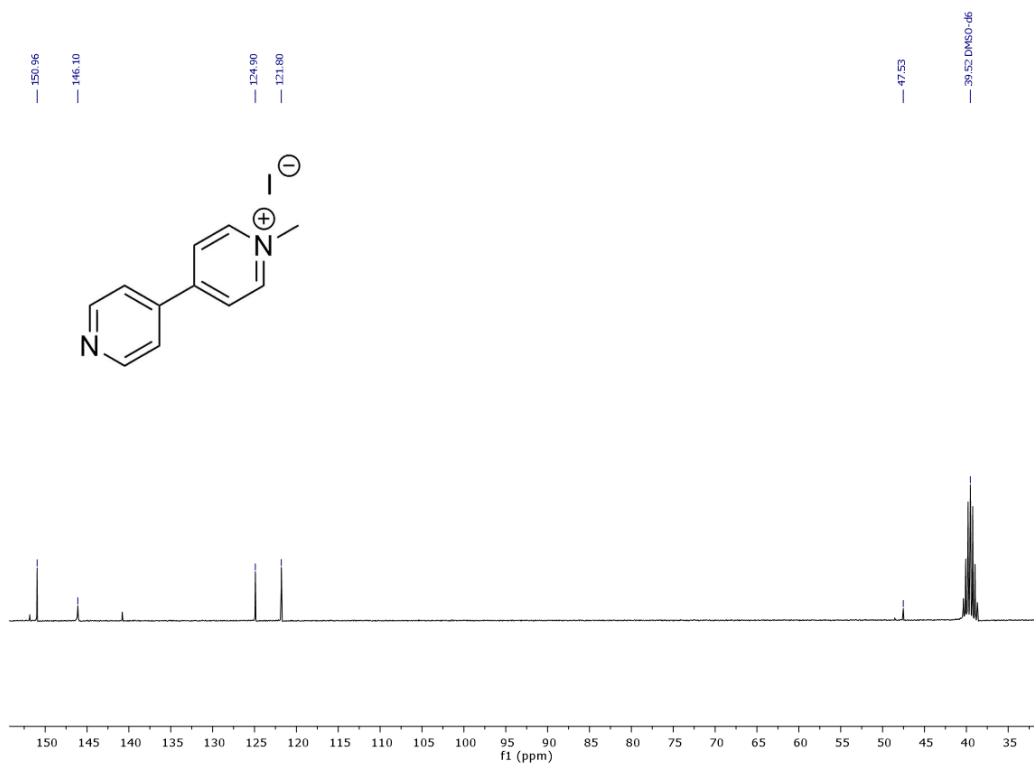
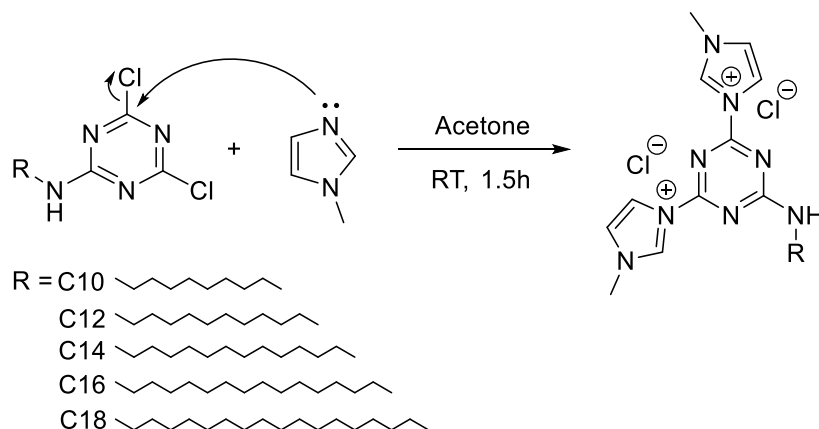


**Figure 3.33**  $^{13}\text{C}$  NMR ( $\text{DMSO-d}_6$ ) of MBP

Figure 3.33 represent the  $^{13}\text{C}$  NMR spectrum of MBP. The signal at 150.96 ppm corresponds to the carbons in ortho to quaternary nitrogen ( $\text{CHCHN}^+$ ), at 146.10 ppm there is the signal from the carbons in ortho to the tertiary nitrogen ( $\text{CHCHN}$ ), the signal at 124.90 ppm corresponds to the carbons in meta to quaternary nitrogen ( $^+\text{NCHCHC}$ ), the signal at 121.80 ppm corresponds to the carbons in meta to tertiary nitrogen atom ( $\text{NCHCHC}$ ), finally, the signal at 47.53 ppm corresponds to the methyl carbon bound to quaternary nitrogen ( $\text{CH}_3\text{N}^+$ ).

### 3.3.3 Synthesis of 3,3'-(6-(alkylamino)-1,3,5-triazine-2,4-diyl)bis(1-methyl-1*H*-imidazol-3-ium) chloride (MATdMIMI)

The synthesis of bis 3,3'-(6-(alkylamino)-1,3,5-triazine-2,4-diyl)bis(1-methyl-1*H*-imidazol-3-ium) chloride (MATdMIMI) was carried out as reported in Scheme 3.18.



**Scheme 3.18** – Synthesis of MATdMIMIs

In this system we chose to use a large excess of imidazole (ratio 1:5) to favor the di-substitution of the triazine ring. The products under the reaction conditions are easily recovered from reaction mixture by simple filtration. The fine white powders recovered were characterized by  $^1\text{H}$  NMR,  $^{13}\text{C}$  NMR, COSY, FT-IR, ESI-MS and m.p. resulting in 3,3'-(6-(decylamino)-1,3,5-triazine-2,4-diyl)bis(1-methyl-1*H*-imidazol-3-ium) chloride (MAT<sub>10</sub>dMIMI), 3,3'-(6-(dodecylamino)-1,3,5-triazine-2,4-diyl)bis(1-methyl-1*H*-imidazol-3-ium) chloride (MAT<sub>12</sub>dMIMI), 3,3'-(6-(tetradecylamino)-1,3,5-triazine-2,4-diyl)bis(1-methyl-1*H*-imidazol-3-ium) chloride (MAT<sub>14</sub>dMIMI), 3,3'-(6-(hexadecylamino)-1,3,5-triazine-2,4-diyl)bis(1-methyl-1*H*-imidazol-3-ium) chloride (MAT<sub>16</sub>dMIMI) (82%) yield and 3,3'-(6-(alkylamino)-1,3,5-triazine-2,4-diyl)bis(1-methyl-1*H*-imidazol-3-ium) chloride (MAT<sub>18</sub>dMIMI). Yields and purity of the different compounds are reported in table 3.8.

**Table 3.8** - Yield in isolated product of MAT<sub>10</sub>dMIMI, MAT<sub>12</sub>dMIMI, MAT<sub>14</sub>dMIMI, MAT<sub>16</sub>dMIMI and MAT<sub>18</sub>dMIMI

| Compounds               | Yield | Purity |
|-------------------------|-------|--------|
| <b>MAT<sub>10</sub></b> | 86%   | 96%    |
| <b>MAT<sub>12</sub></b> | 97%   | 98%    |
| <b>MAT<sub>14</sub></b> | 97%   | 98%    |
| <b>MAT<sub>16</sub></b> | 82%   | 92%    |
| <b>MAT<sub>18</sub></b> | 99%   | 93%    |

*N*-methylimidazole, due to the presence of two nitrogen atoms in the cycle, has the possibility to react in two different positions, leading to the formation of two possible isomers as shown in figure 3.34.

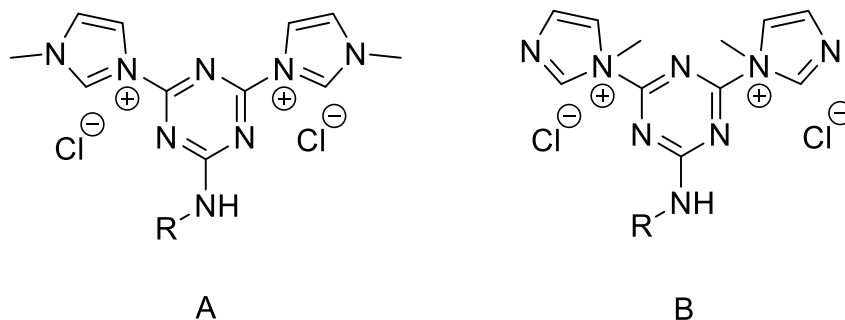


**Figure 3.34** – Possible isomers of MATdMIMI, A) 1,3 disubstituted imidazolium isomer B) 1,1 disubstituted imidazolium isomer

According to Hoffman<sup>[147]</sup>, the *N*-alkylimidazoles in addition reactions with electrophilic groups for the synthesis of dialkylimidazolium salts lead to the formation of the 1,3-disubstituted isomer A rather than the 1,1-disubstituted B. Therefore, it is presumable that all MATdMIMIs are in the form of the A isomer (figure 3.34 A)

The <sup>1</sup>H NMR and <sup>13</sup>C NMR spectrum of MAT<sub>10</sub>dMIMI, MAT<sub>12</sub>dMIMI, MAT<sub>14</sub>dMIMI, MAT<sub>16</sub>dMIMI and MAT<sub>18</sub>dMIMI reported in figure 3.35 and figure 3.36, show almost identical chemical shifts, varying only the integrations of the peaks related to the alkyl chain. As example, therefore, we comment only the <sup>1</sup>H NMR and <sup>13</sup>C NMR spectrum of MAT<sub>12</sub>dMIMI (figures 3.37 - 3.40). Signal assignment was done using both single-dimensional and two-dimensional techniques such as COSY, HMQC, and HMBC.

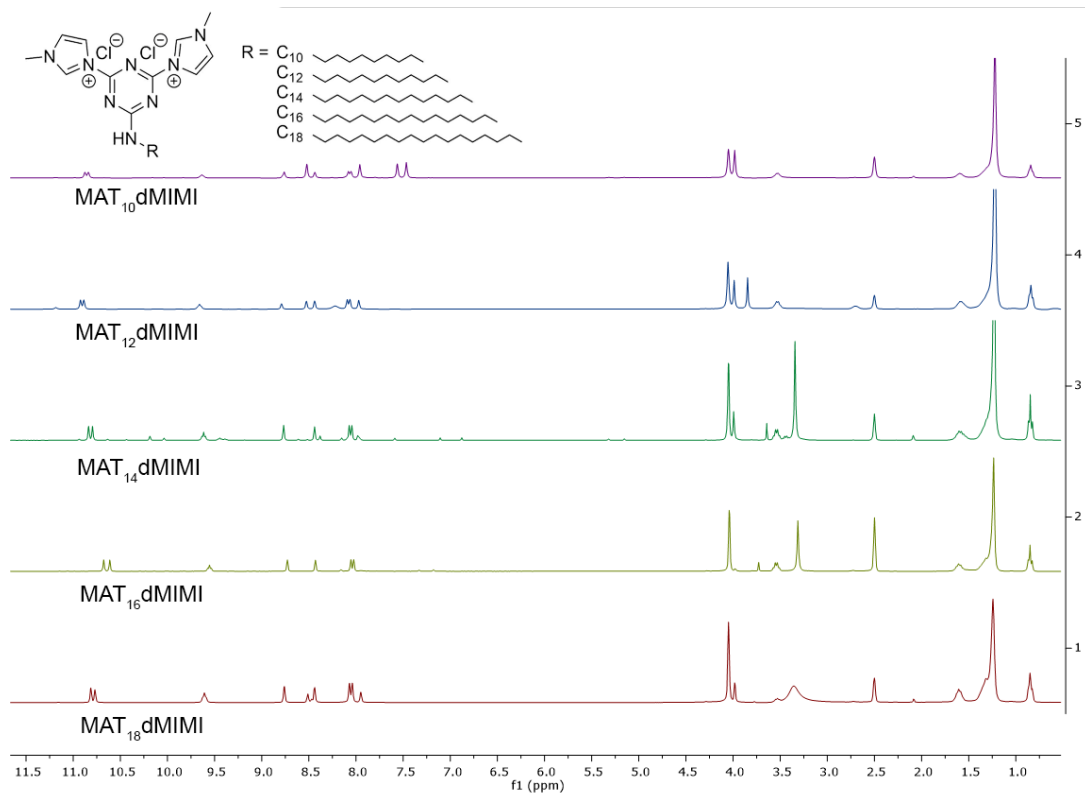
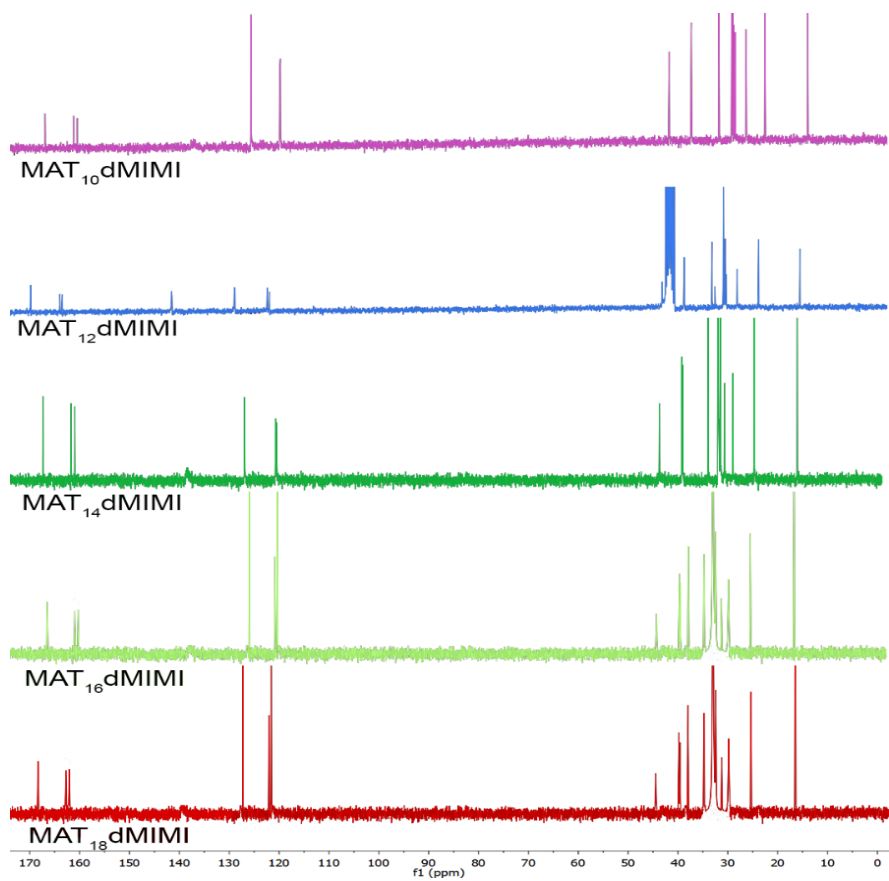
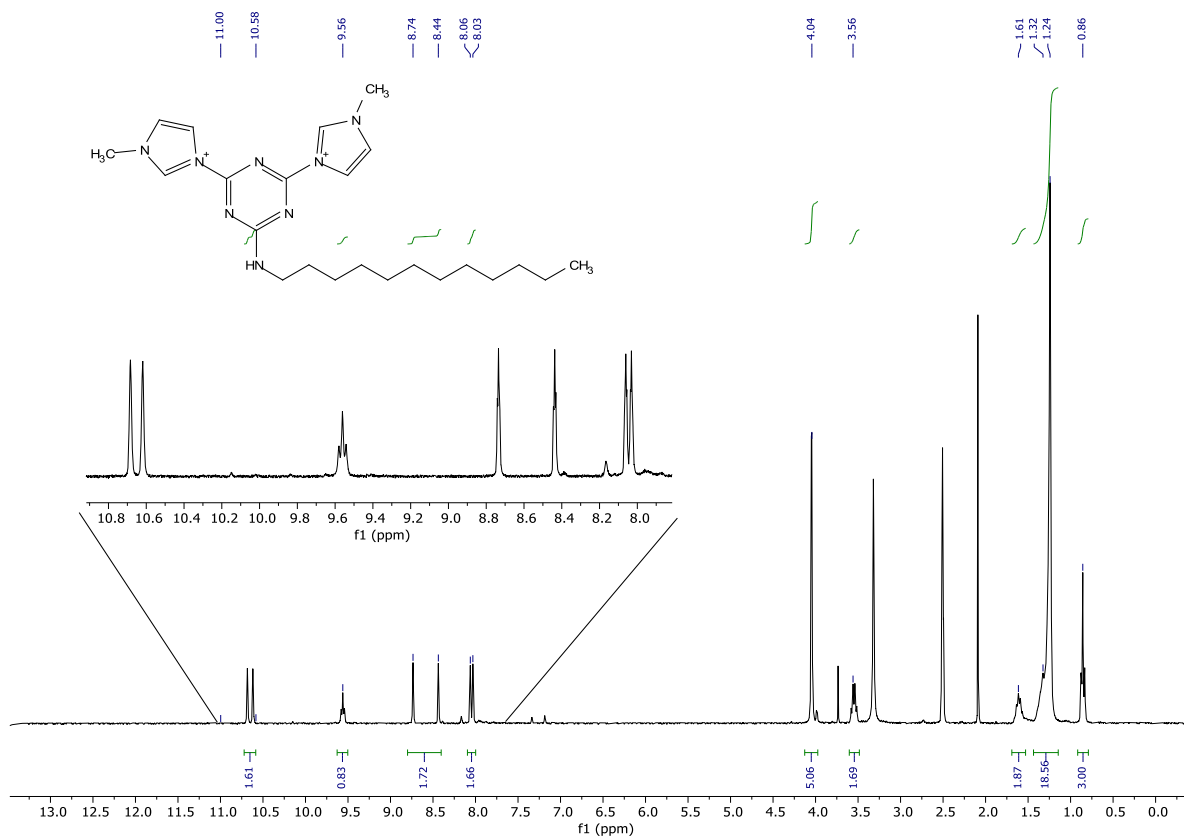


Figure 3.35 - <sup>1</sup>H NMR (DMSO-d<sub>6</sub>) spectrum of MATdMIMIs



**Figure 3.36** -  $^{13}\text{C}$  NMR ( $\text{DMSO-d}_6, \text{D}_2\text{O}$ ) spectra of MATdMIMIs



**Figure 3.37** -  $^1\text{H}$  NMR ( $\text{DMSO-d}_6$ ) spectrum of MAT<sub>12</sub>dMIMI

In figure 3.37 is reported the  $^1\text{H}$  NMR spectrum of MAT<sub>12</sub>dMIMI where the signals between 8.00-11.00 ppm correspond to the hydrogens of the imidazole ring, which appear splitted due to the impediment of the free rotation of the alkyl chain around the Ar-N axis. This behavior creates a pair of atropoisomers (figure 3.38) identifiable by the imidazoline ring signals splitting into two different signals. This behavior is also revealed by COSY spectra (figure 3.39) which show cross picks between the splitted signals. This phenomenon of impediment of free rotation on the (Ar)C-N axis in the amine substituents of chlorotriazines had already been reported in the literature by the group of Katritzky<sup>[148]</sup>. Therefore, the signals at 10.68 ppm and 10.61 ppm can be considered as one that correspond of CH located between the two nitrogen atoms of the ring ( $\text{NCHN}^+$ ), the signal at 9.55 ppm corresponds to hydrogen bound to the terminal nitrogen of the side chain ( $\text{CNHCH}_2$ ), the signals at 8.73 ppm and 8.43 ppm correspond to CH in  $\alpha$  to the quaternary nitrogen of the imidazole ring ( $\text{CHCHN}^+$ ), the signals at 8.05 and 8.02 ppm corresponding to CH in  $\alpha$  to the tertiary nitrogen atom of the imidazole ring ( $\text{CHCHNCH}_3$ ).

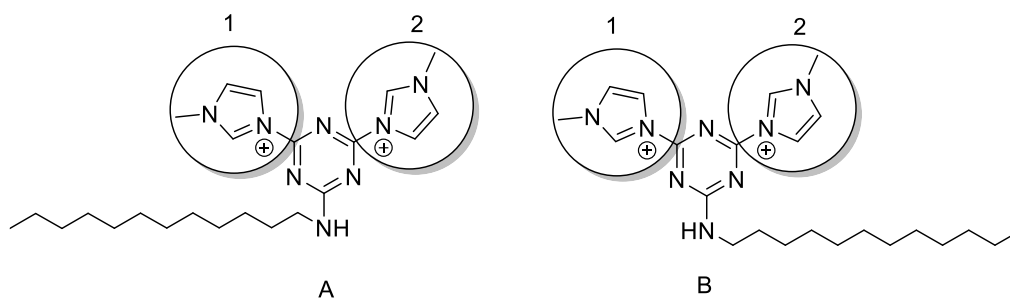


**Figure 3.38** – Representation of the atropisomers pair formed by impediment to free rotation of the Ar-N axis of the alkyl chain

The signal at 4.04 ppm corresponds to the two CH<sub>3</sub> of the imidazole rings (**CH<sub>3</sub>N**), the signal at 3.53 ppm corresponds of the CH<sub>2</sub> of the alkyl chain in α to the terminal amine (**HNCH<sub>2</sub>CH<sub>2</sub>**), at 1.61 ppm corresponds to the signal of CH<sub>2</sub> of the alkyl chain in β to the terminal amine (**HNCH<sub>2</sub>CH<sub>2</sub>CH<sub>2</sub>**), at 1.23 ppm there is the signal ascribable to the nine central CH<sub>2</sub> groups of the chain (**CH<sub>2</sub>(CH<sub>2</sub>)<sub>9</sub>CH<sub>2</sub>**), finally the signal at 0.85 ppm corresponds to the terminal CH<sub>3</sub> of the alkyl chain (**CH<sub>3</sub>CH<sub>2</sub>**), the latter signal was used as a reference for peak integrations.

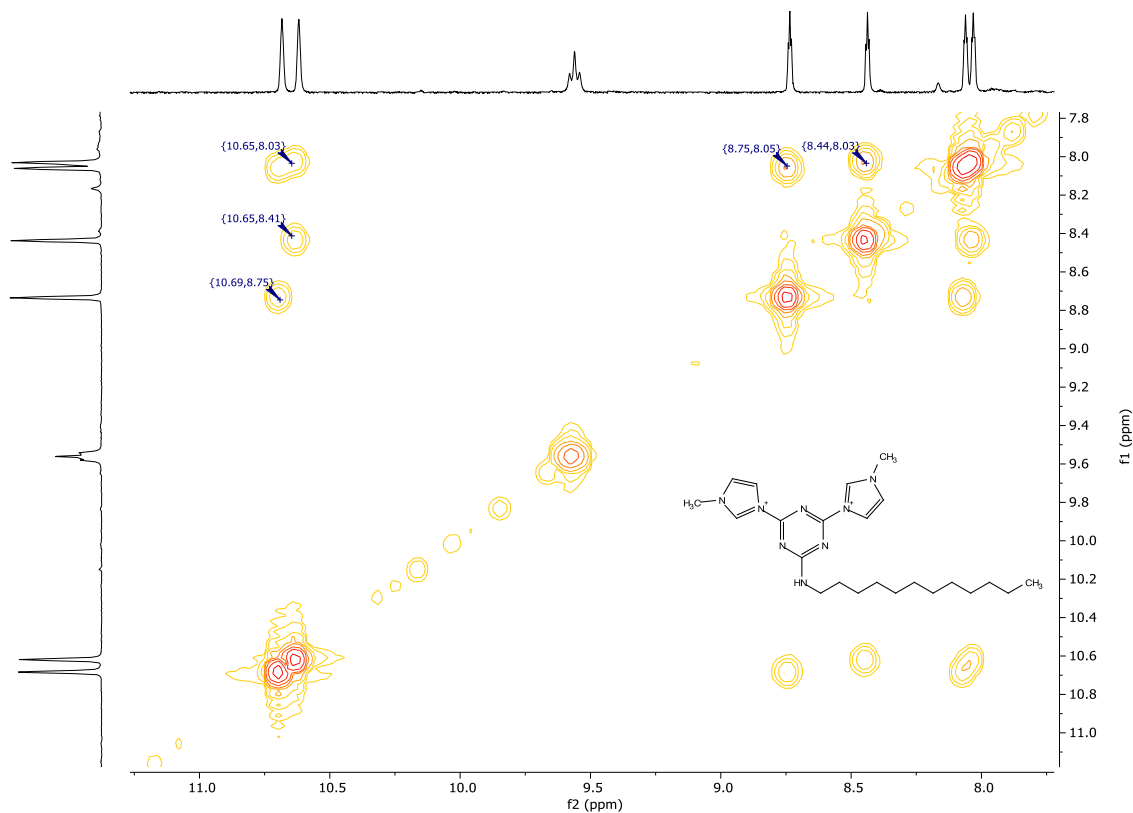


**Figure 3.39** – COSY NMR (DMSO-d<sub>6</sub>) spectrum of MAT<sub>12d</sub>MIMI

The  $^{13}\text{C}$  NMR spectrum of MAT<sub>12</sub>dMIMI is shown in figure 3.40. The signal at 165.59 ppm corresponds to the carbon of the triazine ring bounded to the nitrogen of the alkyl amine ( $\text{N}_2\text{CNH}$ ), the signals at 160.36 and 159.89 ppm correspond to the triazine carbons bounded to the quaternary nitrogen of the methylimidazole substituents that are splitted due to the presence of the two atropoisomers ( $\text{N}_2\text{CN}^+$ ).

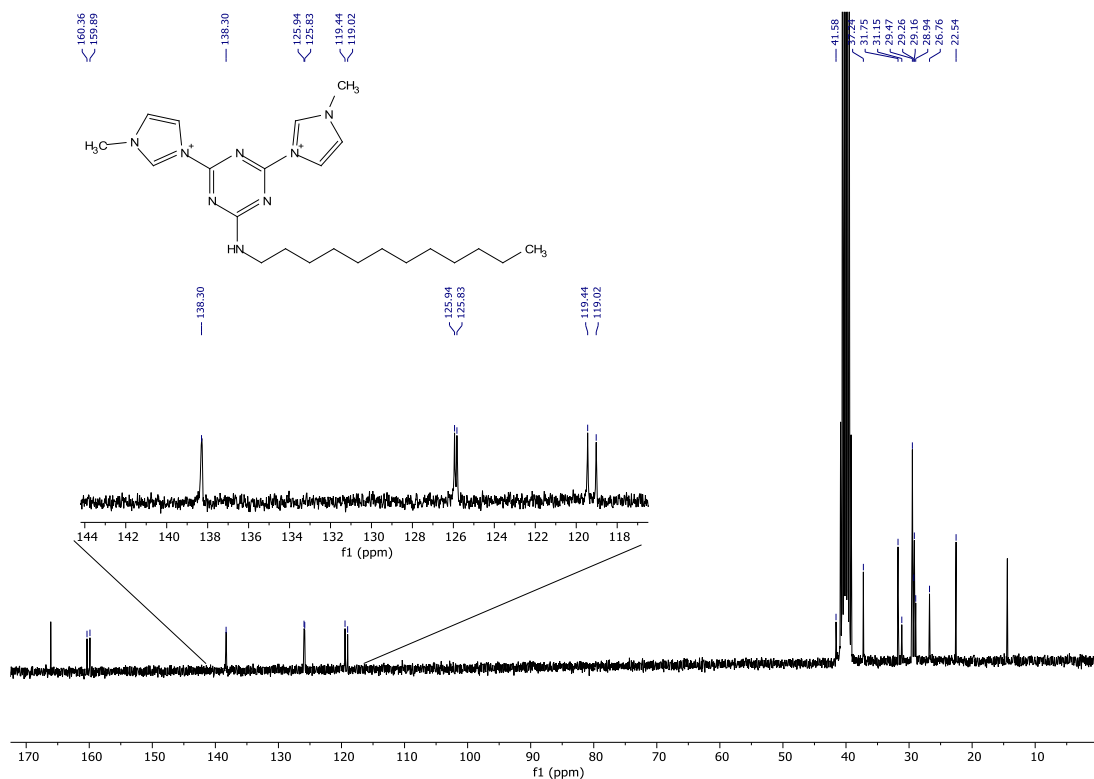


**Figure 3.40** -  $^{13}\text{C}$  NMR (DMSO- $d_6$ ) spectrum of MAT<sub>12</sub>dMIMI

The signals visible in the spectrum at 138.30 ppm, 125.94-125.83 ppm and 119.44-119.02 ppm are assignable to the carbons of the imidazole rings ( $\text{N}^+(\text{CH})\text{N}$ ) ( $\text{C}(\text{CH})\text{N}^+$ ) ( $\text{C}(\text{CH})\text{N}$ ) respectively. The signal at 36.74 ppm is of the primary carbons ( $\text{NCH}_3$ ), the signals at 31.25, 28.97, 28.66, 26.25 and 22.04 ppm correspond to the carbons of the long alkyl chain ( $\text{CH}_2(\text{CH}_2)_9\text{CH}_2$ ) and lastly the signal at 13.91 ppm corresponds to the  $\text{CH}_3$  of the alkyl chain ( $\text{CH}_2\text{CH}_3$ ).

ESI-MS spectra (figure 3.41) show the mass of MATdMIMIs in which the molecular ion peak is characterized by the presence of the double positive charge  $[\text{M}]^{2+}$ .

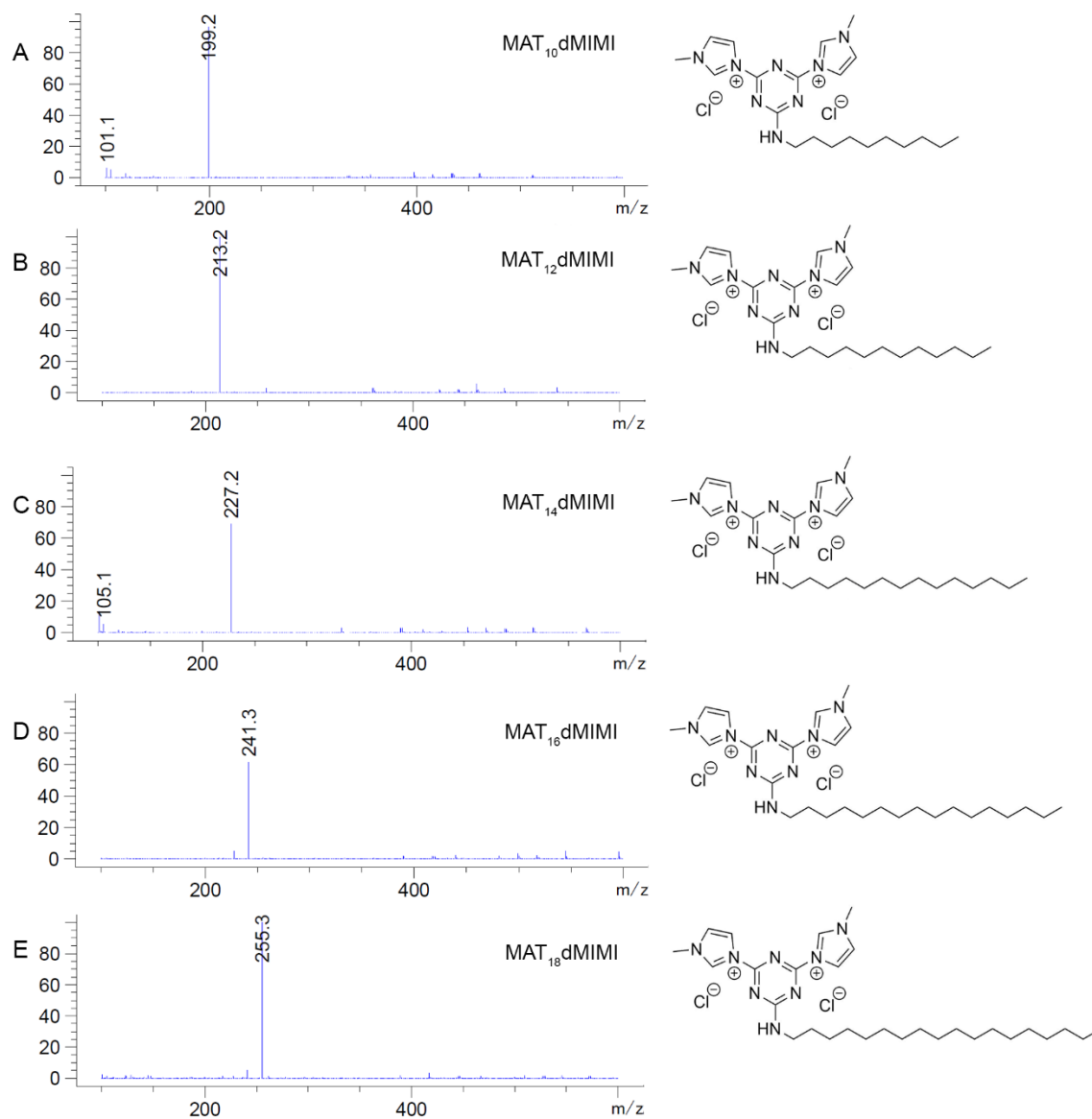


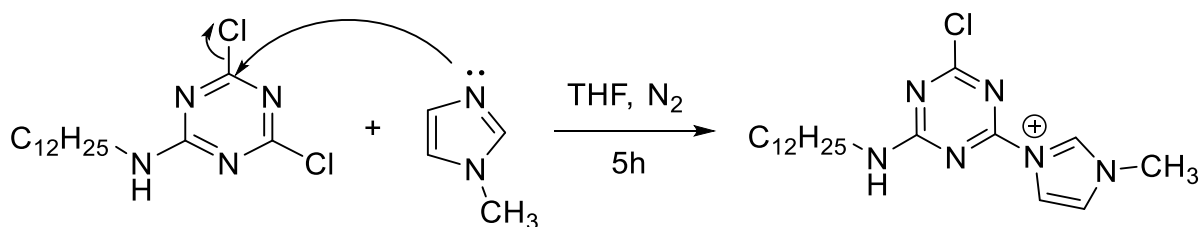
**Figure 3.41** – Mass spectrum of MATdMIMIs A) MAT<sub>10</sub>dMIMI [M]<sup>2+</sup> = 199.2, B) MAT<sub>12</sub>dMIMI [M]<sup>2+</sup> = 213.2, C) MAT<sub>14</sub>dMIMI [M]<sup>2+</sup> = 227.2, D) MAT<sub>16</sub>dMIMI [M]<sup>2+</sup> = 241.3, E) MAT<sub>18</sub>dMIMI [M]<sup>2+</sup> = 255.3



### 3.3.4 Synthesis of 3-(4-chloro-6-(dodecylamino)-1,3,5-triazin-2-yl)-1-methyl-1*H*-imidazol-3-ium chloride (MAT<sub>12</sub>mMIMI)

The reactivity of chlorotriazines towards polymers and surfaces functionalization is well known in the literature<sup>[149-151]</sup> and for industrial applications<sup>[152,153]</sup>. The synthesis of 3-(4-chloro-6-(dodecylamino)-1,3,5-triazin-2-yl)-1-methyl-1*H*-imidazol-3-ium chloride (MAT<sub>12</sub>mMIMI) was carried out to prepare a compound that would be effective as an antimicrobial agent and could be also used to functionalize polymers and surfaces.

In order to achieved this purpose, a chloride needs to be present on the final product which is required for further grafting of the antimicrobial agent to a polymeric structure or a surface. Mono-TQAC species were prepared by reacting MAT with a single methyl imidazole group. The reaction scheme is shown in scheme 3.19 in the presence of MAT<sub>12</sub> and methylimidazole. Preliminarily this triazine was chosen as precursor because, according to the literature, the most active QACs as antimicrobials are those bearing 12 carbon units alkyl chains<sup>[58-61]</sup>.



**Scheme 3.19** – Synthesis of MAT<sub>12</sub>mMIMI

Various experiments were performed with different solvents and in different reaction conditions. The best results were obtained using anhydrous THF under nitrogen atmosphere. The products under the reaction environment are easily recovered from the reaction mixture by simple filtration. The reaction shown to have a conversion of 70% calculated on the weight of the isolated product. The fine white powders recovered were characterized by <sup>1</sup>H NMR, <sup>13</sup>C NMR, COSY, HMQC, FT-IR and m.p. resulting in 3-(4-chloro-6-(dodecylamino)-1,3,5-triazin-2-yl)-1-methyl-1*H*-imidazol-3-ium chloride (MAT<sub>12</sub>mMIMI).

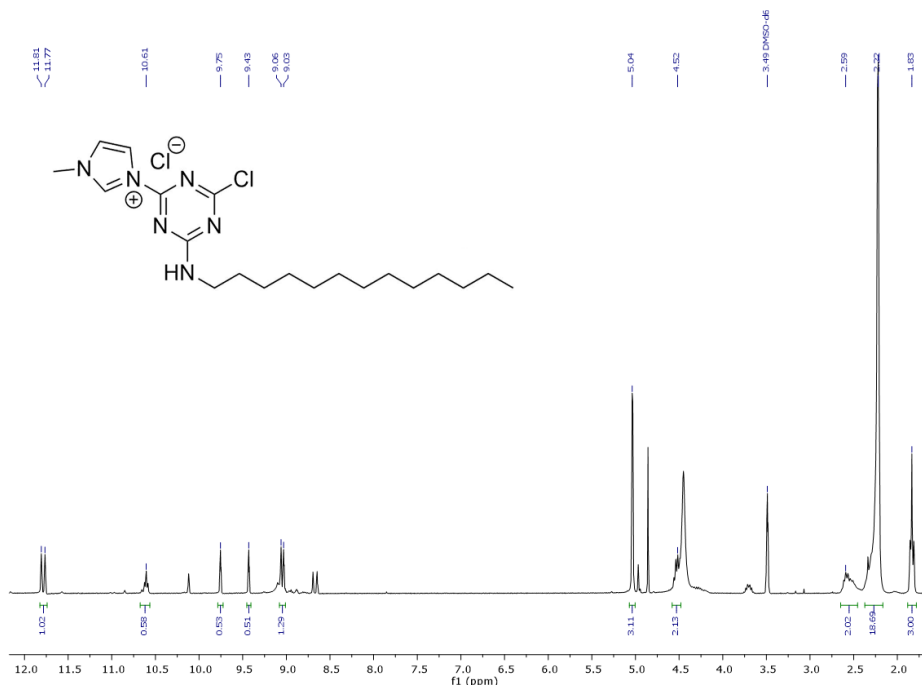


**Figure 3.42** -  $^1\text{H}$  NMR ( $\text{DMSO-d}_6$ ) spectrum of  $\text{MAT}_{12}\text{mMIMI}$

Signal assignment was done using both single-dimensional and two-dimensional techniques such as COSY, HMQC, and HMBC.

As for  $\text{MATdMIMI}$ , also  $^1\text{H}$  NMR of  $\text{MAT}_{12}\text{mMIMI}$  spectrum (figure 3.42) shows a splitting of the signals because of the impediment to free rotation of the alkyl chain. Particularly evident is the splitting of signals at 10.81 and 10.77 ppm which correspond to the imidazole CH between the two nitrogen atoms of the ring ( $\text{NCHN}^+$ ), the signal at 9.61 ppm corresponds to hydrogen bounded to the terminal nitrogen of the side chain ( $\text{CNHCH}_2$ ), the signals at 8.75 and 8.43 ppm corresponding to CH in  $\alpha$  to the quaternary nitrogen of the imidazole ring ( $\text{CHCHN}^+$ ), the signals at 8.05 and 8.02 ppm corresponding to CH in  $\alpha$  to the tertiary nitrogen atom of the imidazole ring ( $\text{CHCHNCH}_3$ ). The presence of the monosubstituted product is confirmed by the integrations of the methyl signal of imidazole at 4.04 ppm ( $\text{CH}_3\text{N}$ ), as a reference for the integrations we used the signal of the methyl protons of the alkyl chain at 0.83 ppm ( $\text{CH}_3\text{CH}_2$ ). At 3.53ppm corresponds the signal of the  $\text{CH}_2$  of the alkyl chain in  $\alpha$  to the terminal amine ( $\text{HNCH}_2\text{CH}_2$ ), the signal at 1.61 ppm corresponds to  $\text{CH}_2$  of the alkyl chain in  $\beta$  to the terminal amine ( $\text{HNCH}_2\text{CH}_2\text{CH}_2$ ) lastly at 1.23 ppm there is the signal that corresponds to the nine central  $\text{CH}_2$  of the chain ( $\text{CH}_2(\text{CH}_2)_9\text{CH}_2$ )

Signals of  $^{13}\text{C}$  NMR spectrum are reported in figure 3.43. The signal at 165.61 ppm corresponds to the triazine carbon atom bonded to the chlorine atom (**ClC**), the signals at 159.86 and 159.39 ppm correspond to the triazine carbons bonded to the quaternary ammonium of the methylimidazole and the alkylamine substituents ( $(\text{N})_2\text{CN}^+$ ) ( $(\text{N})_2\text{CNH}$ ). The signals visible in the spectrum at 137.94 ppm, 125.33-123.10 ppm, 118.97-118.50 ppm are assignable to the carbons of the imidazole ring ( $\text{N}^+(\text{CH})\text{N}$ ) ( $\text{CH}(\text{CH})\text{N}^+$ ) ( $\text{CH}(\text{CH})\text{N}$ ), while the signal at 36.73 ppm belong to  $\text{CH}_3$  carbon (**NCH<sub>3</sub>**) of the imidazole, the signals at 31.29, 29.02, 28.71 and 22.04 ppm correspond to the long alkyl chain carbons and finally the signal at 13.96 ppm corresponds to the primary terminal carbon of the alkyl chain (**CH<sub>2</sub>CH<sub>3</sub>**).

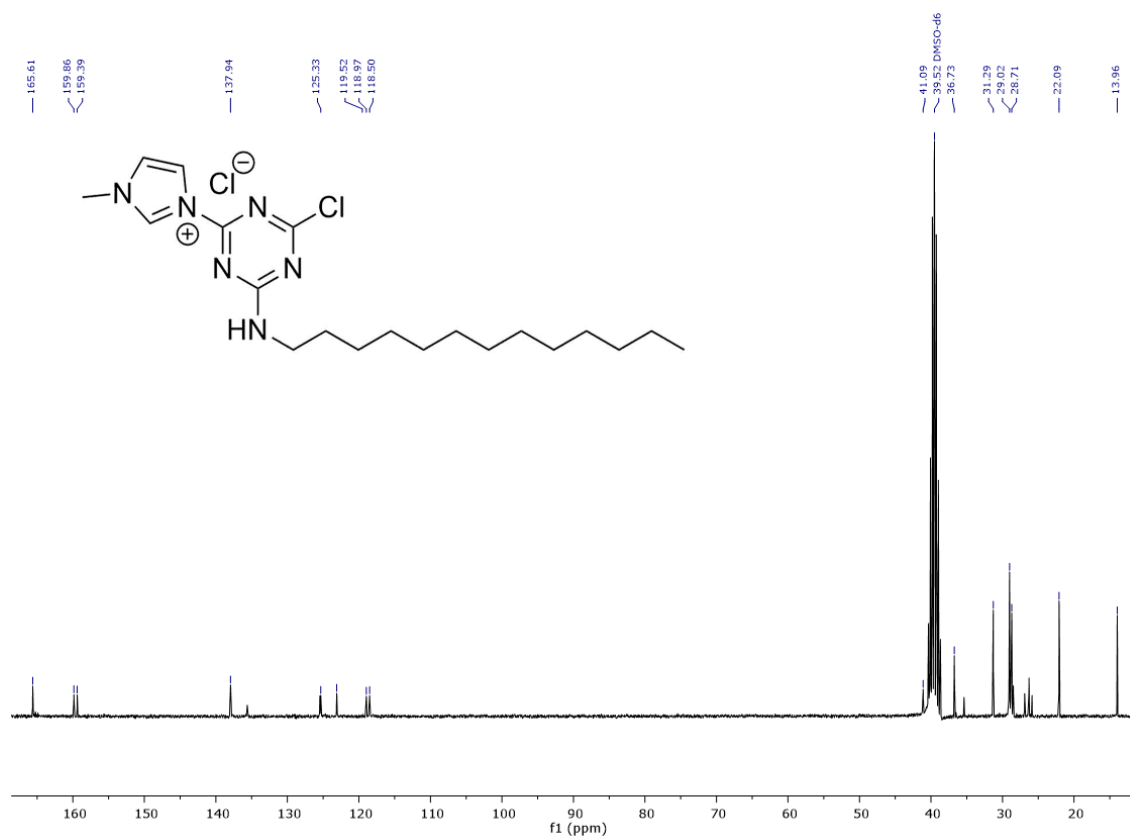


**Figure 3.43** -  $^{13}\text{C}$  NMR (DMSO- $d_6$ ) spectrum of MAT<sub>12</sub>mMIMI

Despite using a strict 1:1 stoichiometry, in most cases a mixture of mono- and di-substituted products was obtained. The cause could be found in the electron-withdrawing inductive effect due to the presence of a quaternary nitrogen on the aromatic ring of the mono-substituted

product which facilitates the next substitution in meta position. This behavior has already been observed in the case of MoPALA-CC and MoPALA-MMT.

Further DFT calculations were performed to compare the relative energies for the formation of MAT<sub>12</sub>mMIMI and MAT<sub>12</sub>dMIMI compounds. It was employed a hybrid EDF2 functional with basis set 6-31G(d,p) in combination with the implicit solvation model C-PCM, considering THF as the solvent ( $\epsilon=7.6$ ). The software used was Spartan 16, installed in a computer based on Intel processors.

The energy change associated with the reaction shown in figure 3.44 is around 6.5 Kcal/mol. The relatively low energy value, although in agreement with experimental results, suggests that small changes in reaction conditions, such as solvent polarity, may be sufficient to lead to the formation of higher substitution products.



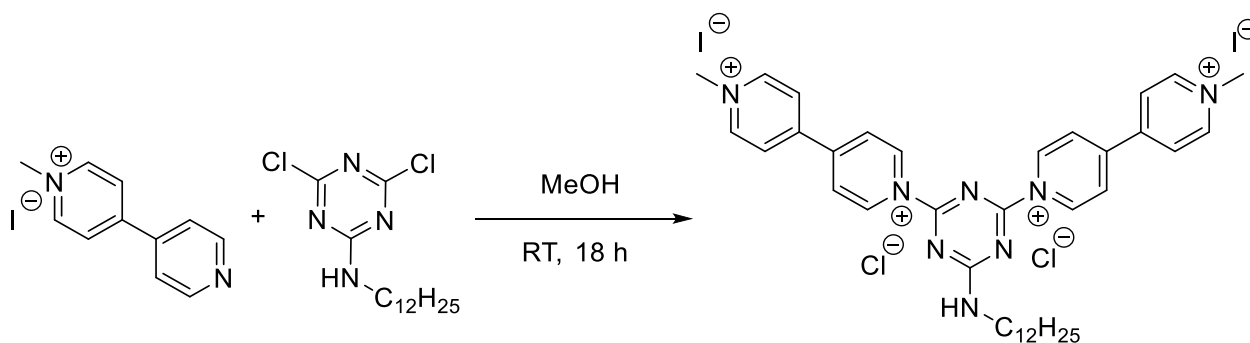
**Figure 3.44** - Comparison of computationally optimized models of MAT<sub>12</sub>, MAT<sub>12</sub>mMIMI and MAT<sub>12</sub>dMIMI

Despite the good result obtained it was difficult to achieve good reproducibility in the reaction performance. The susceptibility of dichloro triazine in forming a mixture of mono and disubstituted products is quite problematic and by repeating the reaction it was not always possible to obtain a satisfactory result. For this reason, further functionalization of polymers with these products has not been carried out and only the antimicrobial activity of the isolated compound has been assessed.

### 3.3.5 Synthesis of 1',1''-(6-(dodecylamino)-1,3,5-triazine-2,4-diyl)bis(1-methyl-[4,4'-bipyridine]-1,1'-diium) dichloride diiodide (MAT<sub>12</sub>MBP)

Multi-charge QACs, as mentioned in chapter 1, appear to have comparable or higher antimicrobial efficiency than bis-QACs<sup>[144,145]</sup>, in particular they appear to be less prone to activate resistance mechanisms in bacteria<sup>[145]</sup>.

Therefore, we investigated the antimicrobial activity of a multi-TQACs obtained via the reaction between MAT<sub>12</sub> and 1-methyl-[4,4'-bipyridin]-1-ium iodide (MBP) (Scheme 3.20). MAT<sub>12</sub> was chosen because, according to the literature, chains with 12 carbon atoms are the most active among the QACs<sup>[58-61]</sup>.



**Scheme 3.20** - Synthesis of MAT<sub>12</sub>dMBP

The reaction was carried out in methanol, unlike the synthesis of MATdMIMIs, which was carried out in acetone. This is due to poor solubility of MBP in acetone, so a more polar solvent was necessary. However, MAT<sub>12</sub>MBP does not precipitate in methanol, therefore, solvent removal was required to recover the product.

The isolated product was then characterized by <sup>1</sup>H NMR, <sup>13</sup>C NMR, COSY, FT-IR and m.p. techniques resulting in 1',1''-(6-(dodecylamino)-1,3,5-triazine-2,4-diyl)bis(1-methyl-[4,4'-bipyridine]-1,1'-diium) dichloride diiodide (MAT<sub>12</sub>dMBP) in 96% yield. Signal assignment was done using both single-dimensional and two-dimensional techniques such as COSY, HMQC, and HMBC.

The  $^1\text{H}$  NMR spectrum of MAT<sub>12</sub>dMBP is reported in figure 3.45. The presence of the disubstituted product is confirmed by the integrals of the four bipyrindyl signals between 9-8 ppm using as reference for the integrations the signal of the methyl protons of the alkyl chain at 0.86 ppm (**CH<sub>3</sub>CH<sub>2</sub>**).

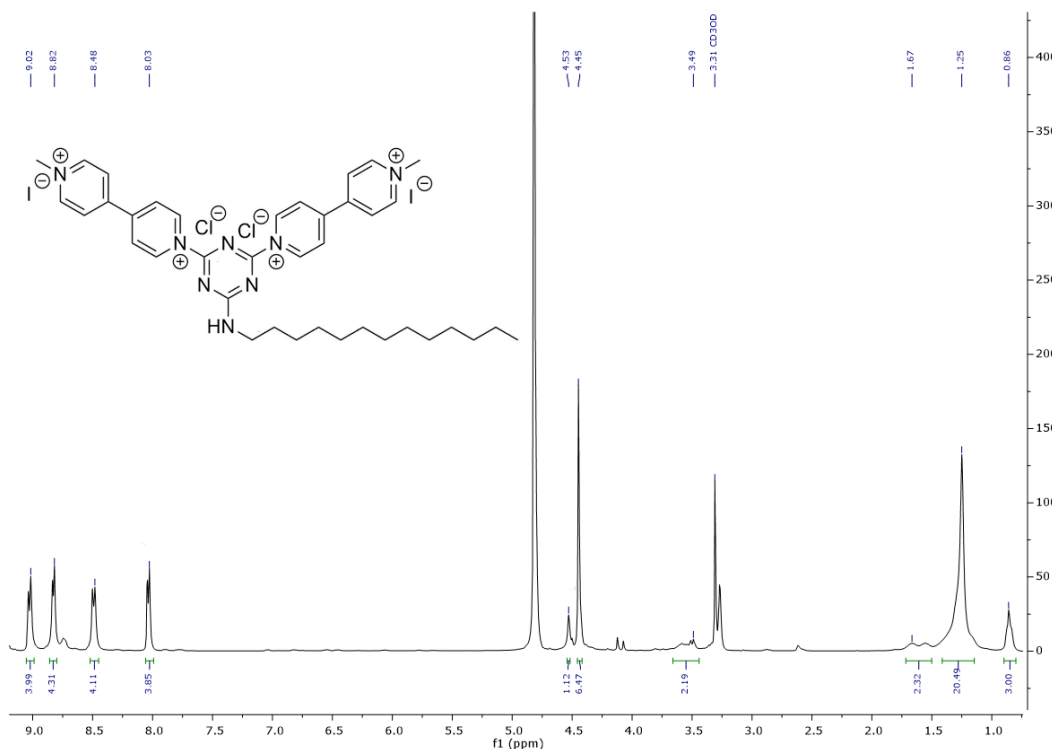


**Figure 3.45** -  $^1\text{H}$  NMR (Methanol- $d_4$ ) spectrum of MAT<sub>12</sub>dBMP

To be able to correctly assign the pyridine  $^1\text{H}$  NMR signals, it was necessary to exploit a COSY spectrum (figure 3.46). There we can see a weak  $^4J_{\text{HH}}$  coupling signal between the pyridine methyl hydrogens at 4.45 ppm (**N<sup>+</sup>CH<sub>3</sub>**) and the pyridine CH hydrogens in ortho at 9.02 ppm (**CH<sub>3</sub>N<sup>+</sup>(CH)**). Consequently, it is easy to find CH in meta (**N<sup>+</sup>CHCH**) at 8.48 ppm by direct  $^3J_{\text{HH}}$  coupling with signals in ortho. The pyridyl residue bounded to triazine, can be recognized by the CH in ortho at 8.82 ppm (**ArN<sup>+</sup>CH**), that are shifted in lower field by the vicinal quaternary nitrogen respect to the CH in meta position at 8.03 ppm (**ArN<sup>+</sup>CHCH**). Similarly to MATdMIMI, the alkyl chain signals are respectively at 3.49ppm (**NHCH<sub>2</sub>CH<sub>2</sub>**), 1.67ppm (**NHCH<sub>2</sub>CH<sub>2</sub>**), 1.25ppm (**CH<sub>2</sub>(CH<sub>2</sub>)<sub>9</sub>CH<sub>2</sub>**), 0.86ppm (**CH<sub>2</sub>CH<sub>3</sub>**), while in methanol the amine hydrogen signal fall at 4.53 ppm.

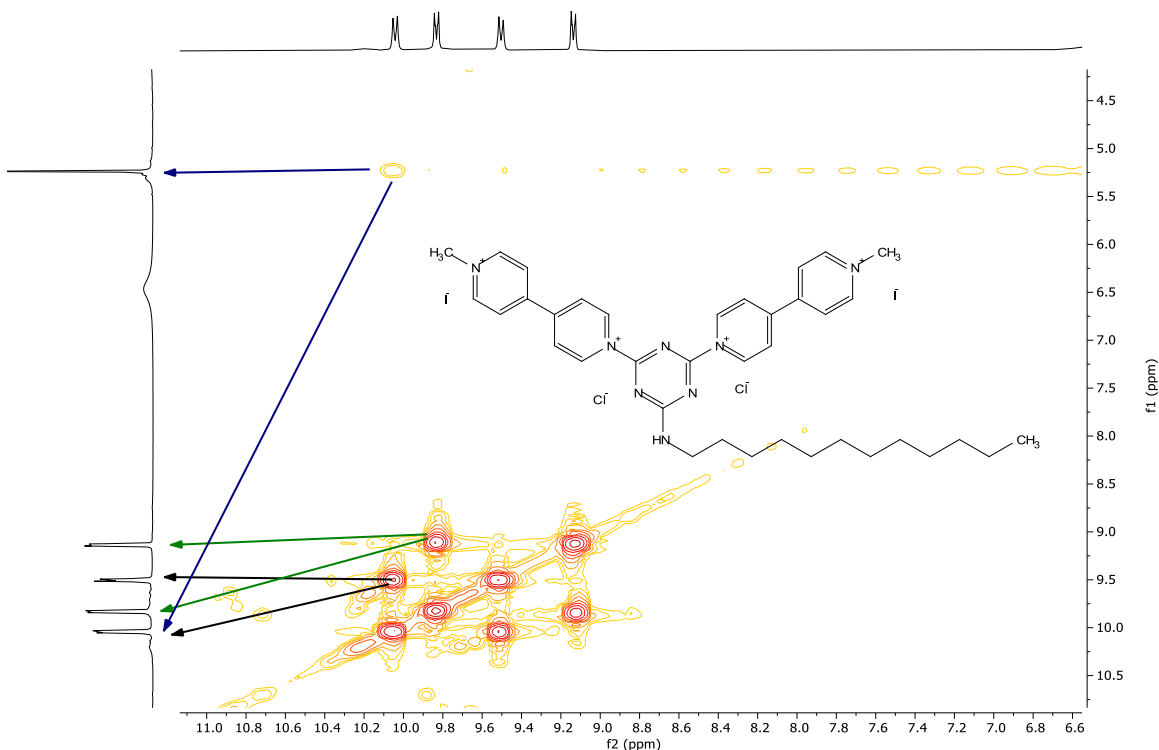


**Figure 3.46** - COSY (Methanol- $d_4$ ) spectrum of MAT<sub>12</sub>dBMP

The  $^{13}\text{C}$  NMR spectrum of MAT<sub>12</sub>dBMP is reported in figure 3.47. The signal at 153.93 ppm corresponds to the triazine carbon atom bonded to the nitrogen of the alkyl amine ( $\text{N}_2\text{CNH}$ ), while the signal at 149.99 and 147.55 ppm correspond to the triazine carbons bonded to the quaternary nitrogen atom of the BMP substituents ( $\text{N}_2\text{CN}^+$ ) splitted for effect of the formation of the twin atropoisomers. The signals visible in the spectrum at 128.29, 127.95, 127.11 and 124.53 ppm are assignable to the carbons of the bipyridine ( $\text{C}(\text{CH})\text{N}^+$ ) rings ( $\text{C}(\text{CH})\text{N}$ ), while the signal at 33.04 ppm is from the methyl carbon ( $\text{NCH}_3$ ), the signals at 30.72, 30.44, 23.71 ppm correspond to the long alkyl chain carbons and finally the signal at 14.43 ppm corresponds to the primary terminal carbon of the alkyl chain ( $\text{CH}_2\text{CH}_3$ ).

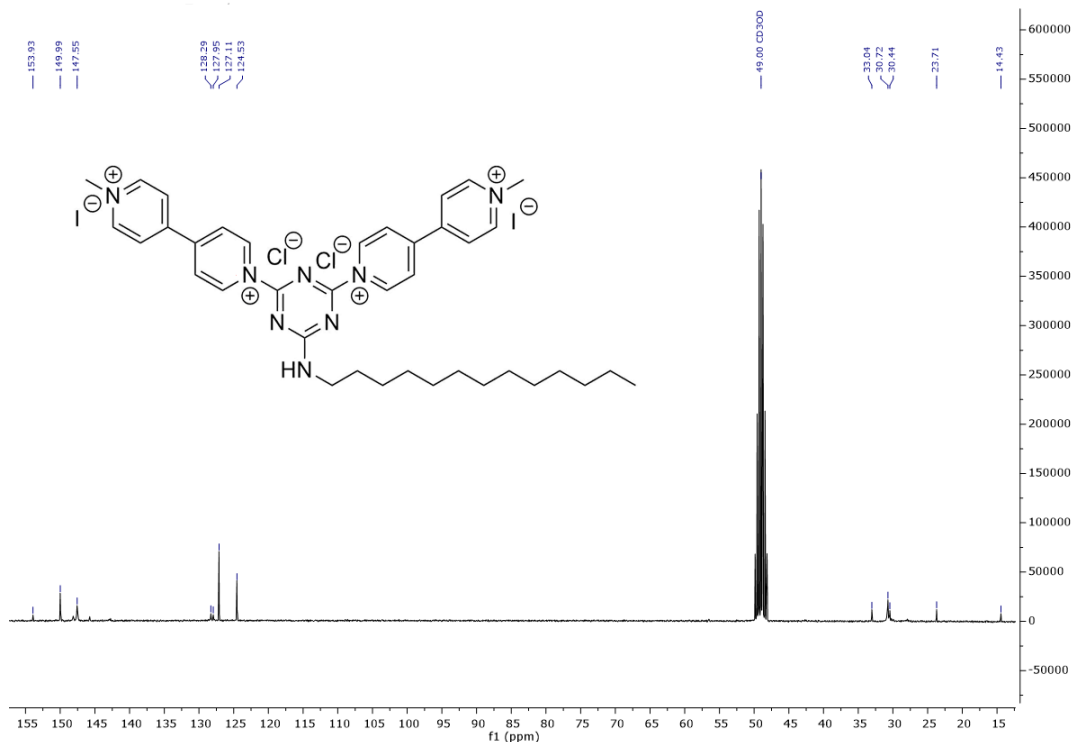


**Figure 3.47** –  $^{13}\text{C}$  NMR (methanol- $d_4$ ) spectrum of MAT<sub>12</sub>dBMP

### 3.4 TQACs biological test and antimicrobial evaluation

All biological tests were performed both in biological and technical triplicate on different bacterial cultures as described in the experimental section (chapter 5.5). The effect of compounds at different concentrations on different bacterial cultures of both Gram positive and Gram negative were evaluated. The data reported represent the minimum inhibition concentration (MIC) at which there is a complete inhibition of bacterial growth. In addition, the cytotoxicity was also evaluated through the  $\text{IC}_{50}$  index, which represents half maximal inhibitory concentration against MRC-5 human fibroblast cell lines.



### 3.4.1 Evaluation of MoPALA-CC, MoPALA-MMT, BuMO-CC and BuMO-MMT TQACs.

Here we report the result of the biological tests performed on the respective MoPALA-CC, MoPALA-MMT, BuMO-CC and BuMO-MMT performed against *Staphylococcus aureus* (ATCC 25923) as Gram positive bacteria and *Escherichia coli* (ATCC 25922) as Gram negative bacteria (table 3.9).

According to Vial and colleagues,<sup>[154-156]</sup> the length of the chain modulates the activity. In figure 3.48 is shown the trend of antimicrobial activity of several different bis-QACs against the *Plasmodium falciparum*, responsible for malaria. According to the authors the antimicrobial activity is heavily influenced by the length of the alkyl chains.

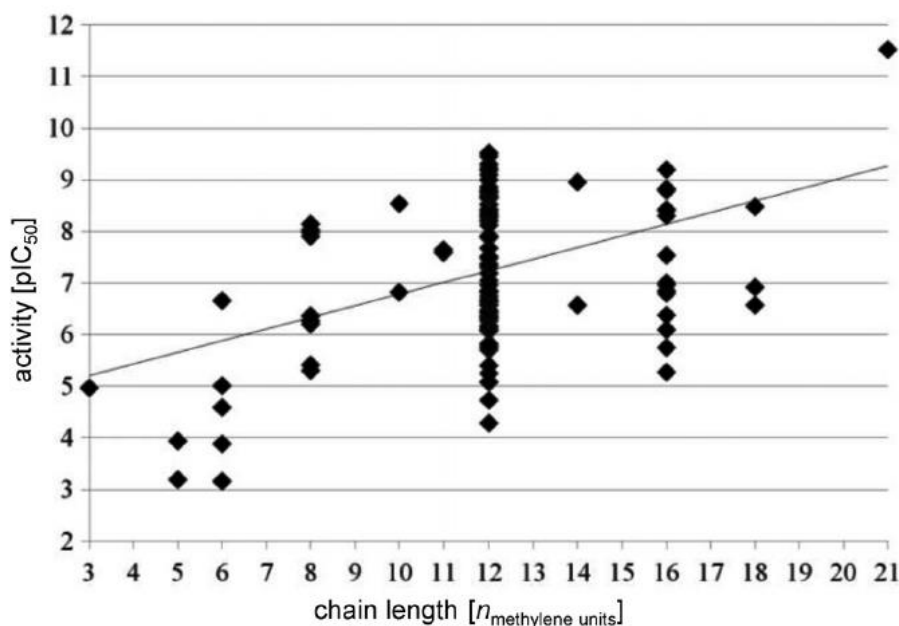


**Figure 3.48** – Chain length-activity correlation of bis-QACs reported by Vial et al.<sup>[154-156]</sup>

As shown in table 3.9 the MIC values for all compounds having a side chain less than 8 carbon units appear to have no activity in bacterial inhibition. In fact, they all have MICs above 400 µg/mL which is the upper limit that was used for this series of tests. All the compounds that have a side chains of 12 and 16 units appear to have activity against the tested strains.

**Table 3.9** - Minimum inhibitory concentration values [ $\mu\text{g/mL}$ ], half maximal inhibitory concentration ( $\text{IC}_{50}$ ) values [ $\mu\text{g/mL}$ ].

| Compound                      | Chain Length | S.aureus <sup>[a]</sup> | E.coli <sup>[b]</sup> | $\text{IC}_{50}$ <sup>[c]</sup> |
|-------------------------------|--------------|-------------------------|-----------------------|---------------------------------|
| <b>BuMO-CC</b>                | 4            | >400                    | >400                  | >1000                           |
| <b>BuMO-MMT</b>               | 4            | >400                    | >400                  | >1000                           |
| <b>MoPALA<sub>4</sub>CC</b>   | 8            | >400                    | >400                  | 25                              |
| <b>MoPALA<sub>4</sub>MMT</b>  | 8            | >400                    | >400                  | 36                              |
| <b>MoPALA<sub>8</sub>CC</b>   | 12           | 50                      | 400                   | 59                              |
| <b>MoPALA<sub>8</sub>MMT</b>  | 12           | 350                     | >400                  | 34                              |
| <b>MoPALA<sub>12</sub>CC</b>  | 16           | 300                     | 200                   | 67                              |
| <b>MoPALA<sub>12</sub>MMT</b> | 16           | >400                    | 300                   | 62                              |
| <b>CPC<sup>[d]</sup></b>      | 12           | 0.5                     | 8                     | -                               |

Minimal inhibitory concentration (MIC) was calculated taking as reference the negative control (bacteria plated onto medium without samples). All the experiments were conducted both in biological and technical triplicate. [a] *Staphylococcus aureus*, [b] *Escherichia coli*, [c]  $\text{IC}_{50}$  values were determined on MRC-5 cells. [d] Cetylpyridinium chloride, data was taken from the work of Minbiole.<sup>[157]</sup>

However, the antimicrobial activities are rather low, especially in comparison with cetylpyridinium chloride (CPC), that is a commercial available QACs. However, the trend of Gram positive species being more susceptible to QACs than Gram negative species is confirmed here as well as by the literature<sup>[74,77]</sup>. The best result is obtained with MoPALA<sub>8</sub>CC that shows a MIC against *Staphylococcus aureus* of 50  $\mu\text{g/mL}$ , the best compound for the inhibition of *Escherichia coli* instead seems to be MoPALA<sub>12</sub>CC.

It is interesting to note that both MoPALA<sub>8</sub>CC and MoPALA<sub>12</sub>CC are, on average, more active than the respective MoPALA<sub>8</sub>MMT and MoPALA<sub>12</sub>MMT. This fact could be related to the different positive charge experienced by the bacterial membrane surface. In fact, while MoPALA-CC possesses two ammonium cations balanced by two chloride anions, MoPALA-MMT possess a zwitterionic behavior for one of the two morpholino groups. In other words, they are both structurally like bis-QACs but act as a mono-QACs which are known to be less efficient than bis-QACs<sup>[158]</sup>.

### 3.4.2 Evaluation of MATdMIMI TQACs

The antimicrobial activity of all compounds was tested against Gram-negative and Gram-positive strains of *Escherichia coli* (ATCC 25922), *Pseudomonas aeruginosa* (CECT 111), *Staphylococcus aureus* (ATCC 25923), *Enterococcus faecalis* (CECT 795) respectively and against fungal strain like *Candida albicans* (CECT 1394) (table 3.10). The results are also reported in figure 3.49.

A general trend in antimicrobial activity was observed, showing an inhibitory effect on all of Gram-positive strains. Between Gram-negative bacteria, *E. coli* strain showed a relevant susceptibility to all the compounds, except for the MAT<sub>18</sub>dMIMI. Instead, only MAT<sub>14</sub>dMIMI seems to be effective against *P. aeruginosa*.

**Table 3.10** - Minimum inhibitory concentration values [ $\mu\text{g/mL}$ ], half maximal inhibitory concentration ( $\text{IC}_{50}$ ) values [ $\mu\text{g/mL}$ ] critical micelle concentration (CMC) values [ $\text{mM}$ ] and logP.

| Compound                     | LogP  | CMC  | S.a. <sup>[a]</sup> | E.c. <sup>[b]</sup> | E.f. <sup>[c]</sup> | P.a. <sup>[d]</sup> | C.a. <sup>[e]</sup> | $\text{IC}_{50}$<br>[f] |
|------------------------------|-------|------|---------------------|---------------------|---------------------|---------------------|---------------------|-------------------------|
| <b>MAT<sub>10</sub>dMIMI</b> | -0.77 | /    | 250                 | 250                 | 125                 | 500                 | >500                | 38                      |
| <b>MAT<sub>12</sub>dMIMI</b> | 0.02  | 20.5 | 7.8                 | 62                  | 62                  | 500                 | 500                 | 41                      |
| <b>MAT<sub>14</sub>dMIMI</b> | 0.81  | 9.3  | 3.9                 | 62                  | 62                  | 250                 | 250                 | 5                       |
| <b>MAT<sub>16</sub>dMIMI</b> | 1.60  | 2.2  | 125                 | 250                 | 62                  | >500                | 250                 | 51                      |
| <b>MAT<sub>18</sub>dMIMI</b> | 2.40  | 1.1  | 250                 | >500                | 62                  | >500                | 250                 | 4                       |
| <b>CPC<sup>[g]</sup></b>     |       |      | 0.5                 | 8                   | 1                   | 63                  | -                   | -                       |

Minimal inhibitory concentration (MIC) was calculated taking as reference the negative control (bacteria plated onto medium without samples). All the experiments were conducted both in biological and technical triplicate. [a] *Staphylococcus aureus*, [b] *Escherichia coli*, [c] *Enterococcus Faecalis*, [d] *Pseudomonas aeruginosa* [f]  $\text{IC}_{50}$  values were determined on MRC-5 cells. [g] Cetylpyridinium chloride, data was taken from the work of Minbiole.<sup>[157]</sup>

However, it is well known that gram-negative species tend to be less susceptible to this class of compounds. About the fungal strain of *C. albicans*, compounds MAT<sub>14</sub>dMIMI, MAT<sub>16</sub>dMIMI and MAT<sub>18</sub>dMIMI have a mild action, and the shortest chain compounds have the weakest

activity. For these reasons MAT<sub>14</sub>dMIMI can be considered a promising broad-spectrum antimicrobial agent.

The minimal inhibitory concentration (MIC) values of cetylpyridinium chloride (CPC), which is one of the most effective QACs on the market, were also taken as a reference to compare with the MIC values of MATdMIMIs. Although CPC remains more efficient, the MIC values of some of the MATdMIMIs are very close to it, especially in the case of *Staphylococcus aureus*.

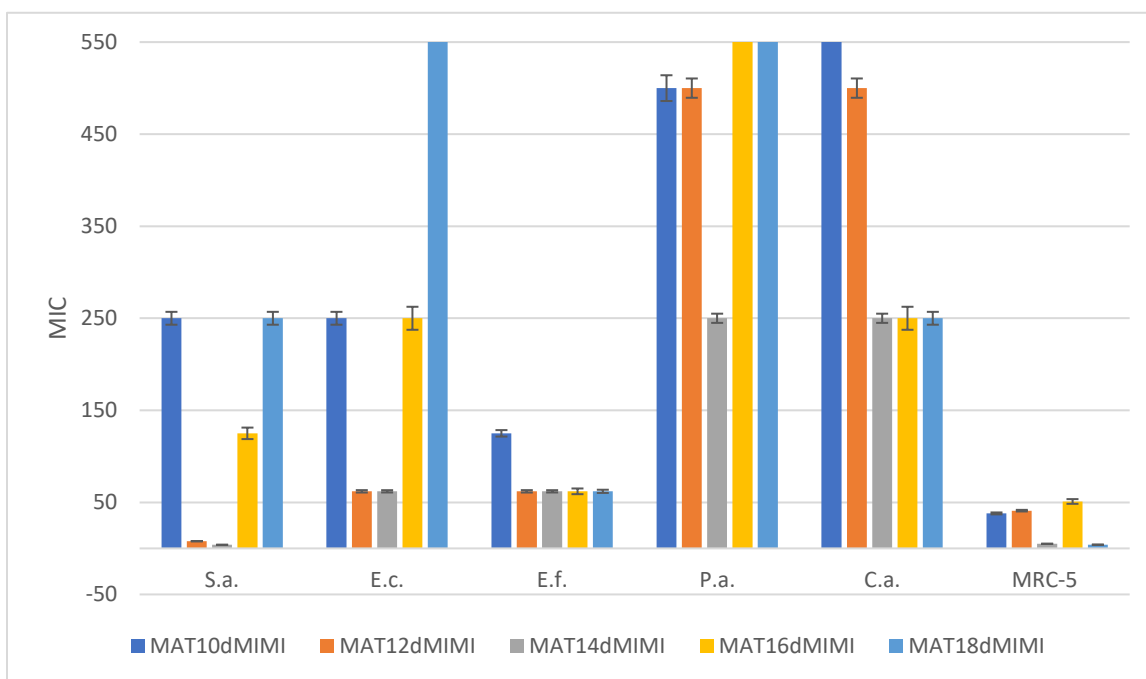


**Figure 3.49** – Graphical representation of minimal inhibitory concentration of MATdMIMI and IC<sub>50</sub> values

About the mode of action of QACs and their derivatives, various opinions have been given, especially about the selectivity of the antimicrobial activity related to chain length. From a general point of view, the biocidal action of QACs lie to his ability to cross membrane or cell wall, and this can explain why Gram-negative are often more resistant than Gram-positive strains<sup>[159]</sup>. We also made a first evaluation of the cytotoxicity of the compounds against the eukaryotic fibroblasts MRC-5 and the results are listed as IC<sub>50</sub> values (table 3.10). The values obtained seem to have a different trend compared to the result for minimal inhibitory concentration (MIC) values. In fact, the most cytotoxic among the MATdMIMI appears to be MAT<sub>18</sub>dMIMI with eighteen long carbon side chain, which nevertheless exhibits the poorest antimicrobial activity. Compounds such MAT<sub>12</sub>dMIMI and MAT<sub>14</sub>dMIMI, although similar in

terms of MIC against all of the tested strains, have very different values of cytotoxicity. While MAT<sub>12</sub>dMIMI shows good MIC values and a rather limited cytotoxicity, MAT<sub>14</sub>dMIMI instead shows a cytotoxicity close of MAT<sub>18</sub>dMIMI.

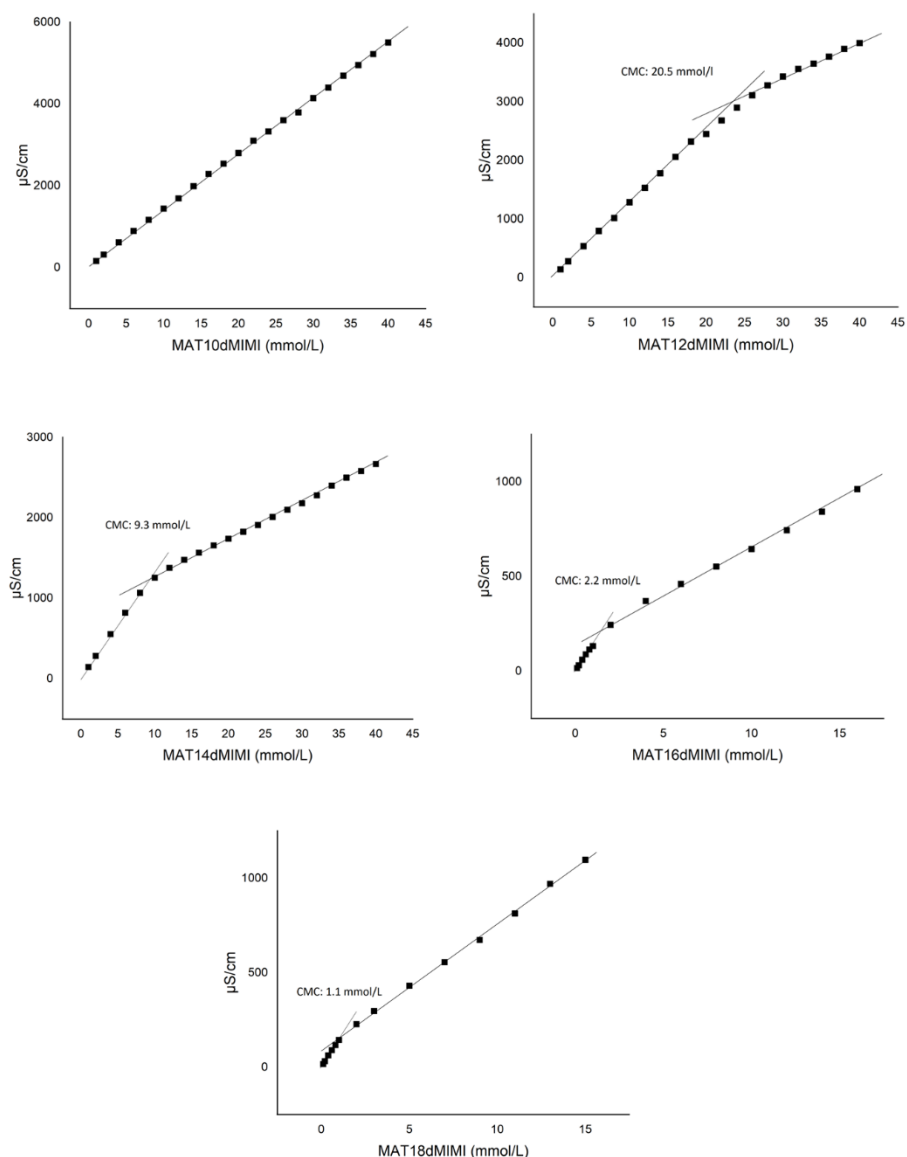


**Figure 3.50** – Conductivity lines of MATdMIMI compounds, change in curve slope indicates CMC.

To justify the results obtained, further analysis were carried out to study possible correlations between the antibacterial and/or cytotoxic activity with the lipophilicity values of the compounds. Using a software (see experimental part, chapter 5.7), we calculated the logP of each compound (table 3.10), which is a coefficient that describes the distribution ratio in a mixture of

two immiscible solvents at equilibrium. The value of critical micelle concentration (CMC) (figure 3.50) was also measured using conductometric method (see experimental part, chapter 5.6).

As expected, the value of CMC and logP increased with the length of carbon side chain. Moreover, as reported figure 3.51 an evident correlation can be drawn between CMC, logP, MIC, and IC<sub>50</sub> values. For MIC values we used the results obtained with *S. aureus* strains, which are the most sensible specie respect to MATdMIMI.

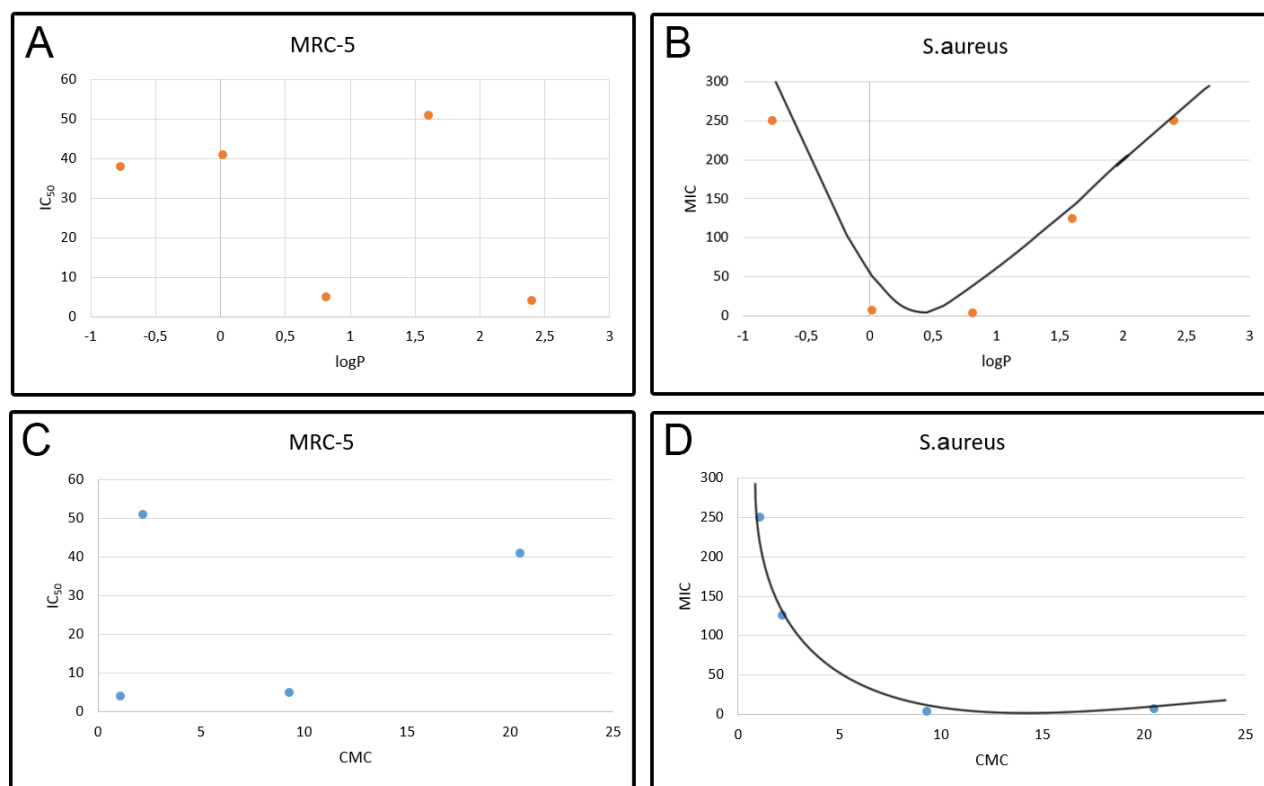


**Figure 3.51** - A-C) Toxicity of the various molecules on MRC-5 cellular line as a function of logP and CMC. B–D) MIC of the various molecules on *S.aureus* strains as a function of logP and CMC

As we can see from figures 3.51 A and 3.51 C, which describe the values of logP and CMC against the values of IC<sub>50</sub> there seems to be no visible trend in graph. On the other hand, in figures 3.51 B and 3.51 D, which represent the MIC against *S. aureus* respect to the values of logP and CMC, the graph may suggest a correlation. In fact, in the case of the logP/MIC graph (figure 3.51 B) it is an evident parabola, that places the lowest MIC values between 0 and 1 logP values. While in the case of the CMC/MIC (figure 3.51 D) the graph describes a geometric figure that can be associated with a curve, where minimum MIC values are found at values

between 10 and 20 mM. Therefore, we can draw the conclusion that the values of CMC and logP, may have a direct impact on the antimicrobial activity of a QACs.

### 3.4.2 Evaluation of MAT<sub>12</sub>mMIMI and MAT<sub>12</sub>MBP

Antimicrobial investigations were performed on *S. aureus* (ATCC 25923) cultures so that they could be compared with the results obtained previously from MATdMIMIs. From the data (table 3.11) it can be seen that the different number of charges on the polar head actually lead to a decrease of antibacterial efficacy. An interesting peculiarity is that, while the difference between MAT<sub>12</sub>mMIMI and MAT<sub>12</sub>dMIMI is contained, the difference between MAT<sub>12</sub>dMIMI and MAT<sub>12</sub>MBP is quite marked. This is in contrast to what is reported in the literature where generally the activities of multi-QACs are comparable than bis-QACs<sup>[144,157,158]</sup>. Further experiments are ongoing to further substantiate these conclusions

**Table 3.1** - Minimum inhibitory concentration values [ $\mu\text{g/mL}$ ] against *S.aureus* of MAT TQACs having 1, 2 and 4 charge

| <b>Compound</b>              | <b>Positive charge</b> | <b>Chain Length</b> | <b>MIC vs S.aureus [<math>\mu\text{g/mL}</math>]</b> |
|------------------------------|------------------------|---------------------|--|
| <b>MAT<sub>12</sub>dMBP</b>  | <b>4</b>               | 12                  | <b>250</b>   |
| <b>MAT<sub>12</sub>mMIMI</b> | <b>1</b>               | 12                  | <b>50</b>  |
| <b>MAT<sub>12</sub>dMIMI</b> | <b>2</b>               | 12                  | <b>7.8</b>   |

Minimal inhibitory concentration (MIC) was calculated taking as reference the negative control (bacteria plated onto medium without samples). All the experiments were conducted both in biological and technical triplicate.

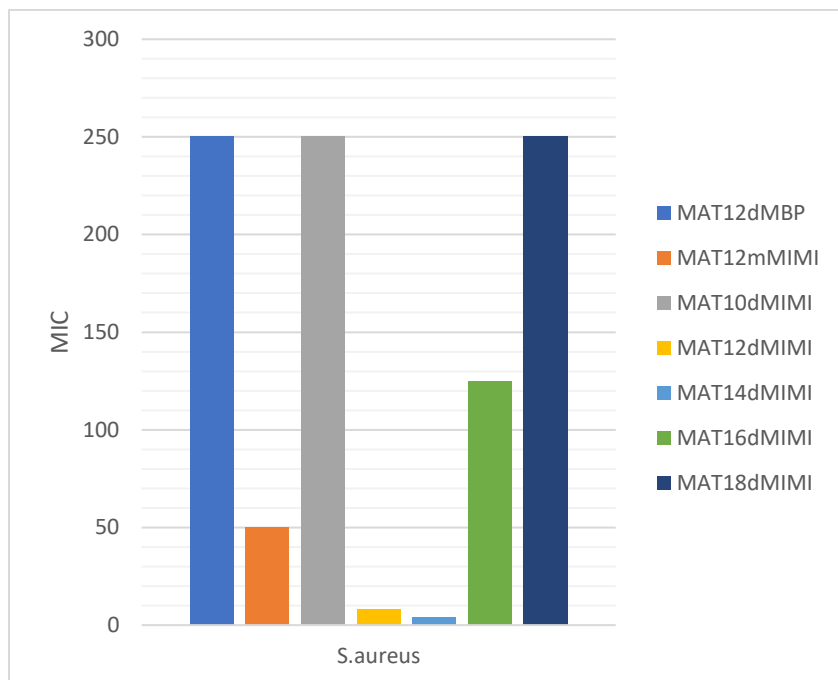


**Figure 3.52** - Graphical representation of minimal inhibitory concentration against *S.aureus* of MATdMIMI, MAT<sub>12</sub>mMIMI and MAT<sub>12</sub>MBP

In Figure 3.52 are reported the MICs values of MAT<sub>12</sub>mMIMI and MAT<sub>12</sub>MBP against MATdMIMIs. It is immediately evident that the 4-charge MAT<sub>12</sub>MBP MIC are comparable with those of MAT<sub>10</sub>MIMI and MAT<sub>18</sub>MIMI MIC, which have the less antimicrobial activity, while the mono-charge MAT<sub>12</sub>mMIMI MIC are close to the performance of MAT<sub>12</sub>dMIMI and MAT<sub>14</sub>dMIMI.



## **CHAPTER 4**

### **CONCLUSIONS**

**Synthesis of new antimicrobial triazine-based quaternary ammonium salts**

The research carried out in this part of the doctoral thesis was focused on the development of new libraries of TQACs derived from the use of chloro 1,3,5-triazines. In addition, the antimicrobial activity of these compounds was also evaluated.

The main results achieved are:

- The identification and optimization of synthetic procedures to achieve *N*-(3-morpholinopropyl)alkyl amides. Amidation reactions were carried out at room temperature in the presence of both DMTMM and CDMT/NMM system. Showing the best performance for the system using preformed DMTMM, achieving more than 70% yield in 3 hours of reaction time and extremely pure products using few work up steps.
- The synthesis of two distinct libraries of TQACs was achieved: one based on morpholino-triazine compounds, inspired by the structure of DMTMM (MoPALA-CC and MoPALA-MMT), and one based on imidazole-morpholino salts (MATdMIMI, MATmMIMI, MATdMBP).
- The results on the synthesis of morpholinic TQACs compounds led us to the conclusion that morpholino-triazine ammonium salts do not undergo dealkylation reaction when highly hindered substituents are present on the morpholinic residue and using dichloro triazines or trichloro triazines. It was further verified that second substitution on the triazine moiety by morpholine is favored due to the activation of the  $\text{NR}_3^+$  group.
- The results on the synthesis of imidazole-triazine TQACs compounds confirmed the ability of dichlorotriazines to form bis-TQACs, with yields significantly higher than those obtained for morpholine TQACs (in all cases above 90%) thanks to the use of less hindered aromatic amines.
- The results of the antimicrobial activity evaluations showed that the two different libraries of TQACs have markedly different performances with regard to antimicrobial activity. The MAT-derived compounds clearly outperform the MoPALA-derived compounds in terms of MIC values, being very close to the most common QACs on the market. In addition, the trend of antimicrobial activities related to the variation of the length of the alkyl side chain is in agreement with data reported in the literature, showing best performances with compounds bearing alkyl chain with 12 and 14 carbon atoms. On the other hand, no antimicrobial activity was found for TQACs having side chain of less than 8 carbon atoms.

**CHAPTER 5**

**EXPERIMENTAL SECTION**

**Synthesis of new antimicrobial triazine-based quaternary ammonium salts**

## 5.1 Methods and instrumentation

All chemicals used were purchased from; Sigma Aldrich, Merck, Alfa Aesar and Fluka with high grade of purity.

All solvents used were analytical grade and were employed without further purification.

NMR spectra were recorded using a Bruker Advance 300 spectrometer operating at a frequency of 300.13 MHz for the proton and 75.4 MHz for carbon and a Bruker UltraShield 400 operating at frequency of 400.00 MHz for the proton and 101.00 MHz for carbon. The deuterated solvents used to do the NMR analyses were; CDCl<sub>3</sub>, D<sub>2</sub>O, Acetone-d<sub>6</sub>, DMSO-d<sub>6</sub> and CD<sub>3</sub>OD purchased from Euriso-top and Sigma Aldrich. The chemical shifts were reported in ppm using TMS (Me<sub>4</sub>Si) as reference.

Chromatographic analyses were performed using an Agilent Technologies 6850 gas chromatograph, with an FID detector and an Agilent HP-5 (cross-linked 5% phenylmethylsiloxane) or Agilent HP-1 (100% methylsiloxane) column. Analyses were conducted at the following temperature ramps:

- HP-1: Ti: 50 °C hold 5 min, rate 20 °C/min, Tf: 230 °C x 35min
- HP-5: Ti: 50 °C hold 5 min, rate 20 °C/min, Tf: 240 °C x 30min

Mass spectra were performed with a GC-MS (Agilent technologies 7820A GC system and A.T. 5977B MSD) and with an ESI-MS (Agilent 6100 Series Quadrupole LC/MS Systems)

FT-IR spectra were recorded using the "Perkin-Elmer" model "Spectrum One" spectrometer. Measurements for FT-IR spectra were performed by preparing KBr disks.

Melting points were performed using a Buchi B-535 Melting Point Apparatus.

The purity of all compounds was calculated by integration of the signals of the relative <sup>1</sup>H NMR spectrum.

## 5.2 Reagents and solvents

### Solvents

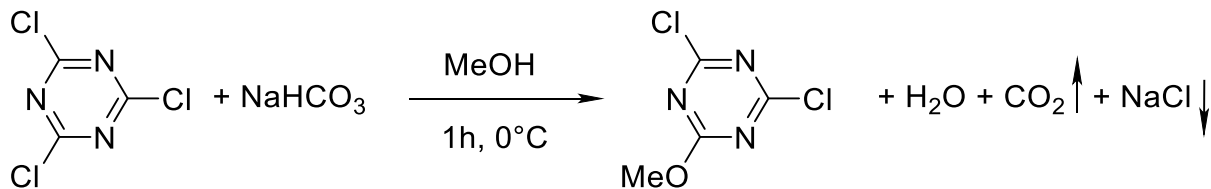
- Acetone
- Acetonitrile
- Dichloromethane
- Diethylether
- Dimethylsulfoxide
- Distilled water
- Hexane
- Methanol
- Tetrahydrofuran
- Toluene

### Reagents

- 3-Morpholinpropylamine (MoPA)
- 4-(4,6-dimethoxy-1,3,5-triazin-2-yl)-4-methyl-morpholinium chloride (DMTMM)
- 4,4'-bipyridine (BP)
- Sodium bicarbonate (NaHCO<sub>3</sub>)
- Butyl imidazole
- Cyanuric chloride (CC)
- Decan-1-amine
- Dodecan-1-amine
- Hexadecan-1-amine
- Methyl-imidazole
- Methyl iodide
- Octadecan-1-amine
- Tetradecan-1-amine
- Dodecanoic Acid

## 5.3 Synthesis of precursors and substituted chloro triazine

### 5.3.1 Synthesis of 2,4-dichloro-6-methoxy-1,3,5-triazine (MMT)



**Scheme 5.1** - Synthesis of MMT

This synthesis has been carried out following the same method proposed by Kaminsky<sup>[123]</sup>

In a 100mL two-neck flask, 0.91g (10.0 mmol) of NaHCO<sub>3</sub> was introduced WITH 30 mL of methanol under magnetic stirring. The mixture was chilled to 0°C in an ice-water bath. Then, 2.0g (10.8 mmol) cyanuric chloride was added to the solution in small aliquots. The reaction was left under constant magnetic stirring, at 0°C, for 1h and monitored by GC. When the reaction was complete, the solvent was removed by rotavapor. Once removed all of methanol, 30 mL of acetone was added in order to solubilize the product and filter out the sodium chloride present as a byproduct. Finally, the filtrated mother liquors are pulled to dry by rotavapor to obtain the finished product. The product results in a white waxy solid. It is characterized by <sup>1</sup>H NMR, <sup>13</sup>C NMR, COSY, HMQC, FT-IR, GC-MS.

Yield: 97%, Purity: 98%.

#### Characterization

**m.p.:** 88°C.

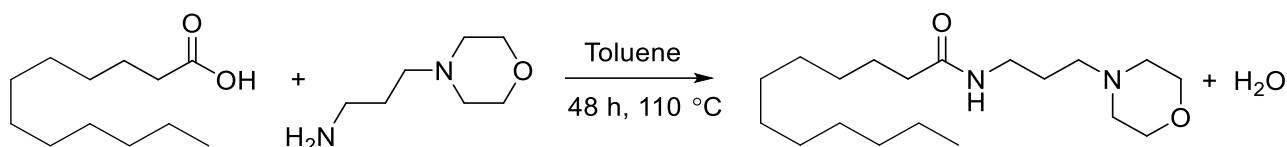
**<sup>1</sup>H NMR** (300 MHz, Acetone-d<sub>6</sub>), δ (ppm): 4.17 (3H, s, -OCH<sub>3</sub>).

**<sup>13</sup>C NMR** (75 MHz, Acetone-d<sub>6</sub>) δ (ppm): 172.76, 172.71, 57.40.

**FT-IR:** (KBr,  $\text{cm}^{-1}$ ): 1528, 1258, 815.

**GC-MS** (m/z): 178.977 [M]<sup>+</sup>, 163.006[M-CH<sub>3</sub>]<sup>+</sup>, 149.988[M-Cl]<sup>+</sup>, 108.064[M-Cl<sub>2</sub>]<sup>+</sup>.

### 5.3.2 Synthesis of N-(3-morpholinopropyl) dodecylamide (via Dean-Stark)



**Scheme 5.2** - Synthesis of N-(3-morpholinopropyl) dodecanamide via heating and water removal

In a 250 mL one-neck flask equipped with magnetic stirring, 4.3 g (30 mmol) dodecanoic acid, 100 mL toluene, and 5.1 g (40 mmol) of excess 3-morpholinopropylamine were added successively. Next, the Dean-Stark trap was set up and the flask was immersed in an oil bath. The solution was allowed to warm to reflux and allowed to proceed for 48 hours. When the reaction was complete, the solution was decanted into a separating funnel and washed with 3 x 30 mL aliquots of water. The recovered organic phase was then anhydriified with anhydrous magnesium sulfate and finally the solvent was removed under reduced pressure on the rotavapor.

The product results in a white waxy solid. It is characterized by <sup>1</sup>H NMR, <sup>13</sup>C NMR, COSY, HMQC, FT-IR, GC-MS.

Yield: 66% Purity 78%.

#### Characterization

**m.p.:** 53,4 °C.

**<sup>1</sup>H NMR** (300 MHz, CDCl<sub>3</sub>), δ (ppm): 0.89 (t, 3H, -CH<sub>2</sub>**CH**<sub>3</sub>), 1.26 (m, 12H, -CH<sub>2</sub>(**CH**<sub>2</sub>)<sub>6</sub>CH<sub>3</sub>), 1.63 (q, 2H, -**CH**<sub>2</sub>CH<sub>2</sub>CO-), 1.71 (q, 2H, -**CH**<sub>2</sub>CH<sub>2</sub>NH-), 2.15 (t, 2H, -**CH**<sub>2</sub>CO-), 2.46 (m, 6H, -

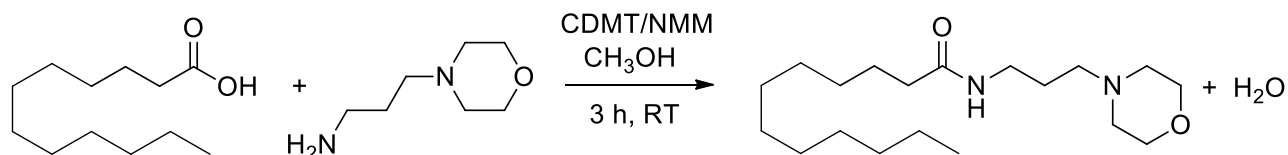
(CH<sub>2</sub>)<sub>2</sub>NCH<sub>2</sub>-, -(CH<sub>2</sub>)<sub>2</sub>NCH<sub>2</sub>-), 3.37 (q, 2H, -CH<sub>2</sub>NH-), 3.72 (t, 4H, -CH<sub>2</sub>OCH<sub>2</sub>-, -CH<sub>2</sub>OCH<sub>2</sub>-), 6.79 (s, 1H, -NHCO-).

<sup>13</sup>C NMR (75 MHz, CDCl<sub>3</sub>), δ (ppm): 172.98, 67.04, 57.86, 53.71, 39.28, 37.12, 31.89, 29.64-29.30, 25.94, 22.65, 14.12.

IR (KBr, cm<sup>-1</sup>): 3312, 2932, 2865, 1652, 1461, 1115.

GC-MS (m/z): 326.310 [M]<sup>+</sup>, 283.330 [M-C<sub>2</sub>H<sub>6</sub>O]<sup>+</sup>, 240.280 [M-C<sub>4</sub>H<sub>9</sub>NO]<sup>+</sup>, 199.150 [M-C<sub>7</sub>H<sub>15</sub>NO]<sup>+</sup>, 127.130 [M-C<sub>12</sub>H<sub>25</sub>NO]<sup>+</sup>, 100.160 [C<sub>5</sub>H<sub>11</sub>NO]<sup>+</sup>.

### 5.3.3 Synthesis of *N*-(3-morpholinopropyl) dodecylamide via CDMT/NMM system



**Scheme 5.3** - Synthesis of *N*-(3-morpholinopropyl) alkylamide using DMTMM as amidation activator

Dodecanoic acid (186 mg, 1.3 mmol) was dissolved in 6 mL of MeOH. Subsequently CDMT (228.2 mg, 1.3 mmol), NMM (131.5 mg, 1.3 mmol), and 3-morpholinopropylamine (153 mg, 1.2 mmol) were added. Yield in amide *N*-(3-morpholinopropyl) dodecylamide was monitored by GC resulting 70% conversion after 3h. The isolated product was isolated via removal of the solvent and triturated with 10 mL of a 1 M NaOH solution.

The product results in a white waxy solid. It is characterized by <sup>1</sup>H NMR, <sup>13</sup>C NMR, COSY, HMQC, FT-IR.

Yield: 42% Purity 98%.



## Characterization

m.p.: 56.4 °C.

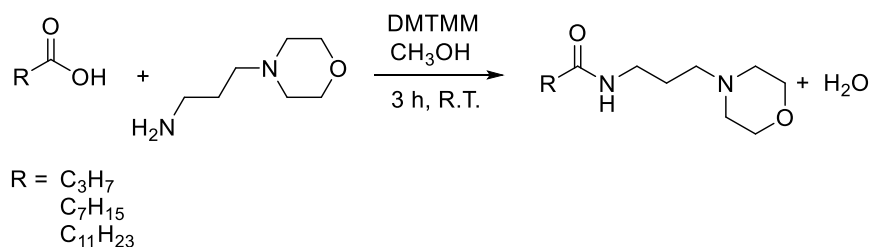
**<sup>1</sup>H NMR** (300 MHz, CDCl<sub>3</sub>), δ (ppm): 0.89 (t, 3H, -CH<sub>2</sub>**CH**<sub>3</sub>), 1.26 (m, 12H, -CH<sub>2</sub>(**CH**<sub>2</sub>)<sub>6</sub>CH<sub>3</sub>), 1.63 (q, 2H, -**CH**<sub>2</sub>CH<sub>2</sub>CO-), 1.71 (q, 2H, -**CH**<sub>2</sub>CH<sub>2</sub>NH-), 2.15 (t, 2H, -**CH**<sub>2</sub>CO-), 2.46 (m, 6H, -(CH<sub>2</sub>)<sub>2</sub>N**CH**<sub>2</sub>-, -(**CH**<sub>2</sub>)<sub>2</sub>NCH<sub>2</sub>-), 3.37 (q, 2H, -**CH**<sub>2</sub>NH-), 3.72 (t, 4H, -CH<sub>2</sub>O**CH**<sub>2</sub>-, -**CH**<sub>2</sub>OCH<sub>2</sub>-), 6.79 (s, 1H, -**NH**CO-).

**<sup>13</sup>C NMR** (75 MHz, CDCl<sub>3</sub>), δ (ppm): 172.98, 67.04, 57.86, 53.71, 39.28, 37.12, 31.89, 29.64-29.30, 25.94, 22.65, 14.12.

**IR** (KBr, cm<sup>-1</sup>): 3312, 2932, 2865, 1652, 1461, 1115.

**GC-MS** (m/z): 326.310 [M]<sup>+</sup>, 283.330 [M-C<sub>2</sub>H<sub>6</sub>O]<sup>+</sup>, 240.280 [M-C<sub>4</sub>H<sub>9</sub>NO]<sup>+</sup>, 199.150 [M-C<sub>7</sub>H<sub>15</sub>NO]<sup>+</sup>, 127.130 [M-C<sub>12</sub>H<sub>25</sub>NO]<sup>+</sup>, 100.160 [C<sub>5</sub>H<sub>11</sub>NO]<sup>+</sup>.

### 5.3.4 Synthesis of N-(3-morpholinopropyl) alkylamide via DMTMM (MoPALA)



**Scheme 5.4** - Synthesis of N-(3-morpholinopropyl) alkylamide using DMTMM as amidation activator

In a 100 mL single-neck flask, one rate of fatty acid and methanol (see table 5.1) were introduced under magnetic stirring. Then, 3-morpholinopropylamine (see table 5.1 for quantities) was added to the solution. Upon complete dissolution, DMTMM (see table 5.1 for quantities) was added. After three hours, the solvent was removed by rotavapor. The resulting powder

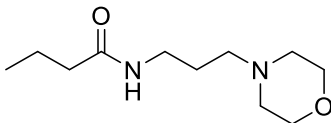
MoPALA<sub>12</sub> was triturated with 25 mL of a 1 M NaOH solution. After 30 minutes, the suspension was filtered on Gooch and washed with three aliquots of distilled water. The solid product was then dried in a reduced pressure desiccator for 24 hours. Instead for MoPALA<sub>4</sub> and MoPALA<sub>8</sub>, which were an oil, the products were resumed with 30 mL of dichloromethane and washed three times with 25 mL of a 1 M NaOH solution inside a separatory funnel. Next, the organic liquors were anhydried with magnesium sulfate powder, filtered, and placed in rotavapor for solvent removal. The product results in a white waxy solid for MoPALA<sub>12</sub> and a yellow oil for MoPALA<sub>4</sub> and MoPALA<sub>8</sub>. All of them was characterized by <sup>1</sup>H NMR, <sup>13</sup>C NMR, COSY, HMQC, FT-IR, GC-MS and m.p.

**Table 5.1** – Experimental data for synthesis of N-(3-morpholinopropyl) alkylamide

|                            | MoPA  | Fatty Acid                            | DMTMM | Methanol | Yield (%) | Purity (%) |
|----------------------------|-------|---------------------------------------|-------|----------|-----------|------------|
| <b>MoPALA<sub>4</sub></b>  |       | (HOOC)C <sub>4</sub> H <sub>7</sub>   |       |          | 60        | 85         |
| <b>mmol</b>                | 12.00 | 10.50                                 | 10.50 |          |           |            |
| <b>g</b>                   | 1.73  | 0.92                                  | 2.93  |          |           |            |
| <b>mL</b>                  |       |                                       |       | 75       |           |            |
| <b>MoPALA<sub>8</sub></b>  |       | (HOOC)C <sub>7</sub> H <sub>15</sub>  |       |          | 62        | 87         |
| <b>mol</b>                 | 12.00 | 10.50                                 | 10.50 |          |           |            |
| <b>g</b>                   | 1.73  | 1.51                                  | 2.93  |          |           |            |
| <b>mL</b>                  |       |                                       |       | 75       |           |            |
| <b>MoPALA<sub>12</sub></b> |       | (HOOC)C <sub>11</sub> H <sub>23</sub> |       |          | 52        | 98         |
| <b>mol</b>                 | 12.00 | 10.50                                 | 10.50 |          |           |            |
| <b>g</b>                   | 1.73  | 2.10                                  | 2.93  |          |           |            |
| <b>mL</b>                  |       |                                       |       | 75       |           |            |

## Characterization

### MoPALA<sub>4</sub>



*N*-(3-morpholinopropyl)butyramide

Chemical Formula: C<sub>11</sub>H<sub>22</sub>N<sub>2</sub>O<sub>2</sub>

Molecular Weight: 214,31

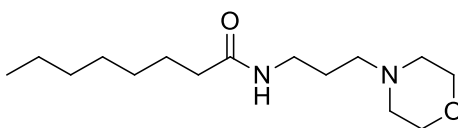
<sup>1</sup>H NMR (300 MHz, CDCl<sub>3</sub>) δ (ppm): 0.85 (t, 3H, -CH<sub>2</sub>**CH**<sub>3</sub>), 1.52 (q, 2H, -CH<sub>2</sub>**CH**<sub>2</sub>CH<sub>3</sub>), 2.13 (t, 2H, -**CH**<sub>2</sub>CO-), 2.42 (m, 6H, -(CH<sub>2</sub>)<sub>2</sub>**NCH**<sub>2</sub>-, -(**CH**<sub>2</sub>)<sub>2</sub>NCH<sub>2</sub>-), 3.30 (q, 2H, -**CH**<sub>2</sub>NH-), 3.75 (t, 4H, -CH<sub>2</sub>**OCH**<sub>2</sub>, -**CH**<sub>2</sub>OCH<sub>2</sub>-), 6.86 (s, 1H, -**NH**CO-).

<sup>13</sup>C NMR (75 MHz, CDCl<sub>3</sub>) δ (ppm): 173.82, 66.12, 56.98, 53.69, 39.10, 37.00, 31.66, 29.27, 25.56, 23.48, 14.00.

IR (KBr, cm<sup>-1</sup>): 3302, 2908, 2859, 1647, 1466, 1109.

GC-MS (m/z): 214.210 [M]<sup>+</sup>, 100.180 [C<sub>5</sub>H<sub>11</sub>NO]<sup>+</sup>, 71.590 [M-C<sub>8</sub>H<sub>15</sub>NO]<sup>+</sup>.

### MoPALA<sub>8</sub>



*N*-(3-morpholinopropyl)octanamide

Chemical Formula: C<sub>15</sub>H<sub>30</sub>N<sub>2</sub>O<sub>2</sub>

Molecular Weight: 270,41

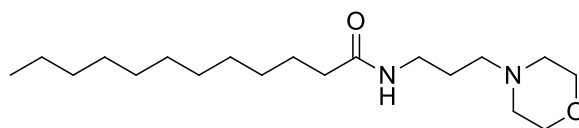
<sup>1</sup>H NMR (300 MHz, CDCl<sub>3</sub>) δ (ppm): 0.86 (t, 3H, -CH<sub>2</sub>**CH**<sub>3</sub>), 1.28 (m, 8H, -CH<sub>2</sub>(**CH**<sub>2</sub>)<sub>6</sub>CH<sub>3</sub>), 1.64 (q, 2H, -**CH**<sub>2</sub>CH<sub>2</sub>CO-), 2.13 (t, 2H, -**CH**<sub>2</sub>CO-), 2.44 (m, 6H, -(CH<sub>2</sub>)<sub>2</sub>**NCH**<sub>2</sub>-, -(**CH**<sub>2</sub>)<sub>2</sub>NCH<sub>2</sub>-), 3.33 (q, 2H, -**CH**<sub>2</sub>NH-), 3.70 (t, 4H, -CH<sub>2</sub>**OCH**<sub>2</sub>, -**CH**<sub>2</sub>OCH<sub>2</sub>-), 6.81 (s, 1H, -**NH**CO-).

**$^{13}\text{C}$  NMR** (75 MHz,  $\text{CDCl}_3$ )  $\delta$  (ppm): 173.06 , 66.98 , 57.72 , 53.69 , 39.10 , 37.00 , 31.66 , 29.27 , 28.98 , 25.87 , 25.07 , 22.55 , 14.00.

**IR** (KBr,  $\text{cm}^{-1}$ ): 3325, 2911, 2869, 1632, 1472, 1106.

**GC-MS** (m/z): 270.230  $[\text{M}]^+$ , 227.230  $[\text{M}-\text{C}_2\text{H}_6\text{O}]^+$ , 127.140  $[\text{M}-\text{C}_8\text{H}_{15}\text{NO}]^+$ , 100.180  $[\text{C}_5\text{H}_{11}\text{NO}]^+$ .

### MoPALA<sub>12</sub>



*N*-(3-morpholinopropyl)dodecanamide

Chemical Formula:  $\text{C}_{19}\text{H}_{38}\text{N}_2\text{O}_2$

Molecular Weight: 326,52

**m.p.:** 52,6 °C.

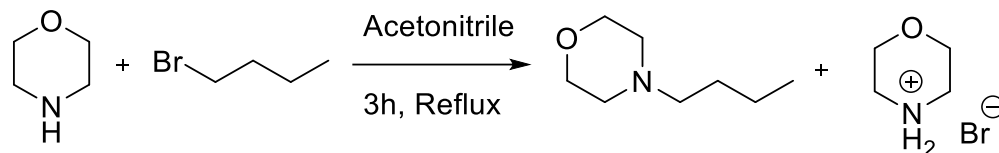
**$^1\text{H}$  NMR** (300 MHz,  $\text{CDCl}_3$ ),  $\delta$  (ppm): 0.89 (t, 3H,  $-\text{CH}_2\text{CH}_3$ ), 1.27 (m, 12H,  $-\text{CH}_2(\text{CH}_2)_6\text{CH}_3$ ), 1.63 (q, 2H,  $-\text{CH}_2\text{CH}_2\text{CO}-$ ), 1.70 (q, 2H,  $-\text{CH}_2\text{CH}_2\text{NH}-$ ), 2.16 (t, 2H,  $-\text{CH}_2\text{CO}-$ ), 2.46 (m, 6H,  $-(\text{CH}_2)_2\text{NCH}_2-$ ,  $-(\text{CH}_2)_2\text{NCH}_2-$ ), 3.36 (q, 2H,  $-\text{CH}_2\text{NH}-$ ), 3.73 (t, 4H,  $-\text{CH}_2\text{OCH}_2-$ ,  $-\text{CH}_2\text{OCH}_2-$ ), 6.78 (s, 1H,  $-\text{NHCO}-$ ).

**$^{13}\text{C}$  NMR** (75 MHz,  $\text{CDCl}_3$ ),  $\delta$  (ppm): 172.99, 67.06, 57.90, 53.74, 39.26, 37.10, 31.89, 29.60-29.32, 25.93, 22.67, 14.10.

**IR** (KBr,  $\text{cm}^{-1}$ ): 3319, 2920, 2870, 1640, 1470, 1113.

**GC-MS** (m/z): 326.320  $[\text{M}]^+$ , 283.310  $[\text{M}-\text{C}_2\text{H}_6\text{O}]^+$ , 240.270  $[\text{M}-\text{C}_4\text{H}_9\text{NO}]^+$ , 199.170  $[\text{M}-\text{C}_7\text{H}_{15}\text{NO}]^+$ , 127.150  $[\text{M}-\text{C}_{12}\text{H}_{25}\text{NO}]^+$ , 100.170  $[\text{C}_5\text{H}_{11}\text{NO}]^+$ .

### 5.3.5 Synthesis of 4-butylmorpholine



**Scheme 5.5** – Synthesis of 4-butylmorpholine by reaction between morpholine and bromobutane

In a 50 mL two-neck flask with magnetic stirring and bubble coolant were introduced 20 ml of acetonitrile, 10.44 g (120.0 mmol) of morpholine and 8.22 g (60.0 mmol) of 1-bromobutane. The mixture is refluxed and allowed to react for 3 hours. At the end of the reaction the resulting mixture is cooled, filtered through silica gel (60 Å) and the liquid is concentrated to reduced pressure. Then the product is purified through vacuum distillation, resulting in pure 4-butylmorpholine as a transparent liquid.

Yield: 86%, Purity: 98%

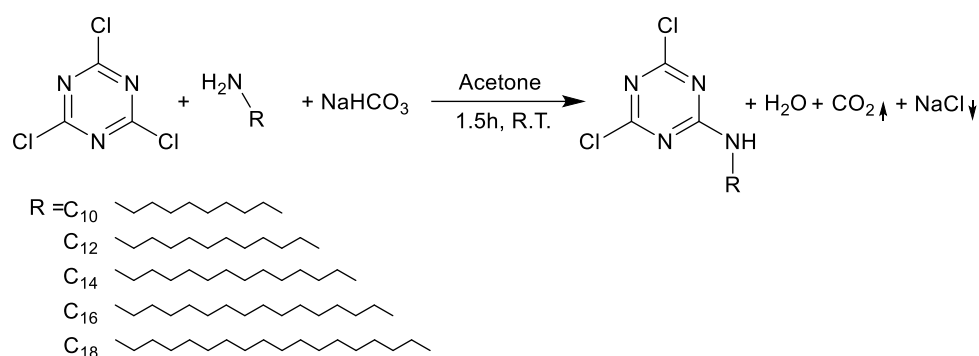
**<sup>1</sup>H NMR** (300 MHz, CDCl<sub>3</sub>) δ (ppm): 0.82 (t, 3H, -CH<sub>2</sub>CH<sub>3</sub>), 1.25 (m, 2H, -CH<sub>2</sub>CH<sub>2</sub>CH<sub>3</sub>), 1.38 (dd, 2H, -CH<sub>2</sub>CH<sub>2</sub>N), 2.28 – 2.16 (m, 2H, -CH<sub>2</sub>N-), 2.33 (t, 4H, -(CH<sub>2</sub>)<sub>2</sub>NCH<sub>2</sub>-), 3.61 (t, 4H, -(CH<sub>2</sub>)<sub>2</sub>O).

**<sup>13</sup>C NMR** (75 MHz, (CDCl<sub>3</sub>) δ (ppm): 66.82, 58.74, 53.68, 28.57, 20.53, 13.87.

**IR** (KBr, cm<sup>-1</sup>): 2952, 2858, 2804, 1452, 1113.

**GC-MS** (m/z): 143.100 [M]<sup>+</sup>.

### 5.3.6 Synthesis of 1,3,5-triazin-2-alkylamine



**Scheme 5.6** – Synthesis of 1,3,5-triazin-2-alkylamine by reaction between cyanuric chloride and alkylamine

In a two-neck flask equipped with an ice bath and magnetic stirring, quantities as shown in Table 5.2, of cyanuric chloride, sodium bicarbonate, and acetone were introduced. The solution was then brought to 0 °C during stirring. An acetone solution of alkyl-1-amine (as reported in Table 5.2) was then placed in a drip funnel. Small amounts of dichloromethane were also added to aid in the solubilization of the higher molecular weight alkylamines. The solution is then dripped into the flask while maintaining it in the ice bath. Upon completion of the addition, the ice bath was removed and the mixture was left to stir for an hour and a half. At the end of the reaction, the suspension was filtered to remove the inorganic salts (NaCl and NaHCO<sub>3</sub>), then the solvent was removed under reduced pressure using a rotavapor. A straw yellow solid is collected. The solid is then purified by precipitation from hexane.

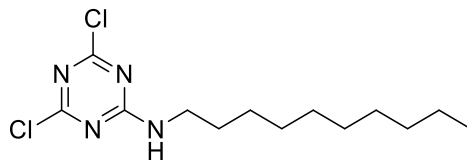
The precipitated product results in a white waxy solid. It is characterized by <sup>1</sup>H NMR, <sup>13</sup>C NMR, COSY, HMQC, FT-IR, GC-MS. The yields are reported in table 5.1

Table 5.2 - Experimental data for MAT synthesis.

|                         | <b>CC</b> | <b>Ammine</b>                                    | <b>NaHCO<sub>3</sub></b> | <b>Acetone</b> | <b>Yield (%)</b> | <b>Purity(%)</b> |
|-------------------------|-----------|--|--------------------------|----------------|------------------|------------------|
| <b>MAT<sub>10</sub></b> |           | H <sub>2</sub> N-C <sub>10</sub> H <sub>21</sub> |                          |                | 51               | 87               |
| <b>mmol</b>             | 13.59     | 13.59  | 25.00                    |                |                  |                  |
| <b>g</b>                | 2.50      | 2.10   | 2.10                     |                |                  |                  |
| <b>mL</b>               |           |  |                          | 50             |                  |                  |
| <b>MAT<sub>12</sub></b> |           | H <sub>2</sub> N-C <sub>12</sub> H <sub>25</sub> |                          |                | 96               | 93               |
| <b>mol</b>              | 0.11      | 0.11   | 0.19                     |                |                  |                  |
| <b>g</b>                | 20.00     | 20.00  | 16.00                    |                |                  |                  |
| <b>mL</b>               |           |  |                          | 50             |                  |                  |
| <b>MAT<sub>14</sub></b> |           | H <sub>2</sub> N-C <sub>14</sub> H <sub>29</sub> |                          |                | 52               | 91               |
| <b>mmol</b>             | 13.59     | 13.59  | 25.00                    |                |                  |                  |
| <b>g</b>                | 2.50      | 2.90   | 2.10                     |                |                  |                  |
| <b>mL</b>               |           |  |                          | 50             |                  |                  |
| <b>MAT<sub>16</sub></b> |           | H <sub>2</sub> N-C <sub>16</sub> H <sub>33</sub> |                          |                | 71               | 94               |
| <b>mmol</b>             | 27.17     | 27.17  | 50.00                    |                |                  |                  |
| <b>g</b>                | 5.00      | 6.50   | 4.20                     |                |                  |                  |
| <b>mL</b>               |           |  |                          | 100            |                  |                  |
| <b>MAT<sub>18</sub></b> |           | H <sub>2</sub> N-C <sub>18</sub> H <sub>37</sub> |                          |                | 50               | 86               |
| <b>mmol</b>             | 27.17     | 27.17  | 50.00                    |                |                  |                  |
| <b>g</b>                | 5.00      | 7.30   | 4.20                     |                |                  |                  |
| <b>mL</b>               |           |  |                          | 100            |                  |                  |

## Characterization

### MAT<sub>10</sub>



4,6-dichloro-*N*-decyl-1,3,5-triazin-2-amine

Chemical Formula: C<sub>13</sub>H<sub>22</sub>Cl<sub>2</sub>N<sub>4</sub>

Molecular Weight: 305,25

**m.p.:** 61°C.

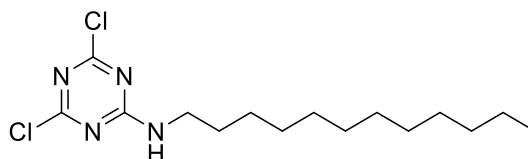
**<sup>1</sup>H NMR** (300 MHz, CDCl<sub>3</sub>) δ (ppm): 6.05 (1H, s, -**NH**CH<sub>2</sub>), 3.45 (2H, m, -NH**CH**<sub>2</sub>CH<sub>2</sub>), 1.60 (2H, q, -NHCH<sub>2</sub>**CH**<sub>2</sub>CH<sub>2</sub>), 1.23 (14H, m, -CH<sub>2</sub>(**C**<sub>7</sub>**H**<sub>14</sub>)CH<sub>3</sub>), 0.85 (3H, m, -CH<sub>2</sub>**CH**<sub>3</sub>).

**<sup>13</sup>C NMR** (75 MHz, CDCl<sub>3</sub>) δ (ppm): 171.13, 169.90, 165.96, 41.72, 32.01, 29.62, 26.77, 22.81, 14.25.

**FT-IR** (KBr, cm<sup>-1</sup>): 3264, 2921-2851, 1620, 851.

**GC-MS** (m/z): 304.100 [M]<sup>+</sup>, 269.140 [M - Cl]<sup>+</sup>, 233.050 [M - 2Cl]<sup>+</sup>, 176.940 [M - C<sub>9</sub>H<sub>19</sub>]<sup>+</sup>.

### MAT<sub>12</sub>



4,6-dichloro-*N*-dodecyl-1,3,5-triazin-2-amine

Chemical Formula: C<sub>15</sub>H<sub>26</sub>Cl<sub>2</sub>N<sub>4</sub>

Molecular Weight: 333,30

**m.p.:** 70°C.

**<sup>1</sup>H NMR** (300 MHz, CDCl<sub>3</sub>) δ (ppm): 6.42 (1H, s, -**NH**-), 3.44 (2H, q, -NH**CH**<sub>2</sub>CH<sub>2</sub>), 1.59 (2H, m, -NHCH<sub>2</sub>**CH**<sub>2</sub>CH<sub>2</sub>), 1.23 (18H, s, -CH<sub>2</sub>(**C**<sub>9</sub>**H**<sub>18</sub>)CH<sub>3</sub>), 0.85 (3H, t, -CH<sub>2</sub>**CH**<sub>3</sub>).

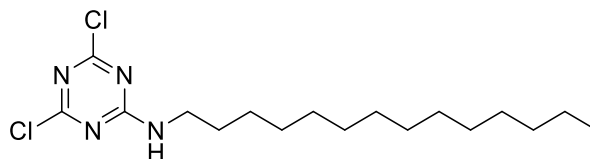


**<sup>13</sup>C NMR** (75 MHz, CDCl<sub>3</sub>) δ (ppm): 171.07, 169.80, 165.92, 41.70, 32.02, 29.73, 26.77, 22.80, 14.22.

**FT-IR:** (KBr, cm<sup>-1</sup>): 3266, 2919-2850, 1630, 848.

**GC-MS** (m/z): 332.170 [M]<sup>+</sup>, 297.210 [M - Cl]<sup>+</sup>, 261.14 [M - 2Cl]<sup>+</sup>, 177.010 [M - C<sub>11</sub>H<sub>23</sub>]<sup>+</sup>.

#### MAT<sub>14</sub>



4,6-dichloro-*N*-tetradecyl-1,3,5-triazin-2-amine

Chemical Formula: C<sub>17</sub>H<sub>30</sub>Cl<sub>2</sub>N<sub>4</sub>

Molecular Weight: 361,36

**m.p.:** 75°C

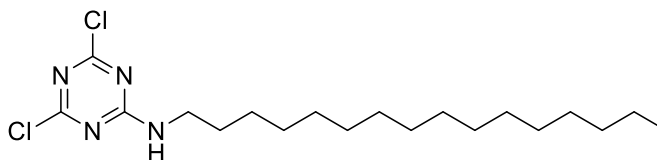
**<sup>1</sup>H NMR** (300 MHz, CDCl<sub>3</sub>) δ (ppm): 5.86 (1H, s, -**NH**-), 3.48 (2H, q, -NH**CH**<sub>2</sub>CH<sub>2</sub>), 1.60 (2H, m, -CH<sub>2</sub>**CH**<sub>2</sub>CH<sub>2</sub>), 1.26 (22H, s, -CH<sub>2</sub>(**C**<sub>11</sub>**H**<sub>22</sub>)CH<sub>3</sub>), 0.88 (3H, t, CH<sub>2</sub>**CH**<sub>3</sub>).

**<sup>13</sup>C NMR** (75 MHz, CDCl<sub>3</sub>) δ (ppm): 171.16, 169.87, 165.98, 41.70, 32.02, 29.77, 26.77, 22.80, 15.06.

**FT-IR:** (KBr, cm<sup>-1</sup>): 3267, 2919-2850, 1630, 848.

**GC-MS** (m/z): 360.210 [M]<sup>+</sup>, 325.260 [M - Cl]<sup>+</sup>, 289.210 [M - 2Cl]<sup>+</sup>, 177.020 [M - C<sub>11</sub>H<sub>23</sub>]<sup>+</sup>.

#### MAT<sub>16</sub>



4,6-dichloro-*N*-hexadecyl-1,3,5-triazin-2-amine

Chemical Formula: C<sub>19</sub>H<sub>34</sub>Cl<sub>2</sub>N<sub>4</sub>

Molecular Weight: 389,41

**m.p.:** 78°C

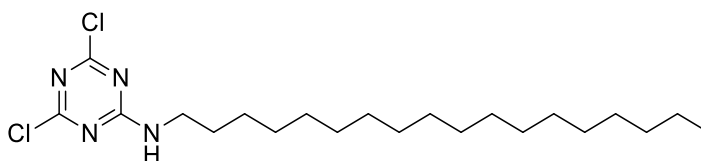
**<sup>1</sup>H NMR** (300 MHz, CDCl<sub>3</sub>) δ (ppm): 6.15 (1H, s, **-NH-**), 3.47 (2H, q, **-NHCH<sub>2</sub>CH<sub>2</sub>**), 1.60 (2H, m, **-NHCH<sub>2</sub>CH<sub>2</sub>CH<sub>2</sub>**), 1.24 (26H, s, **-CH<sub>2</sub>(C<sub>13</sub>H<sub>26</sub>)CH<sub>3</sub>**), 0.87 (3H, t, **-CH<sub>2</sub>CH<sub>3</sub>**).

**<sup>13</sup>C NMR** (75 MHz, CDCl<sub>3</sub>) δ (ppm): 171.18, 169.91, 165.98, 41.70, 32.02, 29.74, 26.77, 22.80, 14.24.

**FT-IR:** (KBr, cm<sup>-1</sup>): 3266, 2919-2850, 1629, 848.

**GC-MS** (m/z): 388.220 [M]<sup>+</sup>, 353.260 [M - Cl]<sup>+</sup>, 317.23 [M - 2Cl]<sup>+</sup>, 176.960 [M - C<sub>11</sub>H<sub>23</sub>]<sup>+</sup>.

**MAT<sub>18</sub>**



4,6-dichloro-*N*-octadecyl-1,3,5-triazin-2-amine

Chemical Formula: C<sub>21</sub>H<sub>38</sub>Cl<sub>2</sub>N<sub>4</sub>

Molecular Weight: 417,46

**m.p.:** 80°C

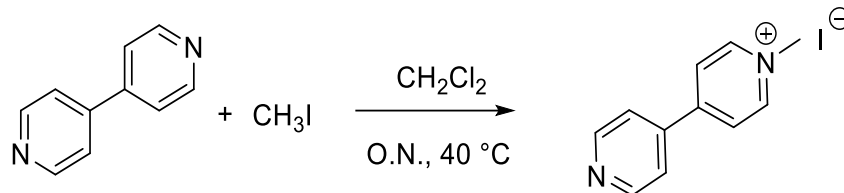
**<sup>1</sup>H NMR** (300 MHz, CDCl<sub>3</sub>) δ (ppm): 5.88 (1H, s, **-NH-**), 3.46 (2H, q, **-NHCH<sub>2</sub>CH<sub>2</sub>**), 1.60 (2H, m, **-NHCH<sub>2</sub>CH<sub>2</sub>CH<sub>2</sub>**), 1.25 (30H, s, **-CH<sub>2</sub>(C<sub>15</sub>H<sub>30</sub>)CH<sub>3</sub>**), 0.87 (3H, t, **-CH<sub>2</sub>CH<sub>3</sub>**).

**<sup>13</sup>C NMR** (75 MHz, CDCl<sub>3</sub>) δ (ppm): 171.19, 169.93, 166.01, 41.70, 32.02, 29.72, 26.77, 22.80, 14.30.

**FT-IR:** (KBr, cm<sup>-1</sup>): 3266, 2918-2849, 1630, 847.

**GC-MS** (m/z): 416.280 [M]<sup>+</sup>, 381.330 [M - Cl]<sup>+</sup>, 345.28 [M - 2Cl]<sup>+</sup>, 176.980 [M - C<sub>11</sub>H<sub>23</sub>]<sup>+</sup>.

### 5.3.7 Synthesis of 1-methyl-[4,4'bipyridin] iodide (MBP)



**Scheme 5.7** – Synthesis route of 1-methyl-[4,4'bipyridin] iodide

This procedure is a modification of the one who was carried in the work of Minbiole<sup>[146]</sup>. In a 250 mL one-neck flask equipped with magnetic stirring, 3.5 g (22.0 mmol) of bipyridyl and 1.7 mL (28.0 mmol) of iodomethane were added in approximately 50 mL of dichloromethane. The reaction was kept at reflux for about 18 hours.

An orange precipitate was formed which was then filtered over Gooch. The collected solid was then dissolved in hot MeOH and by subsequent addition of Et<sub>2</sub>O the solution became yellow by precipitation of a red solid. The solution was then filtered and the mother liquors recovered and the solvent removed under reduced pressure using rotavapor. 3.67g (12.31 mmol) of a yellow solid was recovered. The solid obtained was characterized by <sup>1</sup>H NMR, <sup>13</sup>C NMR, COSY, HMBC, FT-IR and m.p.

#### Characterization

Yield: 56%, Purity: 73%

**m.p.:** 220°C (decomposition)

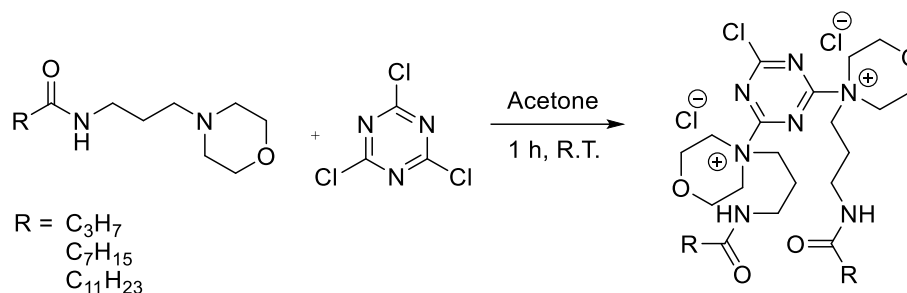
**<sup>1</sup>H NMR** (300 MHz, CDCl<sub>3</sub>) δ (ppm): 9.13 (2H, d, CH**CHN**<sup>+</sup>), 8.86 (2H, dd, CH**CHC**), 8.63 (2H, d, CH**CHN**), 8.05 (2H, dd, CH**CHC**), 4.39 (3H, s, **CH<sub>3</sub>N**<sup>+</sup>).

**<sup>13</sup>C NMR** (75 MHz, CDCl<sub>3</sub>) δ (ppm): 150.96, 146.10, 124.90, 121.80, 47.53.

**FT-IR** (KBr, cm<sup>-1</sup>): 1639, 1465, 811.

## 5.4 Synthesis of triazinyl quaternary ammonium salts

### 5.4.1 Synthesis of 4,4'-(6-chloro-1,3,5-triazine-2,4-diyl)bis(4-(3-alkylamidopropyl) morpholin-4-ium) chloride MoPALA-CC



**Scheme 5.8** – Synthesis of 4,4'-(6-chloro-1,3,5-triazine-2,4-diyl)bis(4-(3-alkylamidopropyl) morpholin-4-ium) chloride by reaction of cyanuric chloride with N-(3-morpholinopropyl)alkylamide

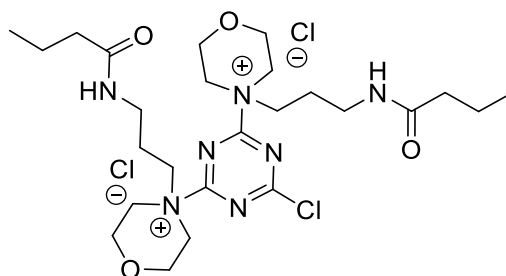
In a 100 mL single neck flask it was placed an aliquot of cyanuric chloride (see table 5.3) in 50 ml of acetone under magnetic stirring. Then N-(3-morpholinopropyl)alkylamide (see table 5.3) was added. After 1 hours of reaction a white precipitate was formed. The solvent was removed with rotavapor and the resulting white powder were triturated in ethyl ether. Then product was collected by filtration on a Gooch funnel and rinsed with cold ethyl ether. The product was left overnight in a low-pressure dryer. The white solid obtained was characterized by <sup>1</sup>H-NMR, <sup>13</sup>C-NMR, COSY, HMQC, FT-IR, m.p. and ESI-MS.

Table 5.3 - Experimental data for synthesis of MoPALA<sub>x</sub>CC

|                               | MoPALA               | CC   | Acetone | Yield (%) | Purity (%) |
|-------------------------------|----------------------|------|---------|-----------|------------|
| <b>MoPALA<sub>4</sub>CC</b>   | MoPALA <sub>4</sub>  |      |         | 19        | 89         |
| mmol                          | 7.40                 | 9.20 |         |           |            |
| g                             | 1.58                 | 1.69 |         |           |            |
| mL                            |                      |      | 50      |           |            |
| <b>MoPALA<sub>8</sub> CC</b>  | MoPALA <sub>8</sub>  |      |         | 18        | 91         |
| mol                           | 7.40                 | 9.20 |         |           |            |
| g                             | 2.00                 | 1.69 |         |           |            |
| mL                            |                      |      | 50      |           |            |
| <b>MoPALA<sub>12</sub> CC</b> | MoPALA <sub>12</sub> |      |         | 15        | 96         |
| mol                           | 7.40                 | 9.20 |         |           |            |
| g                             | 1.73                 | 1.69 |         |           |            |
| mL                            |                      |      | 50      |           |            |

## Characterization

### MoPALA<sub>4</sub>CC



4,4'-(6-chloro-1,3,5-triazine-2,4-diyl)bis(4-(3-butyramidopropyl)morpholin-4-ium) chloride

Chemical Formula: C<sub>25</sub>H<sub>44</sub>Cl<sub>3</sub>N<sub>7</sub>O<sub>4</sub>

Exact Mass: 611,25

<sup>1</sup>H NMR (300 MHz, DMSO) δ (ppm): 0.84 (t, 3H, -CH<sub>2</sub>CH<sub>3</sub>), 1.48 (q, 2H, -CH<sub>2</sub>CH<sub>2</sub>CO-), 1.53 (m, 2H, -CH<sub>2</sub>CH<sub>2</sub>NH-), 2.07 (t, 2H, -CH<sub>2</sub>CO-), 3.10 (q, 2H, -NHCH<sub>2</sub>-), 3.69 (q, 6H, -

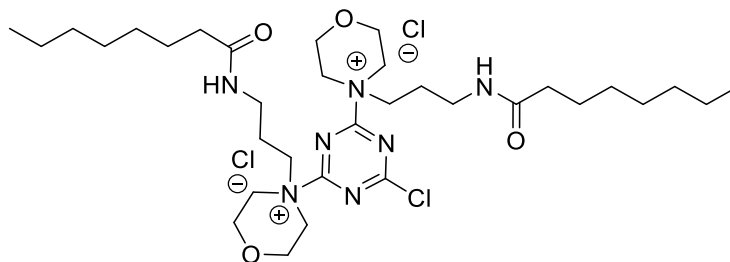
NH(CH<sub>2</sub>)<sub>2</sub>**CH<sub>2</sub>**-, **-CH<sub>2</sub>OCH<sub>2</sub>**-), 3.92 (m, 2H, -CH<sub>2</sub>CN<sup>+</sup>(**CH<sub>2</sub>**)<sub>2</sub>-), 4.35 (m, 2H, -CH<sub>2</sub>CN<sup>+</sup>(**CH<sub>2</sub>**)<sub>2</sub>-), 8.01 (t, 1H, **-NH**).

<sup>13</sup>C NMR (101 MHz, CDCl<sub>3</sub>) δ (ppm): 172.05, 166.54, 164.02, 65.21, 61.68, 57.87, 35.36, 31.24, 29.35, 28.45, 14.15.

FT-IR (KBr, cm<sup>-1</sup>): 2935, 1606, 1312.

ESI-MS (m/z): 522.4 [M]<sup>+</sup> (in the HPLC-ESI condition the triazine Cl group was hydrolyzed at OH group)

### MoPALA<sub>8</sub>CC



4,4'-(6-chloro-1,3,5-triazine-2,4-diyl)bis(4-(3-octanamidopropyl)morpholin-4-ium) chloride

Chemical Formula: C<sub>33</sub>H<sub>60</sub>Cl<sub>3</sub>N<sub>7</sub>O<sub>4</sub>

Exact Mass: 723,38

M.P.: 131.7 °C ;

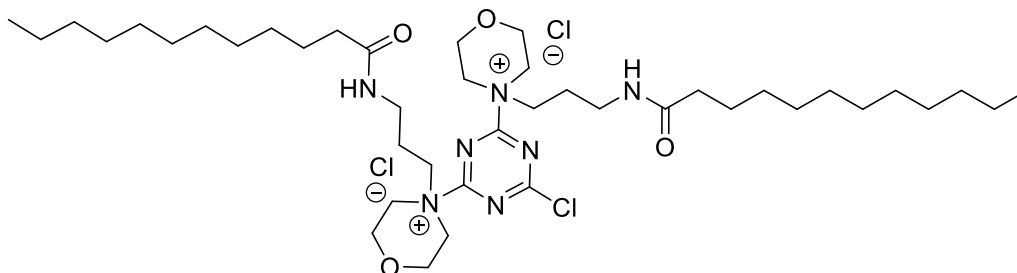
<sup>1</sup>H NMR (300 MHz, (CD<sub>3</sub>)<sub>2</sub>SO) δ (ppm): 0.85 (t, 3H, -CH<sub>2</sub>**CH<sub>3</sub>**), 1.22 (t, 8H, -CH<sub>2</sub>(**CH<sub>2</sub>**)<sub>8</sub>CH<sub>3</sub>), 1.44 (q, 2H, **-CH<sub>2</sub>CH<sub>2</sub>CO-**), 1.59 (m, 2H, **-CH<sub>2</sub>CH<sub>2</sub>NH-**), 2.03 (t, 2H, **-CH<sub>2</sub>CO-**), 3.02 (q, 2H, -NH**CH<sub>2</sub>**-), 3.76 (q, 6H, -NH(CH<sub>2</sub>)<sub>2</sub>**CH<sub>2</sub>**-, **-CH<sub>2</sub>OCH<sub>2</sub>**-), 3.97 (t, 2H, -CH<sub>2</sub>CN<sup>+</sup>(**CH<sub>2</sub>**)<sub>2</sub>-), 4.32 (m, 4H, -CH<sub>2</sub>CN<sup>+</sup>(**CH<sub>2</sub>**)<sub>2</sub>-), 8.03 (t, 1H, **-NH**).

<sup>13</sup>C NMR (75 MHz, (CD<sub>3</sub>)<sub>2</sub>SO) δ (ppm): 172.90, 166.92, 164.53, 65.64, 62.03, 58.23, 35.84, 31.75, 29.51, 29.47, 29.42, 29.28, 29.22, 29.17, 25.62, 22.54, 14.39.

FT-IR (KBr, cm<sup>-1</sup>): 2918, 1620, 1372.

**ESI-MS** (m/z): 327.3[M]<sup>2+</sup>.

**MoPALA<sub>12</sub> CC**



4,4'-(6-chloro-1,3,5-triazine-2,4-diyl)bis(4-(3-dodecanamidopropyl)morpholin-4-ium) chloride

Chemical Formula: C<sub>41</sub>H<sub>76</sub>Cl<sub>3</sub>N<sub>7</sub>O<sub>4</sub>

Exact Mass: 835,50

**M.P.:** 260°C (decomposition)

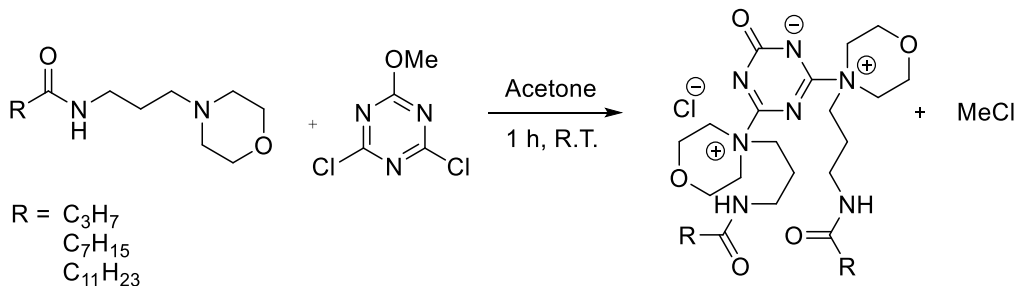
**<sup>1</sup>H NMR** (300 MHz, (CD<sub>3</sub>)<sub>2</sub>SO) δ (ppm): 0.85 (t, 3H, -CH<sub>2</sub>**CH**<sub>3</sub>), 1.23 (t, 16H, -CH<sub>2</sub>(**CH**<sub>2</sub>)<sub>8</sub>CH<sub>3</sub>), 1.44 (q, 2H, -**CH**<sub>2</sub>CH<sub>2</sub>CO-), 1.59 (m, 2H, -**CH**<sub>2</sub>CH<sub>2</sub>NH-), 2.02 (t, 2H, -**CH**<sub>2</sub>CO-), 3.01 (q, 2H, -NH**CH**<sub>2</sub>-), 3.74 (q, 6H, -NH(CH<sub>2</sub>)<sub>2</sub>**CH**<sub>2</sub>-, -**CH**<sub>2</sub>O**CH**<sub>2</sub>-), 3.96 (t, 2H, -CH<sub>2</sub>CN<sup>+</sup>(**CH**<sub>2</sub>)<sub>2</sub>-), 4.32 (t, 2H, -CH<sub>2</sub>CN<sup>+</sup>(**CH**<sub>2</sub>)<sub>2</sub>-), 7.95 (t, 1H, -**NH**-).

**<sup>13</sup>C NMR** (75 MHz, (CD<sub>3</sub>)<sub>2</sub>SO) δ (ppm): 172.41, 166.46, 164.08, 65.13, 61.56, 57.76, 35.36, 35.33, 31.28, 29.05, 29.00, 28.95, 28.82, 28.76, 28.68, 25.16, 22.07, 13.92.

**FT-IR** (KBr, cm<sup>-1</sup>): 2920, 1628, 1368.

**ESI-MS** (m/z): 746.7 (in the HPLC-ESI condition the triazine Cl group was hydrolyzed at OH group).

### 5.4.2 Synthesis of 4,4'-(6-chloro-1,3,5-triazine-2,4-diyl)bis(4-(3-alkylamidopropyl) morpholin-4-ium) chloride (MoPALA-MMT)



**Scheme 5.9** – Synthesis of 4,4'-(6-chloro-1,3,5-triazine-2,4-diyl)bis(4-(3-alkylamidopropyl) morpholin-4-ium) chloride by reaction of MMT with N-(3-morpholinopropyl)alkylamide

In a 100 mL single neck flask it was placed an aliquot of 2,4-dichloro-6-methoxy-1,3,5-triazine (MMT) (see table 5.4) in 50 ml of acetone under magnetic stirring. Then N-(3-morpholinopropyl)alkylamide (see table 5.4) was added. After 1.5 hours of reaction a white precipitate was formed. The solvent was removed with rotavapor and the resulting white powder were triturated in ethyl ether. Then product was collected by filtration on a Gooch funnel and rinsed with cold ethyl ether. The product was left overnight in a low-pressure dryer. The white solid obtained was characterized by  $^1\text{H}$  NMR,  $^{13}\text{C}$  NMR, COSY, HMBC, FT-IR, m.p. and ESI-MS.

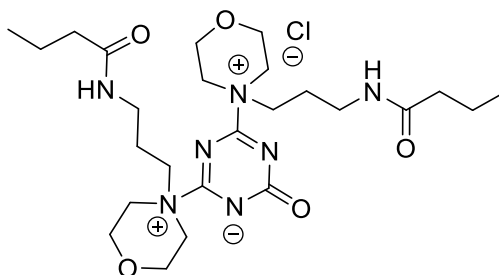


Table 5.4 - Experimental data for synthesis of MoPALA<sub>x</sub>MMT

|                               | MoPALA               | MMT  | Acetone | Yield (%) | Purity (%) |
|-------------------------------|----------------------|------|---------|-----------|------------|
| <b>MoPALA<sub>4</sub>MMT</b>  | MoPALA <sub>4</sub>  |      |         | 15        | 89         |
| mmol                          | 7.40                 | 9.20 |         |           |            |
| g                             | 1.58                 | 1.65 |         |           |            |
| mL                            |                      |      | 50      |           |            |
| <b>MoPALA<sub>8</sub>MMT</b>  | MoPALA <sub>8</sub>  |      |         | 12        | 85         |
| mol                           | 7.40                 | 9.20 |         |           |            |
| g                             | 2.00                 | 1.65 |         |           |            |
| mL                            |                      |      | 50      |           |            |
| <b>MoPALA<sub>12</sub>MMT</b> | MoPALA <sub>12</sub> |      |         | 8         | 87         |
| mol                           | 7.40                 | 9.20 |         |           |            |
| g                             | 1.73                 | 1.65 |         |           |            |
| mL                            |                      |      | 50      |           |            |

## Characterization

### MoPALA<sub>4</sub>MMT



4,6-bis(4-(3-butyramidopropyl)morpholino-4-ium)-2-oxo-2H-1,3,5-triazin-1-ide chloride

Chemical Formula: C<sub>25</sub>H<sub>44</sub>ClN<sub>7</sub>O<sub>5</sub>

Exact Mass: 557,31

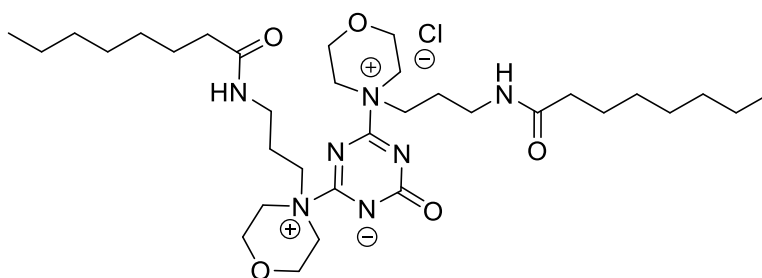
<sup>1</sup>H NMR (300 MHz, (CD<sub>3</sub>)<sub>2</sub>SO) δ (ppm): 0.84 (t, 3H, -CH<sub>2</sub>CH<sub>3</sub>), 1.48 (q, 2H, -CH<sub>2</sub>CH<sub>2</sub>CO-), 1.53 (m, 2H, -CH<sub>2</sub>CH<sub>2</sub>NH-), 2.07 (t, 2H, -CH<sub>2</sub>CO-), 3.10 (q, 2H, -NHCH<sub>2</sub>-), 3.69 (q, 6H, -NH(CH<sub>2</sub>)<sub>2</sub>CH<sub>2</sub>-, -CH<sub>2</sub>OCH<sub>2</sub>-), 3.92 (m, 2H, -CH<sub>2</sub>CN<sup>+</sup>(CH<sub>2</sub>)<sub>2</sub>-), 4.35 (m, 2H, -CH<sub>2</sub>CN<sup>+</sup>(CH<sub>2</sub>)<sub>2</sub>-), 8.01 (t, 1H, -NH-).

**$^{13}\text{C}$  NMR** (75 MHz,  $(\text{CD}_3)_2\text{SO}$ )  $\delta$  (ppm): 172.25, 165.85, 163.92, 66.26, 62.54, 58.83, 35.21, 31.85, 29.74, 28.12, 14.49.

**FT-IR** (KBr,  $\text{cm}^{-1}$ ): 2931, 1635, 1384.

**ESI-MS** (m/z): 522.4[M]<sup>+</sup>.

### MoPALA<sub>3</sub>MMT



4,6-bis(4-(3-octanamidopropyl)morpholino-4-ium)-2-oxo-2H-1,3,5-triazin-1-ide chloride

Chemical Formula:  $\text{C}_{33}\text{H}_{60}\text{ClN}_7\text{O}_5$

Exact Mass: 669,43

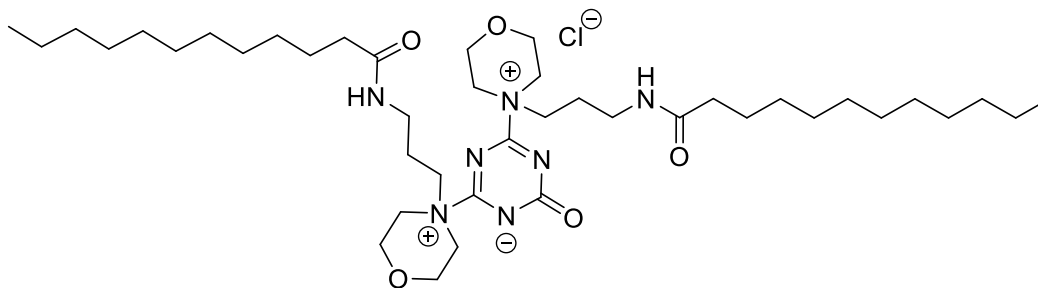
**m.p.:** 149.9 °C ;

**$^1\text{H}$  NMR** (300 MHz,  $(\text{CD}_3)_2\text{SO}$ )  $\delta$  (ppm): 0.85 (t, 3H,  $-\text{CH}_2\text{CH}_3$ ), 1.22 (t, 8H,  $-\text{CH}_2(\text{CH}_2)_6\text{CH}_3$ ), 1.45 (q, 2H,  $-\text{CH}_2\text{CH}_2\text{CO}-$ ), 1.59 (m, 2H,  $-\text{CH}_2\text{CH}_2\text{NH}-$ ), 2.03 (t, 2H,  $-\text{CH}_2\text{CO}-$ ), 3.02 (q, 2H,  $-\text{NHCH}_2-$ ), 3.76 (q, 6H,  $-\text{NH}(\text{CH}_2)_2\text{CH}_2-$ ,  $-\text{CH}_2\text{OCH}_2-$ ), 3.97-4.32 (m, 4H,  $-\text{CH}_2\text{CN}^+(\text{CH}_2)_2-$ ), 8.04 (t, 1H,  $-\text{NH}$ ).

**$^{13}\text{C}$  NMR** (75 MHz,  $(\text{CD}_3)_2\text{SO}$ )  $\delta$  (ppm): 172.88, 166.93, 164.52, 65.64, 62.04, 58.21, 35.83, 31.61, 29.15, 28.90, 25.62, 22.51, 14.37.

**FT-IR** (KBr,  $\text{cm}^{-1}$ ): 2925, 1632, 1359.

**ESI-MS** (m/z): 634.6[M]<sup>+</sup>.

**MoPALA<sub>12</sub>MMT**

4,6-bis(4-(3-dodecanamidopropyl)morpholino-4-ium)-2-oxo-2H-1,3,5-triazin-1-ide chloride

Chemical Formula: C<sub>41</sub>H<sub>76</sub>ClN<sub>7</sub>O<sub>5</sub>

Exact Mass: 781,56

**m.p.:** 115°C

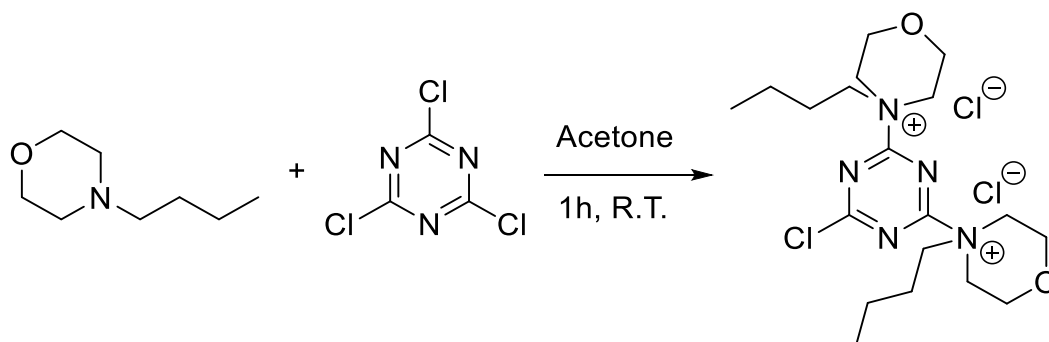
**<sup>1</sup>H NMR** (300 MHz, (CD<sub>3</sub>)<sub>2</sub>SO) δ (ppm): 0.85 (t, 3H, -CH<sub>2</sub>**CH**<sub>3</sub>), 1.22 (t, 16H, -CH<sub>2</sub>(**CH**<sub>2</sub>)<sub>8</sub>CH<sub>3</sub>), 1.44 (q, 2H, -**CH**<sub>2</sub>CH<sub>2</sub>CO-), 1.58 (m, 2H, -**CH**<sub>2</sub>CH<sub>2</sub>NH-), 2.02 (t, 2H, -**CH**<sub>2</sub>CO-), 3.01 (q, 2H, -NH**CH**<sub>2</sub>-), 3.74 (q, 6H, -NH(CH<sub>2</sub>)<sub>2</sub>**CH**<sub>2</sub>-, -**CH**<sub>2</sub>O**CH**<sub>2</sub>-), 3.94-4.32 (m, 4H, -CH<sub>2</sub>CN<sup>+</sup>(**CH**<sub>2</sub>)<sub>2</sub>-), 7.98 (t, 1H, -**NH**-).

**<sup>13</sup>C NMR** (75 MHz, (CD<sub>3</sub>)<sub>2</sub>SO) δ (ppm): 172.88, 166.91, 164.55, 65.64, 62.03, 58.22, 35.84, 35.80, 31.76, 29,52, 29.48, 29.43, 29.29, 29.23, 29.18, 25,63, 22,55,14.40.

**FT-IR** (KBr, cm<sup>-1</sup>): 2925, 1620, 1359

**ESI-MS** (m/z): 746.7 [M]<sup>+</sup>

### 5.4.3 Synthesis of 4-butyl-4-(4,6-dichloro-1,3,5-triazin-2-yl)morpholin-4-ium chloride



**Scheme 5.10** – Synthesis of 4-butyl-4-(4,6-dichloro-1,3,5-triazin-2-yl)morpholin-4-ium chloride by reaction of cyanuric chloride with N-(3-morpholinopropyl)alkylamide

In a 50 mL single neck flask immersed in a ice bath, place 460.0 mg (2.50 mmol) cyanuric chloride in 25 ml of acetone under magnetic stirring. Then 286.0 mg (2.00 mmol) 4-butylmorpholine in small aliquots is added. After one hours, a white precipitate is formed. Then product is filtered through Gooch funnel and rinsed with cold acetone. The product was left overnight in a dryer resulting in pure 4-butyl-4-(4,6-dichloro-1,3,5-triazin-2-yl)morpholin-4-ium chloride. The final product was characterized by  $^1\text{H}$  NMR,  $^{13}\text{C}$  NMR, COSY, HMQC, IR and m.p.

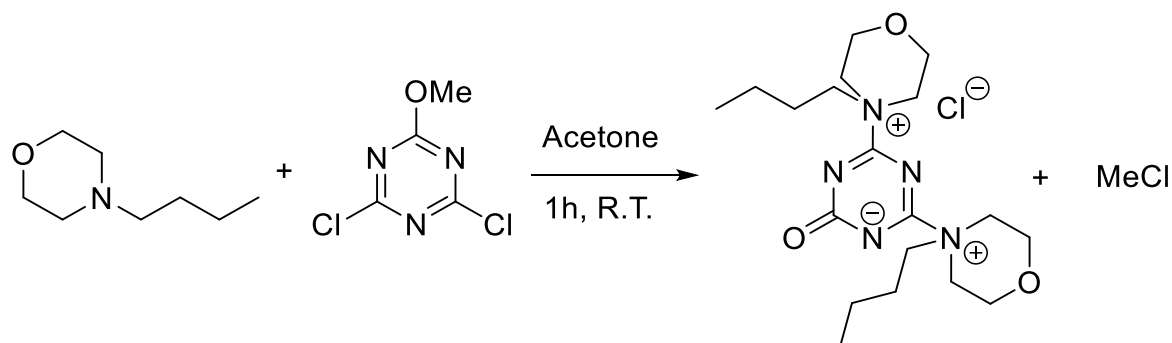
Yield: 26% Purity: 92%.

**$^1\text{H}$  NMR** (300 MHz,  $(\text{CD}_3)_2\text{SO}$ )  $\delta$  (ppm): 0.84 (t, 3H,  $-\text{CH}_2\text{CH}_3$ ), 1.23 (q, 2H,  $-\text{CH}_2\text{CH}_2\text{CH}_3$ ), 1.40 (m, 2H,  $-\text{CH}_2\text{CH}_2\text{N}^+$ ), 3.76 (m, 6H,  $-\text{N}^+\text{CH}_2-$ ,  $-\text{CH}_2\text{OCH}_2-$ ), 3.95 (m, 2H,  $-\text{CH}_2\text{CN}^+(\text{CH}_2)_2-$ ), 4.36 (m, 2H,  $-\text{CH}_2\text{CN}^+(\text{CH}_2)_2-$ ).

**$^{13}\text{C}$  NMR** (75 MHz,  $(\text{CD}_3)_2\text{SO}$ )  $\delta$  (ppm): 166.46, 164.15, 66.83, 61.51, 57.67, 30.62, 23.30, 18.93, 13.27.

**ESI-MS** (m/z): 199.2  $[\text{M}]^{2+}$ .

#### 5.4.4 Synthesis of 4,6-bis(4-butylmorpholino-4-ium)-2-oxo-2*H*-1,3,5-triazin-1-ide chloride



**Scheme 5.11** – Synthesis of 4,6-bis(4-butylmorpholino-4-ium)-2-oxo-2*H*-1,3,5-triazin-1-ide chloride by reaction of MMT with N-(3-morpholinopropyl)alkylamide

In a 50 mL single neck flask immersed in a ice bath, place 450.0 mg (2.50 mmol) of 2,4-dichloro-6-methoxy-1,3,5-triazine (MMT) in 25 ml of acetone under magnetic stirring. Then 286.0 mg (2.00 mmol) 4-butylmorpholine in small aliquots is added. After one hour, a white precipitate is formed. The product is filtered through Gooch funnel and rinsed with cold acetone. The product was left overnight in a dryer resulting in pure 4,6-bis(4-butylmorpholino-4-ium)-2-oxo-2*H*-1,3,5-triazin-1-ide chloride. The final product was characterized by <sup>1</sup>H NMR, <sup>13</sup>C NMR, COSY, HMQC, IR and m.p.

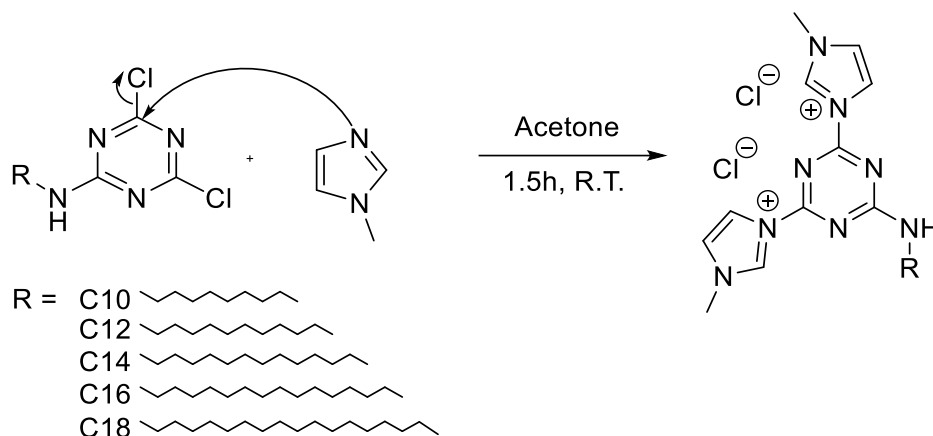
Yield: 20%, Purity: 87%.

**<sup>1</sup>H NMR** (300 MHz, (CD<sub>3</sub>)<sub>2</sub>SO) δ (ppm): 0.84 (t, 3H, -CH<sub>2</sub>CH<sub>3</sub>), 1.23 (q, 2H, -CH<sub>2</sub>CH<sub>2</sub>CH<sub>3</sub>), 1.40 (m, 2H, -CH<sub>2</sub>CH<sub>2</sub>N<sup>+</sup>), 3.75 (m, 6H, -N<sup>+</sup>CH<sub>2</sub>-, -CH<sub>2</sub>OCH<sub>2</sub>-), 3.95 (m, 2H, -CH<sub>2</sub>CN<sup>+</sup>(CH<sub>2</sub>)<sub>2</sub>-), 4.36 (m, 4H, -CH<sub>2</sub>CN<sup>+</sup>(CH<sub>2</sub>)<sub>2</sub>-).

**<sup>13</sup>C NMR** (75 MHz, (CD<sub>3</sub>)<sub>2</sub>SO) δ (ppm): 166.64, 165.15, 66.81, 31.53, 57.60, 30.62, 23.37, 18.97, 13.23.

**ESI-MS** (m/z): 380.3 [M]<sup>+</sup>

### 5.4.5 Synthesis of 3,3'-(6-(alkylamino)-1,3,5-triazin)bis(1-methyl-1*H*-imidazol-3-ium) Chloride (MATdMIMI)



**Scheme 5.12** – Reaction scheme of synthesis of 3,3'-(6-(alkylamino)-1,3,5-triazin)bis(1-methyl-1*H*-imidazol-3-ium) chloride by reaction of methylimidazole and MAT

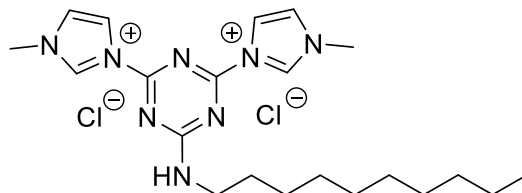
Aliquots of MAT<sub>10,14,16,18</sub>, (see table 5.5) were added in acetone to a 100 ml one-neck flask equipped with magnetic stirring. Aliquots of methylimidazole (MI<sub>mi</sub>) (see table 5.5) were subsequently added to the solution. The reaction was continued for 1.5 hours until a precipitate was formed. The solid was recovered by filtration on Gooch, washed with a little quantity of acetone and dried under vacuum. The white solid obtained was characterized by <sup>1</sup>H NMR, <sup>13</sup>C NMR, COSY, HMQC, FT-IR, m.p. and ESI-MS. Yields and purities are shown in Table 5.5.

**Table 5.5** - Experimental data for synthesis of MATMImi

|                              | <b>MAT</b>        | <b>MImi</b> | <b>Acetone</b> | <b>Yield (%)</b> | <b>Purity (%)</b> |    |
|------------------------------|-------------------|-------------|----------------|------------------|-------------------|----|
| <b>MAT<sub>10</sub>MIMI</b>  | MAT <sub>10</sub> |             |                |                  |                   |    |
| <b>mmol</b>                  | 0.82              | 4.10        |                | 86               | 96                |    |
| <b>g</b>                     | 0.25              | 0.34        |                |                  |                   |    |
| <b>mL</b>                    |                   | 0.33        | 10.00          |                  |                   |    |
| <b>MAT<sub>12</sub> MIMI</b> | MAT <sub>12</sub> |             |                |                  | 97                | 98 |
| <b>mmol</b>                  | 3.00              | 15.00       |                |                  |                   |    |
| <b>g</b>                     | 0.10              | 0.12        |                |                  |                   |    |
| <b>mL</b>                    |                   | 1.19        | 25.00          |                  |                   |    |
| <b>MAT<sub>14</sub> MIMI</b> | MAT <sub>14</sub> |             |                |                  | 97                | 98 |
| <b>mmol</b>                  | 0.69              | 3.46        |                |                  |                   |    |
| <b>g</b>                     | 0.25              | 0.25        |                |                  |                   |    |
| <b>mL</b>                    |                   | 0.24        | 10.00          |                  |                   |    |
| <b>MAT<sub>16</sub> MIMI</b> | MAT <sub>16</sub> |             |                |                  | 82                | 92 |
| <b>mmol</b>                  | 1.23              | 6.15        |                |                  |                   |    |
| <b>g</b>                     | 0.50              | 0.50        |                |                  |                   |    |
| <b>mL</b>                    |                   | 0.49        | 15.00          |                  |                   |    |
| <b>MAT<sub>18</sub> MIMI</b> | MAT <sub>18</sub> |             |                |                  | 99                | 93 |
| <b>mmol</b>                  | 1.13              | 5.67        |                |                  |                   |    |
| <b>g</b>                     | 0.50              | 0.47        |                |                  |                   |    |
| <b>mL</b>                    |                   | 0.45        | 15.00          |                  |                   |    |

## Characterization

### MAT<sub>10</sub>MImi



3,3'-(6-(decylamino)-1,3,5-triazine-2,4-diyl)bis(1-methyl-1*H*-imidazol-3-ium) chloride

Chemical Formula: C<sub>21</sub>H<sub>34</sub>Cl<sub>2</sub>N<sub>8</sub>

Exact Mass: 468,23

**m.p.:** 196°C (decomposition)

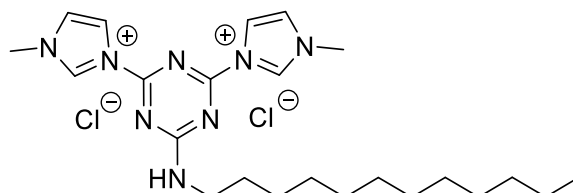
**<sup>1</sup>H NMR** (300 MHz, D<sub>2</sub>O) δ (ppm): 8.40 (2H, d, CH**CHN**CH<sub>3</sub>), 8.34 (2H, d, CH**CHN**CH<sub>3</sub>), 7.69 (2H, dd, CH**CHN**<sup>+</sup>), 4.09 (6H, s, CH<sub>2</sub>**CH**<sub>3</sub>), 3.63 (2H, m, NH**CH**<sub>2</sub>CH<sub>2</sub>), 1.70 (2H, m, CH<sub>2</sub>**CH**<sub>2</sub>CH<sub>2</sub>), 1.23 (14H, m, CH<sub>2</sub>(**C**<sub>7</sub>**H**<sub>14</sub>)CH<sub>3</sub>), 0.83 (3H, m, CH<sub>2</sub>**CH**<sub>3</sub>)

**<sup>13</sup>C NMR** (75 MHz, CDCl<sub>3</sub>) δ (ppm): 164.51, 158.76, 158.07, 123.24, 117.50, 117.37, 35.09, 29.54, 26.98, 26.29, 24.11, 20.38, 11.75

**FT-IR** (KBr, cm<sup>-1</sup>): 3042, 2924-2852, 1626, 1343, 801

**ESI-MS** (m/z): 199.1[M]<sup>2+</sup>

### MAT<sub>12</sub>MImi



3,3'-(6-(dodecylamino)-1,3,5-triazine-2,4-diyl)bis(1-methyl-1*H*-imidazol-3-ium) chloride

Chemical Formula: C<sub>23</sub>H<sub>38</sub>Cl<sub>2</sub>N<sub>8</sub>

Exact Mass: 496,26



**m.p.:** 196°C (decomposition)

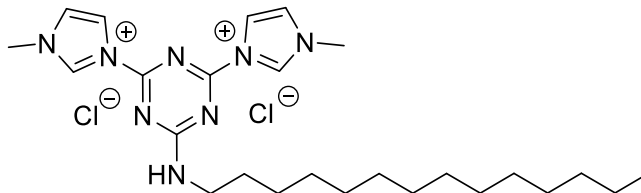
**<sup>1</sup>H NMR** (300 MHz, DMSO)  $\delta$  (ppm): 10.68 (1H, s, CH<sub>3</sub>NCHN<sup>+</sup>), 10.61 (1H, s, CH<sub>3</sub>NCHN<sup>+</sup>), 9.55 (1H, t, CNHCH<sub>2</sub>), 8.73 (1H, s, CHCHNCH<sub>3</sub>), 8.43 (1H, s, CHCHNCH<sub>3</sub>), 8.05 (1H, s, <sup>+</sup>NCHCH), 8.02 (1H, s, <sup>+</sup>NCHCH), 4.04 (6H, s, CH<sub>3</sub>N), 3.53 (2H, q, NHCH<sub>2</sub>CH<sub>2</sub>), 1.61 (2H, m, CH<sub>2</sub>CH<sub>2</sub>CH<sub>2</sub>), 1.24 (18H, s, CH<sub>2</sub>(C<sub>9</sub>H<sub>18</sub>)CH<sub>3</sub>), 0.85 (3H, t, CH<sub>2</sub>CH<sub>3</sub>).

**<sup>13</sup>C NMR** (75 MHz, CDCl<sub>3</sub>)  $\delta$  (ppm): 165.59, 159.84, 159.37, 137.81, 125.43, 125.31, 118.93, 118.51, 36.74, 31.25, 28.97, 28.75, 28.66, 26.25, 22.04, 13.91.

**FT-IR** (KBr, cm<sup>-1</sup>): 3040, 2921-2851, 1626, 1341, 801.

**ESI-MS** (m/z): 213.2[M]<sup>2+</sup>.

### MAT<sub>14</sub>MImi



3,3'-(6-(tetradecylamino)-1,3,5-triazine-2,4-diyl)bis(1-methyl-1H-imidazol-3-ium) chloride

Chemical Formula: C<sub>25</sub>H<sub>42</sub>Cl<sub>2</sub>N<sub>8</sub>

Exact Mass: 524,29

**m.p.:** 177°C (decomposition)

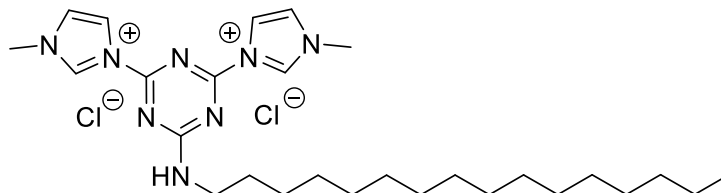
**<sup>1</sup>H NMR** (300 MHz, D<sub>2</sub>O)  $\delta$  (ppm): 8.37 (2H, d, CHCHNCH<sub>3</sub>), 8.32 (2H, d, CHCHNCH<sub>3</sub>), 7.72 (2H, dd, CHCHN<sup>+</sup>), 7.69 (2H, dd, CHCHN<sup>+</sup>), 4.09 (6H, s, CH<sub>2</sub>CH<sub>3</sub>), 3.61 (2H, m, NHCH<sub>2</sub>CH<sub>2</sub>), 1.69 (2H, m, CH<sub>2</sub>CH<sub>2</sub>CH<sub>2</sub>), 1.23 (22H, m, CH<sub>2</sub>(C<sub>11</sub>H<sub>22</sub>)CH<sub>3</sub>), 0.85 (3H, m, CH<sub>2</sub>CH<sub>3</sub>).

**<sup>13</sup>C NMR** (101 MHz, D<sub>2</sub>O)  $\delta$  (ppm): 168.53, 162.87, 162.12, 127.86, 121.61, 121.40, 44.20, 39.66, 39.51, 34.41, 32.36, 32.34, 32.25, 31.97, 31.92, 31.08, 29.40, 25.11, 16.39.

**FT-IR** (KBr, cm<sup>-1</sup>): 3035, 2920-2850, 1624, 1340, 801.

**ESI-MS** (m/z): 227.2[M]<sup>2+</sup>.

**MAT<sub>16</sub>MImi**



3,3'-(6-(hexadecylamino)-1,3,5-triazine-2,4-diyl)bis(1-methyl-1*H*-imidazol-3-ium) chloride

Chemical Formula: C<sub>27</sub>H<sub>46</sub>Cl<sub>2</sub>N<sub>8</sub>

Exact Mass: 552,32

**m.p.:** 200°C (decomposition)

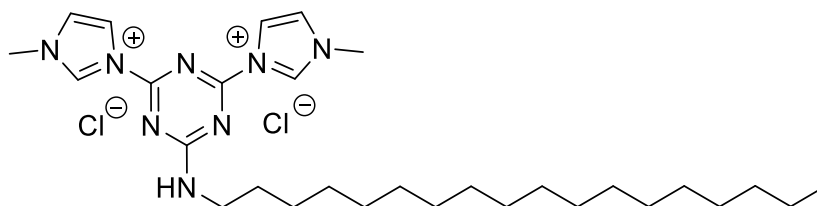
**<sup>1</sup>H NMR** (300 MHz, DMSO) δ (ppm): 10.92 (1H, s, CH<sub>3</sub>NCHN<sup>+</sup>), 10.89 (1H, s, CH<sub>3</sub>NCHN<sup>+</sup>), 9.66 (1H, t, CNHCH<sub>2</sub>), 8.99 (1H, s, CHCHN<sup>+</sup>), 8.79 (1H, s, CHCHN<sup>+</sup>), 8.09 (1H, s, CH<sub>3</sub>NCHCH), 8.06 (1H, s, CH<sub>3</sub>NCHCH), 4.05 (6H, s, CH<sub>3</sub>N), 3.54 (2H, q, NHCH<sub>2</sub>CH<sub>2</sub>), 1.59 (2H, m, CH<sub>2</sub>CH<sub>2</sub>CH<sub>2</sub>), 1.22 (26H, s, CH<sub>2</sub>(C<sub>13</sub>H<sub>26</sub>)CH<sub>3</sub>), 0.84 (3H, t, CH<sub>2</sub>CH<sub>3</sub>).

**<sup>13</sup>C NMR** (101 MHz, CDCl<sub>3</sub>) δ (ppm): 168.34, 162.71, 161.95, 127.25, 122.00, 121.57, 44.45, 39.83, 39.62, 37.99, 34.80, 32.99, 32.42, 31.23, 29.82, 25.38, 16.49.

**FT-IR** (KBr, cm<sup>-1</sup>): 3035, 2918-2850, 1628, 1349, 801.

**ESI-MS** (m/z): 241.3[M]<sup>2+</sup>.

**MAT<sub>18</sub>MImi**



3,3'-(6-(octadecylamino)-1,3,5-triazine-2,4-diyl)bis(1-methyl-1*H*-imidazol-3-ium) chloride

Chemical Formula: C<sub>29</sub>H<sub>50</sub>Cl<sub>2</sub>N<sub>8</sub>

Exact Mass: 580,35

**m.p.:** 220°C

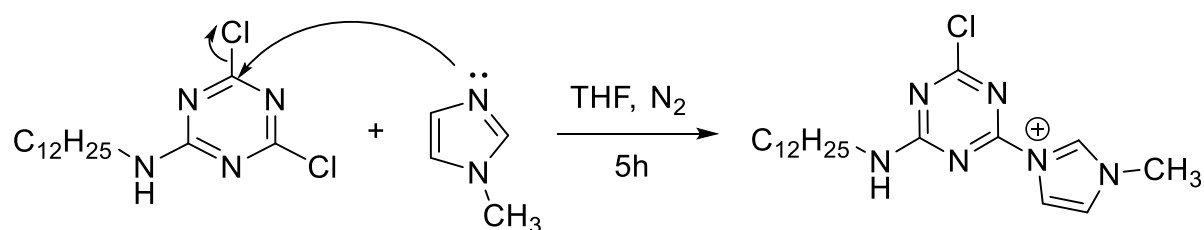
**<sup>1</sup>H NMR** (300 MHz, DMSO)  $\delta$  (ppm): 10.88 (1H, s, CH<sub>3</sub>NCHN<sup>+</sup>), 10.84 (1H, s, CH<sub>3</sub>NCHN<sup>+</sup>), 9.63 (1H, t, CNHCH<sub>2</sub>), 8.05 (1H, s, CHCHN<sup>+</sup>), 7.96 (1H, s, CHCHN<sup>+</sup>), 7.56 (1H, s, CH<sub>3</sub>NCHCH), 7.47 (1H, s, CH<sub>3</sub>NCHCH), 4.05 (6H, s, CH<sub>3</sub>N), 3.52 (2H, q, NHCH<sub>2</sub>CH<sub>2</sub>), 1.60 (2H, m, CH<sub>2</sub>CH<sub>2</sub>CH<sub>2</sub>), 1.22 (30H, s, CH<sub>2</sub>(C<sub>15</sub>H<sub>30</sub>)CH<sub>3</sub>), 0.84 (3H, t, CH<sub>2</sub>CH<sub>3</sub>)

**<sup>13</sup>C NMR** (101 MHz, CDCl<sub>3</sub>)  $\delta$  (ppm): 168.32, 162.67, 161.91, 127.22, 121.50, 121.09, 44.37, 39.83, 39.63, 34.67, 32.81, 32.23, 31.16, 29.75, 25.29, 16.50

**FT-IR** (KBr, cm<sup>-1</sup>): 3089, 2918-2850, 1631, 1353, 801

**ESI-MS** (m/z): 255.3[M]<sup>2+</sup>

#### 5.4.6 Synthesis of 3-(4-chloro-6-(dodecylamino)-1,3,5-triazin-2-yl)-1-methyl-1H-imidazol-3-ium chloride (MAT<sub>12</sub>mMIMI)



**Scheme 3.13** – Synthesis of MAT<sub>12</sub>mMIMI

In a 100 mL two-neck flask equipped with magnetic stirring and a drip funnel, 1g (3.0 mmol) of MAT<sub>12</sub> in 20 mL of THF are introduced and 0.25g (3.0 mol) in 5 mL of THF are introduced into the drip funnel. 3 cycles of vacuum/nitrogen are then performed and the flask is then immersed on ice bath (approx. 0°C). Then the methyl imidazole solution is allowed to drip gently and allowed to react for about 5 h. A white precipitate is formed and the solution is turbid. At the end of the reaction, filtration on paper was performed and the product then placed in a high

vacuum desiccator overnight. The final product was characterized by  $^1\text{H}$  NMR,  $^{13}\text{C}$  NMR, COSY, HMQC, IR and m.p.

Yield: 70%, Purity: 83%.

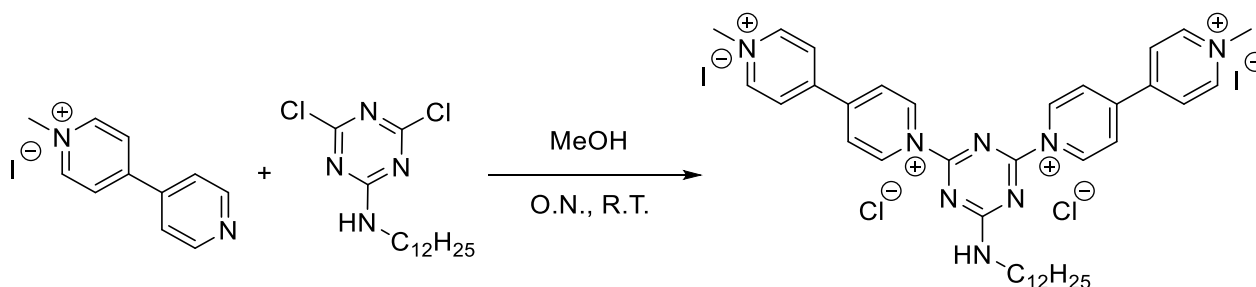
**m.p.:** 137°C

$^1\text{H}$  NMR (300 MHz,  $\text{D}_2\text{O}$ )  $\delta$  (ppm): 8.36 (1H, s,  $\text{CH}_3\text{NCHCH}$ ), 7.68 (1H, s,  $\text{CHCHN}^+$ ), 4.07 (3H, s,  $\text{CH}_3\text{N}$ ), 3.58 (2H, q,  $\text{NHCH}_2\text{CH}_2$ ), 1.66 (2H, m,  $\text{CH}_2\text{CH}_2\text{CH}_2$ ), 1.18 (18H, s,  $\text{CH}_2(\text{CH}_2)_9\text{CH}_3$ ), 0.80 (3H, t,  $\text{CH}_2\text{CH}_3$ )

$^{13}\text{C}$  NMR (75 MHz,  $\text{CDCl}_3$ )  $\delta$  (ppm): 165.61, 159.86, 159.39, 137.94, 125.33, 123.10, 119.52, 118.97, 118.50, 41.09, 36.73, 31.29, 29.02, 28.71, 22.09, 13.96

**FT-IR** (KBr,  $\text{cm}^{-1}$ ): 3035, 2918-2849, 1627, 1340, 845, 801

#### 5.4.7 Synthesis of 1'.1''-(6-(dodecylamino-1,3,5-triazin-2,4,-diyl)bis(1-methyl-[4,4'-bipyridin]-1,1'-io) salt (MAT<sub>12</sub>dMBP)



**Scheme 5.14** – Synthesis of 1'.1''-(6-(dodecylamino-1,3,5-triazin-2,4,-diyl)bis(1-methyl-[4,4'-bipyridin]-1,1'-io) by reaction of 4,6-dichloro-N-dodecyl-1,3,5-triazin-2-amine and 4-methyl-bipyridinium

In a 250 mL single-neck flask equipped with magnetic stirring, 0.5 g (1.5 mmol) of MAT12 and 0.9 g (3.0 mmol) of 4-methyl-bipyridinium were introduced with 20 mL of MeOH. The reaction mixture was kept under stirring, at room temperature, for approximately 10 hours overnight. Subsequently, the solvent was removed by rotary evaporator. The brown solid obtained was

subsequently ground in Et<sub>2</sub>O and finally filtered over Gooch and placed in a vacuum dryer obtaining 1.35g (96.70% yield) of product. The brown solid obtained was characterized by <sup>1</sup>H-NMR, <sup>13</sup>C-NMR, COSY, HMQC, FT-IR and m.p.

Yield: 96%, Purity: 94%.

### Characterization

**m.p.:** 160°C (decomposition)

**<sup>1</sup>H NMR** (300 MHz, D<sub>2</sub>O) δ: 9.02 ppm (4H, d, CH**CHN**<sup>+</sup>CH<sub>3</sub>), 8.82 ppm (4H, dd, CH**CHN**<sup>+</sup>C), 8.48 ppm (4H, d, CH**CHC**), 8.03 ppm (4H, dd, CH**CHC**), 4.53 ppm (1H, s, C**NH**CH<sub>2</sub>), 4.45 ppm (6H, s, **CH**<sub>3</sub>N<sup>+</sup>), 3.49 ppm (2H, q, NH**CH**<sub>2</sub>CH<sub>2</sub>), 1.67 ppm (2H, m, CH<sub>2</sub>**CH**<sub>2</sub>CH<sub>2</sub>), 1.25ppm (2H, s, CH<sub>2</sub>**CH**<sub>2</sub>CH<sub>2</sub>), 0.86 ppm (3H, t, CH<sub>2</sub>**CH**<sub>3</sub>)

**<sup>13</sup>C NMR** (75 MHz, MeOD) δ (ppm): 153.93, 149.99, 147.55, 128.29, 127.95, 127.11, 124.53, 33.04, 30.72, 30.44, 23.71, 14.43

**FT-IR** (KBr, cm<sup>-1</sup>): 2923-2851, 1633, 1465, 810

## 5.5 Biological assays

### Antimicrobial test

All the culture media and pathogenic strains were purchased from Sigma Aldrich. The bacterial and fungal strains were stored at -20°C in glycerol stocks before the use.

The screening of antimicrobial activity of these new molecules was conducted using a 96-well microplate against Staphylococcus aureus ATCC 25923, Escherichia coli ATCC 25922, Enterococcus faecalis CECT 795, Pseudomonas aeruginosa CECT 111 and Candida albicans

CECT 1394. Specifically, we used as culture media Nutrient Broth for *S. aureus*, Tryptic Soy Broth for *P. aeruginosa* and *E. coli*, Brain Heart Infusion for *E. faecalis*, Sabouraud dextrose medium for *C. albicans*. In particular, we made 1:2 serial dilutions from 0.5 to 0,0625 mg/ml of each synthesized compound. After, we inoculated 10<sup>5</sup> CFU/ml of overnight culture of each strain of in a final volume of 0.180 ml of liquid culture medium for each well. The microplate was incubated overnight under stirring (150 rpm) in a thermoshaker at 37°C for bacterial strains and at 25°C for *C. albicans*. Serial dilutions from 10<sup>-6</sup> to 10<sup>-1</sup> of each well were spotted on Petri dishes using spot plating technique. The Petri dishes were incubated overnight at 37°C for bacterial strains and at 25°C for fungal strain, respectively. The Minimum inhibitory concentration (MIC) was taken as the lowest concentration that completely inhibits microbial growth.

## Cell viability assay

MRC-5 fibroblast cells (from ATCC) were maintained at 37 °C in a humidified atmosphere containing 5% CO<sub>2</sub> according to the supplier. Cells (5 × 10<sup>2</sup>) were plated in 96-well culture plates. The day after seeding, vehicle or compounds were added at different concentrations to the medium. Compounds were added to the cell culture at a concentration ranging from 1000 µg/ml to 0.1 µg/ml. Cell viability was measured after 96 h according to the supplier (CellTiter-Glo® luminescence assay, Promega G7571) with a Tecan M1000 PRO instrument. IC<sub>50</sub> values were calculated from logistical dose response curves and performed in triplicates.

## 5.6 Determination of critical micelle concentration

A series of 50 mL variable concentration solutions (40, 38, 36, 34, 32, 30, 28, 26, 24, 22, 20, 18, 16, 14, 12, 10, 8, 6, 4, 2, 1, 0.8, 0.6, 0.4, 0.2, 0.1 mM) of MATdMIMIs in milliQ water were

prepared. Using a XS instruments COND 80+ conductometer calibrated with KCl solutions of known conductivity values, the conductivity value of each solution was recorded at room temperature. The conductivity values in  $\mu\text{S}$  were then plotted on a  $\mu\text{S}$  vs mM graph. The CMC value is marked by the change in slope of the straight line. The intersection of the two lines with different slopes whose values were obtained on Excel calculation software indicates the CMC.

## 5.7 LogP calculation method

The logP values (octanol/water partition coefficients) were calculated in order to estimate the lipophilicity character of compounds. These calculations were achieved using MarvinSketch software (Marvin 16.8.22.0, 2019, ChemAxon (<http://www.chemaxon.com>))

## **CHAPTER 6**

### **REFERENCES**

**Synthesis of new antimicrobial triazine-based quaternary ammonium salts**



- [1] G. B. Lindsay, R. M. Merrill, R.J. Hedin, *The Contribution of Public Health and Improved Social Conditions to Increased Life Expectancy: An Analysis of Public Awareness*, Journal of Community Medicine & Health Education, **2014**, 4 (5), 311.
- [2] A. Fleming, "On the Antibacterial Action of Cultures of a *Penicillium*, with Special Reference to their use in the Isolation of *B. influenzae*", The British Journal of Experimental Pathology, **1929**, 10 (3), 226–236.
- [3] <https://www.cia.gov/library/publications/the-world-factbook/rankorder/2102rank.html>
- [4] M. Avila, N. Said, D.M. Ojcius, *The book reopened on infectious diseases*, Microbes and Infection, **2008**, 10, 942-7.
- [5] A. B. Pandit, J. K. Kumar, *Drinking water disinfection techniques*, CRC Press Taylor& Francis Group, 1<sup>st</sup> ed., **2013**, ISBN: 9781439877418.
- [6] I. Al-Adham, R. Haddadin, P. Collier, Principles and Practice of Disinfection, Preservation and Sterilization, Wiley-VCH, 5<sup>th</sup> ed., **2013**, ISBN 97814443-33251.
- [7] M.Ferri, E. Ranucci, P. Romagnoli, V. Giaccone, *Antimicrobial Resistance: A Global Emerging Threat to Public Health Systems. Critical Reviews*, Food Science and Nutrition, **2015**, 57 (13), 2857-2876.
- [8] A. H. Holmes, L. S. P. Moore, A. Arnfinn, M. Steinbakk, S. Regmi, A. Karkey, P.J. Guerin, L. J. V. Piddock, *Understanding the mechanisms and drivers of antimicrobial resistance*, The Lancet, **2015**, 387 (10014), 176-187.
- [9] V. D'Costa, C. E. King, L. Kalan, M. Morar, W. W. L. Sung, C. Schwarz, D. Froese, G. Zazula, F. Calmels, R. Debruyne, G. B. Golding, H. N. Poinar, G. D. Wright, *Antibiotic resistance is ancient*, Nature, **2011**, 477, 457–461.
- [10] H. K. Allen, J. Donato, H. H. Wang, K. A. Cloud-Hansen, J. Davies, J. Handelsman, *Call of the wild: antibiotic resistance genes in natural environments*, Nature Reviews Microbiology, **2010**, 8, 251–259.
- [11] M.L. Cohen, *Epidemiological factors influencing the emergence of antimicrobial resistance*. Ciba Foundation Symposium. **1997**, 207, 223-31.
- [12] J. Deasy, *Antibiotic resistance: The ongoing challenge for effective drug therapy*, Journal of the American Academy of Physician Assistants, **2009**, 22 (3), 18-22.
- [13] P. M. Adcock, P. Pastor, F. Medley, J. E. Patterson, T. V. Murphy, *Methicillin-Resistant Staphylococcus aureus in Two Child Care Centers*, The Journal of Infectious Diseases, **1998**, 178 (2), 577–580.
- [14] A. H. Suggs, M. C. Maranan, S. Boyle-Vavra, R. Daum, *Methicillin-resistant and borderline methicillin-resistant asymptomatic Staphylococcus aureus colonization in children without identifiable risk factors*, The Pediatric Infectious Disease Journal, **1999**, 18 (5), 410-414.

- [15] F. M. Hussain, S. Boyle-Vavra, R. Daum, *Community-acquired methicillin-resistant Staphylococcus aureus colonization in healthy children attending an outpatient pediatric clinic*, The Pediatric Infectious Disease Journal, **2001**, 20 (8), 763-767.
- [16] E. D. Charlebois, et al. "Population-Based Community Prevalence of Methicillin-Resistant Staphylococcus Aureus in the Urban Poor of San Francisco." Clinical Infectious Diseases, vol. 34, no. 4, **2002**, pp. 425–433.
- [17] World Health Organization, *Antimicrobial resistance: global report on surveillance*, **2014**, ISBN: 9789241564748.
- [18] J. O'Neill, *Tackling drug-resistant infections globally: final report and recommendations*, Government of the United Kingdom, **2016**.
- [19] S. E. Josephson, M. S. Peterson, *Preservation of food by ionizing radiation*, CRC Press Taylor & Francis Group, 1<sup>st</sup> ed., volume 3, **2018**, ISBN: 9781315896892.
- [20] D. S. Morais, R. M. Guedes, M. A. Lopes, *Antimicrobial Approaches for Textiles: From Research to Market*, Materials, **2016**, 9(6), 498.
- [21] P. M. Davidson, T. M. Taylor, S. E. Schmidt, *Chemical Preservatives and Natural Antimicrobial Compounds, Food Microbiology: Fundamentals and Frontiers*, ASM Press, 4th Edition, **2012**, ISBN:9781119739135.
- [22] M. Gołębiowski, M. Dawgul, W. Kamysz, M. I. Boguś, W. Wieloch, E. Włóka, M. Paszkiewicz, E. Przybysz, P. Stepnowski, *Antimicrobial activity of alcohols from Musca domestica*, Journal of Experimental Biology, **2012**, 215, 3419-3428.
- [23] N. V. Harohally, C. Cherita, P. Bhatt, K. A. A. Appaiah, *Antiaflatoxic and Antimicrobial Activities of Schiff Bases of 2-Hydroxy-4-methoxybenzaldehyde, Cinnamaldehyde, and Similar Aldehydes*, Journal of Agricultural and Food Chemistry, **2017**, 65 (40), 8773-8778.
- [24] A. Megahed, B. Aldridge, J. Lowe, *Antimicrobial Efficacy of Aqueous Ozone and Ozone–Lactic Acid Blend on Salmonella-Contaminated Chicken Drumsticks Using Multiple Sequential Soaking and Spraying Approaches*, Frontiers in Microbiology, **2020**, 11.
- [25] M. T. Arias-Moliz, R. Ordinola-Zapata, P. Baca, M. Ruiz-Linares, C. M. Ferrer-Luque, *Antimicrobial Activity of a Sodium Hypochlorite/Etidronic Acid Irrigant Solution*, Journal of Endodontics, **2014**, 40 (12), 1999-2002.
- [26] M. Finnegan, E. Linley, S. P. Denyer, G. McDonnell, C. Simons, J. Maillard, *Mode of action of hydrogen peroxide and other oxidizing agents: differences between liquid and gas forms*, Journal of Antimicrobial Chemotherapy, **2010**, 65 (10), 2108–2115.
- [27] X. Xie, W. Cong, F. Zhao, H. Li, W. Xin, G. Hou, C. Wang, *Synthesis, physicochemical property and antimicrobial activity of novel quaternary ammonium salts*, Journal of Enzyme Inhibition and Medicinal Chemistry, **2018**, 33 (1), 98-105.

- [28] M. E. Vianna, B. P. F. A. Gomes, V. B. Berber, A. A. Zaia, C. C. R. Ferraz, F. J. Souza-Filho, *In vitro evaluation of the antimicrobial activity of chlorhexidine and sodium hypochlorite*, Oral Surgery, Oral Medicine, Oral Pathology, Oral Radiology, and Endodontology, **2004**, 97 (1), 79-84.
- [29] H. Fjeld, E. Lingaas, *Polyhexanide – safety and efficacy as an antiseptic*, Tidsskr Nor Legeforen **2016**; 136, 707.
- [30] M. Rbaa, S. Jabli, Y. Lakhrissi, M. Ouhssine, F. Almalki, T. B. Hadda, S. Messgo-Moumene, A. Zarrouk, B. Lakhrissi. *Synthesis, antibacterial properties and bioinformatics computational analyses of novel 8-hydroxyquinoline derivatives*, Heliyon, **2019**, 5(10).
- [31] W. Mendling, E. R. Weissenbacher, S. Gerber, V. Prasauskas, P. Grob, *Use of locally delivered dequalinium chloride in the treatment of vaginal infections: a review*, Arch Gynecol Obstet, **2016**, 293, 469–484.
- [32] A. Bidossi, M. Bottagisio, R. De Grandi, L. Drago, E. De Vecchi, *Chlorquinaldol, a topical agent for skin and wound infections: anti-biofilm activity and biofilm-related antimicrobial cross-resistance*, Infect Drug Resist. **2019**; 12, 2177-2189.
- [33] A. Tačić, V. Nikolic, L. Nikolic, I. Savic, *Antimicrobial sulfonamide drugs*, Advanced technologies, **2017**, 6 (1), 58-71.
- [34] H. Ullah, S. Ali, *Classification of Anti-Bacterial Agents and Their Functions*, Antibacterial Agents, IntechOpen, **2017**, ISBN: 9789535132004.
- [35] K. Jastrzabek, B. Kolesinska, G. Sabatino, F. Rizzolo, A.M. Papini, Z. J. Kaminski, *Benzyloxy Derivatives of Triazine-based Coupling Reagents Designed for an Efficient Solid Phase Peptide Synthesis on Polystyrene Resin*, International Journal of Peptide Research and Therapeutics, **2007**, 13, 229–236.
- [36] M. Kunishima, T. Ujigawa, Y. Nagaoka, C. Kawachi, K. Hioki and M. Shiro, *Study on 1,3,5-Triazine Chemistry in Dehydrocondensation: Gauche Effect on the Generation of Active Triazinylammonium Species*, Chemistry European Journal, **2012**, 18 (49), 15856-15867.
- [37] I. Mulder, J. Siemens, V. Sentek, W. Amelung, K. Smalla, and S. Jechalke, *Quaternary ammonium compounds in soil: implications for antibiotic resistance development*, Reviews in Environmental Science and Biotechnology, **2018**, 17, 159-185.
- [38] N. Menschutkin, Zeitschrift für Physikalische Chemie, **1890**, 5, 589.
- [39] K. Moonen, D. Ulrichs, D. Scheldeman, *Process for the production of choline hydroxide*, **2013**, WO 2013088575.

- [40] A. Fazlara, S. Chamran, *The Disinfectant Effects of Benzalkonium Chloride on Some Important Foodborne Pathogens*, American-Eurasian Journal of Agricultural & Environmental Sciences, **2012**, 12 (1), 23-29.
- [41] C. Zhou, Y. Wang, *Structure–activity relationship of cationic surfactants as antimicrobial agents*, Current Opinion in Colloid & Interface Science, **2020**, 45, 28-43.
- [42] Y. Li, K. Holmberg, R. Bordes, *Micellization of true amphoteric surfactants*, Journal of Colloid and Interface Science, **2013**, 411, 47-52.
- [43] D. E. Perdew Jr., *Cleansing composition: device and method*, **2003**, US6727210B1.
- [44] S. Shaukat, M. V. Fedotova, S. E. Kruchinin, M. Bešter-Rogač, Č. Podlipnik, R. Buchner, *Hydration and ion association of aqueous choline chloride and chlorocholine chloride*, Physical Chemistry Chemical Physics, **2019**, 21, 10970-10980.
- [45] M. Feoktistova, P. Geserick, M. Leverkus, *Crystal Violet Assay for Determining Viability of Cultured Cells*, Cold Spring Harbor Protocols, **2016**, 4.
- [47] G. Domagk, *A new class of disinfectant*, Deutsche Medizinische Wochenschrift, **1935**; 61, 829-32.
- [48] U. Tezel, S. G. Pavlostathis, *Role of Quaternary Ammonium Compounds on Antimicrobial Resistance in the Environment*, Antimicrobial Resistance in the Environment; 1<sup>st</sup> ed., John Wiley & Sons, **2011**, 349–387.
- [49] M. Bondaryk, M. Staniszevska, P. Zielińska, Zofia Urbańczyk-Lipkowska, *Natural Antimicrobial Peptides as Inspiration for Design of a New Generation Antifungal Compounds*, Journal of Fungi, **2017**, 46 (3).
- [50] J. M. Ageitos, A. Sánchez-Pérez, P. Calo-Mata, T. G. Villa, *Antimicrobial peptides (AMPs): Ancient compounds that represent novel weapons in the fight against bacteria*, Biochemical Pharmacology, **2017**, 133, 117–138.
- [51] M. A. Hanson, B. Lemaitre, *New insights on Drosophila antimicrobial peptide function in host defense and beyond*, Current Opinion in Immunology, **2020**, 62, 22–30
- [52] L. Marcotte, J. Barbeau, M. Lafleur, *Permeability and thermodynamics study of quaternary ammonium surfactants-phosphocholine vesicle system*. Journal of Colloid and Interface Science, **2005**, 292, 219-27.
- [53] J. Haldar, D. An, L. A. de Cienfuegos, J. Chen, A. M. Klibanov, *Polymeric coatings that inactivate both influenza virus and pathogenic bacteria*, Proceedings of the National Academy of Sciences, **2006**, 103, 17667-71.
- [54] R. Kenawy, S. D. Worley, R. Broughton, *The chemistry and applications of antimicrobial polymers: a state-of-the-art review*, Biomacromolecules, **2007**, 8, 1359-84.

- [55] E. Oblak, A. Piecuch, A. Krasowska, J. Luczynski, *Antifungal activity of gemini quaternary ammonium salts*, Microbiological Research, **2013**, 168, 630-8.
- [56] C. L. Schrank, K. P. C. Minbiole, W. M. Wuest, *Are Quaternary Ammonium Compounds, the Workhorse Disinfectants, Effective against Severe Acute Respiratory Syndrome-Coronavirus-2?*, ACS Infectious Diseases, **2020**, 6(7), 1553-1557.
- [57] A. Jain, L. S. Duvvuri, S. Farah, N. Beyth, A. J. Domb, W. Khan, *Antimicrobial polymers*, Advanced Healthcare Materials, **2014**, 3, 1969-85.
- [58] T. Ikeda, H. Hirayama, H. Yamaguchi, S. Tazuke, M. Watanabe, *Polycationic biocides with pendant active groups: molecular weight dependence of antibacterial activity*. Antimicrobial Agents and Chemotherapy, **1986**, 30, 132-6.
- [59] C. Z. Chen, N. C. Beck-Tan, P. Dhurjati, T. K. van Dyk, R. A. LaRossa, S. L. Cooper, *Quaternary ammonium functionalized poly (propylene imine) dendrimers as effective antimicrobials: structure-activity studies*, Biomacromolecules, **2000**, 1, 473-80.
- [60] P. Gilbert, A. Al-Taae, *Antimicrobial activity of some alkyltrimethylammonium bromides*, Letters in Applied Microbiology, **1985**, 1, 101-4.
- [61] L. Caillier, E. T. de Givenchy, R. Levy, Y. Vandenberghe, S. Geribaldi, F. Guittard, *Synthesis and antimicrobial properties of polymerizable quaternary ammoniums*. European Journal of Medicinal Chemistry, **2009**, 44, 3201-8.
- [62] J. He, E. Soderling, P. K. Vallittu, L. V. Lassila, *Investigation of double bond conversion, mechanical properties, and antibacterial activity of dental resins with different alkyl chain length quaternary ammonium methacrylate monomers (QAM)*, Journal of Biomaterials Science, Polymer Edition, **2013**, 24, 565-73.
- [63] M. Kong, X. G. Chen, K. Xing, H. J. Park, *Antimicrobial properties of chitosan and mode of action: a state of the art review*, International Journal of Food Microbiology, **2010**, 144, 51-63.
- [64] A. J. Leitgeb, J. A. Feliciano, H. A. Sanchez, R. A. Allen, K. R. Morrison, K. J. Sommers, R. G. Carden, W. M. Wuest, K. P. C. Minbiole, *Further Investigations into Rigidity-Activity Relationships in BisQAC Amphiphilic Antiseptics*, ChemMedChem, **2020**, 15 (8), 667-670.
- [65] R. C. Kontos, S. A. Schallenhammer, B. S. Bentley, K. R. Morrison, J. A. Feliciano, J. A. Tasca, A. R. Kaplan, M. W. Bezpalko, W. S. Kassel, W. M. Wuest *An Investigation into Rigidity-Activity Relationships in BisQAC Amphiphilic Antiseptics*, ChemMedchem, **2019**, 14(1), 83-87.
- [66] G. Garg, G. S. Chauhan, R. Gupta, J. H. Ahn, *Anion effects on anti-microbial activity of poly[1-vinyl-3-(2-sulfoethyl imidazolium betaine)]*, Journal of Colloid and Interface Science, **2010**, 344, 90-6.

- [67] M. L. Ingalsbe, J. D. Denis, M. E. McGahan, W. W. Steiner, R. Priefer, *Development of a novel expression, ZI MAX/K ZI, for determination of the counter-anion effect on the antimicrobial activity of tetrabutylammonium salts*, Bioorganic & Medicinal Chemistry Letters, **2009**, 19, 4984-7.
- [68] S. K. Sharma, G. S. Chauhan, R. Gupta, J. H. Ahn, *Tuning anti-microbial activity of poly(4-vinyl 2-hydroxyethyl pyridinium) chloride by anion exchange reactions*. Journal of Materials Science: Materials in Medicine, **2010**, 21, 717-24.
- [69] D. Xie, Y. Weng, X. Guo, J. Zhao, R. L. Gregory, C. Zheng, *Preparation and evaluation of a novel glass-ionomer cement with antibacterial functions*, Dental Materials, **2011**, 27, 487-96.
- [70] E. F. Panarin, M. V. Solovskii, N. A. Zaikina, G. E. Afinogenov, *Biological activity of cationic polyelectrolytes*, Die Makromolekulare Chemie, **1985**, 9, 25-33.
- [71] U. Mizerska, W. Fortuniak, J. Chojnowski, R. Halasa, A. Konopacka, W. Werel, *Polysiloxane cationic biocides with imidazolium salt (ImS) groups, synthesis and antibacterial properties*, European Polymer Journal, **2009**, 45, 779-87.
- [72] M. Tischer, G. Pradel, K. Ohlsen, U. Holzgrabe, *Quaternary ammonium salts and their antimicrobial potential: targets or nonspecific interactions?*, ChemMedChem **2012**, 7, 22-31.
- [73] Gottenbos B, Grijpma DW, van der Mei HC, Feijen J, Busscher HJ.;1; Antimicrobial effects of positively charged surfaces on adhering Gram-positive and Gram-negative bacteria. J Antimicrob Chemother **2001**;48:7-13.
- [74] M.C. Jennings, K.P.C. Minbiole, W.M. Wuest, *Quaternary Ammonium Compounds: An antimicrobial Mainstay and Platform for Innovation to Address Bacterial Resistance*, ACS Infectious Disease, **2015**, 1(7), 288-303.
- [75] C.J. Ioannou, G.W. Hanlon, S.P. Denyer, *Action of disinfectant quaternary ammonium compounds against Staphylococcus aureus*, Antimicrobial Agents and Chemotherapy, **2007**, 51 (1), 296-306.
- [76] T. Sumimoto, H. Nagamune, T. Maeda, H. Kourai, *Correlation between the Bacterioclastic Action of a Bis-quaternary Ammonium Compound and Outer Membrane Proteins*, Biocontrol Science, **2006**, 11 (3), 115-124.
- [77] M. C. Jennings, B. A. Buttaro, K. P. C. Minbiole, W. M. Wuest, *Bioorganic Investigation of Multicationic Antimicrobials to Combat QAC-Resistant Staphylococcus aureus*, ACS Infectious Diseases, **2015** 1 (7), 304-309.

- [78] N.W. Gunther, A.A. Wakeel, E.R. Reichenberger, S. Al-Khalifa, K.P.C. Minbiole, *Quaternary ammonium compounds with multiple cationic moieties (multiQACs), provide antimicrobial activity against Campylobacter jejuni*, Food Control, **2018**, 1-34.
- [79] J. Y. Maillard, *Bacterial target sites for biocide action*, Journal of Applied Microbiology, **2002**, 92, 16S–27S
- [80] P. Gilbert, L. E. Moore, *Cationic antiseptics: Diversity of action under a common epithet*, Journal of Applied Microbiology, **2005**, 99(4), 703–715.
- [81] T. Sumimoto, H. Nagamune, T. Maeda, H. Kourai, *Bacterioclastic Action of a Bis-Quaternary Ammonium Compound against Escherichia coli*, Biocontrol Science, **2004**, 9(1-2), 1-9.
- [82] M. P. Pereira, B. I. Tagkopoulos, *Benzalkonium chlorides: uses, regulatory status, and microbial resistance*, Applied and Environmental Microbiology, **2019**, 85.
- [83] F. Merino, S. Rubio, D. Perez-Bendito, *Solid-phase extraction of amphiphiles based on mixed hemimicelle/admicelle formation: Application to the concentration of benzalkonium surfactants in sewage and river water*, Analytical Chemistry, **2003**, 75(24), 6799–6806.
- [84] M. Clara, S. Scharf, C. Scheffknecht, O. Gans, *Occurrence of selected surfactants in untreated and treated sewage*, Water Research, **2007**, 41(19), 4339–4348.
- [85] N. Kreuzinger, M. Fuerhacker, S. Scharf, M. Uhl, O. Gans, B. Grillitsch, *Methodological approach towards the environmental significance of uncharacterized substances—Quaternary ammonium compounds as an example*, Desalination, **2007**, 215(1–3), 209–222.
- [86] E. Martinez-Carballo, A. Sitka, C. Gonzalez-Barreiro, N. Kreuzinger, M. Furhacker, S. Scharf, O. Gans, *Determination of selected quaternary ammonium compounds by liquid chromatography with mass spectrometry. Part I. Application to surface, waste and indirect discharge water samples in Austria*, Environmental Pollution, **2007**, 145(2), 489–496.
- [87] P. Gilbert, A. J. McBain, *Potential impact of increased use of biocides in consumer products on prevalence of antibiotic resistance*, Clin Microbiol Rev, **2003**, 16(2), 189–208.
- [88] M. N. Alekshun, S. B. Levy, *Molecular mechanisms of antibacterial multidrug resistance*, Cell, **2007**, 128(6), 1037–1050.
- [89] M. A. Kohanski, D. J. Dwyer, J. J. Collins, *How antibiotics kill bacteria: From targets to networks*, Nature Reviews Microbiology, **2010**, 8(6), 423–435.
- [90] J. Davies, D. Davies, *Origins and evolution of antibiotic resistance*, Microbiology and Molecular Biology Reviews, **2010**, 74(3), 417–433.
- [91] K. Hegstad, S. Langsrud, B. T. Lunestad, A. A. Scheie, M. Sunde, S. P. Yazdankhah, *Does the wide use of quaternary ammonium compounds enhance the selection and*

- spread of antimicrobial resistance and thus threaten our health?*, Microbial Drug Resistance, **2010**, 16(2), 91–104.
- [92] B. Perichon, P. Courvalin, *Antibiotic resistance*, 1<sup>st</sup> ed., Elsevier, Oxford, **2010**, ISBN: 9780080472461.
- [93] W. H. Gaze, N. Abdousslam, P. M. Hawkey, E. M. H. Wellington, *Incidence of class 1 integrons in a quaternary ammonium compound-polluted environment*, Antimicrobial Agents and Chemotherapy, **2005**, 49(5), 1802–1807
- [94] M. R. Gillings, X. J. Duan, S. A. Hardwick, M. P. Holley, H. W. Stokes HW, *Gene cassettes encoding resistance to quaternary ammonium compounds: A role in the origin of clinical class 1 integrons?* The ISME Journal, **2009**, 3(2), 209–215.
- [95] S. R. Partridge, G. Tsafnat, E. Coiera, J. R. Iredell, *Gene cassettes and cassette arrays in mobile resistance integrons*, FEMS Microbiology Reviews, **2009**, 33(4), 757–784.
- [96] K. Wakabayashi, M. Tsunoda and Y. Suzuki, *Bulletion of the chemical society of Japan*, **1969**, 42, 10.
- [97] R.M. Böhme, Q. Dang, *1,3,5-Triazine*, Encyclopedia of Reagents for Organic Synthesis, **2008**, 1-3.
- [98] K. Huthmacher, D. Most, *Cyanuric Acid and Cyanuric Chloride*, ULLMANN'S Encyclopedia of Industrial Chemistry, **2000**, 1<sup>st</sup> ed., Wiley-VCH, ISBN: 9783527306732.
- [99] G.H. Coleman, R.W. Leeper, C.C. Schulze, *Cyanogen Chloride*, Inorganic Synthesis, **1946**, 2, 90–94.
- [100] L. P. Hammett, *The Effect of Structure upon the Reactions of Organic Compounds. Benzene Derivatives*, Journal of the American Chemical Society, **1937**, 59 (1), 96–103.
- [101] J. McMurry, *Chimica Organica*, **2009**, Piccin, 359-372
- [102] P. Jeschke, M. Witschel, W. Krämer, U. Schirmer, *Modern Crop Protection Compounds*, **2007**, 3<sup>rd</sup> ed., Volume 1, Wiley-VCH, ISBN: 978-3-527-34089-7.
- [103] E.F. Eastin, R.D. Palmer, C.O. Grogan, *Mode of Action of Atrazine and Simazine in Susceptible and Resistant Lines of Corn, Weeds*, **1964**, 12 (1), 49-53
- [104] H. LeBaron, J. McFarland, O. Burnside, *The Triazine Herbicides – 50 years revolutionizing agriculture*, **2008**, 1<sup>st</sup> ed., Elsevier, 13-45, 101-103, ISBN: 9780444511676.
- [105] T. W. Newton, A. McArthur, *Triazine herbicides*, **1988**, US5062882A.
- [106] S. Haggblade, B. Minten, C. Pray, *The Herbicide Revolution in Developing Countries: Patterns, Causes, and Implications*, The European Journal of Development Research, **2017**. 29, 533–559.



- [107] W. O. Smith, jr. S. M. Daniels, *Purification of Phytochrome by Affinity Chromatography on Agarose-Immobilized Cibacron Blue 3GA*, *Plant Physiology*, **1981**, 68, 443-446.
- [108] Z.J. Kamiński, 2-chloro-4,6-disubstituted-1,3,5-triazines a novel group of condensing reagents, *Tetrahedron Letters*, **1985**, 26 (24), 2901-2904.
- [109] M. D'Este, D. Eglin, M. Alini, *A systematic analysis of DMTMM vs EDC/NHS for ligation of amines to Hyaluronan in water*, *Carbohydrate Polymers*, **2014**, 108, 239-246.
- [110] F. Labre, S. Mathieu, P. Chaud, P. Morvan, R. Vallée, W. Helbert, S. Fort, *DMTMM-mediated amidation of alginate oligosaccharides aimed at modulating their interaction with proteins*, *Carbohydrate Polymers*, **2018**, 184, 427-434.
- [111] M. Kunishima, C. Kawachi, J. Morita, K. Terao, S. Tani, F. Iwasaki, S. Tani, *4-(4,6-dimethoxy-1,3,5-triazin-2-yl)-4-methyl-morpholinium chloride: an efficient condensing agent leading to the formation of amides and esters*, *Tetrahedron*, **1999**, 55 (46), 13159-13170.
- [112] Z.J. Kamiński, B. Kolesińska, J. Kolesińska, G. Sabatino, M. Chelli, P. Rovero, M. Błaszczuk, M.L. Główska, A.M. Papini, *N-Triazinylammonium Tetrafluoroborates. A New Generation of Efficient Coupling Reagents Useful for Peptide Synthesis*, *Journal of the American Chemical Society*, **2005**, 127, 16912-16920.
- [113] A. El-Faham, F. Albericio, *Peptide Coupling Reagents, More than a Letter Soup*, *Chemical Reviews*, **2011**, 111, 6557-6602.
- [114] A. Falchi, G. Giacomelli, A. Porcheddu, M. Taddei, *4-(4,6-Dimethoxy-1,3,5-triazin-2-yl)-4-methyl-morpholinium chloride. A Valuable Alternative to PyBOP for Solid Phase Peptide Synthesis*, *Synlett*, **2000**, 2, 275-277.
- [115] J. R. Dunetz, J. Magano, G. A. Weisenburger, *Large-Scale Applications of Amide Coupling Reagents for the Synthesis of Pharmaceuticals*, *Organic Process Research & Development*, **2016**, 20 (2), 140-177.
- [116] V. Beghetto, A. Zancanaro, G. Pozza, *Process for Tanning Leathers with Triazine Derivatives*, **2014**, WO2015/044971 A2.
- [117] V. Beghetto, *Method for the industrial production of 2 halo-4,6-dialcoxy-1,3,5-triazines and their use in the presence of amines*, **2016**, WO2016/103185A3.
- [118] M. Kunishima, C. Kawachi, K. Hioki, K. Terao and S. Tani, *Development of novel polymer-type dehydrocondensing reagents comprised of chlorotriazines*, *Tetrahedron*, **2001**, 57, 1551 -1558.
- [119] R. Sole, V. Gatto, S. Conca, N. Bardella, A. Morandini, V. Beghetto. *Sustainable Triazine-Based Dehydro-Condensation Agents for Amide Synthesis*, *Molecules*. **2021**; 26(1):191.

- [120] R. Sole; V. Gatto; S. Conca, L. Agostinis, N. Bardella, A. Morandini, C. Buranello, V. Beghetto, *Synthesis of Amidation Agents and their Reactivity in Condensation Reactions*, *Synthesis*, **2020**, 1-9.
- [121] P. Farkaš; A. Čížová, S. Bekešová, S. Bystrický, *Comparison of EDC and DMTMM efficiency in glycoconjugate preparation*, *International Journal of Biological Macromolecules*, **2013**, 60, 325–327.
- [122] ] Z. J. Kamiński, P. Paneth, and J. Rudziński, *A Study on the Activation of Carboxylic Acids by Means of 2-Chloro-4,6-dimethoxy-1,3,5-triazine and 2-Chloro-4,6-diphenoxy-1,3,5-triazine*, *The Journal of Organic Chemistry*, **1998**, 63(13), 4248-4255.
- [123] Z. J. Kamiński, *Triazine-based condensing reagents*, *Biopolymers*, **2000**, 55(2), 140-164.
- [124] J. von Braun; K. Heider, E. Müller, *Bromalkylierte aromatische Amine. II. Mitteilung*, *Chemische Berichte*, **1918**, 5.1(1): 273–282.
- [125] S. Paganelli, M. M. Alam; V. Beghetto, A. Scrivanti, E. Amadio; M. Bertoldini; U. Matteoli, *A pyridyl-triazole ligand for ruthenium and iridium catalyzed C = C and C = O hydrogenations in water/organic solvent biphasic systems*, *Applied Catalysis A*, **2015**, 503, 20–25.
- [126] V. Beghetto, A. Scrivanti, M. Bertoldini, M. Aversa, A. Zancanaro, U. Matteoli, *A practical, enantioselective synthesis of the fragrances canthoxal, and silvial, and evaluation of their olfactory activity*, *Synthesis*, **2015**, 47, 272–278.
- [127] U. Matteoli, V. Beghetto, A. Scrivanti, M. Aversa, M. Bertoldini, S. Bovo, *An alternative stereoselective synthesis of (R)-and (S)-rosaphen via asymmetric catalytic hydrogenation*, *Chirality*, **2011**, 23, 779–783.
- [128] R. Sole, L. Taddei, C. Franceschi, V. Beghetto, *Efficient chemo-enzymatic transformation of animal biomass waste for eco-friendly leather production*, *Molecules*, **2019**, 24, 2979.
- [129] P. Zassowski, P. Ledwon, A. Kurowska, A. P. Herman, M. Lapkowski, V. Cherpak, Z. Hotra, P. Turyk, K. Ivaniuk, P. Stakhira, G. Sych, D. Volyniuk and J. V. Grazulevicius, *1,3,5-Triazine and carbazole derivatives for OLED applications*, *Dyes and Pigments*, **2018**, 149, 804-811.
- [130] A. Ullah, F. Iftikhar, M. Arfan, S. T. Batool Kazmi, M. N. Anjum, I .U. Haq, M. Ayaz, S. Farooq, U. Rashid, *Amino acid conjugated antimicrobial drugs: Synthesis, lipophilicity-activity relationship, antibacterial and urease inhibition activity*, *European Journal of Medicinal Chemistry*, **2018**, 145, 140-153.

- [131] J. Fraczyk, Z. Kamiński, J. Katarzynska, B. Kolesinska, *4-(4,6-Dimethoxy-1,3,5-triazin-2-yl)-4-methylmorpholinium Toluene-4-sulfonate (DMT/NMM/TsO<sup>-</sup>) Universal Coupling Reagent for Synthesis in Solution*, *Helvetica Chimica Acta*, **2018**, 101,1-21.
- [132] L. Xiaolian, C. Xuehui, Dalian University of Technology, CN107739367, **2018**, A
- [133] A. Locher, F. Reisser and K. Hofer, Sandoz Ltd., BE636144, **1963**, A
- [134] K. Yamada, Y. Tsukada, Y. Karuo, M. Kitamura, M. Kunishima, *Development of a New Benzylating Reagent Spontaneously Releasing Benzyl Cation Equivalents at Room Temperature*, *Chemistry - A European Journal*, **2014**, 20(38), 12274–12278.
- [135] J. C. Oxley, J. L. Smith, J. S. Moran, *Decomposition of Azo- and Hydrazo-Linked Bis Triazines*, *Journal of Energetic Materials*, **2009**, 27: 63–93.
- [136] N. Fridman, M. Kapon, M. Kaftory, *2-Chloro-4,6-dimethoxy-1,3,5-triazine*, *Acta Crystallographica Section C*, **2003**, 59, 12.
- [137] M. Kaftory, E. Handelsman-benory, *Thermal rearrangement of cyanurates in the solid state*, *Molecular Crystals and Liquid Crystals Science and Technology. Section A*, **1994**, 240, 241-249.
- [138] E. Handelsman-Benory, M. Botoshansky, M. Greenberg, V. Shteiman M. Kaftory, *Methyl Rearrangement of Methoxy-Triazines in the Solid- and Liquid-State*, *Tetrahedron*, **2000**, 56, 6887-6897.
- [139] P. Haegler, L. Joerin, S. Krähenbühl, J. Bouitbir, *Hepatocellular Toxicity of Imidazole and Triazole Antimycotic Agents*, *Toxicological Sciences*, **2017**, 157(1), 183–195.
- [140] V.S. Talismanov, S.V. Popkov, S.S. Zykova, O.G. Karmanova, G.V. Tsaplin, *Design, synthesis and evaluation of antimycotic and fungicidal activities of novel substituted 1-[(2-benzyl-1,3-dioxolan-4-yl)methyl]-1H-imidazoles*, *Journal of Pharmaceutical Sciences and Research*, **2018**, 10(6), 1625-1628
- [141] M. Gaba, C. Mohan, *Development of drugs based on imidazole and benzimidazole bioactive heterocycles: recent advances and future directions*, *Medicinal Chemistry Research*, **2016**, 25,173–210.
- [142] L. Liu, Y. Hu, J. Lu, G. Wang, *An imidazole coumarin derivative enhances the antiviral response to spring viremia of carp virus infection in zebrafish*, *Virus Research*, **2019**, 112-118.
- [143] L. Zhang, X. Peng, G. L. V. Damu, R. Geng, C. Zhou, *Comprehensive Review in Current Developments of Imidazole-Based Medicinal Chemistry. Medicinal*, *Research Reviews*, **2014**, 34(2), 340–437.

- [144] R. A. Allen, M. C. Jennings, M. A. Mitchell, S. E. Al-Khalifa, W. M. Wuest, K. P.C. Minbiole, *Ester- and amide-containing multiQACs: Exploring multicationic soft antimicrobial agents*, *Bioorganic & Medicinal Chemistry Letters*, **2017**, 27(10), 2107-2112.
- [145] N. W. Gunther, A. A. Wakeel, E. R. Reichenberger, S. Al-Khalifa, K. P. C. Minbiole, *Quaternary ammonium compounds with multiple cationic moieties (multiQACs), provide antimicrobial activity against Campylobacter jejuni*, *Food Control*, **2018**, 1-34.
- [146] K. P. C. Minbiole, M. C. Jennings, L. E. Ator, J. W. Black, M. C. Grenier, J. E. LaDow, K. L. Caran, K. Seifert, W. M. Wuest, *From antimicrobial activity to mechanism of resistance: the multifaceted role of simple quaternary ammonium compounds in bacterial eradication*, *Tetrahedron*, **2016**, 1-8.
- [147] K. Hoffman, *Imidazole and Its Derivatives. Part I. The Chemistry of heterocyclic compounds*, Interscience Publishers, **1953**.
- [148] A.R. Katritzky, D.C. Oniciu, I. Ghiviriga, R.A. Barcock, 4,6-Bis- and 2,4,6-tris-(N,N-dialkylamino)-s-triazines: synthesis, NMR spectra and restricted rotations, *J. Chem. Soc. Perkin Trans.*, **1995**, 785-792
- [149] A. Fatona, A. Osamudiamen, M. Moranâ, B. Jose, A. Michael, Rapid, catalyst-free crosslinking of silicones using triazines, *Journal of Polymer Science*, **2020**, 28(14), 1949-1959.
- [150] W. Ma, M. Meng, X. Jiang, B. Tang, S. Zhang, *Synthesis of a water-soluble macromolecular light stabilizer containing hindered amine structures*. *Chinese Chemical Letters*, **2013**, 24(2), 153–155.
- [151] D. M. Lewis, *Developments in the chemistry of reactive dyes and their application processes*, *Coloration Technology*, **2014**, 130(6), 382–412.
- [152] H. Seiler, G. Hegar, *Fibre-reactive dyes, containing both chloro and fluoro triazine radicals*, **1982**, US4507236A
- [153] A. Tzikas, *Azo dyes containing chloro-s-triazine and vinylsulfonyl type fiber-reactive groups*, **1993**, US5233026A
- [154] M. Calas, M. L. Ancelin, G. Cordina, P. Portefaix, G. Piquet, V. Vidal-Sailhan, H. Vial, Antimalarial activity of compounds interfering with Plasmodium falciparum phospholipid metabolism: comparison between mono- and bisquaternary ammonium salts, *Journal of Medicinal Chemistry*, **2000**, 43, 505– 516.
- [155] M. Calas, M. Ouattara, G. Piquet, Z. Ziora, Y. Bordat, M. L. Ancelin, R. Escale, H. Vial, Potent antimalarial activity of 2-aminopyridinium salts, amidines, and guanidines, *Journal of Medicinal Chemistry*, **2007**, 50, 6307 – 6315.

- [156] S. Ortial, S. Denoyelle, S. Wein, O. Berger, T. Durand, R. Escale, A. Pellet, H. Vial, Y. Vo-Hoang, Synthesis and evaluation of hybrid bis-cationic salts as antimalarial drugs, *ChemMedChem*, **2010**, 5, 52–55.
- [157] S. E. Al-Khalifa, Megan C. Jennings, W. M. Wuest, K. P. C. Minbiole, *The Development of Next-Generation Pyridinium-Based multiQAC Antiseptics*, *ChemMedChem*, **2018**, 12(4), 280-283.
- [158] S. Schallenhammer, S. Duggan, K. Morrison, B. Bentley, W. Wuest, K. P. C. Minbiole, Hybrid BisQACs: Potent Biscationic Quaternary Ammonium Compounds Merging the Structures of Two Commercial Antiseptics, *ChemMedChem*, **2017**, 12(23), 1931-1934.
- [159] D. Kwaśniewska, Y. Chen, D. Wieczorek, Biological Activity of Quaternary Ammonium Salts and Their Derivatives, *Pathogens*, **2020**, 9, 459-461.

# **POLYMERIC QACS SYNTHESIS AND THEIR SURFACE ADHESION TREATMENT**

# CHAPTER 7

## INTRODUCTION

### Polymeric QACs synthesis and surface adhesion treatment

In collaboration with:



Supervisors:

**Prof. Kohji Ohno**

## 7.1 Biofilm

The same kind of bacteria may be found in different forms generally referred to as biofilm and planktonic form and their characteristics change. A biofilm is an agglomeration of bacteria held together through a complex mixture of self-produced macromolecules such as; polysaccharides, proteins and DNA.<sup>[1,2]</sup> This form differs from the planktonic state where the bacteria are single separate cells (i.e. floating as single cells in water), whereas the biofilm behaves more like a cellular community, a classic example is dental plaque.

As reported by O'Toole <sup>[3]</sup> biofilm formation has five stages of development (figure 7.1):

1. Initial adhesion: This stage begins with the adhesion of cells to a surface in a reversible manner through weak interactions such as Van der Waals forces <sup>[4]</sup>.
2. Colonization: After reversible adhesion, the bacteria anchor themselves strongly to the surface, developing appendage-forming macromolecules or by producing of a film of polymeric extracellular substances <sup>[5]</sup>.
3. Proliferation: Following permanent anchorage, bacterial cells begin to proliferate <sup>[6,-8]</sup>.

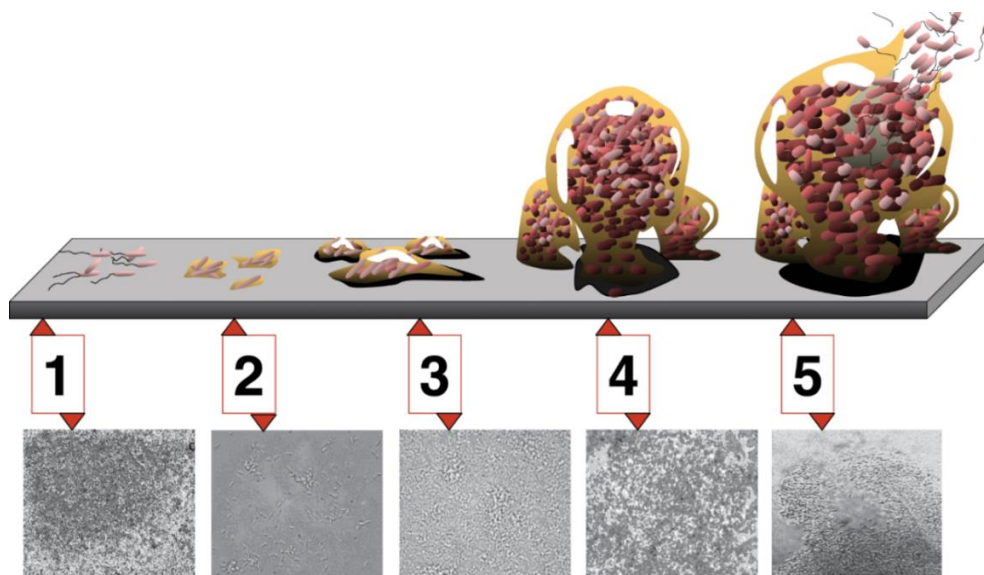


**Figure 7.1** - Development of a biofilm. Stage 1: Initial adhesion. Stage 2: Irreversible attachment and colonization. Stage 3: Proliferation. Stage 4: Maturation. Stage 5: Detachment. Figure adapted from Monroe <sup>[8]</sup>.



4. **Maturation:** The Biofilm has expanded over much of the available surface area in proximity and has produced a large amount of polymeric "shells" that allow for extra protection from the external environment [9].
5. **Detachment:** Once the biofilm is mature there are possible methods of detachment of some cells both in planktonic form or portions of biofilm. The first mechanism is called quorum sensing [10] and produces a series of programmed chemical events within the biofilm itself that lead to a local hydrolysis of the outer polymeric matrix resulting in the detachment of some cells from the biofilm in planktonic form [11]. A second mechanism, generally caused by environmental conditions, generates forces capable of removing a portion of the biofilm from the surface [12]. These portions of biofilm can then be carried away by the flow of the fluid medium in which they are in contact and migrate elsewhere, where they can again adhere to a surface and restart the formation of new biofilms.



**Figure 7.2** Examples of biofilms. *Left:* typical mold in households. *Center:* typical biofouling on a ship hull. *Right:* biofilm of *Pseudomonas aeruginosa* on a catheter

In nature we can find them in many environments (figure 7.2); biofilms may, in some cases, have benign actions positive and are essential for food digestion or sewage processing [13], others can be inconvenient, forming slippery surfaces and/or unpleasant smell, some can generate degradative phenomena for certain materials (for example pipelines) [14] or can be extremely dangerous when occurring inside the human body [6]. In this connection, modern medicine pays much attention to the biofilm phenomenon for human body implants. Biofilms can have disastrous consequences [15-18], especially if diagnosed too late or for implants that are difficult to replace. In fact, the biofilm greatly delays the action of antimicrobials (a value that can change from substance to substance and from biofilm to biofilm) [19]. In some cases,

decrease in antibiotic response up to 500-fold lower has been observed by bacteria in biofilm state compared to the corresponding planktonic form [20-22]. In a similar way, biofilms can also stop immune cell response of infected hosts, making it even more difficult to eradicate within the organism.

## 7.2 New Challenge in infectious diseases

According to the literature, ninety percent of bacterial species in nature exist in the form of biofilms (figure 7.3) [23].

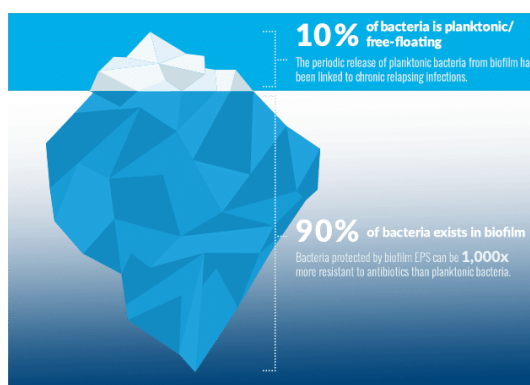


**Figure 7.3** – Representation of the distribution of bacteria in nature between planktonic form and biofilm form, as can be seen from the illustration only 10% are in free form

Ninety percent of bacterial species in nature exist in the form of biofilms (Figure 6.3) [23]. For a medical stand point, biofilms represent a great challenge, since they are involved in the majority of human infections, and are extremely difficult to treat due to their intrinsic tolerance to immune and antimicrobial responses. Biofilms, such as *Pseudomonas aeruginosa*, *Staphylococcus aureus* and *Escherichia coli*, show important virulence mechanisms and are therefore a danger for many medical treatments. Additionally, it should be mentioned that a large number of diseases, such as vaginitis, colitis, conjunctivitis, gingivitis, are directly related to biofilm infections [24-27]. Biofilms may also be responsible of wounds chronic infections, which are also of great concern in the medical field. In fact, very persistent infections are mostly a consequence of biofilm formation from common pathogens (*P. aeruginosa* and *S. aureus* [28]), that in planktonic form would not be problematic. Unfortunately, to date the majority of medical treatments are evaluated against microorganisms in the planktonic form, which, when

employed, are often found to be inactive against biofilms [29,30]. This recalcitrance phenomenon makes them extremely difficult to effectively treat and eradicate. Therefore, new strategies for the prevention, dispersion, and treatment of bacterial biofilms are urgently needed.

### 7.3 Active surfaces for biofilm formation prevention

In nature, there are several examples of how many higher organisms effectively prevent biofilm growth on living tissue. Some aquatic mammals such as whales and dolphins contrast biofilm through passive mechanisms such as secretion of a gel-like substance that prevents the microorganism from taking root, and through active mechanisms the enzymatic digestion of potentially hazardous biological materials [31].

From this animal behavior, several synthetic analogues have been formulated that exploit both passive and active methods by incorporating different antimicrobials into antifouling hydrogels [32] or by using zwitterionic materials [33].

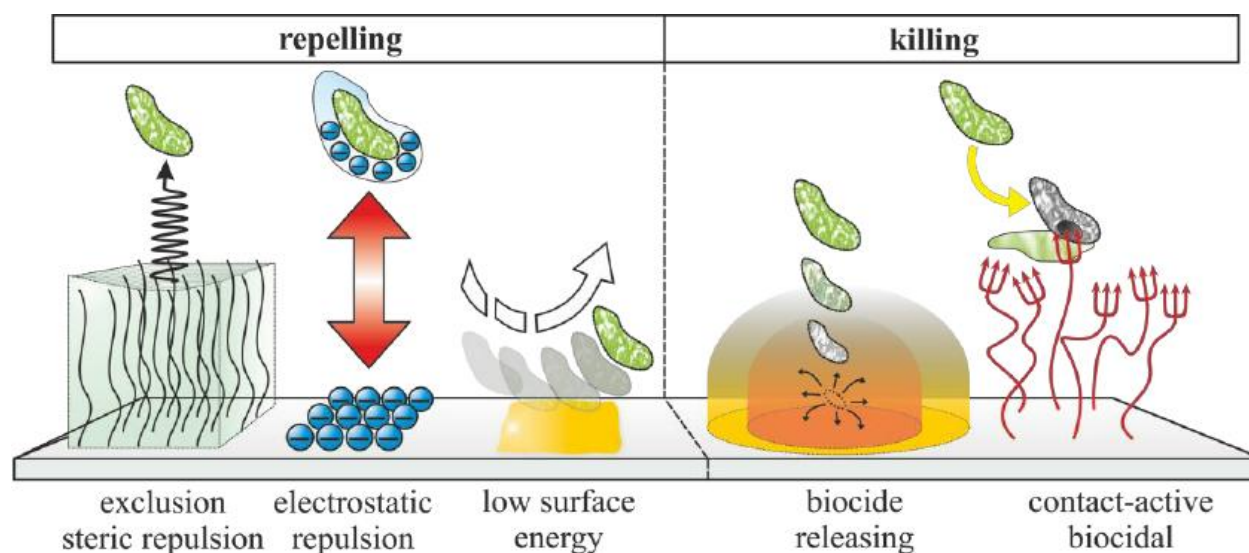


**Figure 7.4** – Different strategies for controlling biofilm formation on surfaces

Many of the passive ways of preventing biofilm formation exploit the physicochemical properties of surfaces such as hydrophilicity, smoothness, electrical charge (figure 7.4). In fact, modulation of these properties can reduce or prevent bacterial adhesion. Hydrophilicity can be modulated using hydrophilic polymer brushes [34-36]. Acting with dispersion forces between the chains and the bacterial cells, preventing them from binding to the surface, a similar concept happens in

steric stabilization of colloids where polymer chains grafted on the surface prevent agglomeration [37]. Hydrophobicity gives the surface lubricating properties towards bacteria decreasing their adhesion, and can be easily achieved by treating the surfaces with polymers such as polyvinylidene fluoride [38] or polydimethylsiloxane [39]. Finally, the smoothness of a surface greatly influences biofilm formation, the rougher a surface is the more prone bacteria will be to cling to it and will be more difficult to remove. Therefore, the use of smooth surfaces decreases the tendency for biofilm formation [40,41].

Active modalities directly kill bacteria by contact and mostly foresee the use of leachable antimicrobials [42,43,44]. Examples of these materials date back to ancient times, and silver is certainly the undisputed leader for these applications [45]. In fact, ancient civilizations used silver containers to better preserve liquid foods and water from bacterial contamination. Even today, there is still much medical interest in silver which is employed, for example, for surface coating [46]. However, it must be considered that silver does not have a selective action on bacteria and has an equally toxic effect on human cells [47]. In fact, silver ions form complexes with various proteins and DNA, and for this reason its use must be limited in medical devices medical devices and food preservation. Other examples of leachable substances used as antibacterial are furanones [48], iodine [49], triclosan [50], nitric oxide [51], hypochlorite [52], antibiotics [53]. However, leaching surfaces have an intrinsic disadvantage that is independent of the specific drug employed: sooner or later the active principle is inevitably exhausted and therefore become ineffective.

This drawback can be circumvented through the immobilization of antimicrobial agents that act by contact on the bacterial cell and cause its death. These antimicrobials can be anchored to the surface via covalent bonding [54,55] or weak interactions [56,57]. Several compounds exhibiting antibacterial activity such as lysozyme [58], antimicrobial peptides [59], and quaternary ammonium salts [60] have also been studied.

## **7.4 Contact-killing surfaces containing quaternary ammonium salts**

Historically speaking, one of the first quaternary ammonium salts immobilized on the surface

was 3-trimethoxysilyl-propyldimethyloctadecyl ammonium chloride, a compound containing a silane group [61]. Like most silanes it can form covalent bonds with silicates, oxides and even polymers activated by surface activation techniques such as plasma treatment and corona treatment [62]. It can also self-polymerize to form long polymer chains. Abbot and Walters [63] have carried out several experiments with these types of silanes by binding them to different surfaces, including fiber metals and silica surfaces, then testing their activities against gram positive, gram negative bacteria, algae and fungi reporting positive antibacterial properties.

More recently, the scientific community has showed much attention to the study of polymeric quaternary ammonium salts derived from common polymers such as polyethyleneimine, polyvinylpyridinium, chitosan and various acrylates [73-76]. These polymers may be immobilized either through grafting techniques (covalent bonding) or by lower energy interactions with the surface (electrostatic and Van der Waals interactions). Surface immobilization has usually been followed by quaternization through various sidechains and counterions [64-67].

#### **7.4.1 Surface containing quaternary ammonium polymers**

The research group of Lin and colleagues reported the practicability of anchor polyethyleneimine chains on glass slides [77]. Authors afterwards used alkyl halide and alkyl halide acid in order to obtain cationic and zwitterionic groups. The evaluation of antimicrobial efficacy was done against different bacterial strains. Sidechains of different lengths (ethyl, butyl, hexyl, dodecyl and octadecyl) were evaluated. The results showed that while neutral and zwitterionic surfaces had no bactericidal activity, those containing cationic groups were effective in eradicating bacterial colony formation. It was also found that the chain length of the alkylating group was decisive and required a carbon chain with more than 4 units.

The group of Haldar and colleagues studied a different approach to immobilization using long alkyl chain polyethyleneimine QACs and “paint” it on glass slides [68]. According to the authors, the advantage of using this polymer, despite the fact that it is not covalently anchored to the surface, lies in its nature of not being soluble in the medium in which the biological tests are done (inoculum) and therefore not being released from the surface. In addition, this study also verified the efficacy of ammonium polymer-treated surfaces against coronaviruses responsible

for seasonal influenza with a 4-log reduction PFU (plaque-forming unit) within minutes.

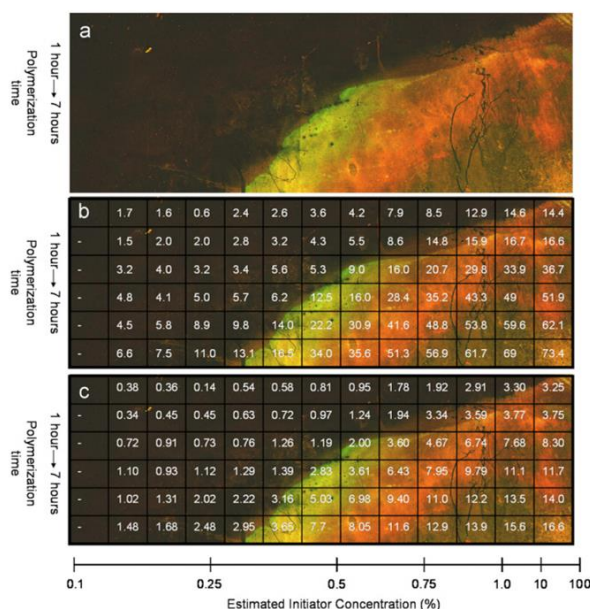


**Figure 7.5** – Concentration gradient of QACs in a slide glass from work of Murata et al [69]. a) Color image of the slide, b) slide with polymer layer thickness data, c) Charge density data in positive charges/cm<sup>2</sup>(x10<sup>15</sup>), measured by fluorescein staining.

All of the previous techniques lack in control of the deposition of ammonium polymers on the surface. To overcome this, Murata's group exploited grafting from techniques in which glass surfaces are initially bounded with initiators and then the polymers chains of dimethylaminoethylmethacrylate have grown using atom transfer radical polymerization (ATRP) techniques [69]. By controlling the initiators surface density and polymerization reaction time, they were able to independently control the polymer density and polymer length, respectively. By fluorescence techniques, the authors were able to determine the charge density and correlate it to the antimicrobial efficacy (figure 7.5). In conclusion, the antimicrobial efficacy was found to depend on surface charge and not on the length of the polymer itself, determining a threshold of  $5 \times 10^{15}$  charges/cm<sup>2</sup> ( $8.30 \times 10^{-9}$  mol/cm<sup>2</sup>) necessary to be effective as an antimicrobial surface.

Furthermore, Milovic and colleagues have reported that bacteria have a tendency to not develop antimicrobial resistance against surfaces modified with polyethyleneimine containing quaternary ammonium groups [70]. This conclusion was possible by repeatedly sampling the bacteria that survived from surface exposure and re-exposing them to fresh surfaces. The authors report that even after 11 consecutive exposures there appears to be no loss of efficacy

in antibacterial action (Figure 7.6). This behavior exhibited by these surfaces opened up encouraging prospective, allowing to reduce the dispersion of QACs into the environment and disfavoring bacterial resistance.

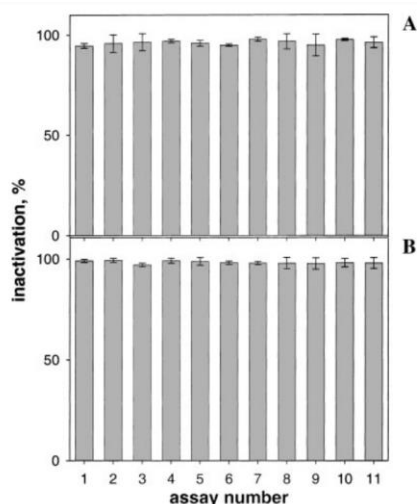


**Figure 7.5** – A series of bactericidal activity assays for amino-glass slides covalently coated with *N*-hexyl, methyl-PEI against *S.aureus* (a) and *E.coli* (b) from work of Milovich et al [70].

## 7.5 Surface grafting techniques

A surface can be functionalized by addition of small molecules, oligomers or even polymers. There are several methods for surface functionalization. Some exploit deposition methods that use weak interactions such as Langmuir-Blodgett technique<sup>[71]</sup> or surface adsorption<sup>[72]</sup> and others exploit immobilization by chemical bond formation<sup>[78,79]</sup>. Each technique clearly has advantages and disadvantages. Chemical grafting techniques have advantages with respect to control and functionalization density<sup>[80]</sup> but are more complicated to exploit in wide substrates.

Chemical grafting can be divided in two different categories: grafting to and grafting from:

- Grafting to (figure 7.6 a): This grafting method involves the use of several functional groups present in the molecules or in the backbone polymer chain <sup>[80,81]</sup>. These functional groups lead to the formation of a chemical bond with the surface due to a coupling reaction with an end-reactive group present on the surface. This method requires a



suitable, preformed polymer, prior to surface immobilization. Common reaction mechanisms used to synthesize these polymers include free-radical polymerization <sup>[83]</sup>, anionic polymerization <sup>[84]</sup>, and living polymerization techniques <sup>[85]</sup>.

- Grafting from (figure 7.6 b): In this technique the immobilized polymer is polymerized directly on the surface. To do this, the surface is first chemically functionalized with functional groups that act as polymerization initiators. The surface is then placed in a solution containing the monomer and polymerization is started. Again, different polymerization techniques can be used here such as ring opening polymerization <sup>[86]</sup>, anionic polymerization <sup>[87]</sup>, atom-transfer radical-polymerization <sup>[88]</sup>, and reversible addition-fragmentation chain transfer <sup>[89]</sup>.

Surface adsorption (figure 7.6 c)

We can consider adsorption phenomena as the adhesion of ions or molecules on a surface belonging to a different phase respect to the surface. This phenomenon can occur in two ways: by physisorption <sup>[90]</sup> or by chemisorption <sup>[91]</sup>. The first mainly involves weak Van der Waals forces while the latter involves weak chemical bonds. Polymers in solution can readily adsorb on various surfaces where there is an attractive interaction between the polymer segments and the surface <sup>[92-94]</sup>. The process of polymer adsorption on a surface is largely governed by the prevailing conditions under which polymer, solvent and surface interact. The adsorption of ions and molecules to polymer surfaces plays a role in many applications including biomedical, structural, coatings, environmental.

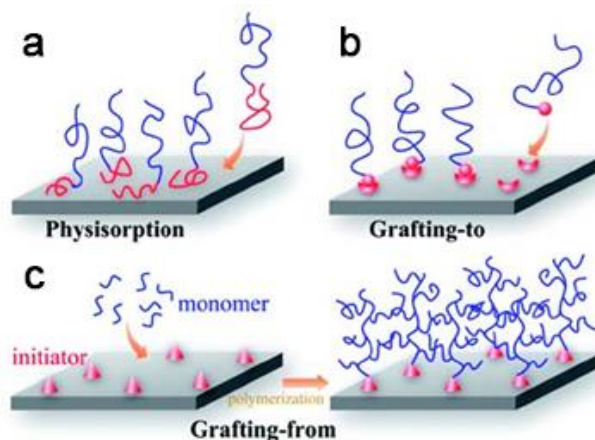


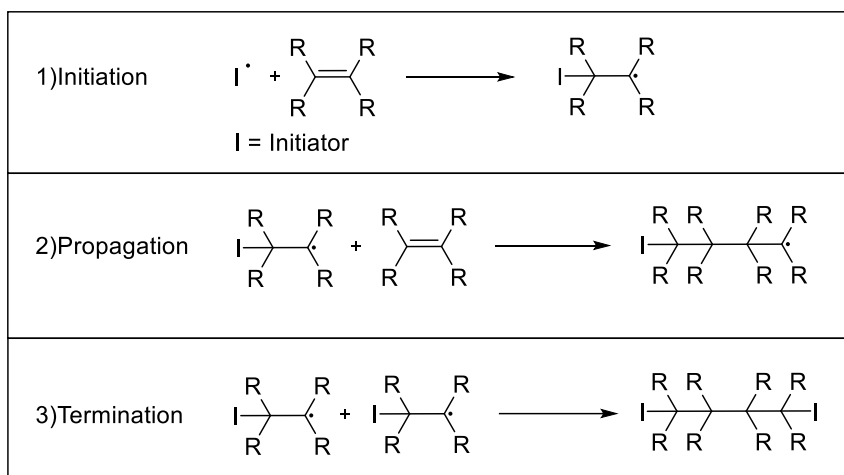
**Figure 7.6** – Different approach in surface polymer anchoring. a) Physisorption: in which the polymers chain



adheres to surface because of Van der Waal forces. b) Grafting to: Anchoring of polymers exploiting a coupling between an end reactive group in the polymer and a functional group onto surface. c) Grafting from: Technique in which a polymerization initiator is immobilized onto surface a then the polymers chains are grown exploiting a living polymerization reaction.

## 7.6 Reversible-deactivation radical polymerization

In the field of polymer chemistry, free-radical polymerization (FRP) was the first polymerization technique studied, and is characterized by a balance of continuous formation (initiation) and quenching (termination) of radicals involved in the reaction (scheme 7.1). This process leads to the formation of polymers with a very wide distribution of molecular weights with a polydispersity ( $\mathcal{D}$ ) of 2 or higher <sup>[95]</sup>.



**Scheme 7.1** – The three reaction steps of a typical free radical polymerization. The resulting polymers depends on the kinetic rate of these reactions.

It is a versatile technique, as it can be performed under different conditions and with a wide variety of monomers. But the poor control of the final microstructure of macromolecules limits its use in many fields such as in the synthesis of block copolymers or other complex microstructures. The latter can be synthesized using living polymerization techniques, well known is the case of anionic polymerization <sup>[96]</sup>, which allows the synthesis of low dispersion polymers, but has the disadvantage of a limited choice of monomers and can be performed only under extremely demanding reaction conditions.

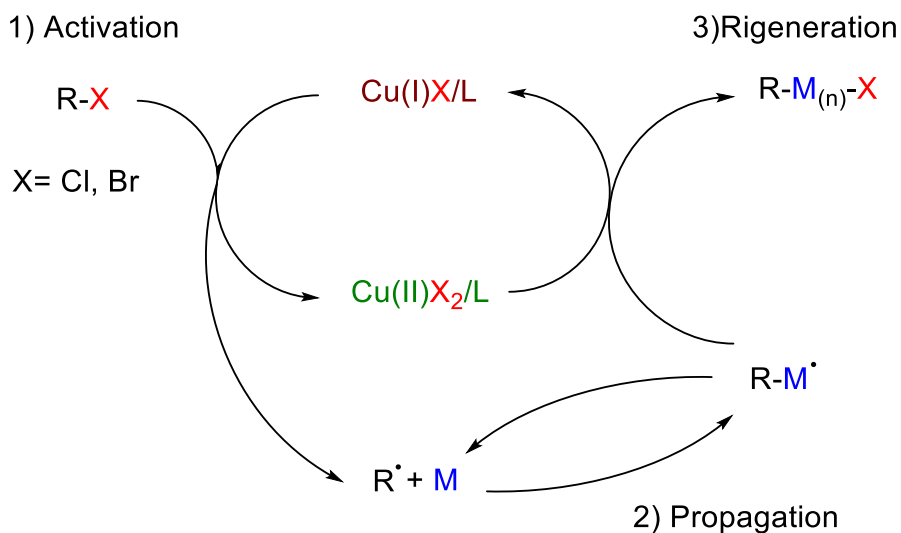
Reversible-deactivation radical polymerization (RDRP) belongs to that group of polymerizations that retain the characteristics of living polymerization but are characterized by radical reactions [97]. The result of such a process will be a polymer with low Đ and predetermined molar mass. Currently, the mechanisms that ensure this living character are mainly three:

- Atom transfer radical polymerization (ATRP)
- Nitroxide-mediated polymerization (NMP)
- Reversible addition-fragmentation chain transfer (RAFT)

In this thesis, the technique of Atom transfer radical polymerization was employed and thus will further be discussed below, leaving out the other two.

### 7.6.1 Atom transfer radical polymerization (ATRP)

In ATRP, a transition-metal catalyst is used to reversibly activate halide-terminated dormant chains. The principal mechanism is outlined in scheme 6.2.



**Scheme 6.2** – General scheme for an ATRP reaction.

Many different metal complexes that have been employed, particularly those of Cu [98], Fe [99], Ru [100], Ni [101] and Os [102]. Metals activate the "dormant" halogen-containing species by

generating radicals via an electron transfer process, and the metal is oxidized to a higher oxidation state. This oxidation process is reversible, and generates an equilibrium that is predominantly shifted to the left of chemical equation. During propagation each chain grows at the same rate in a living/dormant polymer chain formation cycle, allowing to obtain polymers with similar molecular weights and a very low  $\bar{D}$ . Therefore, to achieve an ideal balance of living/dormant species, all polymerization components (initiator, catalyst, ligand and solvent) must be optimized in such a way that the concentration of the dormant species is higher than that of the propagating radical compounds, but not so high that the reaction slows down or stops <sup>[103]</sup>. The number of final chains is determined by the number of initiators but in order to ensure a low  $\bar{D}$  it is necessary that the initiator is activated quickly, or at least faster than the rate of propagation <sup>[104]</sup>.

ATRP reactions, unlike anionic polymerizations, tolerate variable reaction conditions and are compatible with different monomers and functional groups <sup>[105]</sup>. These reactions are simple to carry out and catalysts such as copper or iron complexes, using simple pyridine-based ligands, are inexpensive. Additionally, by working on the structure of the initiator, different polymer architectures can be generated. For example, if an initiator has multiple alkyl halide groups it is possible to generate star-shaped polymers <sup>[106]</sup>, or they can be immobilized on a surface to generate a dense polymeric brush <sup>[107]</sup>.

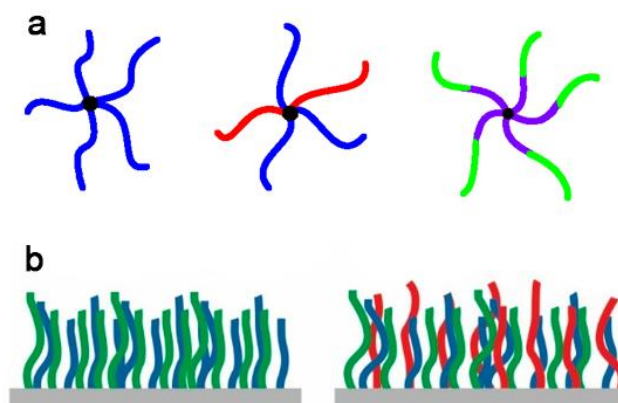


**Figure 6.7** – Structure representation of different star-like polymers (a) and superficial polymer brush (b)

## **CHAPTER 8**

### **SCOPE OF THE WORK**

**Polymeric QACs synthesis and surface adhesion treatments**

This work was carried out during my time spent at the Institute for Chemical Research, Kyoto University in Uji City, Japan. The purpose of this study is to evaluate the possibility of developing different polymeric structures containing 2-*N*-morpholinoethyl methyl methacrylate for the preparation of polymeric TQACs by exploiting the high reactivity of chlorotriazines towards morpholino residues.

In particular, we focused on the synthesis of block polymers that could be used in the functionalization of polypropylene film surfaces through “grafting to” techniques that exploit the physisorption of polymer chains with the surface. In fact, surfaces containing QACs are of great interest in the control of biofilm formation, the advantage of using these surfaces lies in their ability to inhibit the growth of microorganisms without releasing substances into the environment. This makes them very attractive in terms of environmental preservation and control of dispersion of antimicrobials in the environment.

The objectives that were set in this part of the thesis were:

- The identification of optimal reaction conditions and molar ratios between reactants in atom transfer radical polymerization reactions
- Synthesis of different AB and ABA block copolymers containing polystyrene and poly2-*N*-morpholinoethyl methyl methacrylate
- Quaternization of morpholino residues with chloro triazines to obtain polymeric TQACs
- Surface functionalization of PP films with polymeric TQACs and evaluation of efficacy in inhibiting biofilm formation of *Staphylococcus aureus* and *Escherichia coli*.

## **CHAPTER 9**

### **RESULT AND DISCUSSION**

**Polymeric QACs synthesis and surface adhesion treatments**

## 9.1 Introduction

The work here reported foresees the synthesis of diblock copolymers and triblock copolymers containing styrene, methyl methacrylate (MMA) and 2-*N*-morpholinoethyl methacrylate (MEMA) (figure 9.1), exploiting atom transfer radical polymerization (ATRP) a living radical polymerization technique. Polymers achieved with this technique have been further functionalized with halo-1,3,5-triazine derivatives in order to obtain various polymeric TQACs and test their use in surface functionalization.

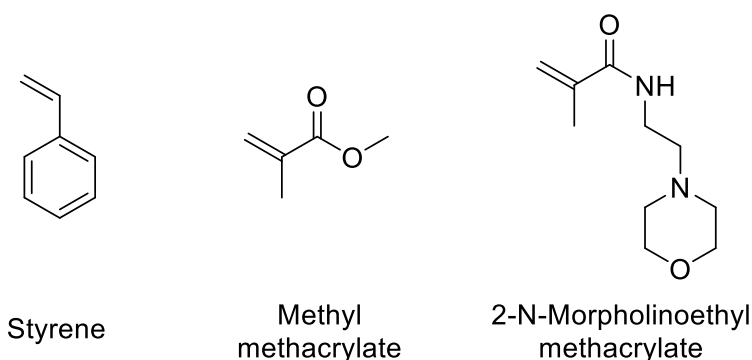


**Figure 9.1** – Structure of styrene, methyl methacrylate e 2-*N*-morpholinoethyl methacrylate

In fact, the ultimate goal of this part of the work was to prepare polymeric films employed for contact-killing antimicrobial surface treatments. This purpose was achieved by simple deposition of polymeric TQACs.

The mechanism by which these block copolymers can be anchored onto surfaces is well known in the literature and is promoted by physisorption phenomena <sup>[90]</sup> (figure 9.2). Taking advantage of this behavior, we sought to devise a series of A-B and A-B-A block polymers containing TQACs that could be physisorbed onto polypropylene film surfaces.

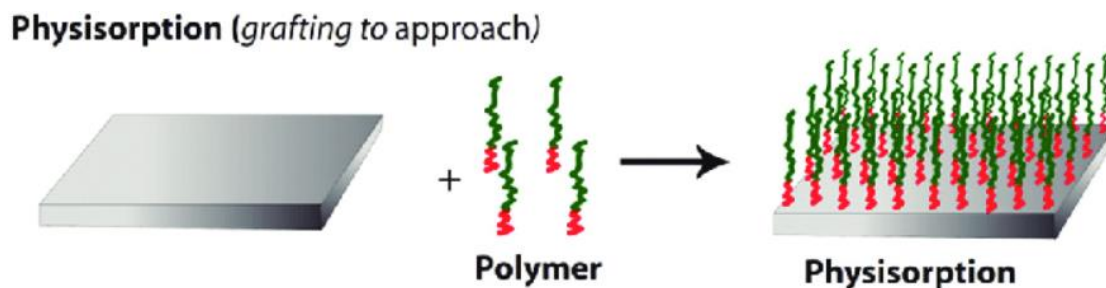


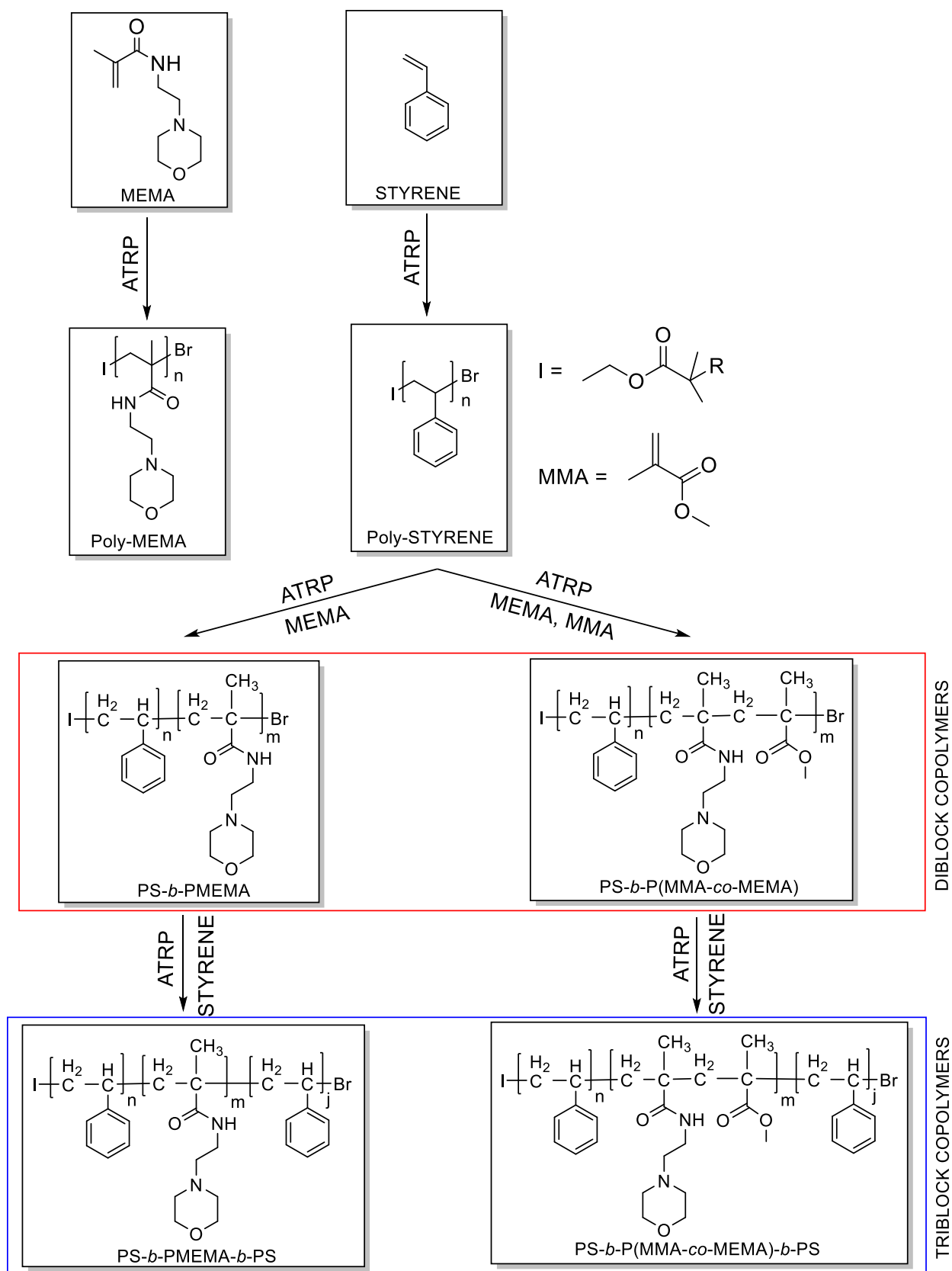
**Figure 9.2** – Physisorption of block copolymers on a surface

The choice of the monomers was based on both commercial availability and properties of the resulting polymers. Polymers such as polystyrene and polymethylmethacrylate are able to adsorb on various neutral surfaces <sup>[108]</sup> and may be used as "anchor" segments. The morpholino residue of MEMA on the other hand, was used to achieve quaternization with MAT<sub>12</sub> to obtain anchored TQACs. The antimicrobial properties of the surface were evaluated by biofilm inhibition towards bacterial species such as *Staphylococcus aureus* and *Escherichia coli*.

## 9.2. Atom transfer radical polymerization (ATRP) polymers synthesis and characterization

In the following paragraphs, the syntheses and characterization of polymers and block copolymers obtained exploiting different atom transfer radical polymerization techniques will be discussed. All polymers were characterized by GPC and the performance of the reaction evaluated in terms both of monomer conversion and polydispersity ( $\bar{M}_w/\bar{M}_n$ ). A general scheme of the polymer synthesis is reported below (scheme 9.1).





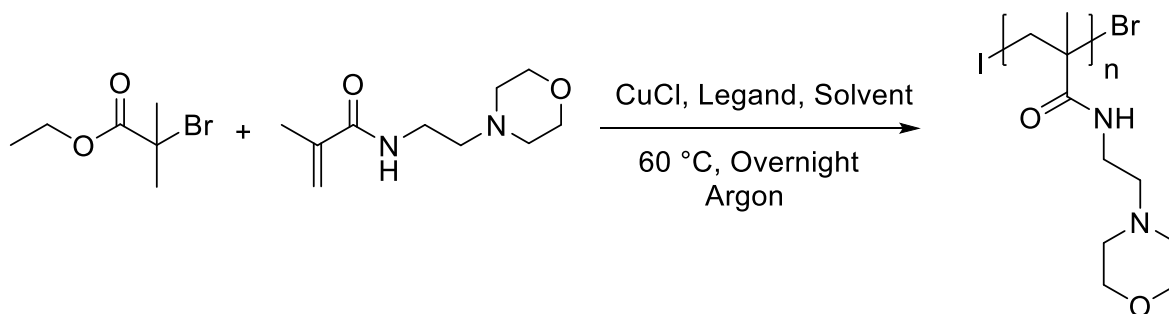
**Scheme 9.1** – General scheme of block copolymers synthesis

## 9.2.1 Synthesis of poly-2-*N*-morpholinoethyl methacrylate (PMEMA)

Initially, we evaluated the performance of ATRP in the polymerization of MEMA under different solvent and ligand conditions. In fact, parameters such as solvent, ligand, catalyst and the reagents molar ratio, were tested and their influence on the polymer characteristics verified.

In determining the various ligands, we followed the indications on their activity reported by Matyjaszewski et al. <sup>[103]</sup>. In fact, the activity of the ligand in ATRP polymerization decreases in the order of; alkylamine = pyridine > alkyl imine >> aryl imine > arylamine. Therefore, an alkylamine ligand (*N,N',N'',N'''*-pentamethyl diethylene triamine) and a pyridine ligand (4,4'-dinonyl-2,2'-dipyridyl) were chosen.

The following scheme shows the general synthesis of poly-2-*N*-morpholinoethyl methacrylate (PMEMA) (scheme 9.2).



**Scheme 9.2** - Synthesis of poly-2-*N*-morpholinoethyl methacrylate

**Table 9.1** – Experimental data for PMEMA

| Run          | Monomer            | Ligand           | Solvent |
|--------------|--------------------|------------------|---------|
| <b>1</b>     | MEMA               | PMDETA           | DMF     |
| <i>ratio</i> | 200 <sup>[a]</sup> | 2 <sup>[a]</sup> | 50wt%   |
| <b>2</b>     | MEMA               | dNbpy            | Anisole |
| <i>ratio</i> | 200 <sup>[a]</sup> | 2 <sup>[a]</sup> | 50wt%   |

Reaction conditions: Initiator EBiB 0.01mmol, catalyst CuCl 0.01mmol, reactions carried on inert atmosphere for 18h at 60 °C, [a] mmol

The reaction was carried out in two different solvents in the presence of two different ligands: in DMF, in combination with *N,N',N'',N'''*-pentamethyl diethylene triamine (PMDETA) and anisole, in combination with 4,4'-dinonyl-2,2'-dipyridyl (dNbpy). Ethyl 2-bromoisobutyrate (EBiB) was used as initiator in all polymerizations, while CuCl was used as catalyst. Results achieved in preliminary polymeric experiments are reported in table 9.2.

**Table 9.2** - Analysis data for PMEMA

| Run | Conversion <sup>[a]</sup> | M <sub>n</sub> <sup>[b]</sup> | M <sub>w</sub> <sup>[b]</sup> | Đ    | Repeating units <sup>[c]</sup> |
|-----|---------------------------|-------------------------------|-------------------------------|------|--------------------------------|
| 1   | 47%                       | 18.400 Da                     | 34.400 Da                     | 1.87 | 172                            |
| 2   | 85%                       | 24.900 Da                     | 36.700 Da                     | 1.47 | 183                            |

[a] Calculated on isolate product [b] Calculated with GPC (THF), PMMA standards were used to calibrate the GPC system [c] Calculated on average M<sub>w</sub> of the polymer

In table 9.2 are reported molecular weights (M<sub>n</sub> and M<sub>w</sub>) determined by GPC analysis, conversions, and average repeating units of the final polymer calculated on average M<sub>w</sub> of the polymer. Both runs show a similar M<sub>w</sub>, and best performance was obtained with the second run showing higher conversion and polydispersity, producing more homogeneous PMEMA with a higher monomer conversion; thus further experiments were carried out in these way.

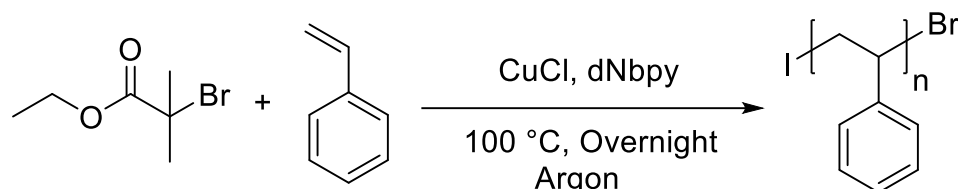
### 9.2.2 Synthesis of polystyrene-*b*-poly-2-*N*-morpholinoethyl methacrylate diblock copolymers (PS-*b*-PMEMA)

In the following section, the synthesis of diblock A-B copolymers formed by an A segment consisting of a polystyrene and a B segment consisting of a PMEMA will be discussed.

In general, diblock copolymers may be synthesized carrying out two ATRP polymerization in sequence. As explained in chapter 7.6, the ATRP polymerization leads to the shift of the

terminal halide present on the radical initiator along the growing polymer chain. In the final polymer the halogen atom, the bromine atom of ethyl 2-bromoisobutyrate, will be in terminal position, as in our case. This terminal bromine is also active towards a second polymerization reaction, allowing us to control the sequence of the blocks by simply varying the monomer for each polymerization step.

We started with the preparation of the A segment composed of polystyrene, the reaction scheme is shown below (scheme 9.3).



**Scheme 9.3** - Synthesis of polystyrene

The reaction was carried out in absence of solvent using CuCl as catalyst and dNbpy as ligand. Different syntheses were carried out in order to determine optimal polymerization condition. This was made by varying the molar ratios of the reactants as reported in table 9.3. Isolation of the polymer was performed by simple precipitation in methanol.

**Table 9.3** – Different reaction conditions adopted for the synthesis of polystyrene

| Run | Styrene(mmol) | CuCl(mmol) | dNbpy(mmol) | Reaction time |
|-----|---------------|------------|-------------|---------------|
| 1   | 20            | 0.025      | 0.055       | 18 h          |
| 2   | 1             | 0.01       | 0.02        | 16 h          |
| 3   | 10            | 0.01       | 0.02        | 24 h          |

Reaction conditions: EBiB 0.01mmol, reactions carried in Argon atmosphere at 100 °C

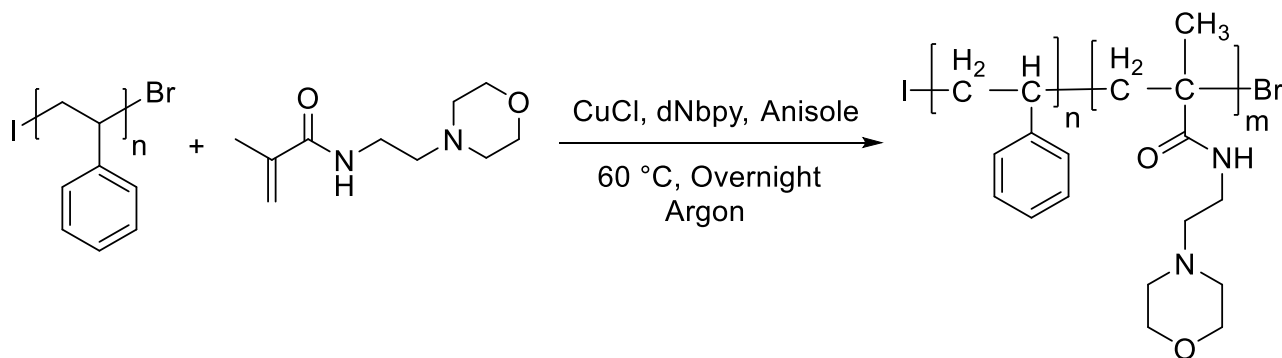
Table 9.4 shows the results obtained in various runs. In the first experiment, where a large excess of styrene was used, we obtained a much heavier polymer compared to the others. The two polymers recovered from second and third runs are comparable in terms of molecular weight and polydispersity, showing much better polydispersity compared to first run.

**Table 9.4** – Molecular weight, polydispertion and conversion of polystyrene in different reaction conditions.

| Run | $M_n^{[a]}$ | $M_w^{[a]}$ | $M_n/M_w^{[a]}$ | Conversion <sup>[b]</sup> | Styr. r.u. <sup>[c]</sup> |
|-----|-------------|-------------|-----------------|---------------------------|---------------------------|
| 1   | 64.300 Da   | 94.100 Da   | 1.46            | 70 %                      | 904                       |
| 2   | 7.800 Da    | 8.300 Da    | 1.12            | 54 %                      | 80                        |
| 3   | 10.100 Da   | 12.200 Da   | 1.11            | 76 %                      | 117                       |

[a] Calculated with GPC (THF), PMMA standards were used to calibrate the GPC system [b] Calculated on isolate product [c] Styrene repeating units, calculated on average  $M_w$  of the polymer.

Then, the synthesis of the second B segment consisting of PMEMA was carried out (Scheme 9.4).

**Scheme 9.4** - Synthesis of polystyrene-*b*-[poly-2-*N*-morpholinoethyl methacrylate] deblock copolymer

The reaction was carried out in anisole, using CuCl as catalyst and dNbpy as ligand. Several experiments were performed varying the molar ratio of the reactants in order to optimize reaction conditions (Table 9.5). The isolation of the polymer from the reaction mixture was performed by precipitation in hexane.

**Table 9.5** – Molar ratio for the synthesis of PS-*b*-PMEMA

| Run | MEMA(mmol) | CuCl (mmol) | dNbpy(mmol) | Reaction time |
|-----|------------|-------------|-------------|---------------|
| 1   | 10         | 0.025       | 0.055       | 18 h.         |
| 2   | 10         | 0.05        | 0.11        | 18 h.         |
| 3   | 10         | 0.025       | 0.055       | 24 h          |
| 4   | 10         | 0.025       | 0.055       | 12 h          |
| 5   | 10         | 0.025       | 0.055       | 24 h          |
| 6   | 10         | 0.025       | 0.055       | 12 h          |
| 7   | 2          | 0.025       | 0.055       | 18 h.         |

Reaction conditions: PS-Br 0.01mmol, reactions carried in Argon atmosphere at 60 °C and 50wt% Anisole as solvent

In table 9.6 are reported the results achieved in the various polymerization experiments performed starting from PS block of 94.100 Da (■), 12.200 Da (■), and 8.300 Da (■), synthesized as reported in section 9.2.1. On average we obtained block polymers with a  $M_w$  ranging from 150.000 Da to 200.000 Da, except for one case (run 5) where a different molar ratio of the reagents was used, obtaining a lower  $M_w$  (90.600 Da). The polydispersity varied between 1.3 and 1.8, in all cases higher than the starting block. When PS segments with high  $M_w$  were used (94.100 Da, runs 1 and 2), very low monomer conversions were measured, resulting in a modest PMEMA segment compared to the PS segment.

**Table 9.6** - Analysis data for PS-*b*-PMEMA

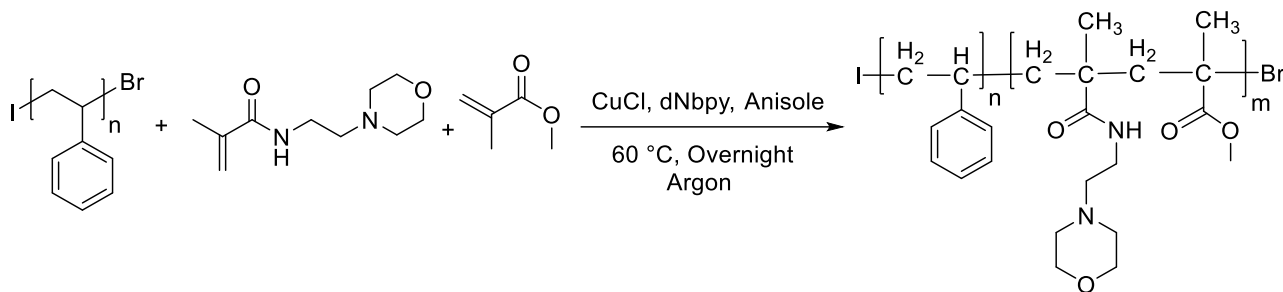
| Run | M <sub>n</sub> <sup>[a]</sup> | M <sub>w</sub> <sup>[a]</sup> | M <sub>n</sub> /M <sub>w</sub> <sup>[a]</sup> | Conversion <sup>[b]</sup> | PS r.u. <sup>[c]</sup> | MEMA r.u. <sup>[d]</sup> |
|-----|-------------------------------|-------------------------------|---|---------------------------|------------------------|--------------------------|
| 1   | 92.500 Da                     | 142.000 Da                    | 1.53  | 19 %                      | 904                    | 518                      |
| 2   | 108.000 Da                    | 197.700 Da                    | 1.82  | 28 %                      | 904                    | 667                      |
| 3   | 142.900 Da                    | 239.700 Da                    | 1.63  | 58 %                      | 117                    | 1137                     |
| 4   | 116.000 Da                    | 168.200 Da                    | 1.44  | 41 %                      | 117                    | 780                      |
| 5   | 124.200 Da                    | 199.000 Da                    | 1.60  | 47 %                      | 80                     | 953                      |
| 6   | 111.000 Da                    | 171.600 Da                    | 1.54  | 50 %                      | 80                     | 816                      |
| 7   | 67.600 Da                     | 90.600 Da                     | 1.34  | 69 %                      | 80                     | 411                      |

■ Starting from PS block of 94 100 Da, 
 ■ Starting from PS block of 12 200, 
 ■ Starting from PS block of 8 300 Da, 
 [a] Calculated with GPC (THF), PMMA standards were used to calibrate the GPC system [b] Calculated on isolate product [c] PS repeating units[d] MEMA repeating units, calculated on average M<sub>w</sub> of the polymer.

### 9.2.3 Synthesis of polystyrene-*b*-[poly-2-*N*-morpholinoethyl methacrylate-co-polymethyl methacrylate] diblock copolymer (PS-*b*-(PMEMA-co-PMMA))

The possibility to synthesize a diblock copolymer consisting in a polystyrene A-block and a copolymer B-block composed of a 1:1 ratio of 2-*N*-morpholinoethyl methacrylate and methyl methacrylate (MMA) was further investigated. This choice was made with the purpose of reducing the content of morpholino residues along the chain respect PS-*b*-PMEMA. In fact, from the experience we have acquired in the synthesis of MoPALA-CC and MoPALA-MMT TQACs, we have understood that hindered morpholines have difficulty in reacting with dichlorotriazines. Therefore, the our idea was that using a chain containing less morpholine residues could help the subsequent quaternization process.

Below is reported the scheme of the synthesis of polystyrene-*b*-[poly-2-*N*-morpholinoethyl methacrylate-co-polymethylmethacrylate] (PS-*b*-(PMEMA-co-PMMA)) (scheme 9.5).



**Scheme 9.5** - Synthesis of polystyrene-*b*-[poly-2-*N*-morpholinoethyl methacrylate-*co*-polymethyl methacrylate] diblock copolymer

The reaction was carried out using 0.01 mmol of PS starting block copolymer (8.300 Da), 2 mmol of MEMA, 2 mmol of MMA, 0.025 mmol of CuCl as catalyst and 5.5 mmol of dNbpy as ligand in anisole 75%wt in inert atmosphere at 60 °C for 18h. Isolation of the polymer from the reaction environment was performed by precipitation in hexane. The result of the polymerization is a polymer with a  $M_w$  value around 126.300 Da with a polydispersity of 1.35. The conversion of the monomer is around 74%, calculated from the weight isolate product. Since the reactivity towards radical polymerization of MMA and MEMA are similar, we can consider the average repeating unit of block B consisting of one unit of MMA and one unit of MEMA. The resulting (PS-*b*-(PMEMA-*co*-PMMA)) diblock copolymer obtained starting from PS block of 8.300 Da (■) show a monomer conversion of 74% calculated from the weight of the isolated product. The GPC analysis showed a polymer having  $M_n$ : 93 000 Da,  $M_w$ : 126 300 Da,  $M_n/M_w$ :1.35, average styrene repeating units: 80, average MEMA-MMA repeating units: 393 calculated on average  $M_w$  of the polymer.



### 9.2.4 Synthesis of polystyrene-*b*-poly-2-*N*-morpholinoethyl methacrylate-*b*-polystyrene triblock copolymers (PS-*b*-PMEMA-*b*-PS) and polystyrene-*b*-[poly-2-*N*-morpholinoethyl methacrylate-co-polymethyl methacrylate]-*b*-polystyrene triblock copolymer (PS-*b*-(PMEMA-co-PMMA)-*b*-PS)

The preparation of some triblock copolymers consisting in A-B-A structure was also investigated. The preparation of these structures was done with the aim of improving the surface adhesion of the polymer which, having two blocks capable of physisorption on the polypropylene films, should ensure greater adhesion than polymers having only one PS block (Figures 9.3).

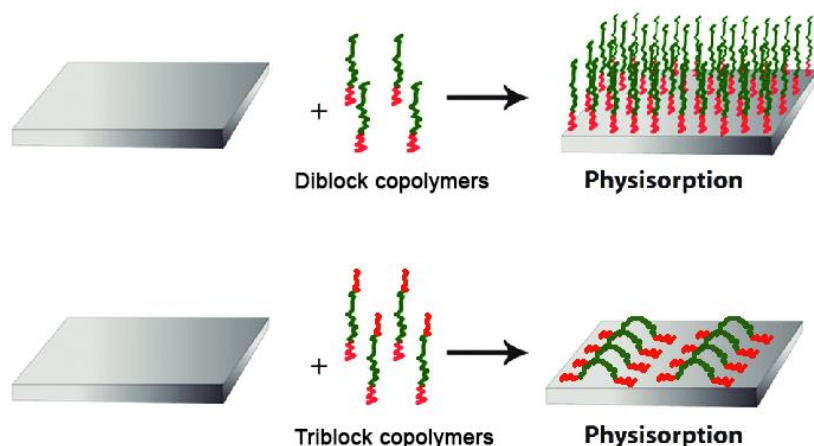
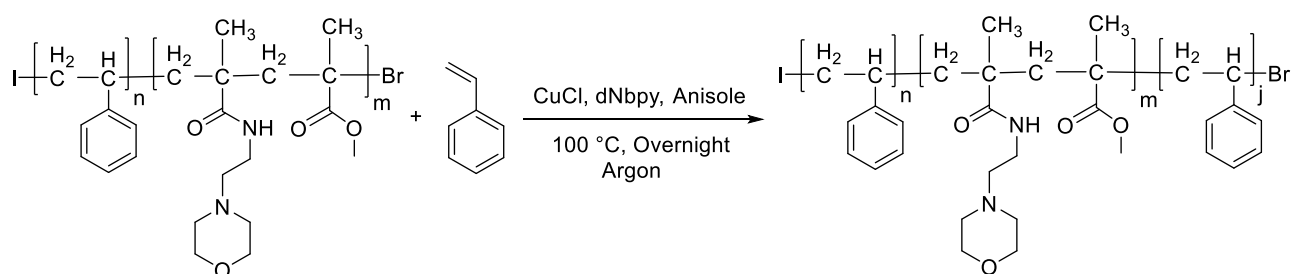


**Figure 9.3** – Representation of different surface physisorption of diblock copolymers and triblock copolymers

The synthesis of polystyrene-*b*-poly-2-*N*-morpholinoethyl methacrylate-*b*-polystyrene triblock copolymers (PS-*b*-PMEMA-*b*-PS) and polystyrene-*b*-[poly-2-*N*-morpholinoethyl methacrylate-co-polymethyl methacrylate]-*b*-polystyrene triblock copolymer (PS-*b*-(PMEMA-co-PMMA)-*b*-PS) is reported in schemes 9.6 and 9.7.



**Scheme 9.6** - Synthesis of polystyrene-*b*-[poly-2-*N*-morpholinoethyl methacrylate]-*b*-polystyrene triblockcopolymer



**Scheme 9.7** - Synthesis of polystyrene-*b*-[poly-2-*N*-morpholinoethyl methacrylate-*co*-polymethylmetacrilate]-*b*-polystyrene triblockcopolymer

The syntheses were conducted in anisole using CuCl as the catalyst and dNbpy as ligand. The reaction molar ratios are given in Table 9.7. In Run 1 and 2, PS-*b*-MEMA from 171 600 Da block copolymer was used as starting block copolymer in order to obtain the corresponding PS-*b*-PMEMA-*b*-PS, while in run 2, PS-*b*-(PMEMA-*co*-PMMA) was used as the starting polymer in order to obtain the corresponding PS-*b*-(PMEMA-*co*-PMMA)-*b*-PS.

**Table 9.7**– Molar ratio for the synthesis of PS-*b*-PMEMA-*b*-PS (Run 1) and PS-*b*-(PMEMA-*co*-PMMA)-*b*-PS (Run 2).

| Run | Styrene | CuCl | dNbpy |
|-----|---------|------|-------|
| 1   | 10      | 0.01 | 0.02  |
| 2   | 3       | 0.01 | 0.02  |
| 3   | 3       | 0.01 | 0.02  |

■ Starting from PS-MEMA block of 171 600 Da, ■ Starting from PS-(PMEMA-*co*-PMMA) block of 126 300 Da, Reaction condition: Starting block 0.01 mmol, reaction carried in Argon atmosphere for 24h at 100°C in anisole 75%wt

Results of the two polymerization reactions are reported in table 9.8. In the first run, for the synthesis of PS-*b*-PMEMA-*b*-PS, a large excess of styrene was used which led to the formation of a heavy PS end section. In fact, the final product turned out to have a  $M_w$  around 300.000 Da, with final polystyrene fraction of about 1200 repeating units. We have therefore decreased the amount of styrene to try to obtain a second block of PS with a length comparable to the first one. In the second run we therefore obtained a lower molecular weight product, having the initial and final PS segments of similar size. In the third run, which represents the synthesis of PS-*b*-(PMEMA-*co*-PMMA)-*b*-PS triblock copolymer, the same ratios were used as in run 2, obtaining a comparable result.

**Table 9.8** - Analysis data for PS-*b*-(PMEMA-*co*-PMMA)

| Run | $M_n$ <sup>[a]</sup> | $M_w$ <sup>[a]</sup> | $M_n/M_w$ <sup>[a]</sup> | Conversion <sup>[b]</sup> | PS r.u. <sup>[c]</sup> | MEMA r.u. <sup>[d]</sup> |
|-----|----------------------|----------------------|--------------------------|---------------------------|------------------------|--------------------------|
| 1   | 196.600 Da           | 299.000 Da           | 1.52                     | 51 %                      | 1308                   | 816                      |
| 2   | 123.200 Da           | 180.200 Da           | 1.46                     | 71 %                      | 166                    | 816                      |
| 3   | 94.400 Da            | 132.700 Da           | 1.40                     | 73 %                      | 142                    | 393                      |

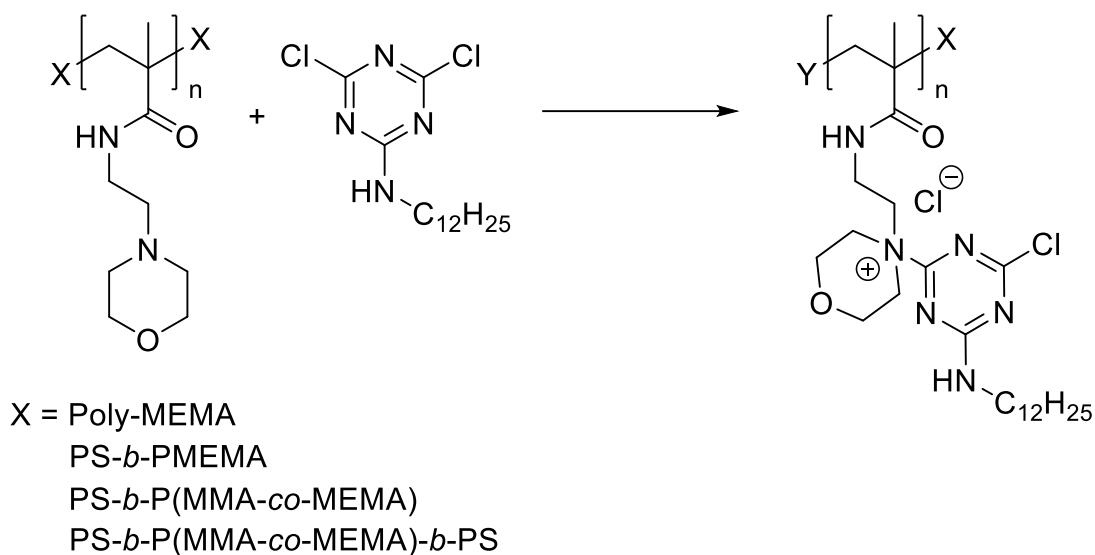
■ Starting from PS-MEMA block of 171 600 Da, ■ Starting from PS-(PMEMA-*co*-PMMA) block of 126 300 Da [a] Calculated with GPC (THF), PMMA standards were used to calibrate the GPC system [b] Calculated on isolate product [c] Repeating units of the two PS block [d] MEMA repeating units, calculated on average  $M_w$  of the polymer.

### 9.3 Synthesis of polymeric TQACs

In this chapter, the use of MAT<sub>12</sub> as a chloro-1,3,5-triazine derivative for the quaternization of morpholine residues of the various polymer chains obtained, will be discussed. The choice of MAT<sub>12</sub> was made taking into account both the presence of the alkyl side chain (an essential criterion for the antimicrobial activity) and the reactivity of dichloro triazine species towards morpholines moieties. In fact, according to the results obtained from the antimicrobial tests on MATdMIMI and also according to data reported in the literature<sup>[109-112]</sup>, the QACs having a side chain between 12 and 14 carbons units are those with the highest performance in terms of

antimicrobial activity. Moreover, on the basis of the experience gained with the synthesis of MoPALA-CC and MoPALA-MMT, we realized that it was essential to use a chlorotriazine having two or three chlorine atoms for quaternization of hindered morpholines.

Several quaternization reactions were performed (Scheme 9.8) with different polymers and different reaction conditions (Table 9.9). In many cases an extremely compact and insoluble polymer was obtained.



**Scheme 9.8** – General scheme of quaternization of MEMA units in various block copolymers

An excess of MAT<sub>12</sub> was used in all tests. This should disfavor cross-linking by creating an environment with low free morpholino residues. Anhydrous solvents and inert atmosphere reactions were also used in some trials. Despite many trials, the only product that resulted soluble was the polymer obtained in run 6 where PS-*b*-(PMEMA-*co*-MMA)-*b*-PS was used.

The latter appears as a fine yellow powder, soluble in polar solvents such as DMSO or H<sub>2</sub>O/THF mixtures (20/80). Figure 9.5 shows the polymer in the various synthetic steps from the first synthesis of PS block A until quaternization with MAT<sub>12</sub>.

Dichloro triazine like MAT<sub>12</sub>, as we have seen in the first part of the thesis, easily lead to the formation of a bis-TQACs. This behavior, discussed extensively in Sections 3.2.4 and 3.3.4, is difficult to control, and is complicated to manage in order to obtain mono TQACs. The obtaining of insoluble products can be explained as the ease of both chlorine residues of MAT<sub>12</sub> to react.

In fact, MAT<sub>12</sub> can lead to the formation of cross-linking bonds between chains, leading to the formation of an extremely hard and insoluble material (Figure 9.4).

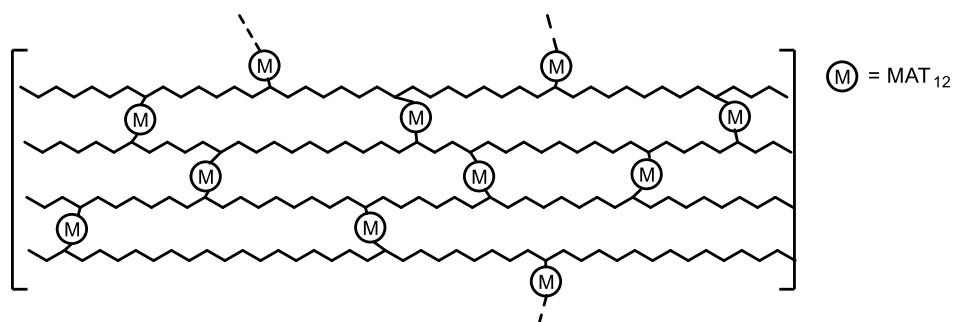


**Figure 9.4** - Crosslinking action of MAT<sub>12</sub>

**Table 9.9** – Experimental condition for synthesis of polymeric TQACs

| Run              | Starting polymer                                    | M <sub>w</sub> <sup>[b]</sup> | Temperature | Solvent                | Time  | Solubility                   |
|------------------|---|-------------------------------|-------------|------------------------|-------|------------------------------|
| 1                | PMEMA   | 36.600 Da                     | 25 °C       | Acetone                | 1.5 h | Insoluble                    |
| 2                | PMEMA   | 36.600 Da                     | -12 °C      | Acetone                | 1.5 h | Insoluble                    |
| 3 <sup>[a]</sup> | PMEMA   | 36.600 Da                     | -94 °C      | THF <sup>[c]</sup>     | 10 h  | Insoluble                    |
| 4 <sup>[a]</sup> | PS- <i>b</i> -PMEMA                                 | 171.600 Da                    | -94 °C      | THF <sup>[c]</sup>     | 10 h  | Insoluble                    |
| 5 <sup>[a]</sup> | PS- <i>b</i> -(PMEMA- <i>co</i> -MMA)               | 126.300 Da                    | -10 °C      | Acetone <sup>[c]</sup> | 2 h   | Insoluble                    |
| 6 <sup>[a]</sup> | PS- <i>b</i> -(PMEMA- <i>co</i> -MMA)- <i>b</i> -PS | 132.700 Da                    | 0 °C        | THF <sup>[c]</sup>     | 5 h   | H <sub>2</sub> O/THF<br>DMSO |

[a] Reaction carried out in inert atmosphere using 1:5 ratio of MEMA/MAT<sub>12</sub>, [b] M<sub>w</sub> of starting polymer [c] Anhydrous solvent

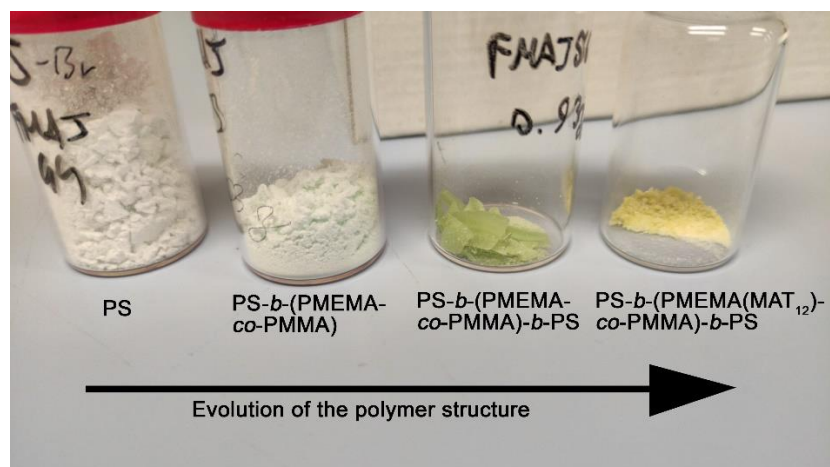


**Figure 9.5** – Synthetic steps in the formation of polymeric TQACs

The polymer obtained from run 6 was characterized by  $^1\text{H}$  NMR (Figure 9.6) using COSY for peak assignment, resulting in polystyrene-*b*-[4-(4-chloro-6-(dodecylamino)-1,3,5-triazin-2-yl)-4-(2-methacrylamidoethyl) morpholin-4-ium chloride-co-polymethylmethacrylate]-*b*-polystyrene triblock copolymer (PS-*b*-(PMAT<sub>12</sub>MEMA-co-PMMA)-*b*-PS). The degree of quaternization of the morpholino groups was calculated to be 81% from the weight of the isolated product, and 79% from the NMR spectrum.

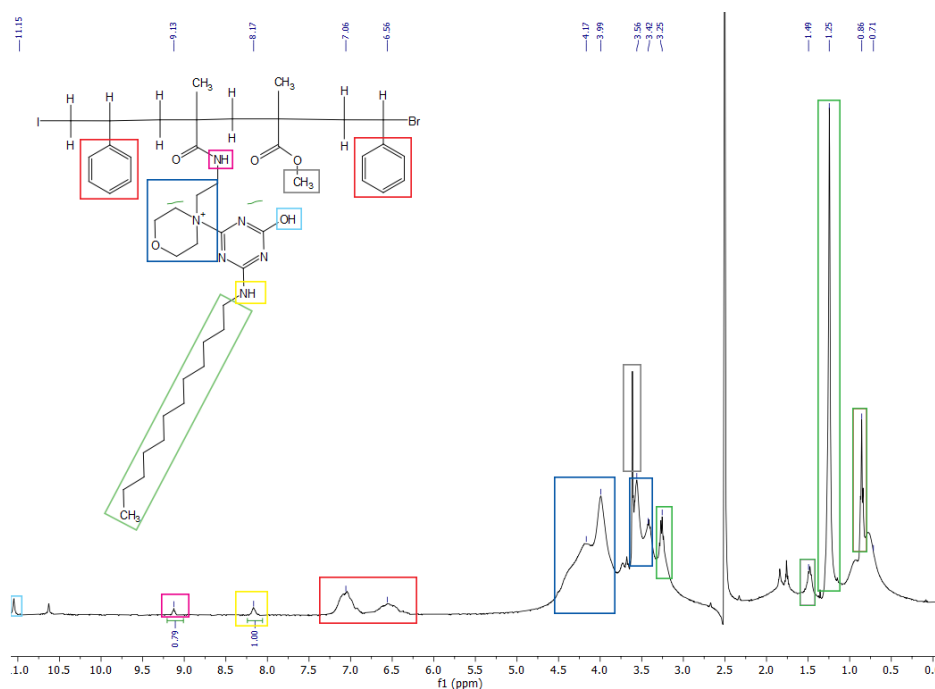


**Figure 9.6** –  $^1\text{H}$  NMR spectrum of (PS-*b*-(PMAT<sub>12</sub>MEMA-co-PMMA)-*b*-PS)

In  $^1\text{H}$  NMR spectrum of (PS-*b*-(PMAT<sub>12</sub>MEMA-*co*-PMMA)-*b*-PS) following relevant signals have been assigned: at 0.86 ppm the signal of the terminal methyl of the long alkyl chain ( $\text{CH}_2\text{CH}_3$ ), at 1.25 ppm the signal corresponds to the nine central  $\text{CH}_2$  groups present on the chain ( $\text{CH}_2(\text{CH}_2)_9\text{CH}_3$ ), at 1.49 ppm the signal of  $\text{CH}_2$  of the alkyl chain in  $\beta$  position to the terminal amine ( $\text{HNCH}_2\text{CH}_2\text{CH}_2$ ), at 3.25 ppm the signal of the  $\text{CH}_2$  of the alkyl chain in  $\alpha$  position to the terminal amine ( $\text{HNCH}_2\text{CH}_2$ ), at 3.42 the signal of  $\text{CH}_2$  in  $\alpha$  to the oxygen of the morpholino ring ( $\text{CH}_2\text{OCH}_2$ ), at 3.52 ppm the signal of the  $\text{CH}_2$  belonging to MMA ester ( $\text{OCH}_3$ ). At 3.99 and 4.17 there are two broad signals that belong to the  $\text{CH}_2$  in  $\alpha$  to the nitrogen of morpholino ring ( $\text{CH}_2\text{N}^+(\text{CH}_2)_2$ ) and the  $\text{CH}_2$  of the ethyl chain of MEMA in  $\alpha$  to the nitrogen ( $\text{CH}_2\text{CH}_2\text{N}^+(\text{CH}_2)_2$ ), signals at 6.56 and 7.06 ppm are due to the aromatic residues of polystyrene (**Ar**), at 8.17 ppm falls the signal of the amide hydrogen of MEMA (**NH**) while at 9.13 falls the signal of the amine hydrogen belonging to the alkyl chain linked to the triazine ring (**NH**). The latter two signals were used as a reference to calculate the degree of quaternization. Finally, at 11.15 ppm the signal corresponds to an OH indicating that the second chloride of the triazine ring was hydrolyzed during the reaction.

#### 9.4 Polypropylene film surface modification with (PS-*b*-(PMAT<sub>12</sub>MEMA-*co*-PMMA)-*b*-PS) triblock copolymer

The deposition on a surface of a polypropylene (PP) film of the PS-*b*-(PMAT<sub>12</sub>MEMA-*co*-PMMA)-*b*-PS was then investigated. The deposition was done dispersing with an airbrush 25 mL solutions of  $\text{H}_2\text{O}/\text{THF}$  containing 100mg, 50mg, 25mg, 12.5mg of PS-*b*-(PMAT<sub>12</sub>MEMA-*co*-PMMA)-*b*-PS, respectively. A4 size polypropylene sheets (210x297 mm, 623.7  $\text{cm}^2$ , 28.25 g) were used as the surface.

Successful deposition was investigated using dyne tests to assay the change in surface tension between the untreated and modified PP films (figure 9.7).

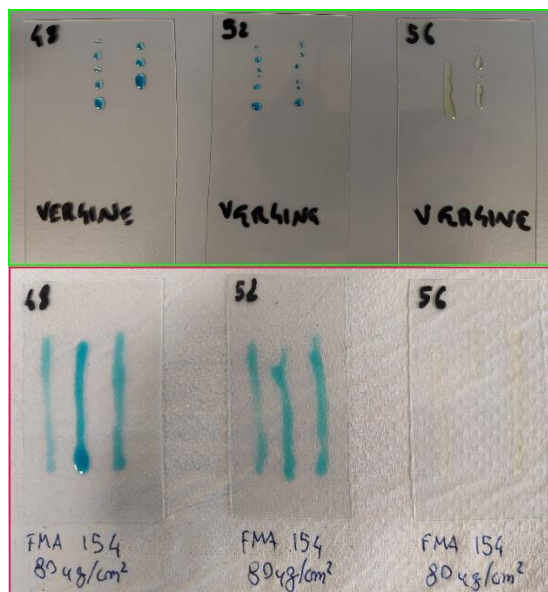


**Figure 9.7** – Dyne test for surface tension assay, top virgin polypropylene film, bottom modified polypropylene film

As shown in figure 9.7 the dyne test is an experiment where liquid mixtures of known surface tension are used to determine the level of adhesion of a liquid to a plastic surface or other materials. The formation of droplets after a few seconds indicates that the surface has a lower surface tension than the liquid.

As shown in Table 9.10 the dyne tests were performed on both untreated and modified PP surfaces. It can be seen that in all tests the surface tension of the modified surfaces is always higher than the starting one, and this behavior remains unchanged also after ultrasonic washing. The washing tests were performed with the scope to preliminarily verifying how sensitive the deposited polymeric TQACs was to leaching. According to the tests there seems to be no appreciable difference between washed and unwashed samples.



**Table 9.10** – Dyne test for surface modified PP foil.

| Dyne | Virgin PP | 100mg <sup>[a]</sup> | 100mg <sup>[a,b]</sup> | 50mg <sup>[a]</sup> | 50mg <sup>[a,b]</sup> | 25mg <sup>[a]</sup> | 25mg <sup>[a,b]</sup> | 12.5mg <sup>[a]</sup> | 12.5mg <sup>[a,b]</sup> |
|------|-----------|----------------------|------------------------|---------------------|-----------------------|---------------------|-----------------------|-----------------------|-------------------------|
| 48   | ✗         | ✓                    | ✓                      | ✓                   | ✓                     | ✓                   | ✓                     | ✓                     | ✓                       |
| 52   | ✗         | ✓                    | ✓                      | ✓                   | ✓                     | ✓                   | ✓                     | ✓                     | ✓                       |
| 56   | ✗         | ✓                    | ✓                      | ✓                   | ✓                     | ✓                   | ✓                     | ✓                     | ✓                       |

[a] Amount of deposited sample in an A4 sheet of polypropylene [b] Washed with water in ultrasonic bath for 20 min, ✓ = Higher wettability ✗ = Lower wettability

## 9.5 Polypropylene modified surface antibiofilm evaluation

The films obtained as above described, were used for biological investigations. Biofilm inhibition tests were performed using strains of *Staphylococcus aureus* as Gram-positive bacteria and *Escherichia coli* as Gram-negative bacteria. Tests were performed by immersing a film sample in an inoculated culture broth to promote bacterial growth and biofilm formation on the surface of the sample. Upon completion of growth, cells that remained adhered to the surface were detached using an ultrasonic bath by re-immersing the sample in fresh liquid medium. The resulting liquid from sonication was then plated at various dilutions in order to perform microbial count.

The results of the inhibition tests are reported in Table 9.11 as  $\text{Log}_{10}(\text{CFU/mL})$ .

**Table 9.11** – Biofilm inhibition tests of modified PP surfaces

| <i>Staphylococcus aureus</i> <sup>[a]</sup> |                               |      | <i>Escherichia coli</i> <sup>[b]</sup> |                               |      |
|---|-------------------------------|------|--|-------------------------------|------|
| Sample                                      | Log <sub>10</sub> (c.f.u./mL) | S.D. | Sample                                 | Log <sub>10</sub> (c.f.u./mL) | S.D. |
| Control (PP)                                | 8.22                          | 0.12 | Control (PP)                           | 7.6                           | 0.13 |
| 12.5 mg                                     | 7.69                          | 0.67 | 1.25 mg                                | 7,18                          | 0,27 |
| 12.5 mg <sup>[c]</sup>                      | 7.85                          | 0.41 | 12.5 mg <sup>[c]</sup>                 | 7,09                          | 0,32 |
| 25 mg                                       | 8.47                          | 0.14 | 25 mg                                  | 7,56                          | 0,39 |
| 25 mg <sup>[c]</sup>                        | 8.20                          | 0.31 | 25 mg <sup>[c]</sup>                   | 7,20                          | 0,19 |
| 50 mg                                       | 8.03                          | 0.10 | 50 mg                                  | 7.88                          | 0.22 |
| 50 mg <sup>[c]</sup>                        | 8.30                          | 0.14 | 50 mg <sup>[c]</sup>                   | 7.08                          | 0.39 |
| 100 mg                                      | 7.62                          | 0.23 | 100mg                                  | 7.35                          | 0.12 |

[a] CECT 59 [b] CECT 434 [c] Washed with water in ultrasonic bath for 20 min

In many of the tests performed, there was no significant reduction. Data in table 9.11 show in some cases, samples in which a smaller amount of deposited TQACs had a higher abatement. This could be attributed to the poor control of polymer deposition on the surface, generating non-homogeneous dispersion of TQACs on the surface. In any case, total abatement was never found, even in the highest concentration samples. It is not clear if this fact is due to an insufficient concentration of TQACs on the surface or if it is due to the low antimicrobial activity of the polymer itself or other phenomena. Unfortunately, it was not possible to evaluate the MIC of the isolated TQACs polymer in solution because of its insolubility in the biological media where bacteria grow.

Further investigations are ongoing to improve the performance of polymer dispersion and film deposition to achieve better performing inhibition surfaces.

## **CHAPTER 10**

### **CONCLUSIONS**

**Polymeric QACs synthesis and surface adhesion  
treatments**

The research in this part of the Ph.D. thesis has focused on the familiarization of living radical polymerization techniques. Several protocols were developed in the synthesis of various block copolymers containing morpholino groups and their quaternarization with chloro-triazines to produce polymeric TQACs. Some polymeric TQACs were then used in the surface functionalization of polypropylene sheets and evaluated in biofilm inhibition tests.

The main results obtained were:

- Optimization of the catalytic system and conditions for PMEMA synthesis
- Development of different synthesis protocols for the production of block copolymers based on styrene, 2-*N*-morpholyethyl methyl methacrylate and methyl methacrylate with different molecular weights with low polydispersity.
- Production of polymeric TQACs by post-polymerization quaternization of morpholino residues in various block copolymers containing 2-*N*-morpholioethyl methyl methacrylate.
- Surface functionalization of polypropylene sheets with polymeric TQACs
- Biological evaluation of polypropylene surface samples functionalized with TQACs in the inhibition of biofilm formation.

Future investigations on the surface adhesion and antibiofilm activity of polymeric TQACs will be necessary to better understand the mechanisms of biofilm inhibition for encourage further development of these technologies.

# **CHAPTER 11**

## **EXPERIMENTAL SECTION**

**Polymeric QACs synthesis and surface adhesion**

## 11.1 Methods and instrumentation

Methyl methacrylate (MMA, 98%), copper(I) chloride (CuCl, 99.9%), 4,4'-dinonyl-2,2'-dipyridyl (dNbpy, 97%) Iodomethane (MeI 99.5%) were purchased from Wako Pure Chemicals, Osaka, Japan. Ethyl 2-bromoisobutyrate (EBiB, 98%) were obtained from Tokyo Chemical Industry, Tokyo, Japan. Styrene (S, 99%) were received from Nacalai Tesque Inc., Osaka, Japan, N,N,N',N'',N''-pentamethyldiethylenetriamine (PMDETA; 99%), 2-N-Morpholinoethyl methacrylate (MEMA, 95%) were purchased from Sigma-Aldrich, St. Louis, Missouri, USA.

Gel permeation chromatography (GPC) analyses using tetrahydrofuran (THF) as an eluent at a flow rate of 0.8 mL/min were carried out at 40 °C on a Shodex GPC-101 highspeed liquid chromatography system equipped with a guard column (Shodex GPC KF-G), two 30 cm mixed columns (Shodex GPC LF-806, exclusion limit =  $1.5 \times 10^7$ ), and a differential refractometer (Shodex RI-71S). PS standards were used to calibrate the GPC system. This system was used for characterization of poly styrene (PS), poly-MEMA(PMEMA), PS-*b*-PMEMA, PS-*b*-MEMA-*b*-PS, PS-*b*-P(MMA-co-MEMA), PS-*b*-P(MMA-co-MEMA)-*b*-PS.

<sup>1</sup>H-NMR and <sup>13</sup>C-NMR spectra were recorded on a JNM-ECA600 (JEOL, Tokyo, Japan) spectrometer operating at frequency of 600.00 MHz and Bruker UltraShield 400 operating at frequency of 400.00 MHz for the proton and 101.00 MHz for carbon with tetramethylsilane as an internal standard

## 11.2 Reagents and solvents used

### Solvents

- Acetone
- Acetonitrile
- Anisole
- Dichloromethane

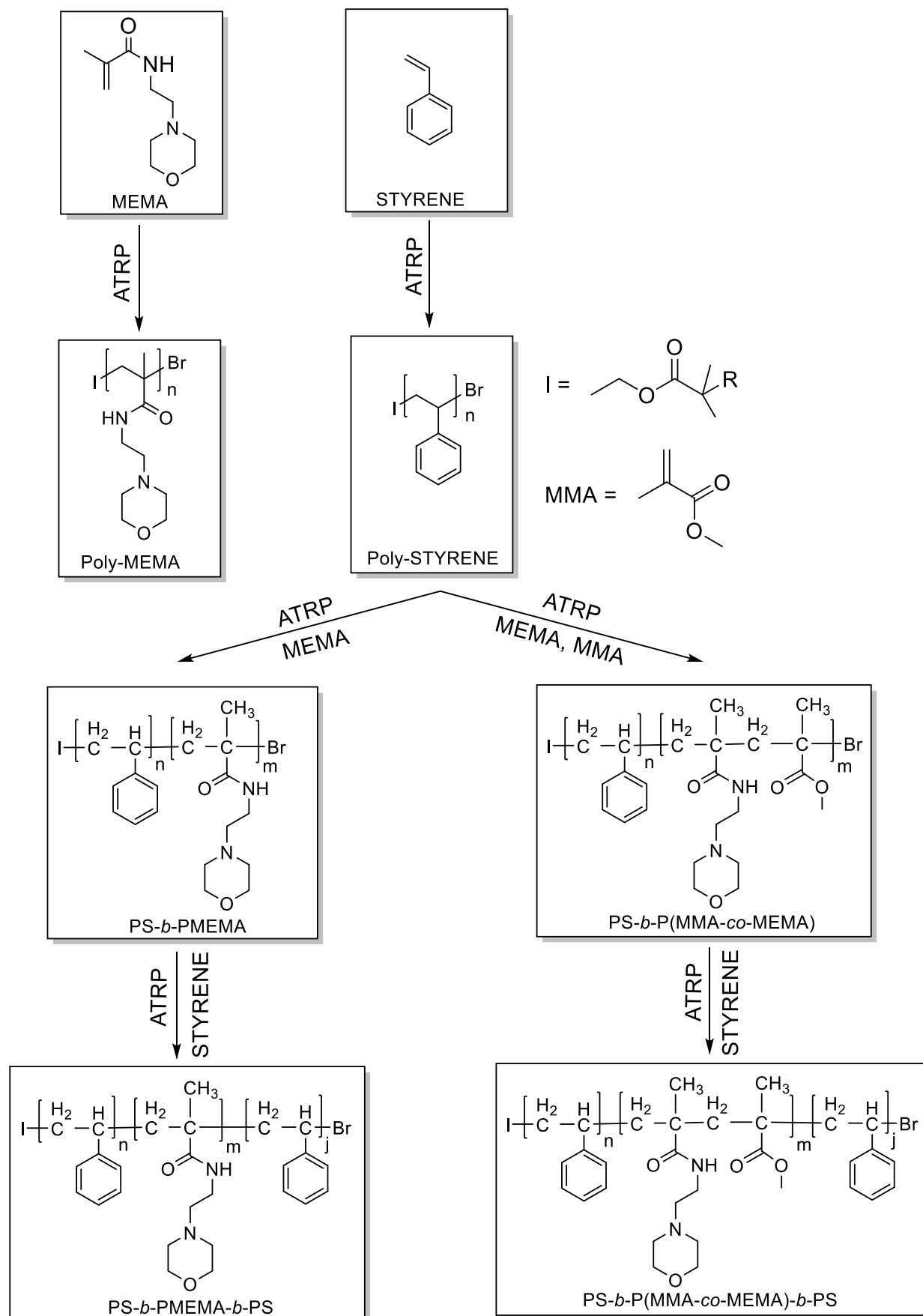
- Dimethylformamide
- Dimethylsulfoxide
- Hexane
- Methanol
- Tetrahydrofuran

### Reagents

- 2-*N*-Morpholinoethyl methacrylate
- 4,4'-dinonyl-2,2'-dipyridyl
- Copper(I) chloride
- Ethyl 2-bromoisobutyrate
- Iodomethane
- MAT<sub>12</sub>
- Methyl methacrylate
- N,N,N',N'',N'''-pentamethyldiethylenetriamine
- Styrene

## 11.3 Atom transfer radical polymerization (ATRP) polymers synthesis and characterization

A general scheme is reported below for the synthesis of various polymers and block-copolymers exploiting the atom transfer radical polymerization reaction using styrene, methylmetacrilate and 2-*N*-morpholinoethyl methacrylate as monomers (scheme 11.1).

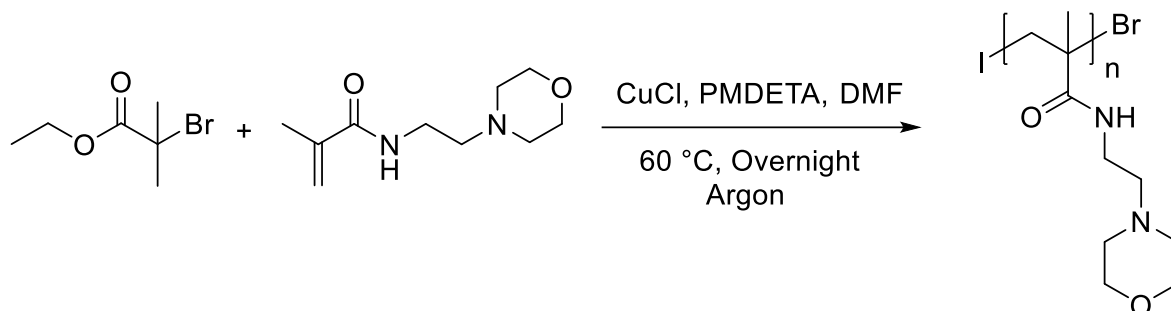




**Scheme 11.1** – General scheme of polymers synthesis

### 11.3.1 Synthesis of poly-2-*N*-morpholinoethyl methacrylate (PMEMA)

In DMF:



**Scheme 11.2** - Synthesis of poly-2-*N*-morpholinoethyl methacrylate in DMF

Into a test tube fitted with a ground neck are introduced; 10 mg (0.051 mmol) of ethyl 2-bromoisobutyrate (EBiB), 2043 mg (10.25 mmol) of 2-*N*-Morpholinoethyl methacrylate (MEMA), 17.74 mg (0.102 mmol) of *N,N',N'',N'''*-pentamethyldiethylenetriamine (PMDETA) and 2 g of DMF. Some argon is then allowed to flux within the solution using a needle for 5 minutes. Within a glove-box, 5.07 mg (0.051 mmol) of CuCl is then withdrawn and poured into the solution under argon flow. The solution is then sealed with a cap and allowed to react overnight at 60 °C in an oil bath equipped with a tilting plate. The resulting polymer is recovered using a dialysis bag (3.5 kDa cut off) in water. The polymer is recovered by solvent removal and drying in a high vacuum oven at 60 °C.

Conversion (isolated product): 47%

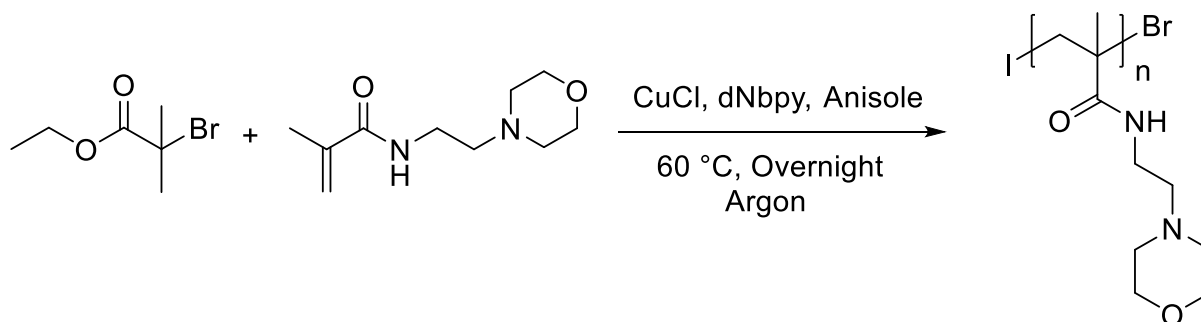
GPC analysis (THF):  $M_n$ : 18 400 Da

$M_w$ : 34 400 Da

Polydispersity ( $M_n/M_w$ ): 1.87

MEMA repeating units: 172

In anisole:



**Scheme 11.3** - Synthesis of poly-2-*N*-morpholinoethyl methacrylate in Anisole

Into a test tube fitted with a ground neck are introduced; 10 mg (0.051 mmol) of ethyl 2-bromoisobutyrate (EBiB), 2043 mg (10.25 mmol) of 2-*N*-Morpholinoethyl methacrylate (MEMA), 41.8 mg (0.102 mmol) of 4,4'-dinonyl-2,2'-dipyridyl (dNbpy) and 2.1 g of anisole. Some argon is then allowed to flow into the solution using a needle for 5 minutes. Within a glove-box, 5.0 mg (0.051 mmol) of CuCl is then withdrawn and poured into the solution under argon flow. The solution is then sealed with a cap and allowed to react overnight at 60 °C in an oil bath equipped with a tilting plate. The resulting polymer is recovered by precipitation in hexane, filtered, and dried in a high vacuum oven at 60 °C.

Conversion (isolated product): 85%

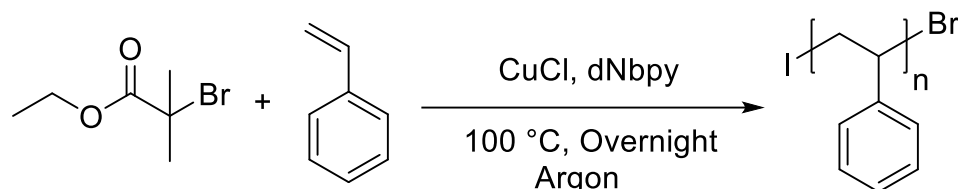
GPC analysis (THF): Mn: 24 900 Da

Mw: 36 700 Da

Polydispersity ( $M_n/M_w$ ): 1.47

MEMA repeating units: 183

### 11.3.2 Synthesis of polystyrene (PS)



**Scheme 11.4** - Synthesis of polystyrene

Into a test tube fitted with a ground neck are introduced; ethyl 2-bromoisobutyrate (EBiB), styrene and 4,4'-dinonyl-2,2'-dipyridyl (dNbpy) (see table 11.1 for quantities). Some argon is then allowed to flow into the solution using a needle for 5 minutes. Within a glove-box, CuCl is then withdrawn and poured into the solution under argon flow. The solution is then sealed with a cap and allowed to react overnight at 100 °C in an oil bath equipped with magnetic stirring. The resulting polymer is recovered by precipitation in methanol, filtered, and dried in a high vacuum oven at 60 °C.

**Table 11.1** – Experimental data for synthesis of polystyrene

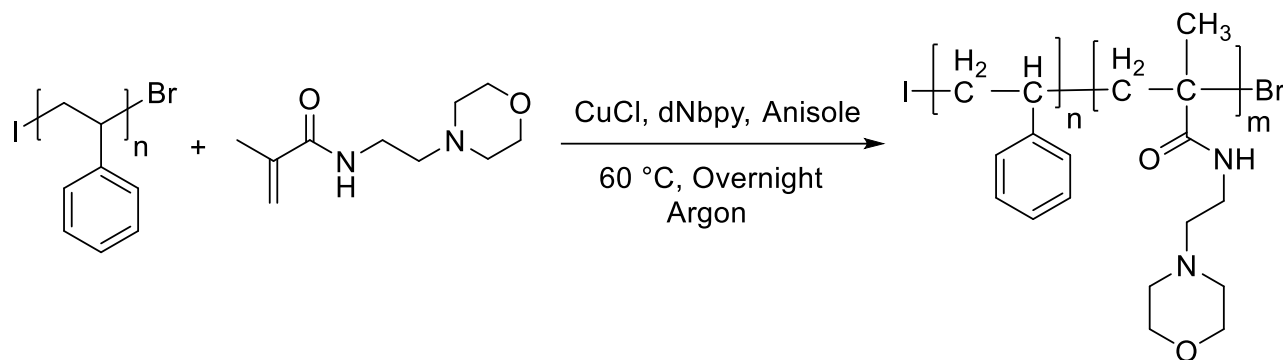
| <i>Run</i> | <i>EBiB</i>          | <i>dNbpy</i>          | <i>Styrene</i>        | <i>CuCl</i>          | <i>Reaction time</i> |
|------------|----------------------|-----------------------|-----------------------|----------------------|----------------------|
| 1          | 3.7 mg<br>0.019 mmol | 43.1 mg<br>0.105 mmol | 4000 mg<br>38.40 mmol | 4.7 mg<br>0.048 mmol | 18 h.                |
| 2          | 171 mg<br>0.88 mmol  | 726 mg<br>1.78 mmol   | 9253 mg<br>88.9 mmol  | 87.1 mg<br>0.88 mmol | 16 h                 |
| 3          | 56.5 mg<br>0.29 mmol | 236 mg<br>0.58 mmol   | 3000 mg<br>28.84 mmol | 28.7 mg<br>0.29 mmol | 24 h                 |

**Table 11.2** - Experimental analysis for synthesis of polystyrene.

| <i>Run</i> | $M_n^{[a]}$ | $M_w^{[a]}$ | $M_n/M_w^{[a]}$ | <i>Conversion</i> <sup>[b]</sup> | <i>Styr. r.u.</i> <sup>[c]</sup> |
|------------|-------------|-------------|-----------------|----------------------------------|----------------------------------|
| 1          | 64 300 Da   | 94 100 Da   | 1.46            | 70 %                             | 904                              |
| 2          | 7 800 Da    | 8 300 Da    | 1.12            | 54 %                             | 80                               |
| 3          | 10 100 Da   | 12 200 Da   | 1.11            | 76 %                             | 117                              |

[a] Calculated with GPC (THF), PS standards were used to calibrate the GPC system. [b] Conversion on isolate product. [c] Styrene repeating units

### 11.3.3 Synthesis of polystyrene-*b*-[poly-2-*N*-morpholinoethyl methacrylate] diblockcopolymer (PS-*b*-(PMEMA))



**Scheme 11.5** - Synthesis of polystyrene-*b*-[poly-2-*N*-morpholinoethyl methacrylate] diblockcopolymer

Into a test tube fitted with a ground neck are introduced; polystyrene with Br terminal group (PS-Br), 2-*N*-Morpholinoethyl methacrylate (MEMA) 4,4'-dinonyl-2,2'-dipyridyl (dNbpy) and 50% wt anisole (see table 11.3 for quantities). Some argon is then allowed to flow into the solution using a needle for 5 minutes. Within a glove-box, CuCl is then withdrawn and poured into the solution under argon flow. The solution is then sealed with a cap and allowed to react overnight at 60 °C in an oil bath equipped with a tilting plate. The resulting polymer is recovered by precipitation in hexane, filtered, and dried in a high vacuum oven at 60 °C.

**Table 11.3** – Experimental data for synthesis of polystyrene-*b*-[poly-2-*N*-morpholinoethyl methacrylate] diblockcopolymer

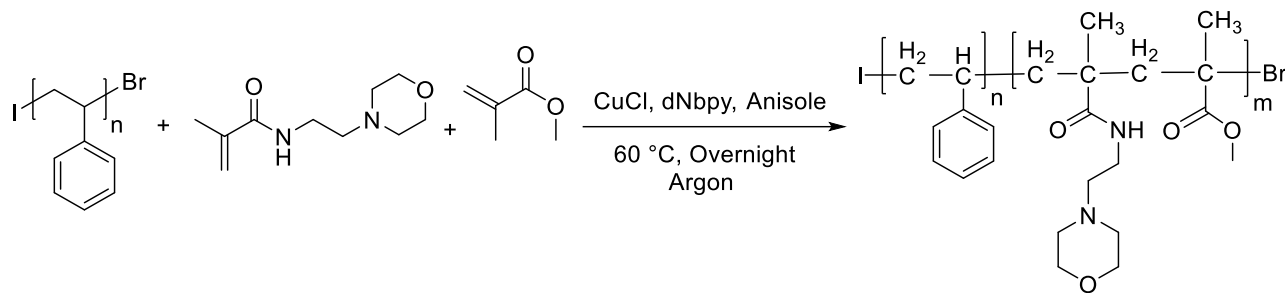
| <i>Run</i> | <i>PS-Br</i>                           | <i>dNbp</i>           | <i>MEMA</i>           | <i>CuCl</i>           | <i>Anisole</i> | <i>Reaction time</i> |
|------------|--|-----------------------|-----------------------|-----------------------|----------------|----------------------|
| 1          | 941 mg<br>0.010 mmol<br>$M_w$ : 94 100 | 24.5 mg<br>0.060 mmol | 2000 mg<br>10.00 mmol | 2.5 mg<br>0.025 mmol  | 50% wt         | 18 h.                |
| 2          | 941 mg<br>0.010 mmol<br>$M_w$ : 94 100 | 49.1 mg<br>0.120 mmol | 2000 mg<br>10.00 mmol | 5.0 mg<br>0.050 mmol  | 50% wt         | 18 h.                |
| 3          | 166 mg<br>0.020 mmol<br>$M_w$ : 8 300  | 44.8 mg<br>0.110 mmol | 4000 mg<br>20.0 mmol  | 5.0 mg<br>0.050 mmol  | 50% wt         | 24 h                 |
| 4          | 166 mg<br>0.020 mmol<br>$M_w$ : 8 300  | 44.8 mg<br>0.110 mmol | 4000 mg<br>20.0 mmol  | 5.0 mg<br>0.050 mmol  | 50% wt         | 12 h                 |
| 5          | 333 mg<br>0.040 mmol<br>$M_w$ : 8 300  | 89.7 mg<br>0.220 mmol | 1600 mg<br>8.00 mmol  | 10.0 mg<br>0.100 mmol | 50% wt         | 18 h.                |
| 6          | 224 mg<br>0.020 mmol<br>$M_w$ : 12 200 | 44.8 mg<br>0.110 mmol | 4000 mg<br>20.0 mmol  | 5.0 mg<br>0.050 mmol  | 50% wt         | 24 h                 |
| 7          | 224 mg<br>0.020 mmol<br>$M_w$ : 12 200 | 44.8 mg<br>0.110 mmol | 4000 mg<br>20.0 mmol  | 5.0 mg<br>0.050 mmol  | 50% wt         | 12 h                 |

**Table 11.4** - Experimental analysis for synthesis of polystyrene. [a] Calculated with GPC (THF), PS standards were used to calibrate the GPC system. [b] Conversion on isolate product. [c] 2-*N*-morpholinoethyl methacrylate repeating units

| <i>Run</i> | $M_n^{[a]}$ | $M_w^{[a]}$ | $M_w/M_n^{[a]}$ | <i>Conversion</i> <sup>[b]</sup> | <i>MEMA r.u.</i> <sup>[c]</sup> |
|------------|-------------|-------------|-----------------|----------------------------------|---------------------------------|
| 1          | 92 500 Da   | 142 000 Da  | 1.53            | 19 %                             | 518                             |
| 2          | 108 000 Da  | 197 700 Da  | 1.82            | 28 %                             | 667                             |
| 3          | 124 200 Da  | 199 000 Da  | 1.60            | 47 %                             | 953                             |
| 4          | 111 000 Da  | 171 600 Da  | 1.54            | 50 %                             | 816                             |
| 5          | 67 600 Da   | 90 600 Da   | 1.34            | 69 %                             | 411                             |
| 6          | 142 900 Da  | 239 700 Da  | 1.63            | 58 %                             | 1137                            |
| 7          | 116 000 Da  | 168 200 Da  | 1.44            | 41 %                             | 780                             |

[a] Calculated with GPC (THF), PS standards were used to calibrate the GPC system. [b] Conversion on isolate product. [c] 2-*N*-morpholinoethyl methacrylate repeating units

### 11.3.4 Synthesis of polystyrene-*b*-[poly-2-*N*-morpholinoethyl methacrylate-co-polymethylmethacrylate] diblockcopolymer (PS-*b*-(PMEMA-co-PMMA))



**Scheme 11.6** - Synthesis of polystyrene-*b*-[poly-2-*N*-morpholinoethyl methacrylate-co-polymethylmethacrylate] diblockcopolymer

Into a test tube fitted with a ground neck are introduced; 333 mg (0.040 mmol) of polystyrene with Br terminal group (PS-Br,  $M_w$ : 8 300 Da), 1600 mg (8.0 mmol) of 2-*N*-Morpholinoethyl methacrylate (MEMA), 800 mg (8.0 mmol) of methyl methacrylate (MMA), 89.7 mg (0.22 mmol) of 4,4'-dinonyl-2,2'-dipyridyl (dNbpy) and 50% wt anisole. Some argon is then allowed to flow into the solution using a needle for 5 minutes. Within a glove-box, 10mg (0.10 mmol) of CuCl is then withdrawn and poured into the solution under argon flow. The solution is then sealed with a cap and allowed to react overnight at 60 °C in an oil bath equipped with a tilting plate. The resulting polymer is recovered by precipitation in hexane, filtered, and dried in a high vacuum oven at 60 °C.

Conversion (isolated product): 74%

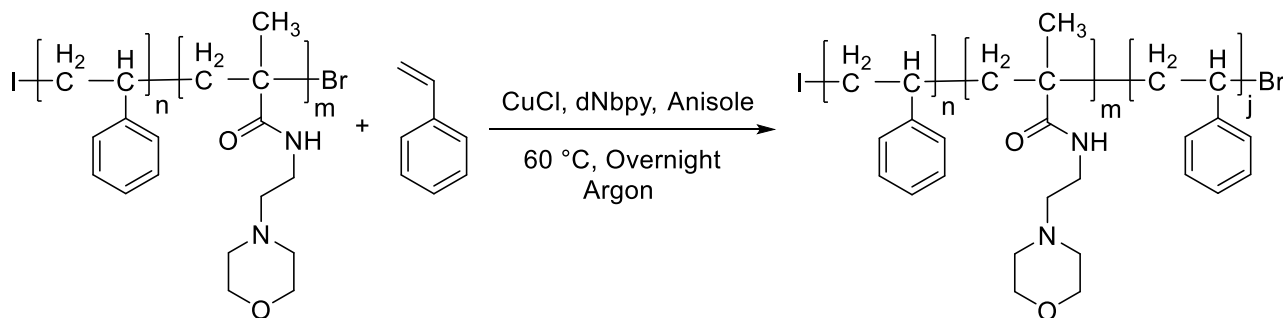
GPC analysis (THF):  $M_n$ : 93 000 Da

$M_w$ : 126 300 Da

Polydispersity ( $M_n/M_w$ ): 1.35

MEMA-MMA repeating units: 393

### 11.3.5 Synthesis of polystyrene-*b*-[poly-2-*N*-morpholinoethyl methacrylate]-*b*-polystyrene triblockcopolymer (PS-*b*-PMEMA-*b*-PS)



**Scheme 11.7** - Synthesis of polystyrene-*b*-[poly-2-*N*-morpholinoethyl methacrylate]-*b*-polystyrene triblockcopolymer

Into a test tube fitted with a ground neck are introduced; 1000 mg (0.0058 mmol) of polystyrene-*b*-[poly-2-*N*-morpholinoethyl methacrylate] diblockcopolymer with Br terminal group (PS-*b*-MEMA-Br,  $M_w$ : 171 600 Da), 600 mg (5.82 mmol) of styrene, 4.74 mg (0.011 mmol) of 4,4'-dinonyl-2,2'-dipyridyl (dNbpy) and 75% wt anisole. Some argon is then allowed to flow into the solution using a needle for 5 minutes. Within a glove-box, 0.5 mg (0.005 mmol) of CuCl is then withdrawn and poured into the solution under argon flow. The solution is then sealed with a cap and allowed to react for 24 hours at 100 °C in an oil bath equipped with a magnetic stirring. The resulting polymer is recovered by precipitation in hexane, filtered, and dried in a high vacuum oven at 60 °C.

Conversion (isolated product): 51%

GPC analysis (THF):  $M_n$ : 196 600 Da

$M_w$ : 299 000 Da

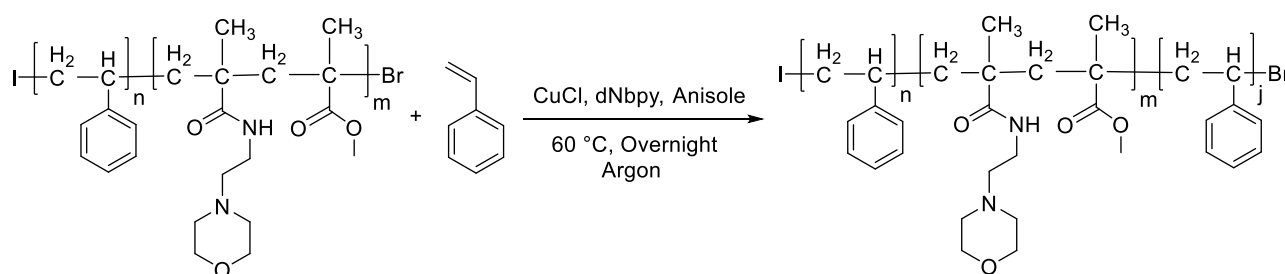
Polydispersity ( $M_w/M_n$ ): 1.52

Initial styrene repeating units: 80

MEMA repeating units: 816

Final styrene repeating units: 1228

### 11.3.6 Synthesis of polystyrene-*b*-[poly-2-*N*-morpholinoethyl methacrylate-co-polymethylmethacrylate]-*b*-polystyrene triblockcopolymer (PS-*b*-(PMEMA-co-PMMA)-*b*-PS)



**Scheme 11.7** - Synthesis of polystyrene-*b*-[poly-2-*N*-morpholinoethyl methacrylate-co-polymethylmethacrylate]-*b*-polystyrene triblockcopolymer

Into a test tube fitted with a ground neck are introduced; 1262 mg (0.01 mmol) of polystyrene-*b*-[poly-2-*N*-morpholinoethyl methacrylate-co-polymethylmethacrylate] diblockcopolymer with Br terminal group (PS-*b*-(MEMA-co-MMA)-Br,  $M_w$ : 126 300 Da), 312 mg (3.0 mmol) of styrene, 8.1 mg (0.022 mmol) of 4,4'-dinonyl-2,2'-dipyridyl (dNbpy) and 75% wt anisole. Some argon is then allowed to flow into the solution using a needle for 5 minutes. Within a glove-box, 1.0 mg (0.01 mmol) of CuCl is then withdrawn and poured into the solution under argon flow. The solution is then sealed with a cap and allowed to react for 24 hours at 100 °C in an oil bath equipped with a magnetic stirring. The resulting polymer is recovered by precipitation in hexane, filtered, and dried in a high vacuum oven at 60 °C.

Conversion (isolated product): 73%

GPC analysis (THF):  $M_n$ : 94 400 Da

$M_w$ : 132 700 Da

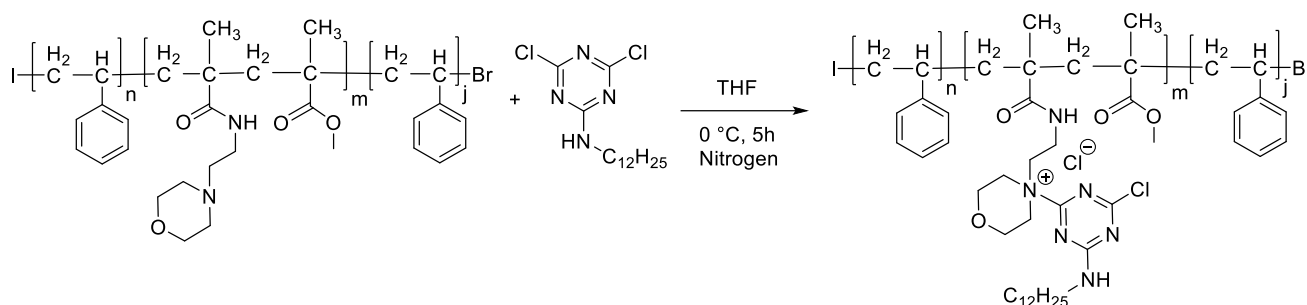


Polydispersity ( $M_n/M_w$ ): 1.40

Initial styrene repeating units: 80

Final styrene repeating units: 62

## 11.4 Synthesis of polystyrene-*b*-[4-(4-chloro-6-(dodecylamino)-1,3,5-triazin-2-yl)-4-(2-methacrylamidoethyl) morpholin-4-ium chloride-co-polymethyl metacrylate]-*b*-polystyrene triblock copolymer (PS-*b*-(PMAT<sub>12</sub>MEMA-co-PMMA)-*b*-PS)



**Scheme 11.11** - Synthesis of polystyrene-*b*-[4-(4-chloro-6-(dodecylamino)-1,3,5-triazin-2-yl)-4-(2-methacrylamidoethyl)morpholin-4-ium chloride-co-polymethylmetacrylate]-*b*-polystyrene triblockcopolymer (PS-*b*-(PMAT<sub>12</sub>MEMA-co-PMMA)-*b*-PS)

In a 100 mL double-necked glass flask equipped with a magnetic stirring rod, drip funnel, and two-way stopcock fitted with a balloon, 1660 mg (5 mmol) of 4,6-dichloro-N-dodecyl-1,3,5-triazin-2-amine (MAT<sub>12</sub>) and 40 mL of anhydrous THF are placed. In the drip funnel, 500 mg (0.0037 mmol,  $M_w$ : 134 700, MEMA-MMA: 1,459 mmol) of polystyrene-*b*-[poly-2-N-morpholinoethyl methacrylate-co-polymethylmethacrylate]-*b*-polystyrene triblockcopolymer (PS-*b*-(MEMA-co-MMA)-*b*-PS) and 10 mL of anhydrous THF are placed. After five vacuum/nitrogen cycles, the balloon is immersed in an ice bath. The solution of (PS-*b*-(PMEMA-co-MMA)-*b*-PS) is allowed to drip gently and allowed to react for a further 5 hours after the end

of addition. A yellowish powdery precipitate is formed. The product is recovered by filtration and allowed to dry in a high vacuum desiccator at room temperature.

Isolated product: 890 mg

Quaternization yield:

79% (calculated on NMR)

81% (calculated on isolate product)

$^1\text{H NMR}$  (400 MHz, DMSO),  $\delta$  (ppm): 0.86 (t,  $-\text{CH}_2\text{CH}_3$ ), 1.25 (broad,  $-\text{CH}_2(\text{CH}_2)_9\text{CH}_3$ ), 1.49 (q,  $-\text{CH}_2\text{CH}_2\text{NH}-$ ), 3.25 (broad,  $\text{HNCH}_2\text{CH}_2$ ), 3.42 (broad,  $\text{CH}_2\text{OCH}_2$ ), 3.52 (s,  $-\text{OCH}_3$ ), 3.99 (broad,  $\text{CH}_2\text{N}^+(\text{CH}_2)_2$ ), 4.17 ( $\text{CH}_2\text{CH}_2\text{N}^+(\text{CH}_2)_2$ ).

## 11.5 Polypropylene film surface modification with (PS-b-(PMAT<sub>12</sub>MEMA-co-PMMA)-b-PS) triblockcopolymer

Three 25 ml solutions were prepared using a THF/H<sub>2</sub>O mixture (ratio 80:20) containing; 100mg, 50 mg, 25 mg, 12.5 mg of (PS-b-(PMAT<sub>12</sub>MEMA-co-PMMA)-b-PS) respectively. A4-sized polyethylene sheets (210x297 mm, 623.7 cm<sup>2</sup>, 28.25 g) were then washed in isopropanol in a ultrasonic bath. The solutions were then atomized using an airbrush and deposited over each side of the sheet.

Dyne tests were performed on both virgin PP surfaces and PP (PS-b-(PMAT<sub>12</sub>MEMA-co-PMMA)-b-PS)) (Table 11.7) to assay the change in surface tension.

**Table 11.7** – Dyne test for surface modified PP foil.

| Dyne | Virgin PP | 100mg <sup>[a]</sup> | 100mg <sup>[a,b]</sup> | 50mg <sup>[a]</sup> | 50mg <sup>[a,b]</sup> | 25mg <sup>[a]</sup> | 25mg <sup>[a,b]</sup> | 12.5mg <sup>[a]</sup> | 12.5mg <sup>[a,b]</sup> |
|------|-----------|----------------------|------------------------|---------------------|-----------------------|---------------------|-----------------------|-----------------------|-------------------------|
| 48   | ✗         | ✓                    | ✓                      | ✓                   | ✓                     | ✓                   | ✓                     | ✓                     | ✓                       |
| 52   | ✗         | ✓                    | ✓                      | ✓                   | ✓                     | ✓                   | ✓                     | ✓                     | ✓                       |
| 56   | ✗         | ✓                    | ✓                      | ✓                   | ✓                     | ✓                   | ✓                     | ✓                     | ✓                       |

[a] Amount of deposited sample in an A4 sheet of polypropylene [b] Washed with water in ultrasonic bath for 20 min, ✓ = Higher wettability ✗ = Lower wettability

## 11.6 Biofilm formation inhibition assay on surfaces

The inhibition assay was conducted on film samples with a size of 22x22mm (968mm<sup>2</sup> considering both faces) using bacterial strains of *Staphylococcus aureus* (CECT 59) and *Escherichia coli* (CECT 434) previously sterilized with UV light. Using 6-wells plates, samples were then immersed in 1 mL of culture broth (Nutrient Broth for *S. aureus* and Tryptic Soy Broth for *E. coli*) and then 50 µL of bacterial inoculum was added, in order to start with 10<sup>6</sup> CFU/mL. The samples were then incubated at 37 °C for 24 h under gentle stirring. After incubation, the samples were rinsed with sterile saline to discard spent culture medium. Samples were immersed in 1 mL of fresh recovery broth and placed in an ultrasonic bath for half an hour. Cells detached from the surface were then collected and plated in serial dilutions from 10<sup>-1</sup> to 10<sup>-6</sup> and grown overnight at 37°C. All the experiments were conducted both in biological and technical triplicate using a virgin PP film as positive control (100% growth).

# **CHAPTER 12**

## **REFERENCES**

**Polymeric QACs synthesis and surface adhesion**

- [1] I. W. Sutherland, *The Biofilm Matrix – an Immobilized but Dynamic Microbial Environment*, Trends in microbiology, **2001**, 9, 222-227.
- [2] C. B. Whitchurch, T. Tolker-Nielsen, P. C. Ragas, J. S. Mattick, *Extracellular DNA Required for Bacterial Biofilm Formation*, Science, **2002**, 295, 1487-1487.
- [3] G. O’Toole, H. B. Kaplan, R. Kolter, *Biofilm Formation as Microbial Development*, Annual Review of Microbiology, **2000**, 54(1), 49–79.
- [4] K. Hori, S. Matsumoto, *Bacterial adhesion: From mechanism to control*, Biochemical Engineering Journal, **2010**, 48(3), 424–434.
- [5] H. Dang, C. R. Lovell, *Microbial Surface Colonization and Biofilm Development in Marine Environments*, Microbiology and Molecular Biology Reviews, **2015**, 80 (1) 91-138.
- [6] H. F. Jenkinson, H. M. Lappin-Scott, *Biofilms Adhere to Stay*, Trends in microbiology, **2001**, 9, 9-10.
- [7] J. D. Bryers, *Biofilms and the Technological Implications of Microbial Cell Adhesion*, Colloids and Surfaces B: Biointerfaces, **1994**, 2, 9-23.
- [8] D. Monroe, *Looking for Chinks in the Armor of Bacterial Biofilms*, Plos Biology **2007**, 5, 2458-2461.
- [9] M. Otto, *Staphylococcal Infections: Mechanisms of Biofilm Maturation and Detachment as Critical Determinants of Pathogenicity*, Annual Review of Medicine, **2013**, 64:1, 175-188.
- [10] Y. H. Li, X. Tian, *Quorum Sensing and Bacterial Social Interactions in Biofilms*, Sensors, **2012**, 12(3), 2519-2538.
- [11] J.W. Costerton, P. S. Stewart, E. P. Greenberg, *Bacterial Biofilms: A Common Cause of Persistent Infections*, Science, **1999**, 284, 1318-1322.
- [12] C. A. Fux, S. Wilson, P. Stoodley, *Detachment Characteristics and Oxacillin Resistance of Staphylococcus aureus Biofilm Emboli in an In Vitro Catheter*, Infection Model Journal of Bacteriology, **2004**, 186(14), 4486-4491.
- [13] Z. U. Khan, I. Naz, A. Rehman, M. Rafiq, N. Ali & S. Ahmed, *Performance efficiency of an integrated stone media fixed biofilm reactor and sand filter for sewage treatment*, Desalination and Water Treatment, **2015**, 54:10, 2638-2647.
- [14] P. Tribedi, A.K. Sil, *Low-density polyethylene degradation by Pseudomonas sp. AKS2 biofilm*, Environ Sci Pollut Res, **2013**, 20, 4146–4153

- [15] T. R. Neu, C. E. De Boer, G. J. Verkerke, H. K. Schutte, G. Rakhorst, H. C. Van der Mei, H. J. Busscher, *Biofilm Development in Time on a Silicone Voice Prosthesis — a Case Study*, *Microbial Ecology in Health and Disease*, **1994**, 7, 27-33.
- [16] E. Everaert, H. F. Mahieu, B. Van de Belt-Gritter, A. Peeters, G. J. Verkerke, H. C. Van der Mei, H. J. Busscher, *Biofilm Formation in Vivo on Perfluoro-Alkylsiloxane-Modified Voice Prostheses*, *Archives of Otolaryngology-Head & Neck Surgery*, **1999**, 125, 1329-1332.
- [17] T. R. Neu, H. C. Van der Mei, H. J. Busscher, F. Dijk, G. J. Verkerke, *Biodeterioration of Medical-Grade Silicone Rubber Used for Voice Prostheses: A Sem Study*, *Biomaterials*, **1993**, 14, 459-464.
- [18] G. J. Elving, H. C. Van der Mei, H. J. Busscher, R. Van Weissenbruch, F. Albers, *Influence of Different Combinations of Bacteria and Yeasts in Voice Prosthesis Biofilms on Air Flow Resistance*, *Antonie Van Leeuwenhoek International Journal of General and Molecular Microbiology*, **2003**, 83, 45-55.
- [19] A. Corbin, B. Pitts, A. Parker, P. S. Stewart, *Antimicrobial Penetration and Efficacy in an In Vitro Oral Biofilm Model*, *Antimicrobial Agents and Chemotherapy*, **2011**, 55 (7), 3338-3344.
- [20] I. Williams, W. A. Venables, D. Lloyd, F. Paul, I. Critchley, *The Effects of Adherence to Silicone Surfaces on Antibiotic Susceptibility in Staphylococcus aureus*, *Microbiology*, **1997**, 143, 2407-2413.
- [21] R. C. Evans, C. J. Holmes, *Effect of Vancomycin Hydrochloride on Staphylococcus epidermidis Biofilm Associated with Silicone Elastomer*, *Antimicrobial Agents and Chemotherapy*, **1987**, 31, 889-894.
- [22] J. W. Costerton, Z. Lewandowski, D. E. Caldwell, D. R. Korber, H. M. Lappin-Scott, *Microbial Biofilms*, *Annual Review of Microbiology*, **1995**, 49, 711-745.
- [23] O. E. Petrova, K. Sauer, *Sticky situations: key components that control bacterial surface attachment*, *Journal of Bacteriology*, **2012**, 194(10), 2413-2425.
- [24] D. Machado, J. Castro, A. Palmeira-de-Oliveira, J. Martinez-de-Oliveira, N. Cerca, *Bacterial vaginosis biofilms: challenges to current therapies and emerging solutions*. *Front. Microbiol.*, **2016**, 6:1528.

- [25] E. C. Von Roseninge, G. A. O'May, S. Macfarlane, G. T. Macfarlane, M. E. Shirtliff, *Microbial biofilms and gastrointestinal diseases*, *Pathog*, **2013**, Dis. 67, 25–38.
- [26] I. Behlau, M. S. Gilmore, *Microbial biofilms in ophthalmology and infectious disease*. *Arch. Ophthalmol*, **2008**, 126, 1572–1581.
- [27] A. P. Vieira Colombo, C. B. Magalhães, F. A. Hartenbach, R. Martins do Souto, C. M. Silva-Boghossian. *Periodontal-disease-associated biofilm: a reservoir for pathogens of medical importance*. *Microbial. Pathog*. **2016**, 94, 27–34.
- [28] A. Omar, J. B. Wright, G. Schultz, R. Burrell, P. Nadworny. *Microbial biofilms and chronic wounds*, *Microorganisms*, **2017**, 5:9.
- [29] J. W. Costerton, K. J. Cheng, G. G. Geesey, T. I. Ladd, J. C. Nickel, M. Dasgupta, T. J. Marrie, *Bacterial biofilms in nature and disease*, *Annu. Rev. Microbiol*, **1987**, 41, 435–464.
- [30] D. Lebeaux, J. M. Ghigo, C. Beloin, *Biofilm-related infections: bridging the gap between clinical management and fundamental aspects of recalcitrance toward antibiotics*, *Microbiol. Mol. Biol. Rev.* , **2014**, 78, 510–543.
- [31] C. Baum, L. G. Fleischer, D. Roessner, W. Meyer, D. Siebers, *A Covalently Cross-Linked Gel Derived from the Epidermis of the Pilot Whale Globicephala Melas*, *Biorheology*, **2002**, 39, 703-717.
- [32] G. Cheng, H. Xue, G. Li, S. Jiang, *Integrated Antimicrobial and Nonfouling Hydrogels to Inhibit the Growth of Planktonic Bacterial Cells and Keep the Surface Clean*, *Langmuir*, **2010**, 26, 10425-10428.
- [33] S. Jiang, Z. Cao, *Ultralow-Fouling, Functionalizable, and Hydrolyzable Zwitterionic Materials and Their Derivatives for Biological Applications*, *Advanced Materials*, **2010**, 22, 920-932.
- [34] I. Fundeanu, H. C. Van der Mei, A. J. Schouten, H. I. Busscher, *Polyacrylamide Brush Coatings Preventing Microbial Adhesion to Silicone Rubber*, *Colloids and Surfaces B-Biointerfaces*, **2008**, 64, 297-301.
- [35] Y. Zhang, N. Kohler, M. Zhang, *Surface Modification of Superparamagnetic Magnetite Nanoparticles and Their Intracellular Uptake*, *Biomaterials*, **2002**, 23, 1553-1561.

- [36] I. C. Saldarriaga Fernández, H. J. Busscher, S. W. Metzger, D. W. Grainger, H. C. Van der Mei, *Competitive Time- and Density-Dependent Adhesion of Staphylococci and Osteoblasts on Crosslinked Poly(Ethylene Glycol)-Based Polymer Coatings in Co-Culture Flow Chambers*, *Biomaterials*, **2011**, 32, 979-984.
- [37] S. Elbasuney, *Sustainable steric stabilization of colloidal titania nanoparticles*, *Applied Surface Science*, **2017**, 409, 438–447.
- [38] R. Brady, *Clean Hulls without Poisons: Devising and Testing Nontoxic Marine Coatings*, *Journal of Coatings Technology*, **2000**, 72, 45-56.
- [39] S. Krishnan, C. J. Weinman, C. K. Ober, *Advances in Polymers for Anti-Biofouling Surfaces*, *Journal of Materials Chemistry*, **2008**, 18, 3405-3413
- [40] K. Subramani, R. E. Jung, A. Molenberg, C. Hammerle, *Biofilm on Dental Implants: A Review of the Literature*, *The International Journal of Oral & Maxillofacial Implants*, **2008**, 24, 616-626.
- [41] M. Quirynen, C. Bollen, *The Influence of Surface Roughness and Surface-Free Energy on Supra-and Subgingival Plaque Formation in Man*, *Journal of Clinical Periodontology*, **1995**, 22, 1-14.
- [42] F. Siepmann, J. Siepmann, M. Walther, R. J. MacRae, R. Bodmeier, *Polymer Blends for Controlled Release Coatings*, *Journal of Controlled Release*, **2008**, 125, 1-15.
- [43] M. Kazemzadeh-Narbat, B. F. L. Lai, C. Ding, J. N. Kizhakkedathu, R. E. W. Hancock, R. Wang, *Multilayered Coating on Titanium for Controlled Release of Antimicrobial Peptides for the Prevention of Implant-Associated Infections*. *Biomaterials*, **2013**, 34, 5969-5977.
- [44] I. Zhuk, F. Jariwala, A. B. Attygalle, Y. Wu, M. R. Libera, S. A. Sukhishvili, *Self-Defensive Layer-by-Layer Films with Bacteria-Triggered Antibiotic Release*, *ACS Nano*, **2014**, 8, 7733-7745.
- [45] J. Y. Maillard, P. Hartemann, *Silver as an Antimicrobial: Facts and Gaps in Knowledge*, *Critical Reviews in Microbiology*, **2013**, 39, 373-383.
- [46] W. Sim, R. T. Barnard, M. A. T. Blaskovich, Z. M. Ziora, *Antimicrobial Silver in Medicinal and Consumer Applications: A Patent Review of the Past Decade, (2007–2017)*, *Antibiotics*, **2018**, 7(4):93.



- [47] C. Greulich, D. Braun, A. Peetsch, J. Diendorf, B. Siebers, M. Epple, M. Köller, *The Toxic Effect of Silver Ions and Silver Nanoparticles Towards Bacteria and Human Cells Occurs in the Same Concentration Range*, RSC Advances, **2012**, 2, 6981-6987.
- [48] R. de Nys, M. Givskov, N. Kumar, *Furanones*, Prog Mol Subcell Biol, **2006**, 42:55–86
- [49] K. G. Kristinsson, B. Jansen, U. Treitz, *Antimicrobial activity of polymers coated with iodine-complexed polyvinylpyrrolidone*, J Biomater Appl, **1991**, 5:173–184
- [50] A. J. Kugel, L. E. Jarabek, J. W. Daniels, *Combinatorial materials research applied to the development of new surface coatings XII: novel, environmentally friendly antimicrobial coatings derived from biocide-functional acrylic polyols and isocyanates*, J Coat Technol Res, **2009**, 6:107–121
- [51] B. J. Nablo, M. H. Schoenfisch, *Antibacterial properties of nitric oxide-releasing sol-gels. J Biomed Mater Res*, **2003**, A 67A:1276–1283
- [52] Li Y, Worley SD (2001) Biocidal copolymers of N-haloacryloxymethylhydantoin. J Bioact Compat Polym 16:493–506
- [53] P. A. Norowski, J. D. Bumgardner, *Biomaterial and antibiotic strategies for periimplantitis: a review*, J Biomed Mater Res B Appl Biomater, **2009**, 88:530–543.
- [54] G.T. Hermanson, *Bioconjugate Techniques*, Second Edition, 2nd ed, Academic Press, **2008**.
- [55] C. Hein, X. Liu, D. Wang, *Pharmaceutical Research*, **2008**, 25, 2216-2230.
- [56] S. Krishnan, R.J. Ward, A. Hexemer, K.E. Sohn, K.L. Lee, E.R. Angert, D.A. Fischer, E.J. Kramer, C.K. Ober, *Langmuir*, **2006**, 22, 11255-11266.
- [57] J. Lichter, K. Van Vliet, and M. Rubner, *Macromolecules*, **2009**, 42, 8573-8586.
- [58] A. K. Muszanska, H. J. Busscher, A. Herrmann, H. C. Van der Mei, W. Norde, *Pluronic–Lysozyme Conjugates as Anti-Adhesive and Antibacterial Bifunctional Polymers for Surface Coating*, Biomaterials, **2011**, 32, 6333-6341.
- [59] A. K. Muszanska, E. T. J. Rochford, A. Gruszka, A. A. Bastian, H. J. Busscher, W. Norde, H. C. Van der Mei, A. Herrmann, *Antiadhesive Polymer Brush Coating Functionalized with Antimicrobial and Rgd Peptides to Reduce Biofilm Formation and Enhance Tissue Integration*, Biomacromolecules, **2014**, 15, 2019-2026.

- [60] A. Kugel, S. Stafslie, B. J. Chisholm, *Antimicrobial Coatings Produced by "Tethering" Biocides to the Coating Matrix: A Comprehensive Review*, *Progress in Organic Coatings*, **2011**, 72, 222-252.
- [61] R. L. Gettings, W. C. White, *Polym. Mater. Sci. Eng.*, **1987**, 57, 181-5.
- [62] I. Novák; A. Popelka; I. Krupa; I. Chodák; I. Janigová; T. Nedelčev; M. Špírková; A. Kleinová, *High-density polyethylene functionalized by cold plasma and silanes*, **2012**, 86(12).
- [63] A. J. Isquith, E. A. Abbott, P. A. Walters, *Appl Microbiol*, **1972**, 24, 859-863
- [64] Z. Li, D. Lee, X. Sheng, R. E. Cohen, M. F. Rubner, *Langmuir*, **2006**, 22, 9820-9823.
- [65] K. Lewis and A. Klibanov, *Trends in Biotechnology*, **2005**, 23, 343-348.
- [66] N. Milovic, J. Wang, K. Lewis, A. Klibanov, *Biotechnology and Bioengineering*, **2005**, 90, 715-722.
- [67] S. Wong, Q. Li, J. Veselinovic, B. Kim, A. Klibanov, P. Hammond, *Biomaterials*, **2010**, 31, 4079-4087.
- [68] J. Haldar, D. An, L. de Cienfuegos, J. Chen, A. Klibanov, *Proceedings of the National Academy of Sciences of the United States Of 103*, **2006**, 17667-17671
- [69] H. Murata, R. Koepsel, K. Matyjaszewski, A. Russell, *Biomaterials*, **2007**, 28, 4870-4879
- [70] N. Milovic, J. Wang, K. Lewis, and A. Klibanov, *Biotechnology and Bioengineering*, **2005**, 90, 715-722.
- [71] A. Kausar, *Survey on Langmuir–Blodgett Films of Polymer and Polymeric Composite*, *Polymer-Plastics Technology and Engineering*, **2017**, 56:9, 932-945
- [72] A. Boujemaoui, C. Cobo Sanchez, J. Engström, C. Bruce, L. Fogelström, A. Carlmark, E. Malmström, *Polycaprolactone Nanocomposites Reinforced with Cellulose Nanocrystals Surface-Modified via Covalent Grafting or Physisorption: A Comparative Study*, *ACS Applied Materials & Interfaces*, **2017**, 9 (40), 35305-35318.
- [73] L. D. Zubris, K. P. C. Minbiole, W. M. Wuest, Willia, *Current Topics in Medicinal Chemistry*, **2017**, 17(3), 305-318.

- [74] P. Elena, K. Miri, *Formation of contact active antimicrobial surfaces by covalent grafting of quaternary ammonium compounds*, Colloids and Surfaces B: Biointerfaces, **2018**, 169,195-205.
- [75] M. Delfi, M. Ghomi, A. Zarrabi, R. Mohammadinejad, Z. B. Taraghdari, M. Ashrafizadeh, E. N. Zare, T. Agarwal, V. V. T. Padil, B. Mokhtari, F. Rossi, G. Perale, M. Sillanpaa, A. Borzacchiello, M. T. Kumar, P. Makvandi, *Functionalization of Polymers and Nanomaterials for Biomedical Applications: Antimicrobial Platforms and Drug Carriers*. Prosthesis. **2020**, 2(2),117-139.
- [76] O. Sakinehi, K. Ali, *Modification of chitosan and chitosan nanoparticle by long chain pyridinium compounds: Synthesis, characterization, antibacterial, and antioxidant activities*, Carbohydrate Polymers, **2019**, 208, 477-485.
- [77] J. Lin, S. Qiu, K. Lewis, and A. Klibanov, *Bactericidal properties of flat surfaces and nanoparticles derivatized with alkylated polyethylenimines*, Biotechnology Progress, **2002**, 18, 1082-1086.
- [78] B. Zdyrko; I. Luzinov, *Polymer Brushes by the "Grafting to" Method*, Macromolecular Rapid Communication, **2011**, 32(12), 859–869.
- [79] H. Kitano; T. Kondo; T. Kamada; S. Iwanaga; M. Nakamura; K. Ohno, *Anti-biofouling properties of an amphoteric polymer brush constructed on a glass substrate*, **2011**, 88(1), 455–462.
- [80] Y. Uyama, K. Kato, Y. Ikada, *Surface modification of polymers by grafting*. Advance in Polymer Science, **1998**,137,1.
- [81] K. Kim , T. K. An , J. Kim , Y. J. Jeong , J. Jang , H. Kim , J. Y. Baek , Y.-H. Kim , S. H. Kim, C. E. Park, *Grafting Fluorinated Polymer Nanolayer for Advancing the Electrical Stability of Organic Field-Effect Transistors*, Chemistry of Materials, **2014**, 26 , 6467-6476.
- [82] P. Paoprasert , J. W. Spalenka , D. L. Peterson , R. E. Ruther , R. J. Hamers , P. G. Evans, P. Gopalan, *Grafting of poly(3-hexylthiophene) brushes on oxides using click chemistry*, Journal of Materials Chemistry, **2010**, 20, 2651-2658.
- [83] V. K. Thakur, M. K. Thakur, R. K. Gupta, *Graft Copolymers from Natural Polymers Using Free Radical Polymerization*, International Journal of Polymer Analysis and Characterization, **2013**, 18,7.

- [84] S. Ito, R. Goseki, T. Ishizone, A. Hirao, *Synthesis of well-controlled graft polymers by living anionic polymerization towards exact graft polymers*. *Polymer Chemistry*, **2014**, 5(19), 5523.
- [85] M. Tizzotti; A. Charlot; E. Fleury; M. Stenzel; J. Bernard, *Modification of Polysaccharides Through Controlled/Living Radical Polymerization Grafting—Towards the Generation of High Performance Hybrids*, *Macromolecular Rapid Communication*, **2010**, 31(20), 1751–1772.
- [86] I. M. Rutenberg, O. A. Scherman , R. H. Grubbs , W. R. Jiang , E. Garfunkel, Z. Bao , *Journal of the American Chemical Society*, **2004**, 126 , 4062-4063
- [87] M. Sato, T. Kato, T. Ohishi, R. Ishige, N. Ohta, K. L. White, T. Hirai, A. Takahara, *Precise Synthesis of Poly(methyl methacrylate) Brush with Well-Controlled Stereoregularity Using a Surface-Initiated Living Anionic Polymerization Method*, *Macromolecules*, **2016**, 49 (6), 2071-2076.
- [88] B. Lego, M. François, W. G. Skene, S. Giasson, *Polymer Brush Covalently Attached to OH-Functionalized Mica Surface via Surface-Initiated ATRP: Control of Grafting Density and Polymer Chain Length*, *Langmuir*, **2009**, 25 (9), 5313-5321
- [89] S. P. Le-Masurier, G. Gody, S. Perrier, A. M. Granville, *One-pot polymer brush synthesis via simultaneous isocyanate coupling chemistry and “grafting from” RAFT polymerization*. *Polymer Chemistry*, **2014**, 5(8), 2816.
- [90] Q. Zhou, X. Lei, J. Li, B. Yan, Q. Zhang, *Antifouling, adsorption and reversible flux properties of zwitterionic grafted PVDF membrane prepared via physisorbed free radical polymerization*, *Desalination*, **2014**, 337, 6–15.
- [91] C. Lv, Q. Xue, D. Xia, M. Ma, J. Xie, H. Chen, *Effect of Chemisorption on the Interfacial Bonding Characteristics of Graphene–Polymer Composites*, *The Journal of Physical Chemistry C*, **2010**, 114(14), 6588-6594.
- [92] M. E. Alf; A. Asatekin; M. C. Barr; S. H. Baxamusa; H. Chelawat; G. Ozaydin-Ince; C. D. Petruczok; R. Sreenivasan; W. E. Tenhaeff; N. J. Trujillo; S. Vaddiraju; J. Xu; K. K. Gleason, *Chemical Vapor Deposition of Conformal, Functional, and Responsive Polymer Films*, *Advanced Materials*, **2010**, 22(18), 1993–2027.
- [93] R. Zhang, Y. Su, X. Zhao, Y. Li, J. Zhao, Z. Jiang, *A novel positively charged composite nanofiltration membrane prepared by bio-inspired adhesion of*

- polydopamine and surface grafting of poly(ethylene imine)*, Journal of Membrane Science, **2014**, 470, 9–17.
- [94] G. J. Fleer, J. Lyklema, *Adsorption from Solution at the Solid/Liquid Interface*; Academic Press: New York, **1983**.
- [95] G. Odian, *Principles of Polymerization*, 3rd ed., John Wiley & Sons, Inc., New York, **1991**.
- [96] H. Zhang, N. Alkayal, Y. Gnanou, N. Hadjichristidis, *Anionic polymerization and polyhomologation: an ideal combination to synthesize polyethylene-based block copolymers*, Chemical Communications, **2013**, 49(79), 8952-
- [97] A. D: Jenkins, R. G. Jones, G. Moad, *Terminology for reversible-deactivation radical polymerization previously called "controlled" radical or "living" radical polymerization (IUPAC Recommendations 2010)*, Pure and Applied Chemistry. **2009**, 82 (2): 483–491.
- [98] J. Pan, B. Zhang, X. Jiang, L. Zhang, Z. Cheng, X. Zhu, *Cu(II)-mediated atom transfer radical polymerization of methyl methacrylate via a strategy of thermo-regulated phase-separable catalysis in a liquid/liquid biphasic system: homogeneous catalysis, facile heterogeneous separation, and recycling*. Macromolecular Rapid Communication, **2014**
- [99] F. Di Lena, K. Matyjaszewski, K, Progress in Polymer Science. **2010**, 35, 959-1021.
- [100] D. He, S. Kyun Noh, W. Seok Lyoo, *In situ-generated Ru(III)-mediated ATRP from the polymeric Ru(III) complex in the absence of activator generation agents*, Polymer chemistry, **2011**, 49(21),4594-4602.
- [101] E. Duquesne, J. Habimana, P. Degée, P. Dubois, *Nickel-Catalyzed Supported ATRP of Methyl Methacrylate Using Cross-Linked Polystyrene Triphenylphosphine as Ligand*, Macromolecules, **2005**, 38(24), 9999-10006.
- [102] W. A. Braunecker, Y. Itami, K. Matyjaszewski, *Osmium-Mediated Radical Polymerization*, Macromolecules **2005** 38 (23), 9402.
- [103] Matyjaszewski, Krzysztof; Xia, Jianhui, *Atom Transfer Radical Polymerization*. Chemical Review, **2001**, 101(9),2921–90.
- [104] W. Tang, Y. Kwak, W. Braunecker, N. V. Tsarevsky, M. L. Coote, K. Matyjaszewski, *Understanding Atom Transfer Radical Polymerization: Effect of Ligand and Initiator*

*Structures on the Equilibrium Constants*, Journal of the American Chemical Society, **2008**,130(32), 10702-10713.

- [105] J. M. G Cowie, V. Arrighi, *In Polymers: Chemistry and Physics of Modern Materials*; CRC Press Taylor and Francis Group, **2008**; 3rd Ed,82–84
- [106] K. Jankova, M. Bednarek, S. Hvilsted, *Star polymers by ATRP of styrene and acrylates employing multifunctional initiators*, Polymer Chemistry, **2005** 43(17), 3748-3759.
- [107] Y. Tsujii, K. Ohno, S. Yamamoto, A. Goto, T. Fukuda, *Structure and Properties of High-Density Polymer Brushes Prepared by Surface-Initiated Living Radical Polymerization*. In: Jordan R. (eds) *Surface-Initiated Polymerization*, Advances in Polymer Science, **2006**, 197. Springer, Berlin, Heidelberg.
- [108] W. Lee, Y. Kim, S.Jo, S. Park, H. Ahn, D. Yeol Ryu, *Irreversible Physisorption of PS-*b*-PMMA Copolymers on Substrates for Balanced Interfacial Interactions as a Versatile Surface Modification*, ACS Macro Letters, **2019**, 8(5), 519-524.
- [109] T. Ikeda, H. Hirayama, H. Yamaguchi, S. Tazuke, M. Watanabe, *Polycationic biocides with pendant active groups: molecular weight dependence of antibacterial activity*. Antimicrobial Agents and Chemotherapy, **1986**,30:132-6.
- [110] C. Z. Chen, N. C. Beck-Tan, P. Dhurjati, T. K. van Dyk, R. A. LaRossa, S. L. Cooper, *Quaternary ammonium functionalized poly (propylene imine) dendrimers as effective antimicrobials: structure-activity studies*, Biomacromolecules, **2000**,1:473-80.
- [111] P. Gilbert, A. Al-Taae, *Antimicrobial activity of some alkyltrimethylammonium bromides*, Letters in Applied Microbiology, **1985**;1:101-4.
- [112] L. Caillier, E. T. de Givenchy, R. Levy, Y. Vandenberghe, S. Geribaldi, F. Guittard, *Synthesis and antimicrobial properties of polymerizable quaternary ammoniums*. European Journal of Medicinal Chemistry, **2009**, 44, 3201-8.

## RINGRAZIAMENTI

Ogni volta che si raggiunge un traguardo, che sia esso grande o piccolo, lo si raggiunge sia col proprio impegno, ma anche con l'indispensabile supporto di tutte quelle persone che nel piccolo o nel grande ci hanno aiutato durante tutto il percorso.

Giungere alla conclusione di un dottorato è un grande traguardo e non sarebbe mai stato possibile senza l'aiuto e il supporto della mia famiglia, che ha sempre creduto in me anche nei momenti più difficili. Se ora sono diventato quello che sono lo devo soprattutto a loro, per avermi guidato senza mai impormi nulla. Grazie.

Ringrazio Francesca, la mia dolce metà, che nonostante i tre anni di lontananza non mi ha mai fatto mancare il suo amore e il suo supporto. Consolandomi nei momenti di tristezza e comprendendomi in quelli più burrascosi.

Ringrazio anche i miei amici più cari per le epiche serate passate tra una sessione di gaming e una pizza assieme.

Voglio ringraziare il Prof. Kohji Ohno e tutto il gruppo di ricerca di Chimica dei Polimeri dell'Institute of Chemical Research per avermi regalato un'esperienza indimenticabile nei loro centri di ricerca alla Kyoto University.

Infine ringrazio tutto il gruppo di Chimica Organica Industriale della Prof. Beghetto per la grande opportunità concessami e il supporto durante il percorso.

## ACKNOWLEDGEMENTS

Every time you achieve a goal, be it big or small, you do it with your own commitment, but also with the indispensable support of all those people who, in a small or big way, have helped you along the way.

Reaching the conclusion of a PhD is a great achievement and it would never have been possible without the help and support of my family, who always believed in me even in the most difficult moments. If I have now become what I am, I owe it above all to them for having guided me without ever imposing anything on me. Thank you.

I would like to thank Francesca, my better half, who in spite of three years of distance has never let me lack her love and support. Consoling me in moments of sadness and understanding me in the stormiest ones.

I also thank my closest friends for the epic evenings spent between a gaming session and a dinner of pizza together.

I would like to thank Prof. Kohji Ohno and all the research group of Polymer Chemistry of the Institute of Chemical Research for giving me an unforgettable experience in their research centers at Kyoto University.

Finally, I would like to thank all the Industrial Organic Chemistry group of Prof. Beghetto for the great opportunity given to me and the support during the course.